5-16-2008

Water Quality Modeling of Freshwater Diversions in the Pontchartrain Estuary

Rachel Roblin
University of New Orleans

Water Quality Modeling of Freshwater Diversions in the Pontchartrain Estuary

A Thesis

Submitted to the Graduate Faculty of the
University of New Orleans
in partial fulfillment of the
requirements for the degree of

Master of Science
in
Engineering
Civil and Environmental Engineering

by

Rachel J. Roblin

B.Sc. Queen's University, Canada, 2003

May, 2008

Acknowledgements

First and foremost, I would like to thank my major professor, Dr. Alex McCorquodale. His unending patience, immeasurable knowledge and enthusiastic approach to his work are truly inspiring. I am grateful to have had the opportunity to work under his supervision for the last two years.

I would also like to thank the other members of my committee, Dr. Ioannis Georgiou, Dr. Gianna Cothren and Dr.Donald Barbé. Their guidance and support of my research are much appreciated.

Jennifer Schindler, who helped analyze the extensive datasets that were collected during this research, also deserves a thank-you as does my colleague and friend, Gabriel Retana.

I would also like to say a special thank you to my mother Pat, my sister Emily, my father Andrew and my boyfriend Matt, who have supported, encouraged and loved me unconditionally throughout my life and from afar these last two years.

Finally, I would like to acknowledge the entities that made this research possible. This research was funded by: the U.S. Environmental Protection Agency (EPA) through a contract with the Lake Pontchartrain Basin Foundation (LPBF); and the National Oceanic and Atmospheric Administration (NOAA) through a Pontchartrain Restoration Program (PRP) grant and a Coastal Louisiana Ecosystem Assessment and Restoration (CLEAR) sub-contract.

Table of Contents

List of Figures

List of Tables

Abstract

A 1-D tidal, salinity and water quality model that analyzes the general effects freshwater diversions have on the water quality of the Pontchartrain Estuary over a 17-year period is presented here. Using the modeled live algae concentrations in conjunction with the algal bloom probability model results produces an accurate prediction of algal bloom occurrences between 1990 and 2006. The model predicts that the addition of freshwater diversions into Maurepas swamp and increases to flow in the Bonnet Carré Spillway may cause more intense and frequent algal blooms to occur around the Pontchartrain Estuary. The model also predicts that high nutrient input events that occur earlier in the year (January/February) will not likely have algal blooms associated with them. When nutrient input events (even small events) occur in the late spring or early summer, algal blooms have a high probability of occurring when the salinity, temperature and light levels are sufficient.

Keywords: Lake Pontchartrain, water quality modeling, algal blooms, freshwater diversions, Bonnet Carré Spillway

1.0 Introduction

1.1 The Pontchartrain Estuary

The Pontchartrain Estuary is located north of New Orleans in southeast Louisiana and is composed of three lakes: Lake Maurepas, Lake Pontchartrain and Lake Borgne. The Pontchartrain Estuary is located in a shallow depression between the alluvial ridge of the Mississippi River to the west, the sloping uplands to the north, the Pearl River basin to the east and Mississippi Sound to the south (U.S. Army Corps of Engineers (USACE), 1982).

Lake Maurepas, located the furthest west, is connected to Lake Pontchartrain via Pass Manchac. Lake Borgne is located the furthest east and is connected to the Gulf of Mexico in the east and Lake Pontchartrain in the west by two natural tidal passes: the Rigolets and Chef Menteur. The Inner Harbor Navigation Canal (INHC), located on the south shore of Lake Pontchartrain, connects Lake Pontchartrain to: the Mississippi River through a lock; and the Mississippi River Gulf Outlet (MRGO) via the Gulf Intracoastal Waterway (GIWW). The Mississippi River periodically flows into Lake Pontchartrain through the Bonnet Carré Spillway, located in the southwest corner of Lake Pontchartrain. Figure 1.1 shows an overview of the Pontchartrain Estuary area.

The Pontchartrain Estuary is a brackish estuary where salinities vary from 1 ppt in the east to 6 ppt in the west. Figure 1.2 shows the variation in salinity concentration around the Pontchartrain Estuary that was calculated using data from the U.S. Geological Survey (USGS), the U.S. Army Corps of Engineers (USACE), the National Oceanic and Atmospheric Administration (NOAA) and the University of New Orleans (UNO).

Lake Maurepas is a relatively fresh lake that has three rivers flowing into it: the Amite River, the Tickfaw River, and the Natalbany River. Freshwater flows into Lake Pontchartrain from tributaries located in the north (mainly the Tangipahoa River, and the Tchefuncte River) and storm water canals in New Orleans. Freshwater also flows into Lake Pontchartrain through the Bonnet Carré Spillway when Mississippi River stages are high. Freshwater enters Lake Borgne from the Pearl River. The Pearl River water also has the potential to enter Lake Pontchartrain through the Rigolets and Chef Menteur tidal passes during flood tide conditions. McCorquodale et al. (2007) estimated that 5-10% of the Pearl River water flows through the two tidal passes into Lake Pontchartrain. Saltwater enters Lake Pontchartrain through the IHNC and through the two tidal passes.

The spring tidal range in Lake Pontchartrain is approximately 0.15 m and the peak exchange flows on the spring ebb and flood tides through all of the passes (IHNC, Chef Menteur, Rigolets and Pass Manchac) are approximately 8,800 m^3/s (McCorquodale et al., 2007). Haralampides (2000) determined that 5%, 27%, 11% 57% and 11% of the exchange flow is carried through the IHNC, Chef Menteur, Rigolets and Pass Manchac passes respectively.

Some important physical parameters of the Pontchartrain Estuary are listed in Table 1.1. For additional information about the hydrologic characteristics of Lake Pontchartrain refer to McCorquodale et al. (2001).

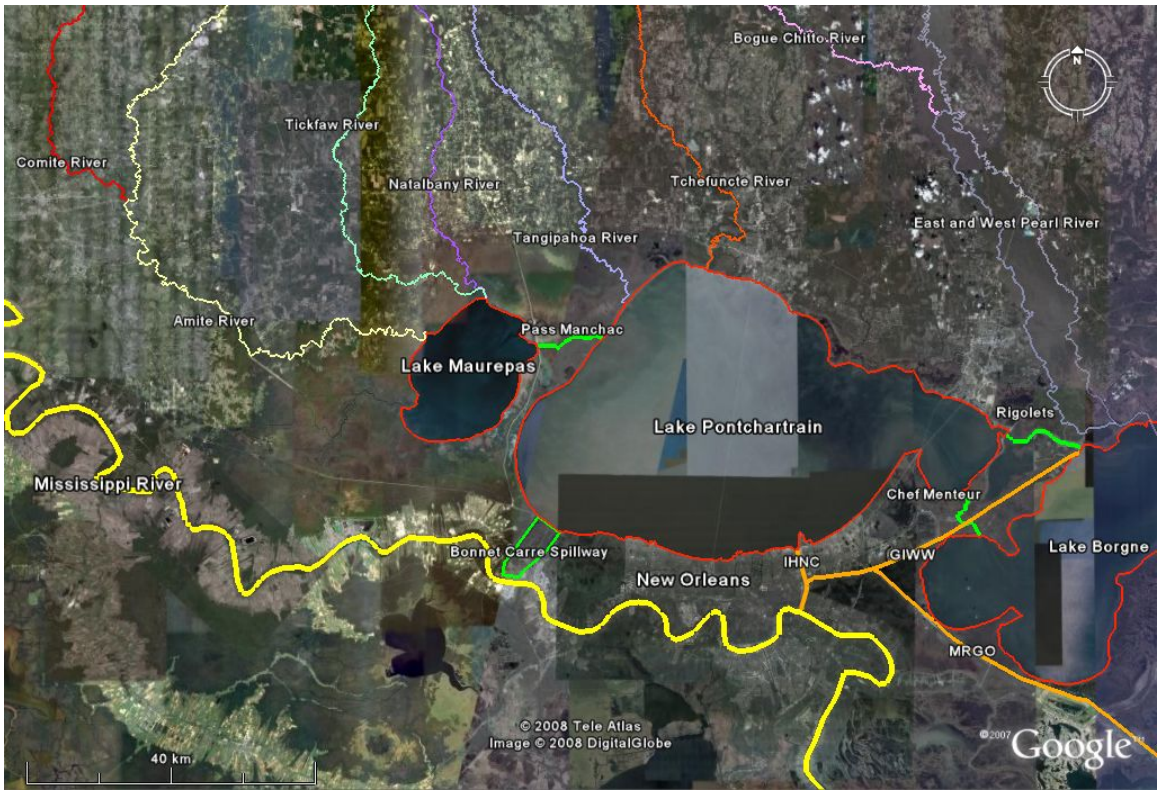

Figure 1.1 Overview of the Pontchartrain Estuary.

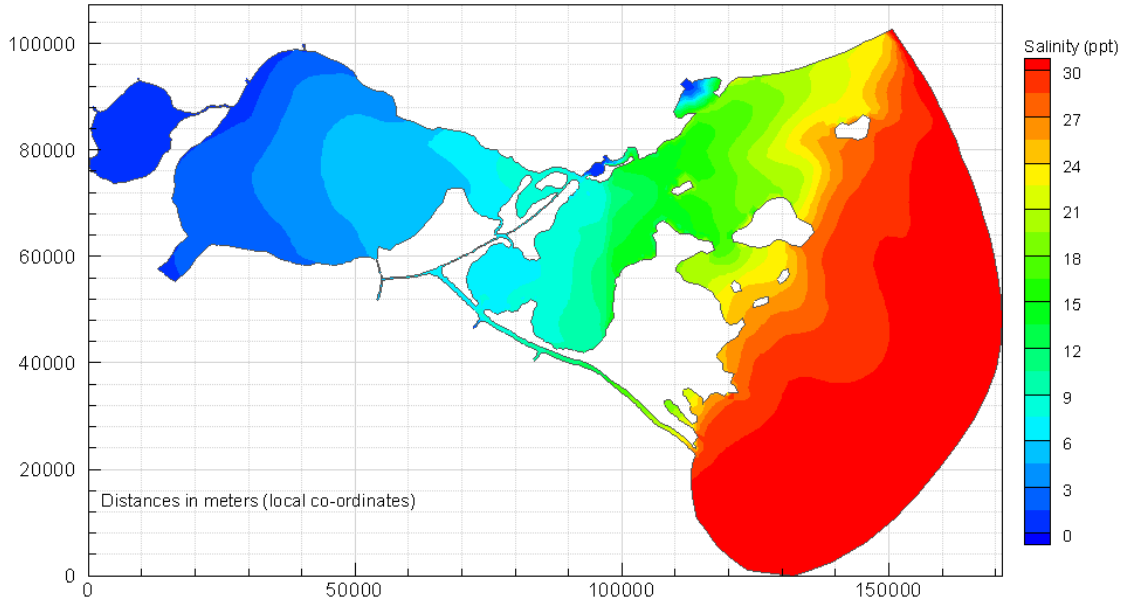

Figure 1.2 Salinity concentrations around the Pontchartrain Estuary based on average conditions for the last 10 years (McCorquodale et al., 2007).

Table 1.1 Important Lake Pontchartrain Estuary physical parameters.

Lake Pontchartrain average depth	3.7 m
Lake Pontchartrain north-south axis	40.2 km
Lake Pontchartrain east-west axis	64.4 km
Lake Pontchartrain surface area	1632 km^2
Lake Pontchartrain tides	diurnal; mean range of 0.11 m
Lake Pontchartrain tidal prism	$1.6x10^8$ m^3
Lake Pontchartrain water column	generally well mixed
Lake Pontchartrain stratification	stronger at certain times near the IHNC
The Rigolets Pass total length average depth cross-sectional area	 14.5 km 8 m 7500 m^2
Chef Menteur Pass total length average depth cross-sectional area	 11.3 km 13 m 2422 m^2
IHNC-MRGO total length average depth cross-sectional area	 30 km 7.5 m 1125 m^2
Pass Manchac total length average depth cross-sectional area	 15 km 8 m 2924 m^2
Lake Maurepas surface area	233 km^2
Lake Maurepas average depth	3.0 m
Lake Borgne surface area	550 km^2
Lake Borgne average depth	2.7 m

- Adapted from Haralampides (2000)

1.2 The Mississippi River Delta Plain

The Mississippi River flows from Lake Itasca in Minnesota to the Gulf of Mexico over a distance of 3,800 km. Approximately 3.25 million square kilometres, comprising 31 states or 41% of the United States, drain into the River (Barry, 1997). Historically, the Mississippi River was unrestricted and was able to freely switch its course and flood its banks each year. The historic switching of the Mississippi River created a series of six deltaic complexes over the past 7,000 years that together form the Mississippi River Delta Plain (Roberts, 1997). The complexes from oldest to youngest are called: Maringouin/Sale Cypremort; Teche; St. Bernard; Lafourche; Balize; and Atchafalaya/Wax Lake. The Balize delta (also known as the Birds-foot delta), located at the mouth of Mississippi River, and the Atchafalaya delta, located at the mouth of the

Atchafalaya River, are the only complexes that are still active today. The Mississippi Delta Plain covers an area of approximately 30,000 km^2 and accounts for 41% of the wetlands in the United States (Coleman et al., 1998).

In the 1970's, the Mississippi River nearly switched its course to the Atchafalaya River course (a more direct route to the Gulf of Mexico). However, because river migration is inconvenient to settlement and navigation, a control structure was built just north of Red River Landing, LA to prevent this switch from occurring. The Old River Control Structure (Auxiliary Structure) diverts 30% of the Mississippi River flow through the structure into the Atchafalaya River. Levees have been built along most of the Mississippi Rivers banks to fix the Rivers course and prevent flooding of settled areas. As a result of these levees, the Mississippi River stage now increases within the riverbanks during flood periods instead of overtopping the banks and distributing freshwater, rich with sediment and nutrients, over the floodplain.

Nutrients and sediments enter the Mississippi River from both point and non-point sources. Point sources enter the river from defined areas (wastewater treatment plant or storm sewer outfalls) whereas non-point sources contribute loads from undefined large areas (runoff, erosion, etc). The nutrients and sediments that enter the river are currently either released into the Gulf of Mexico at the Mississippi or Atchafalaya River mouths or are directed into specific areas via diversions (Caernarvon diversion, Bonnet Carré Spillway, etc). Over the past half-century, agricultural activities in the Upper Mississippi Basin have greatly increased the nutrient concentrations in the Lower Mississippi River (McCorquodale course notes, 2007). The high concentrations of nutrients flowing into the Gulf of Mexico have contributed to the formation of large hypoxic (oxygen depleted) areas in the Gulf of Mexico in the spring and summer (Rabalais et al., 2002). Sediment loads in the Mississippi River have decreased by nearly 70% since 1850 as a result of damming, land use changes, and a decline in discharge (Kesel, 1988).

The lack of connection between the River and its floodplain due to the constrictions along its length (levees, control structures, etc.) has contributed to the deterioration of the Mississippi Delta Plain (Kesel, 1989). Without the annual influx of nutrients and sediments from the river (combined with other anthropogenic and natural factors such as canal dredging and hurricanes), wetland areas are not able to support as rich or diverse communities and are not able to keep pace with sea level rise or subsidence (Kesel, 1989; Day and Templet, 1990; Day et al., 2000). Between 1956 and 2004, the deltaic plain of the Mississippi River lost over 2,975 km^2 of land due to a complex suite of causes (Barras, 2006). Hurricanes Katrina and Rita, which hit the Louisiana coast in 2005, converted an additional 562 km^2 of marsh to open water (Barras, 2006).

1.3 Freshwater diversions

1.3.1 General

In the wake of the extensive damage caused by Hurricanes Katrina and Rita, hurricane protection and coastal restoration have become two of Louisiana's top priorities for recovery. The State Master Plan has proposed fourteen diversions along the length of the Mississippi River (CPRA, 2007). These freshwater diversions hope to re-establish the dynamic interaction between the River and its floodplain by delivering needed freshwater, sediment and nutrients to help restore and build wetland areas (DeLaune et al, 2006; Demcheck, 1996).

Freshwater diversions can be beneficial in a number of ways. They reduce pressure on levees downstream, decrease salinities in wetland areas, enhance marsh productivity and

diversity though nutrient delivery, help wetland areas keep pace with sea level rise and can be beneficial to recreational and commercial fisheries in the long-term (DeLaune, 2003; Lane, 2001; Lake Pontchartrain Basin Foundation (LPBF), 2005). However, freshwater diversions can have negative impacts associated with them as well. Besides the fact that they can be cost prohibitive and are typically long-term projects, they can also cause adverse environmental impacts such as cyanobacterial algal blooms, short-term displacement of species (brown shrimp, speckled trout, redfish and blue crab), mortality of oysters as well as hypoxia and fish kills (Brammer, 2007; Turner and Boyer, 1997; LPBF, 2005).

One major freshwater diversion, the Bonnet Carré Spillway, currently exists between the Mississippi River and the southwest corner of Lake Pontchartrain. The State Master Plan has proposed two new small freshwater diversions that will connect the Mississippi River to Maurepas Swamp.

1.3.2 Bonnet Carré Spillway

As a result of the constrictions (levees, control structures, etc.) along the length of the Mississippi River, the River is no longer hydraulically connected to the Delta Plain where the Pontchartrain Estuary is located. The only connection between the River and the Estuary currently exists at the Bonnet Carré Spillway. The Bonnet Carré Spillway is located along a natural crevasse between the Mississippi River and Lake Pontchartrain, approximately 52 km upriver from New Orleans (Figure 1.3). The two main features of the Bonnet Carré Spillway are the 2.1 km weir located on the east bank of the Mississippi River and the 9.2 km long natural spillway. The Bonnet Carré Spillway was constructed in 1931 after the great flood of 1927 with the intent of alleviating excess pressure on the levees at New Orleans during high river stages. Water is diverted from the Mississippi River to Lake Pontchartrain by mechanically opening bays along the weir. Table 1.2 lists some physical characteristics of the Spillway.

The Bonnet Carré Spillway has many habitat areas including bottomland hardwood forests, cypress swamps, canals and ponds. Due to the habitat diversity, the spillway is home to a wide variety of species and has become a heavily visited outdoor recreation area with approximately 250,000 visitors each year. It has also become a source of sediment for the many restoration projects in the area.

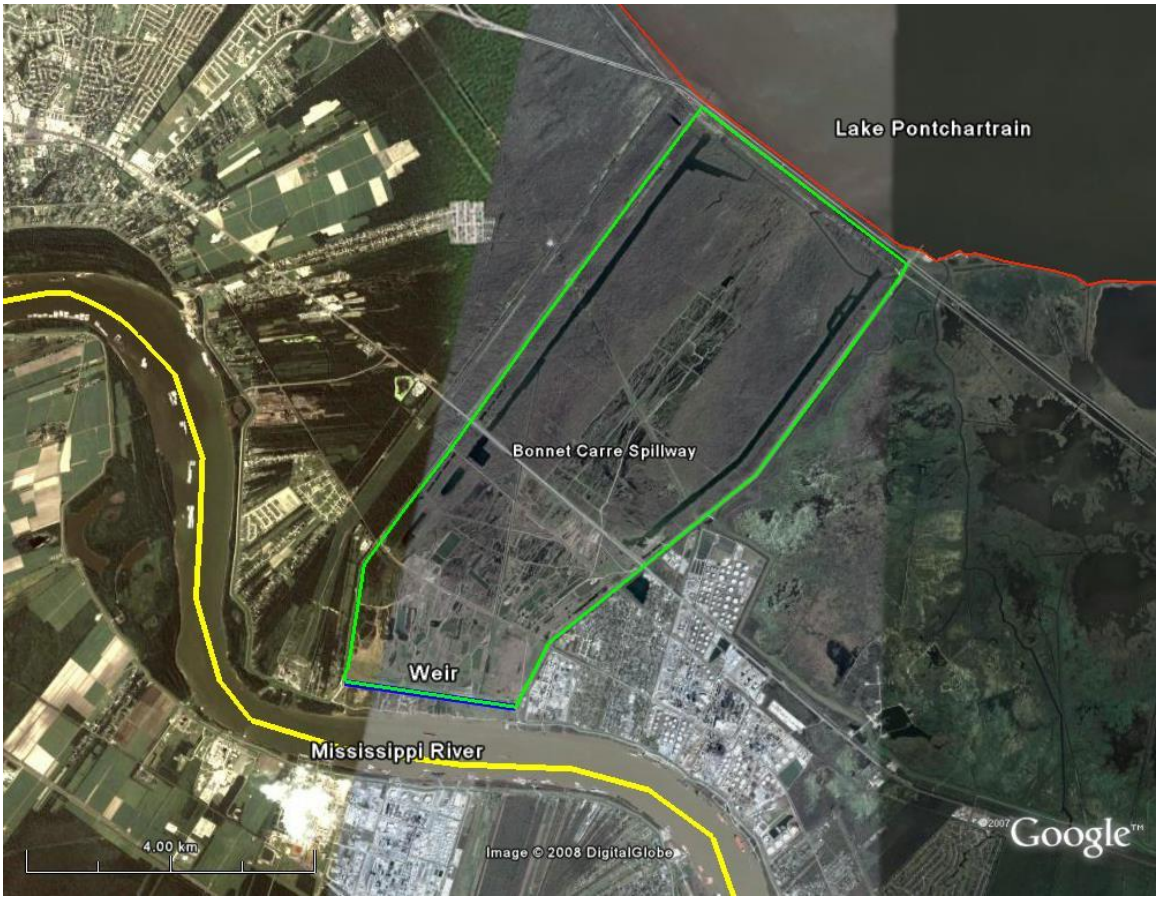

Figure 1.3 Overview of the Bonnet Carré Spillway.

Table 1.2 Physical characteristics of the Bonnet Carré Spillway (Gibbs, 2005).

Design capacity	7000 m^3/s
Weir length	2135 m
Number of bays/Width of bays	350/6.1 m
Elevation of 174 bays	4.57 m (NAVD 88) Brantley, 2008, personal communication
Elevation of 176 bays	5.18 m (NAVD 88) Brantley, 2008, personal communication
Number of creosote timbers per bay	20
Spillway length	9.2 km
Spillway area	30.8 km^2
Width of spillway at River	2,350 m
Width of spillway at Lake	3,780 m

1.3.3 Proposed diversions

The State Master Plan has proposed three freshwater diversions projects in the Pontchartrain Estuary basin area. Two new small diversions (flows between 30 m^3/s to 140 m^3/s) are anticipated at Hope Canal and Convent/Blind River near Gramercy, LA. These two diversions are expected to increase organic deposition and improve biological productivity in Maurepas Swamp via the influx of the nutrient and sediment rich Mississippi River water. The

third proposed freshwater diversion project involves breaching the spoil banks along the Amite River Diversion Canal in eight locations. The openings will be 12m wide and designed to each divert an average of approximately 7 m^3/s during flood events on the Amite River. This introduction of freshwater is also expected to improve biological productivity and increase deposition in Maurepas Swamp.

Maurepas Swamp drains into Lake Maurepas which is hydraulically connected to Lake Pontchartrain via Pass Manchac. As a result of this connection, the proposed freshwater diversions, however small, have the potential to impact water quality in the Pontchartrain Estuary. The effect of the timing and delivery of freshwater from these diversions needs to be investigated to determine the effect on water quality in the Pontchartrain Estuary.

1.4 Problem statement

In the wake of the extensive damage caused by Hurricanes Katrina and Rita, hurricane protection and coastal restoration have become two of Louisiana's top priorities for recovery. For the first time, local, state and federal agencies are working together using a coast-wide recovery approach that incorporates natural restoration measures with artificial protection measures. One common example of this pairing of natural and artificial solutions is the construction of freshwater diversions, which reconnect rivers to their floodplains. The State Master Plan has proposed two such diversions that flow from the Mississippi River into Maurepas Swamp, located at the southwest corner of Lake Maurepas. These diversions are anticipated to increase organic deposition and improve biological productivity in Maurepas Swamp via the influx of the nutrient and sediment rich Mississippi River water. It is important to understand how the proposed freshwater diversions will affect the water quality in the Pontchartrain Estuary (which includes Lake Maurepas, Lake Pontchartrain and Lake Borgne). It is particularly important to determine if unintended consequences associated with excess sediment or nutrient delivery (for example algal blooms) will occur.

The effects of similar freshwater diversions have been looked at previously in the Pontchartrain Estuary (Haralampides, 2000; Georgiou, 2002; McCorquodale et al., 2004; Dortch et al., 2007). Each of these efforts has involved complex hydrodynamic and water quality models that can only simulate relatively short time-periods (on the order of one year) due to the extensive computing requirements that are required. There is a need to develop a simplistic model that can be run quickly over long time periods to determine the general effects freshwater diversions may have on the water quality in the Pontchartrain Estuary. The simplistic model can then be used as a screening tool to focus more complex hydrodynamic and water quality modeling studies.

A 1-D tidal, salinity and water quality model that analyzes the general effects freshwater diversions have on the water quality of the Pontchartrain Estuary over a 17-year period is presented here. This model is computationally efficient and can easily assess the effects of different timing, duration and quantity of flow scenarios over long time periods. The 17-year period from 1990 to 2006 was selected since adequate data records are present in the Estuary for calibration and validation of the model and shell dredging in the Pontchartrain Estuary was banned beginning in 1990.

1.5 Objectives

There are several objectives that have been outlined for this project. The ultimate goals are:

- To develop, calibrate and apply a 1-D tidal, salinity and water quality model for the Upper Pontchartrain Estuary; and
- To investigate the long-term effects of different management scenarios on the water quality of the Upper Pontchartrain Estuary.

These management scenarios include:

- Effect of the proposed freshwater diversions into Maurepas Swamp on water quality in the Pontchartrain Estuary,
- Effect of increased leakage events from the Bonnet Carré Spillway on water quality in the Pontchartrain Estuary, and
- Effect of timing of complete Bonnet Carré Spillway openings on Pontchartrain Estuary water quality.

1.6 Methodology

The general procedure to accomplish the objectives outlined in Section 1.2 is:

- Review existing literature to develop an understanding of water quality issues (both physical and ecological/biological) that are pertinent in the Pontchartrain Estuary,
- Collect long-term physical (hydrological, meteorological, etc.) and water quality data records from stations located within the Pontchartrain Estuary drainage basin,
- Develop average annual and daily records from the long-term datasets for input into the model,
- Create the 1-D tidal, salinity and water quality model
- Calibrate the model to the data collected from the Pontchartrain Estuary between 1990 and 1994,
- Validate the model to the data collected from the Pontchartrain Estuary between 1995-2006,
- Impose the new management scenarios on the calibrated and validated model from 1990 to 2006.

2.0 Literature review

2.1 Water quality

2.1.1 Classification of the Pontchartrain Estuary

Bodies of water can be classified based on their rate of primary productivity. Three classifications generally result from this type of analysis: oligotrophic, mesotrophic or eutrophic. Oligotrophic, mesotrophic and eutrophic waters generally have low, medium and high rates of primary productivity associated with them (Dodson, 2005). Oligotrophic lakes are generally fresh water systems, located high in the watershed (away from agricultural activities) that have low inorganic nutrient inputs; high water quality; clear waters, and high oxygen concentrations (above 2 mg/L). Eutrophic systems usually occur lower in the watershed and have high inorganic nutrient inputs (especially nitrate or phosphate), low water quality, a murky green or brown appearance, and some areas with hypoxic (low oxygen) or anoxic (no oxygen) conditions (Dodson, 2005).

The Pontchartrain Estuary can be classified as an oligotrophic to mesotrophic system (LPBF, 2005). The Pontchartrain Estuary occurs low in the watershed but receives relatively low inputs of nutrients, silts and clays from runoff. The inputs can stimulate phytoplankton production, but do not significantly lower the water clarity of the Estuary (LPBF, 2005). The presence of grassbeds and Rangia clams helps keep the water clear in the Estuary (LPBF, 2005). Water quality is generally good in the Estuary, but can become low close to outfalls or tributary mouths where inorganic nutrient inputs are higher. Water quality also decreases around the Estuary in response to the high nutrient loadings from the Mississippi River water that enters Lake Pontchartrain during the periodic Bonnet Carré Spillway openings. The salinity regime in the Pontchartrain Estuary is relatively low due to the narrow tidal passes and small tidal fluctuations. The oxygen concentrations are generally sufficient, however, large anoxic areas extending out from the IHNC, occupying a sixth of the bottom of Lake Pontchartrain, have been documented in the Estuary (Schurtz and St. Pe', 1984). Georgiou (2000, 2002, and 2003) documented and modeled the introduction of high salinity water entering Lake Pontchartrain from the IHNC. His model showed how the dense, high salinity water entering Lake Pontchartrain from the IHNC stratifies and produces anoxic areas.

2.1.2 Primary productivity growth limitations

Howarth (1988) concluded that estuarine and coastal marine ecosystems are mostly limited by nitrogen, however, he also noted that phosphorous limited and ecosystems limited by both nitrogen and phosphorous may occur. The Pontchartrain Estuary, which has a high capacity to assimilate (convert inorganic or organic nitrogen to organic compounds) dissolved nitrogen, is considered to be nitrogen limited (McCorquodale, 2007). Nitrogen limited means that other nutrient concentrations are generally sufficient and primary productivity in the Estuary relies on the delivery of nitrogen.

Alfred C. Redfield found that ecological interactions in marine water cause relatively constant ratios of carbon (C), nitrogen (N), and phosphorous (P) to occur. When these nutrients are readily available, primary productivity will occur at optimal rates, however if one nutrient is low, the other two nutrients will be used less and slower rates of primary productivity will occur. The optimal ratio, termed the "Redfield ratio", was found to be 106:16:1 (C:N:P) for each

nutrient atom (Dodson, 2005). For the normal nutrient loading case, Lake Pontchartrain has a N:P ratio in the range of 1 to 8, which tends to make it nitrogen limited (Thomann and Mueller, 1987).

Nutrient ratios are not the only factors that affect the growth of primary producers. Ismail (1999), Haralampides (2000), and Dortch (1999, 2001) found that primary productivity is also limited by water temperature, light, turbidity level; and salinity concentrations.

2.1.3 Factors affecting water quality on the Pontchartrain Estuary

When nitrogen is added to the Estuary, primary productivity (growth of phytoplankton, benthic macrophytes and macroalgae) increases and can be beneficial to the ecosystem (Rabalais, 2002). However, if nitrogen is added in excess, degradation to the ecosystem may occur. As primary productivity increases, turbidity increases and light penetration throughout the water column decreases. The decrease in light penetration affects the growth of submerged aquatic vegetation (SAV) and degrades essential habitat areas (Rabalais, 2002). Excess nutrients can also cause water quality degradation when their loads exceed the capacity for assimilation. The water quality degradation can cause detrimental effects on the ecosystem and ecosystem functioning such as harmful algal blooms, fish kills, habitat loss and anoxic zones (Rabalais, 2002).

As mentioned previously, water quality is generally good in the Estuary, but can become low close to outfalls or tributary mouths where inorganic nutrient inputs are higher. Water quality also decreases around the Estuary in response to the high nutrient loadings from the Mississippi River water that enters Lake Pontchartrain during the periodic Bonnet Carré Spillway openings. Water quality in the Estuary also has the potential to decrease in response to the proposed freshwater diversions that will allow Mississippi River water to flow into Maurepas Swamp.

2.1.4 Water quality management around the Pontchartrain Estuary

To improve the water quality in the Estuary it is essential to control the nutrient loads that flow into the Estuary. Nutrients loads can be reduced at both point and non-point sources. Nutrient reduction programs are being implemented around the Pontchartrain Estuary. The Lake Pontchartrain Basin Foundation (LPBF) is currently working on a project to reduce fecal coliform loadings in the Tangipahoa River watershed. The LPBF is providing assistance, technical training, and innovative technology to WWTP operators and is helping dairy farmers dig storage lagoons to reduce the fecal coliform concentrations in the river. These efforts will also help to reduce nutrients in the Tangipahoa River and Lake Pontchartrain. The LPBF, using similar practices throughout the Bogue Falaya/Tchefuncte Watershed, achieved in-stream improvements of 20% to 80% on eight tributaries in three years (LPBF, 2005).

Khairy (2000) used the Soil and Water Assessment Tool (SWAT) model to address the effect of land-use management practices and their associated nutrient loadings on water quality in receiving waters. His study of the Tangipahoa River watershed found that by managing the amount of chemicals (fertilizers and pesticides), animal wastes and urban inputs, the degree of water quality degradation in surface and subsurface systems in the watershed is lessened. However, he found that the reductions in surface runoff and erosion due to improved land-use management strategies do not necessarily reduce sediment and nutrient yields proportionally.

Nutrient loads entering the Estuary from the Mississippi River should also be lessened. Mississippi River nutrient loads can be reduced by either decreasing the flow through the diversions or by diverting the water through more densely vegetated areas that can uptake the nutrients. Changing the timing of the diversions from the Mississippi River so that they occur during cooler conditions could also improve water quality

2.2 Historic conditions

2.2.1 Flood events on the Lower Mississippi River

The Lower Mississippi River is greatly influenced by the events that occur in the Upper Mississippi River Valley. Heavy precipitation and large snowmelt can cause stages in the Lower Mississippi River to increase dramatically. Table 2.1 documents the top seven flood events that occurred between 1927 and 1997 in terms of stage, volume and number of days. Overall, 1927 was the worst flood year during this period. The last eight major floods occurred in 1973, 1974, 1975, 1979, 1983, 1984, 1993 and 1997 (Trotter et al., 1998). Heavy rains in the Upper Mississippi Valley this spring (2008) have caused flood conditions to be declared on the Lower Mississippi River. The stage at the USACE Mississippi River gage at Red River, LA was measured to be 18.46 m on April 22, 2008. This is only 2.4 cm lower than the peak stage of 18.7 m recorded during the 1997 flood at the Red River gage on March 25-26, 1997. Assuming the peak stage has already been reached, the 2008 flood is the 3rd largest flood that has occurred in the last 71 years (in terms of stage) on the Lower Mississippi River.

Table 2.1 Record stage, volume and flood days from 1927-1997 on the Mississippi River at Red River Landing, LA.[1]

Record Stage in meters (Year)	Record Volume in m^3/s (Year)	Record Number of Flood Days (Year)
18.7 (1997)	51,000 (1927)	135 (1927)
18.6 (1927)	43,000 (1945)	115 (1983)
18.4 (1983)	42,500 (1973)	99 (1973,1979)
18.3 (1945)	42,000 (1997)	90 (1974)
18.0 (1979)	41,000 (1983)	79 (1975)
17.7 (1973)	40,000 (1979)	76 (1945)
17.2 (1975)	34,500 (1975)	69 (1997)

[1]Adapted from Trotter et al. (1998).

2.2.2 Bonnet Carré Spillway openings

The Bonnet Carré Spillway was constructed after the great flood of 1927 to alleviate pressure on the levees located further downstream, particularly in the New Orleans area. During flood conditions on the River, the weir located along the entrance to the Spillway can be opened, rerouting water through the Spillway to Lake Pontchartrain and the Gulf of Mexico, decreasing river stages and flows downstream. Many factors (environmental, hydrological, structural, navigational and legal) are taken into account when deciding whether or not to open the Spillway during flood conditions (Gibbs, 2005). When the factors indicate (current and predicted

conditions) that unacceptable stresses will be placed on downstream levees, then the Spillway is opened (Gibbs, 2005). Since the Spillway's construction, the weir has been opened nine times: eight during high flow events, and once for experimental purposes. Table 2.2 summarizes the opening events below. The Bonnet Carré Spillway was also opened on April 11th, 2008 in response to the high water levels on the Mississippi River. The details regarding this event are not listed in Table 2.2 since the event is still in progress.

Table 2.2 Bonnet Carré Spillway openings (Gibbs, 2005).

Opening date	Closing Date	Bays open	Maximum flow (m^3/s)
Jan. 30, 1937	Mar. 7, 1937	285	6,000
Mar. 23, 1945	May 18, 1945	350	9,000
Feb. 10, 1950	Mar. 19, 1950	350	6,300
Apr. 8, 1973	Jun. 21, 1973	350	5,500
Apr. 14, 1975	Apr. 26, 1975	225	3,100
Apr. 18, 1979	May 21, 1979	350	5,400
May 20, 1983	Jun. 23, 1983	350	7,600
Apr. 20, 1994	May 27, 1994	4+	400
Mar. 17, 1997	Apr. 18, 1997	298	6,900

In addition to the opening events listed above, Mississippi River water occasionally leaks through the timber gates of the weir during high River stages. These leakage events usually occur during the late winter or spring when water levels are high (above the base of weir) and do not normally exceed 300 m^3/s (Gibbs, 2005).

Mississippi River water contains high concentrations of nutrients and sediments (see section 3.3.2 for monthly distribution of concentrations). McCorquodale et al. (2007) estimated the concentration of nitrates and dissolved inorganic nitrogen (DIN) in the Mississippi River (c 2000) to be on the order of 1.0 mg/L and 2.0 mg/L, respectively. These concentrations are higher than the background concentrations typically found in Lake Pontchartrain for DIN of 0.01-0.05 mg/L. When Mississippi River water enters Lake Pontchartrain, the background concentrations of nutrients and sediments will increase. The increase in nutrients could have adverse environmental impacts on the water quality in the Pontchartrain Estuary. The next few sections will look at some of the impacts that have been observed during the last few Bonnet Carré Spillway opening events.

2.2.3 1979 opening of the Bonnet Carré Spillway

Demcheck et al (1996) made a comparison between water quality parameters recorded between 1974 and 1984 and those recorded during the 1979 Bonnet Carré Spillway opening. The opening caused an increase in the background nitrite plus nitrate as nitrogen concentrations around the entire Lake. Concentrations increased: from: 0.02 mg/L to 1.1 mg/L three and a half kilometres northwest of the Chef Menteur tidal pass: from less than 0.10 mg/L to 0.22 mg/L at Bayou Lacombe (northeast Lake Pontchartrain), and from 0.16 mg/L to 0.23 mg/L at the mouth of Pass Manchac. Demcheck et al. (1996) also found substantial decreases in inorganic

constituents, indicating a shift towards a freshwater system around Lake Pontchartrain during the release.

2.2.4 1994 opening of the Bonnet Carré Spillway

The USACE looked at operating the Bonnet Carré Spillway more frequently for purposes other than flood control in the 1980's. They specifically looked at reducing salinities in Lake Pontchartrain to directly increase oyster catches. However, since the effects of the diverted freshwater on other areas of the Lake Pontchartrain ecosystem were poorly understood, an experimental opening was scheduled to assess any unintended consequences that might occur.

River stages were high during the spring of 1994 and an experimental opening was scheduled. Leakage occurred from April 20th to May 15th before four bays were opened on May 16th. The bays were open for 12 days and the average flow into the spillway was 400 m^3/s (Demcheck et al., 1996). Many groups took samples during the opening and their findings are summarized below.

Demcheck et al. (1996) found that a freshwater plume extended approximately 6.4 to 9.7 km into Lake Pontchartrain during the opening. Initially, the river water was 4 °C colder than the lake water and moved in a layer beneath the lake water until it warmed and began to mix. The water moving through the spillway was observed to travel mostly via channels.

Lane et al. (2001) looked at the decay of nutrients and sediment during the 1994 opening of the Bonnet Carré Spillway by comparing water quality measurements from the Mississippi River at St. Francisville to measurements taken in the spillway. They found that total suspended sediment concentrations decreased by 82-83%, nitrite + nitrate concentrations decreased by 28-42%, total nitrogen concentrations decreased by 26-30% and total phosphorous concentrations decreased by 50-59% throughout the length of the spillway. They speculated that the nutrient reductions could be due to the forested wetlands that are present in the spillway and also conjectured that the reduction in phosphorous may be due to the phosphate anion (PO_4^{3-}) sorption onto charged clay particles.

Lane et al. (1999) also looked at nutrient removal efficiencies at the Caernarvon freshwater diversion, located approximately 20 km downstream from New Orleans. The Caernarvon diversion has a flow capacity of 226 m^3/s and was found to have nitrite + nitrate, total nitrogen and total phosphorous removal efficiencies of 88-97%, 32-57% and 0-46% respectively between the diversion and the first monitoring station 18 km into the wetland. These reductions are slightly higher than their findings at the Bonnet Carré Spillway. The Bonnet Carré reductions are likely lower due to the shorter Bonnet Spillway length (9 km vs. 18 km) and the presence of channels and sparser wetland vegetation located in the spillway.

Turner (1999) suggests that total nitrogen can be reduced by up to 20% in the Bonnet Carré Spillway during low flows. However, during higher flows Turner postulated that nitrogen uptake would be negligible since natural systems have low retention rates, large spatial areas, a general absence of below ground flow, and short temporal overland flows. The low uptake rates might also be associated with the relatively low nutrient concentrations of river water (as opposed to those of sewage treatment discharge). The nutrient reductions observed by Lane et al. (1999, 2001) are therefore only valid for low flows through the Bonnet Carré Spillway (low flows are assumed to be less than 500 m^3/s).

2.2.5 1997 opening of the Bonnet Carré Spillway

Above normal spring rains and snowmelt in 1997 resulted in the fourth largest flood since 1927. A volume of 42,000 m^3/s and a record stage of 18.7 m were measured at Red River Landing in LA. To prevent flooding and potential levee failures downstream, the Bonnet Carré Spillway was opened for a one-month period between March 17th and April 18th with an average flow of 6,900 m^3/s. Although the diversion of River water into Lake Pontchartrain prevented a flood downstream, major environmental consequences were observed throughout the basin.

The 1997 opening of the Bonnet Carré spillway and it's input of high nutrient loads from the River caused a major algal bloom around the Pontchartrain Estuary. Two blooms of toxin producing algae (*Anabena circinalis. and Microcystis aeruginosa*) were observed on Lake Pontchartrain from June through July (Dortch et al., 1999, Poirrier et al., 1998). Dortch et al. (1998) noted that both of these genera are stimulated by excess nutrients and are capable of positive buoyancy, allowing them to avoid light limitation in turbid waters.

The Louisiana Department of Health and Hospitals (LDHH) issued an advisory limiting recreational use of the Pontchartrain Estuary in the summer of 1997 as a result of these harmful algal blooms (HAB). The algal bloom persisted for four months, extended over a large spatial area and transformed the Pontchartrain Estuary into a foul smelling, discoloured body of water. The full extent of the algal bloom can be seen below in the satellite image provided by the USGS (Figure 2.1). The blue green algae *Anabaena spiroides* was also present on the lake in late May (Poirrier et al., 1998).

The algal blooms caused by the 1997 Bonnet Carré Spillway opening had a deleterious effect on the benthos in Lake Pontchartrain as indicated by decreases in species diversity, abundance, and number of taxa (Brammer, 2007). The blooms also caused oyster bed harvests to close for a number of months and detrimentally effected fisheries (production, harvests, etc.) around the lake. Poirrier et al. (1998) observed fish kills at the mouth of Bayou St. John (south shore of Lake Pontchartrain) on June 15, near the mouth of Bayou Lacombe on June 22, and eastward of Goose Point (northeast Lake Pontchartrain) on July 29. However, the USACE (1998) found that within one year after the opening, the fisheries in the Lake had recovered and by some reports exceeded the pre-opening productivity.

Lane et al. (1999) found that the algal bloom eventually ended as a result of nitrogen limitations in the Lake. Lake Pontchartrain acts as a sink for nitrate. Nitrate is reduced predominantly by denitrification but reductions due to assimilation are also important. Dortch et al. (1998) also came to this conclusion based on the samples they took in Lake Pontchartrain.

Day et al. (1999) found that Mississippi River water moved along the south shore and flowed out predominantly through the Chef Menteur tidal pass. They also looked at the reduction of nutrient concentrations from the River to the Lake during the 1997 opening. They found that within two weeks, two stations located in the southwest area of Lake Pontchartrain had become completely fresh and had similar nutrient concentrations to those in the river. These conditions persisted for one month after the closure and then quickly reduced to pre-opening levels. Day et al. (1999) are in agreement with the conclusion made by Lane et al. (1999) regarding the quick return to pre-opening nitrogen concentrations. Their observation that nutrient concentrations in the Lake were equivalent to those in the river agrees with Turner (1999).

McCorquodale et al. (1998) observed that the initial plume of Mississippi River water remained near the south shore of the lake. After it stayed near the south shore for approximately ten days, the plume moved northward as it was pushed by southeasterly winds. After about three

weeks, they observed that the spillway plume occupied 80-90% of the lake area and after one month, the plume occupied the entire lake and reduced a significant portion of Lake Borgne salinities. Salinities on the south shore of Lake Pontchartrain were observed to return to pre-opening levels by August 29, 1997 while the north shore salinity values did not return to normal until late October. McCorquodale et al. (1998) calculated a 12 day mean residence time for chemicals entering Lake Pontchartrain from the 1997 Bonnet Carré Spillway opening.

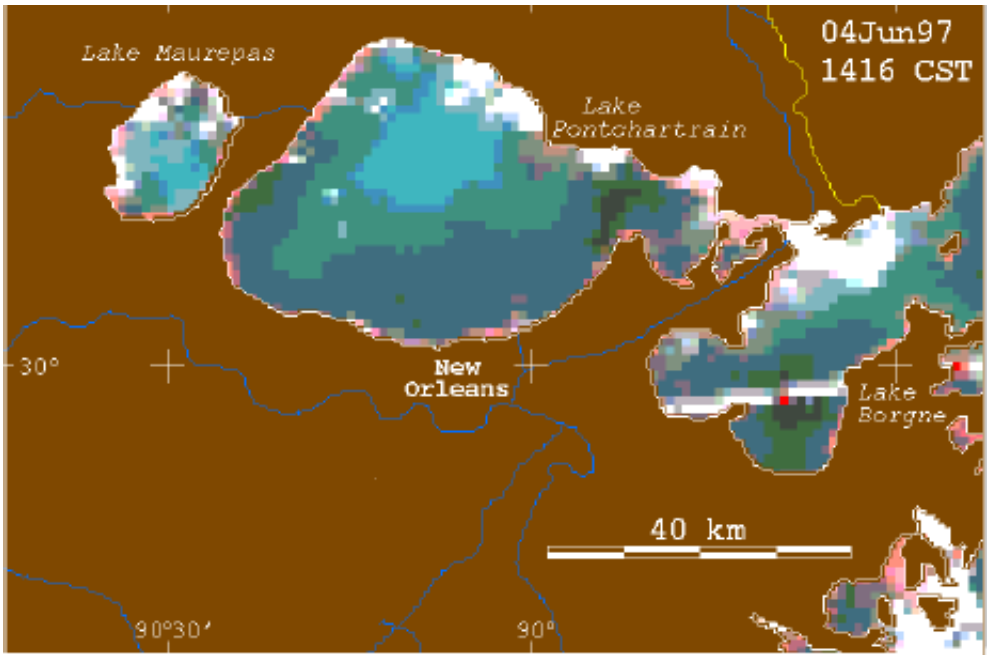

Figure 2.1 Satellite image of June 4, 1997 algal bloom (Courtesy of USGS http://coastal.er.usgs.gov/pontchartrain/imagery/figures/jun0497pontab.html).

2.2.6 2008 opening of the Bonnet Carré Spillway

Flood conditions were declared on the Lower Mississippi River in the spring of 2008 (when this report was published). The USACE gage located on the Mississippi River at the Bonnet Carré Spillway measured stages above the elevation of base of the weir beginning at the end of March. Stages were measured above 4.57 m (elevation of 174 bays) from March 17, 2008 and 5.18 m (elevation of 176 bays) from March 30, 2008 (both elevation are measured with respect to NAVD88, Brantley, 2008, personal communication). Leakage occurred through the timber pins as a result of these high stages. Figure 2.2 shows a photo of the leakage occurring through the weir on April 11, 2008 when the river stage at the Red River, LA gage was measured to be 17.75m.

Figure 2.2 Photo showing leakage through the weir at the Bonnet Carré Spillway on April 11th, 2008.

The Mississippi River Commission President Brigadier General Michael J. Walsh, commander of the USACE Mississippi Valley Division in Vicksburg Mississippi called for the Bonnet Carré Spillway to be opened on April 11, 2008. The decision was made to ensure that the Mississippi River flow volume did not exceed 35,400 m^3/s at New Orleans. The spillway is estimated to be open for approximately a two to four week period. Without opening the Spillway the stage was expected to crest at 5.18 m at the New Orleans gage (USACE, 2008). Measurements are being taken around the Pontchartrain Estuary by the USGS, the LPBF and other groups to determine how the opening will affect water quality. Figure 2.3 shows the Mississippi River water flowing through an open gate on April 17th, 2008.

Figure 2.3 Photo showing flow through the open gates of the weir at the Bonnet Carré Spillway on April 15th, 2008.

2.2.7 Observed algal blooms in the Pontchartrain Estuary

A few other algal blooms have been observed around the Pontchartrain Estuary in addition to the algal bloom described above in 1997. In June of 1993, Poirrier et al. (1998) observed a small bloom of the blue green algae *Anabaena circinalis* near Mandeville. A more extensive surface bloom was also observed in late June 1994 as was a major bloom of *Anabaena circinalis* from mid June to the end of July in 1995. The 1995 bloom had surface accumulations covering most of the lake during the peak and fish kills associated with it.

3.0 Data collection and analysis

3.1 Available data

A number of different organizations regularly collect data around the Pontchartrain Estuary. The most extensive and accessible datasets are collected by: the U.S. Geological Survey (USGS); the Louisiana Department of Environmental Quality (LADEQ); the U.S. Army Corps of Engineers (USACE); the Louisiana Universities Marine Consortium (LUMCON) and the National Climatic Data Center (NCDC). Figure 3.1 shows all of the stations that were used in this study. All of the physical, meteorological and water quality datasets were combined, analyzed and used as input into the 1-D tidal, salinity and water quality model.

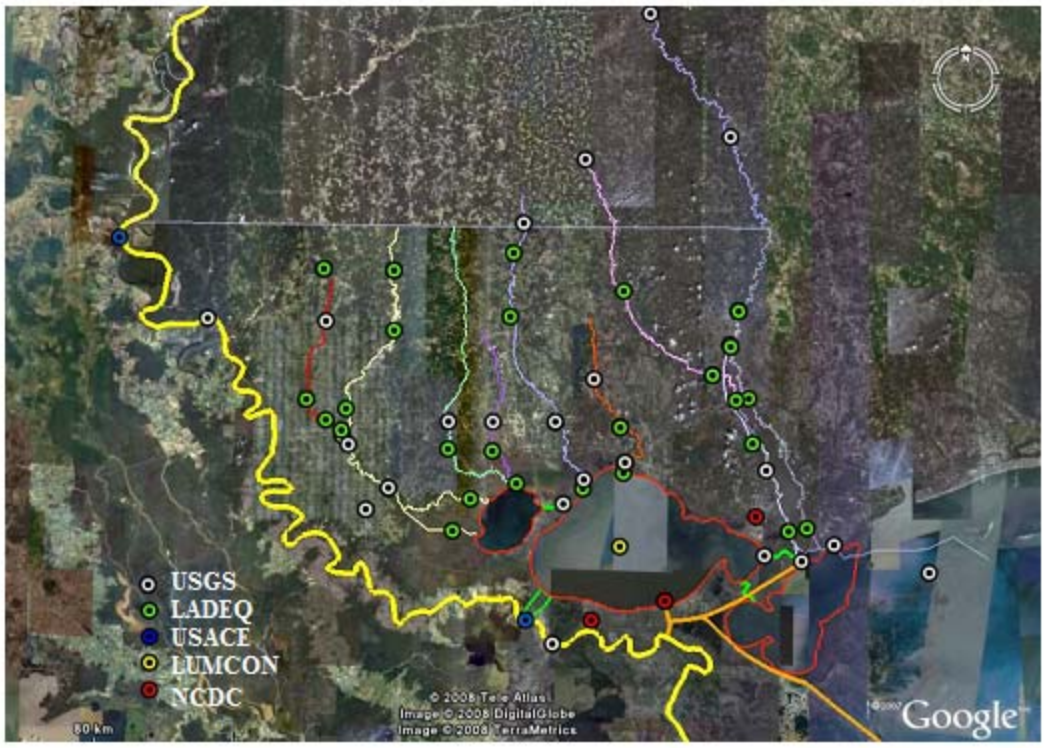

Figure 3.1 Stations used in the Pontchartrain Estuary analysis.

The USGS continuously measures and records numerous physical parameters on many of the rivers, streams and bayous that flow into the Pontchartrain Estuary. They also take periodic water quality measurements at these sites. Additionally, the USGS continuously monitors some water quality and physical parameters at a few sites in Lake Pontchartrain. All of the data measured by the USGS is available online. The LADEQ is primarily responsible for measuring water quality in the rivers, streams and bayous that flow into the Pontchartrain Estuary. The water quality datasets are taken regularly and makeup an extensive long-term dataset that is available on DVD by request only. The USACE has a few stations located around the Pontchartrain Estuary. The USACE gages used in this analysis were located on the Mississippi River and have long-term datasets that can be downloaded from the web. The NCDC measures

climatic data around the Pontchartrain Estuary. All NCDC sites are located over land and daily datasets can be downloaded from their website. LUMCON has one buoy station located in western Lake Pontchartrain. This buoy records both meteorological and hydrological parameters that can be downloaded from the web.

3.2 Tributary analyses

3.2.1 Tributary discharge analysis

The USGS measures discharge at most of the tributaries flowing into the Pontchartrain Estuary. Table 3.1 lists the 21 stations that were used to analyze the discharge characteristics in the Pontchartrain Estuary.

Table 3.1 USGS stations used in Tributary discharge analysis.

USGS Site Number	Site Name	Drainage Area (km^2)	Length of Discharge Record (years)
7377000	Amite River near Darlington, LA	1,502	48
7378500	Amite River near Denham Springs, LA*	3,315	68
7380120	Amite at Port Vincent, LA	4,134	8
7375280	Tangipahoa River at Osyka, MS	409	10
7375500	Tangipahoa River at Robert, LA*	1673	68
7375000	Tchefuncte River near Folsom, LA*	247	56
7375800	Tickfaw River at Liverpool, LA	232	18
7376000	Tickfaw River at Holden, LA	640	66
7376500	Natalbany River at Baptist, LA*	206	63
2490500	Bogue Chitto near Tylertown, MS	1,274	62
2492000	Bogue Chitto River near Bush, LA*	3,142	69
2486000	Pearl River at Jackson, MS	8,213	88
2488000	Pearl River at Rockport, MS	11,800	28
2488500	Pearl River near Monticello, MS	12,932	68
2489000	Pearl River near Columbia, MS	14,815	32
2489500	Pearl River near Bogalusa, LA*	17,024	68
2492600	Pearl River at Pearl River, LA	21,999	6
301141089320300	East Pearl River at CSX Railrd nr Claimborne, MS	22,466	2
7380224	Black Bayou near Duplessis, LA	9.5	5
7377500	Comite River nr Olive Branch, LA	376	64
7378000	Comite River near Comite, LA*	736	62

*Refers to gages that were used to input discharge data into the model.

To properly characterize discharge in our model, it was essential to analyze discharge in the Pontchartrain Estuary area over a long-term period. First, relationships between gages located along the same tributary were analyzed. Average annual daily discharge per unit area was compared between upstream and downstream gages on six rivers to look at how flow changed as it moved downstream (only six rivers had more than one gage located along their length). On the Amite River, a relationship between average annual daily discharge per unit area was created between the upstream gage at Darlington and the downstream gage at Denham Springs (See Figure 3.2). A nearly linear relationship was revealed. Similar results were found for the other five rivers and are shown in Table 3.2 below (the associated figures are shown in Appendix A). These linear relationships indicate that discharge is relatively independent of location in each tributary.

The same conclusion was made when assessing the discharge at each gage in the watershed. Figure 3.3 shows that the average annual daily discharge per unit area does not vary with location. Therefore, we can conclude that discharge is constant around the Pontchartrain Estuary basin. This seems reasonable since the topography and climate are fairly consistent throughout the watershed. From the relationship in Figure 3.3 (Q_{ave}= 0.018637(DA$^{)-0.018577}$), the average long-term daily flow into the Pontchartrain Estuary can be calculated as 0.0156 $m^3/s/km^2$ or 190.5 m^3/s (using a drainage area of 12,173 km^2).

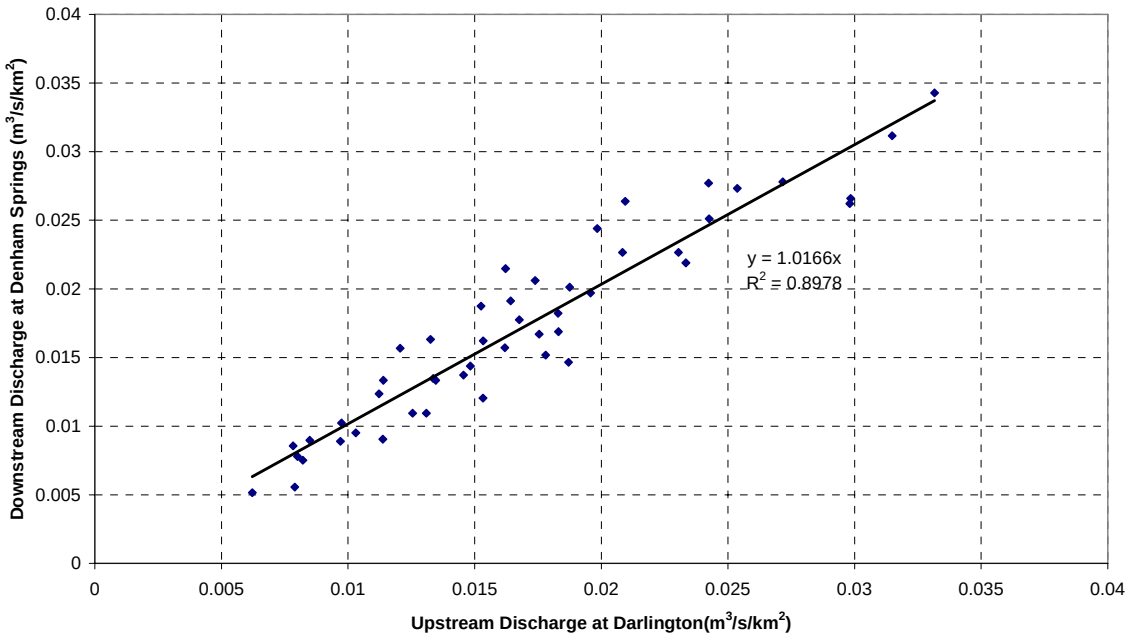

Figure 3.2 Relationship between downstream and upstream average annual daily discharge per unit area for the Amite River.

Table 3.2 Correlations between downstream and upstream daily tributary discharges.

River	Downstream Gage	Upstream Gage	Downstream discharge as a function of upstream discharge ($m^3/s/km^2$)	R^2 Error
Amite	Denham Springs	Darlington	$Q_{downstream} = 1.0166*Q_{upstream}$	0.8978
Tangipahoa	Robert	Osyka	$Q_{downstream} = 0.9165*Q_{upstream}$	0.7893
Bogue Chitto	Bush	Tylertown	$Q_{downstream} = 1.026*Q_{upstream}$	0.9212
Pearl	Bogalusa	Jackson	$Q_{downstream} = 1.1119*Q_{upstream}$	0.8577
Tickfaw	Holden	Liverpool	$Q_{downstream} = 1.0723*Q_{upstream}$	0.9450
Comite	Comite	Olive Branch	$Q_{downstream} = 1.0468*Q_{upstream}$	0.9383

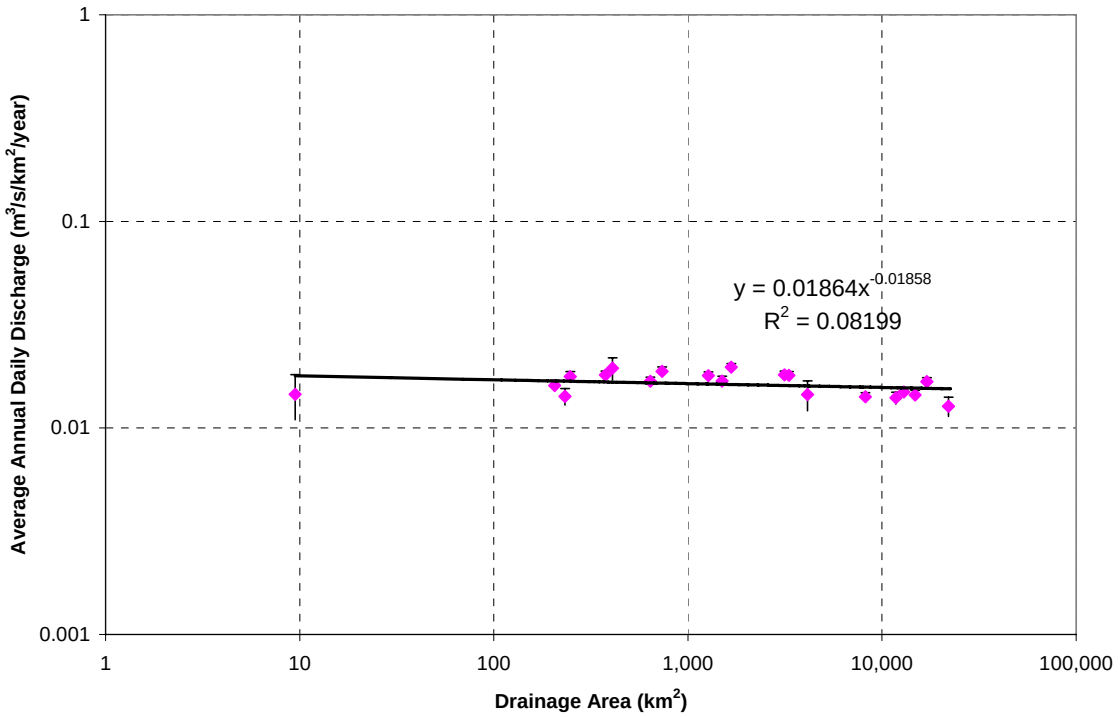

Figure 3.3 Relationship between average annual daily discharge per unit area and drainage area.

3.2.2 Tributary nitrite + nitrate as nitrogen loading analysis

Both the USGS and LADEQ periodically measure nitrite+nitrate as nitrogen concentrations in the tributaries around the Pontchartrain Estuary basin. Fifteen USGS stations had limited filtered and unfiltered data for nitrite + nitrate as nitrogen. The LADEQ data had an extensive nitrite + nitrate as nitrogen dataset (23 sites with long-term records). A list of all of the stations used in the analysis, along with detailed plots are available in Appendix A.

Nitrogen loading is probably the most important factor for predicting the occurrence of algal blooms. As such, it is essential that the loads coming into the Pontchartrain Estuary are

accurately accounted for. The USGS measures nitrite + nitrate as nitrogen concentration in mg/L and the LADEQ measures it in ppm (equivalent units). In order to calculate a load, a relationship needs to be developed in terms of discharge. The USGS took some instantaneous measurements at the same time that the samples were taken while the LADEQ did not measure discharge simultaneously. According to the long-term discharge analysis (see section 3.2.1), discharge is independent of drainage area in the Pontchartrain Estuary basin. Therefore daily discharge from the nearest gage can be applied to the measured concentrations to create a relationship without introducing large errors.

For example, on the Amite River, four USGS stations and six LADEQ stations had nitrite + nitrate as nitrogen concentration data while only three USGS stations had daily discharge data. Figure 3.4 shows a close up of the USGS (white points) and the LADEQ (green points) stations on the Amite River. The closest USGS gage with discharge data was applied to the stations with concentration data. If daily discharge was not available at the closest gage for the sample date, it was either calculated from the flow relationships for each tributary (Table 3.2) or left blank if no data was available. Table 3.3 below shows the sites used in the analysis on the Amite River with the USGS discharge gage assignments.

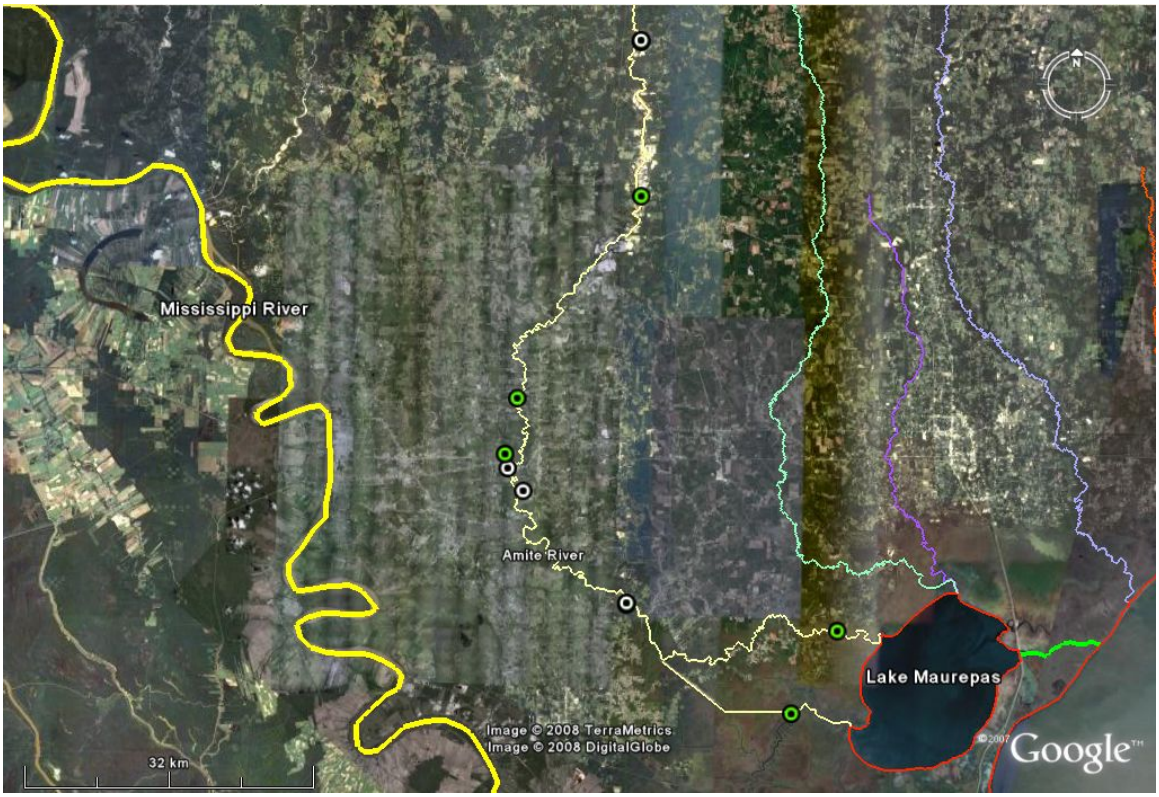

Figure 3.4 Map of the USGS and LADEQ stations used in the nitrite + nitrate as nitrogen analysis.

Table 3.3 Stations used in the nitrite + nitrate as nitrogen analysis on the Amite River.

Entity	Site Number	Site Name	USGS Gage assigned for Discharge
USGS	7377000	Amite River near Darlington, LA	Amite River near Darlington, LA
USGS	7378500	Amite River near Denham Springs, LA	Amite River near Denham Springs, LA
USGS	7380120	Amite at Port Vincent, LA	Amite at Port Vincent, LA
USGS	7378510	Amite River at 4th Camp near Denham Springs	Amite River near Denham Springs, LA
LADEQ	43	Amite River at Port Vincent, Louisiana	Amite at Port Vincent, LA
LADEQ	228	Amite River at mile 6.5, at Clio, Louisiana	Amite at Port Vincent, LA
LADEQ	268	Amite River Diversion Canal north of Gramercy, Louisiana	Amite at Port Vincent, LA
LADEQ	44	Amite River west of Darlington, Louisiana	Amite River near Darlington, LA
LADEQ	119	Amite River at Grangeville, Louisiana	Amite River near Denham Springs, LA
LADEQ	118	Amite River at Magnolia, Louisiana	Amite River near Denham Springs, LA

Figure 3.5 shows the relationship between discharge and nitrite + nitrate as nitrogen on the Amite River. A clear trend can be seen from this figure. Concentrations reach a peak at a discharge of approximately 0.03 $m^3/s/km^2$ and then decrease with either increasing or decreasing discharge. The observed trend is somewhat intuitive since at small discharges and corresponding runoff events, concentrations will be low and as discharge and runoff increase, the amount of nutrients carried into the tributaries will increase. However, at some point, more rainfall and associated runoff will not increase the concentration of nutrients in the receiving waters. Either a limit of available nutrients will be reached from within the watershed or dilution effects will take effect within the tributary itself.

Similar results were observed on the Tangipahoa, Bogue Chitto, Pearl and Tickfaw Rivers. The Natalbany and Comite Rivers showed a slight increase in concentration with increasing discharge and the Tchefuncte River showed a slight decrease in concentration with increasing discharge. The equations developed for each equation are shown in Table 3.4.

Real-time measurement of nitrite+nitrate as nitrogen were available at USGS Station 7375690 Tangipahoa River below Bedico Creek near Madisonville, LA. Daily averages were computed from the real-time data and compared to our daily predictions on the Tangipahoa River. Figure 3.6 shows the comparison between the measured and predicted datasets over time. The prediction seems to capture the general trend of the measured real-time data. Figure 3.7 looks at the measured data vs. discharge. The predicted trend line fits the dataset well again.

These relationships were used to develop a long-term estimate of nitrogen loading into the Pontchartrain Estuary. Figure 3.8 below shows the average annual daily nitrite + nitrate as

nitrogen loading per unit area. As drainage area increases daily nitrogen loads decrease. For a drainage area of 12,173 km^2, an average daily load of approximately 2,658 kg/day enters the Pontchartrain Estuary (or 0.2184 kg/day/km^2).

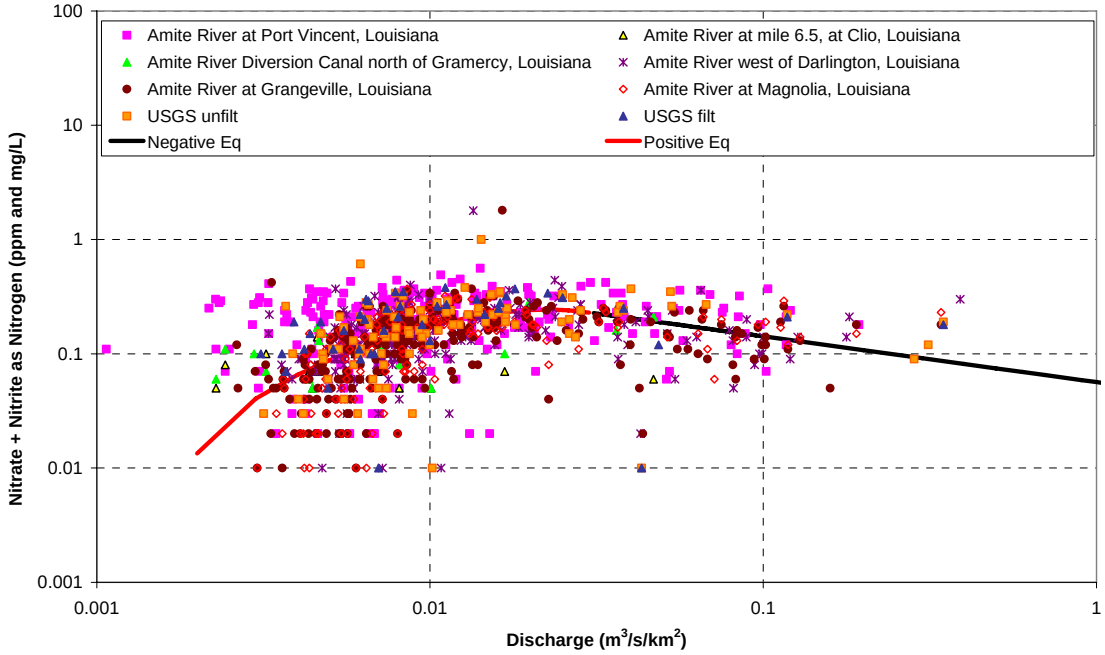

Figure 3.5 Relationship between nitrate + nitrite as nitrogen concentration and discharge for the Amite River.

Table 3.4. Relationships between discharge and nitrite + nitrate as nitrogen concentrations.

River	Nitrite + Nitrate as Nitrogen Concentration (mg/L) for Discharges less than the Splitting Value ($m^3/s/km^2$)	Splitting Value ($m^3/s/km^2$)	Nitrite + Nitrate as Nitrogen Concentration (mg/L) for Discharges greater than the Splitting Value ($m^3/s/km^2$)
Amite River	$-637673*Q^6 + 514426*Q^5 - 150380*Q^4 + 20231*Q^3 - 1280.5*Q^2 + 33.093*Q - 0.0478$	0.03	$0.0565*Q^{-0.4}$
Tangipahoa River	$-8752700*Q^6 + 1190100*Q^5 - 1225500*Q^4 + 352260*Q^3 - 5621.6*Q^2 + 93.372*Q - 0.27777$	0.0252	$0.1298*Q^{-0.343}$
Bogue Chitto	$-5171400*Q^6 + 2928600*Q^5 - 609660*Q^4 + 58800*Q^3 - 2794.9*Q^2 + 61.067*Q - 0.14389$	0.02	$0.127*Q^{-0.2525}$
Pearl	$-24171000*Q^6 + 9579300*Q^5 - 1452100*Q^4 + 105550*Q^3 - 3774.2*Q^2 + 59.312*Q - 0.081608$	0.014	$0.0377*Q^{-0.437}$
Tickfaw	$21{,}000*Q^3 - 2{,}550*Q^2 + 86*Q - 0.225$	0.008	$0.15*Q^{-0.15}$
Tickfaw (cont).		0.027	$0.0251*Q^{-0.65}$
Natalbany	$0.25*Q^{0.07}$		
Comite	$0.4247*Q^{0.2398}$		
Tchefuncte	$0.093*Q^{-0.085}$		

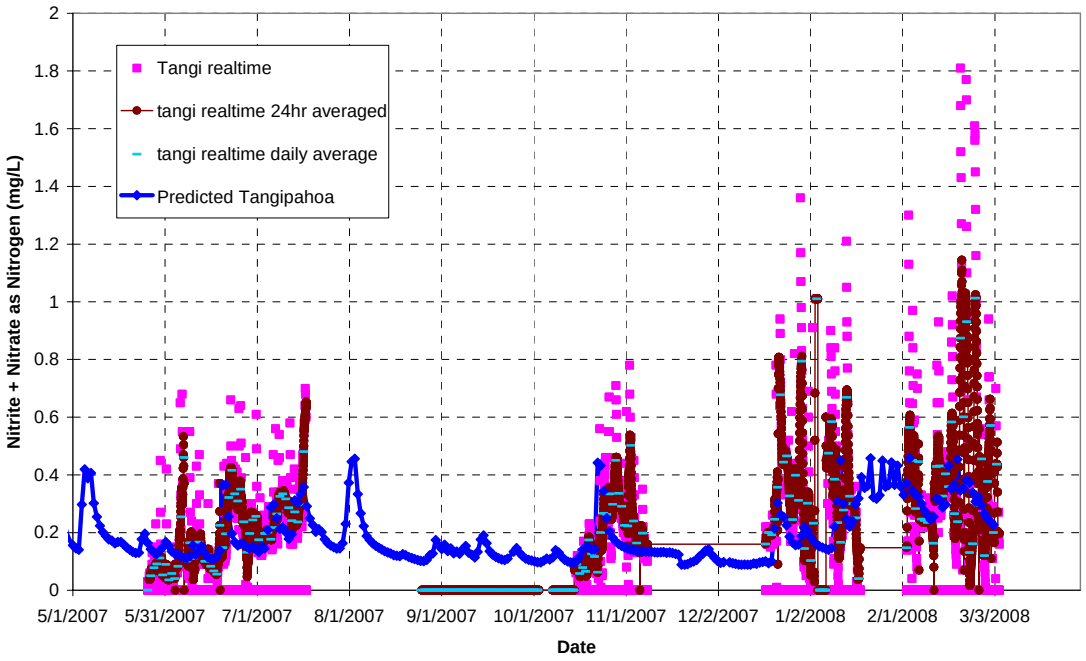

Figure 3.6 Comparison between nitrate + nitrite as nitrogen real-time measurements and predicted results on the Tangipahoa River.

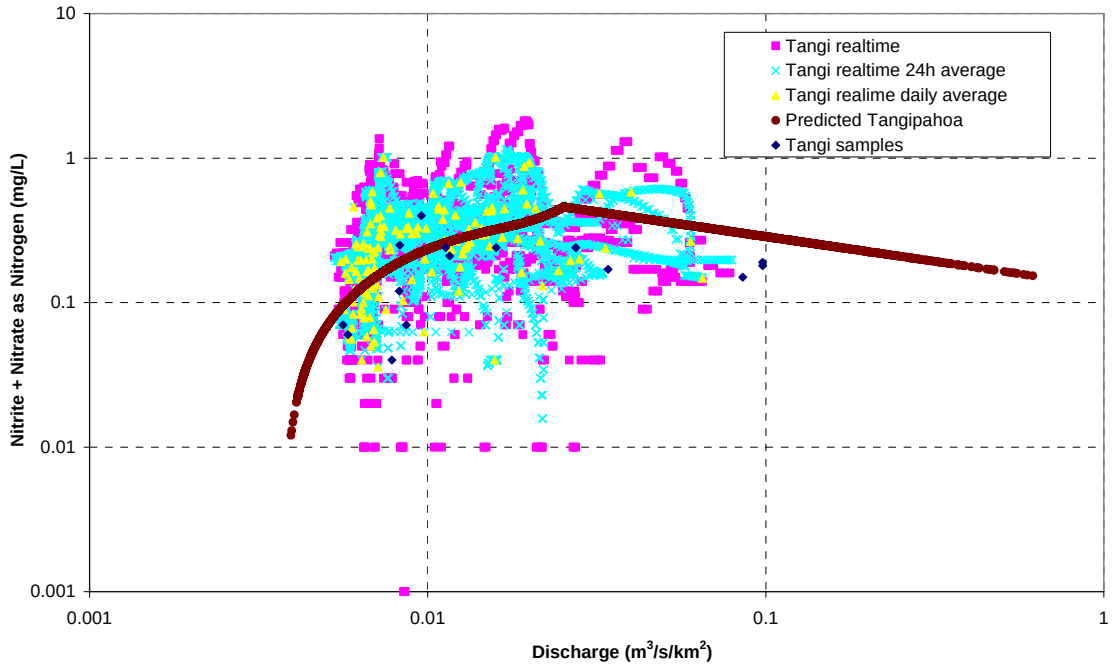

Figure 3.7 Nitrate + nitrite as nitrogen real-time measurements and predicted results as a function of discharge on the Tangipahoa River.

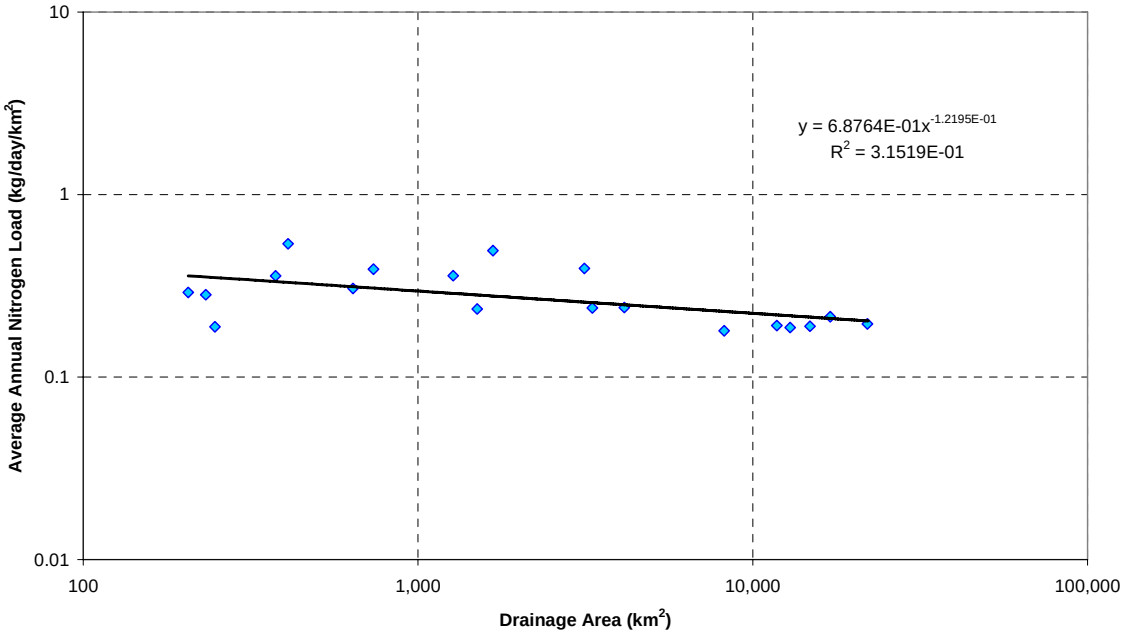

Figure 3.8. Relationship between average annual daily nitrate + nitrite as nitrogen load and drainage area.

3.2.3 Tributary phosphorous load analysis

Both the USGS and LADEQ also periodically measure phosphorous concentrations in the tributaries around the Pontchartrain Estuary basin. Fourteen USGS stations had limited filtered and unfiltered data for phosphorous. The LADEQ data had an extensive phosphorous dataset (23 sites with long-term records). The same sites as those used in the nitrite + nitrate as nitrogen analysis were used with the exception of USGS 7375230 Tchefuncte River at Madisonville, LA.

The same procedure as that above (section 3.2.2) was used to calculate the phosphorous loading into the Pontchartrain Estuary. The results for phosphorous concentration as a function of discharge per unit area for the Amite River are shown in Figure 3.9. Phosphorous concentrations appear to be independent of discharge. The results were similar for every river in the Pontchartrain Estuary basin (see Appendix A). Therefore, average phosphorous concentrations were assumed constant and are shown in Table 3.5. These concentrations were used to develop long-term loading into the Estuary as a function of drainage area (see Figure 3.10). Average annual long-term phosphorous loading was estimated to be 0.1475 kg/day/km^2 or 1,796 kg/day for a 12,174 km^2 watershed.

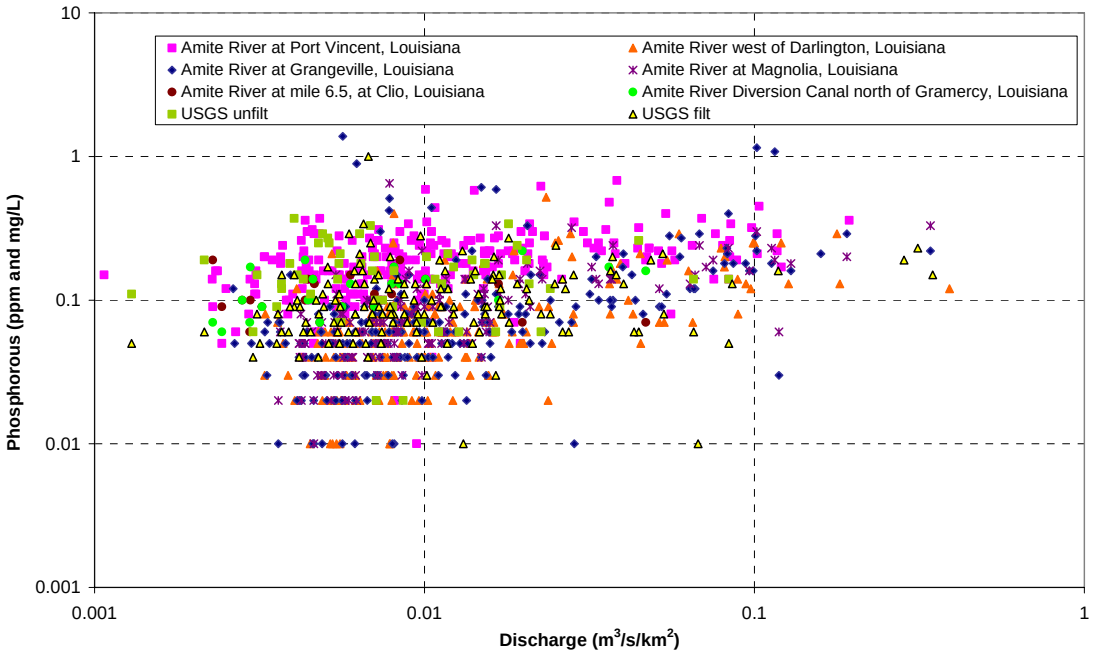

Figure 3.9 Relationship between phosphorous concentration and discharge for the Amite River.

Table 3.5. Average phosphorous concentrations around the Pontchartrain Estuary basin.

River	Average Phosphorous Concentration (mg/L)	Standard Deviation for Phosphorous Concentrations
Amite River	0.1234	0.1126
Bogue Chitto	0.0887	0.0657
Comite River	0.1655	0.1423
Natalbany River	0.1981	0.0808
Pearl River	0.1096	0.0943
Tangipahoa River	0.1187	0.1043
Tchefuncte River	0.0992	0.0672
Tickfaw River	0.1076	0.0654

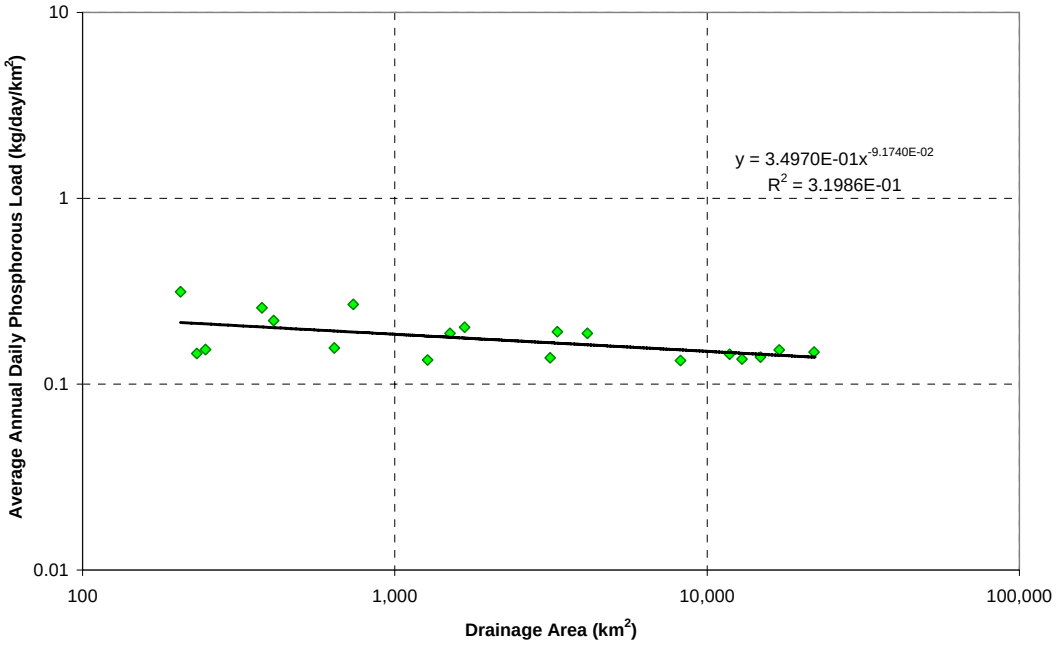

Figure 3.10 Relationship between average annual daily phosphorous load and drainage area.

3.2.4 Tributary ammonia load analysis

The USGS was the only entity that took direct measurements of ammonia in the tributaries flowing into the Pontchartrain Estuary. Short records were available at nine USGS locations distributed on the Amite, Tangipahoa, Bogue Chitto, Pearl and Tchefuncte Rivers. Figure 3.11 shows the relationship between measured ammonia concentrations and discharge per unit area on the Amite River (organic nitrogen concentrations are also included). As with phosphorous, there does not seem to be any dependency on discharge. Therefore, average values were calculated and used to predict long-term average ammonia loading into the Pontchartrain Estuary basin (Figure 3.12). The average concentration values used for each river are shown in Table 3.6. Ammonia concentrations were not measured on the Natalbany, Tickfaw and Comite Rivers. Concentrations on these rivers were predicted from the long-term loading results shown

in Figure 3.12. The pink, square points in Figure 3.12 represent the estimates for these rivers. Average annual long-term ammonia loading was estimated to be 0.2202 kg/day/km^2 or 2,681 kg/day for a 12,174 km^2 watershed.

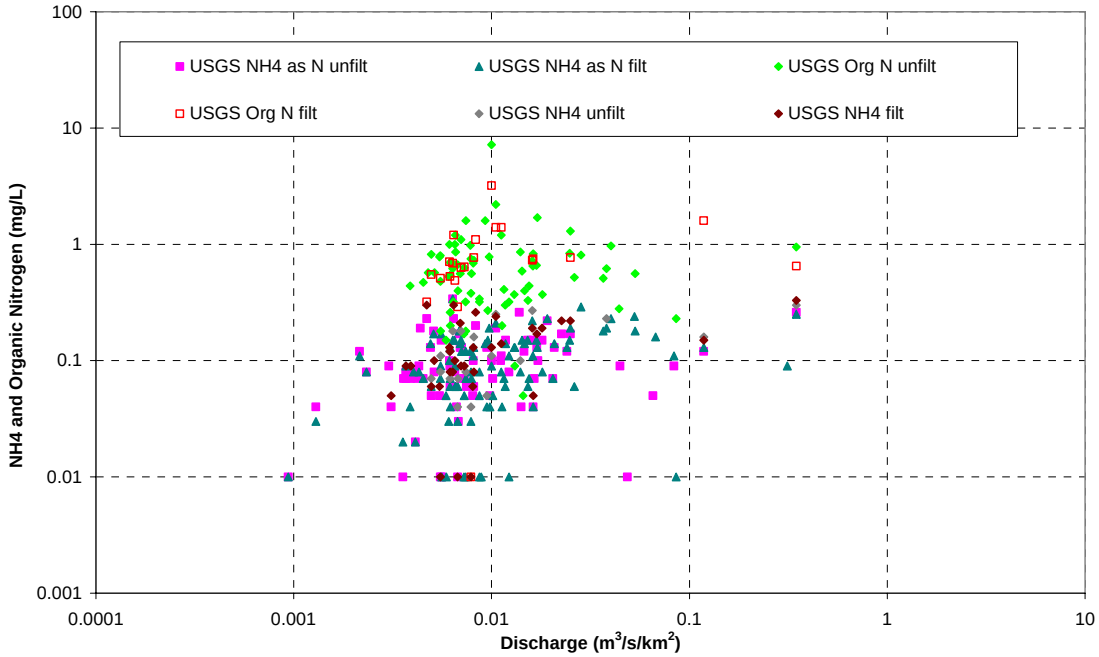

Figure 3.11 Relationship between ammonia concentration and discharge for the Amite River (organic nitrogen concentrations included).

Table 3.6 Average ammonia concentrations around the Pontchartrain Estuary basin.

River	Average Ammonia Concentration (mg/L)	Standard Deviation for Ammonia Concentrations
Amite River	0.10976	0.07155
Bogue Chitto	0.06806	0.05547
Pearl River	0.09625	0.11306
Tangipahoa River	0.08706	0.07200
Tchefuncte River	0.06693	0.07219
Comite River	0.17326	
Natalbany River	0.22419	
Tickfaw River	0.19562	

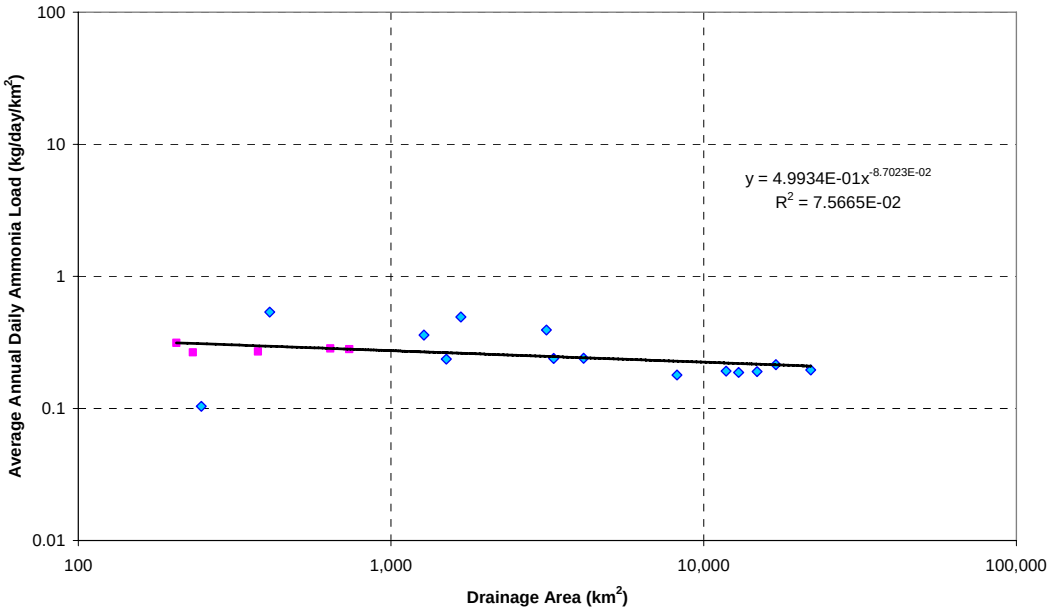

Figure 3.12 Relationship between average annual daily ammonia load and drainage area.

3.2.5 Tributary organic nitrogen load analysis

The USGS was the only entity that took direct measurements of organic nitrogen in the tributaries flowing into the Pontchartrain Estuary. Organic nitrogen was measured at ten USGS locations distributed on the Amite, Tangipahoa, Bogue Chitto, Pearl and Tchefuncte Rivers. The LADEQ took indirect measurements of organic nitrogen concentrations. The LADEQ has an extensive dataset of Total Kjeldahl Nitrogen (TKN), which is a measurement of ammonia and organic nitrogen added together. Therefore, since ammonia concentrations in the tributaries are known (section 3.2.4), organic nitrogen concentrations can be inferred from the LADEQ's TKN measurements. Organic nitrogen concentrations were calculated using this approach since the LADEQ dataset is more robust than that of the USGS. The USGS dataset was instead used to look at the percent errors between the datasets.

Figure 3.13 shows the relationship between measured TKN concentrations and discharge per unit area on the Amite River. As with phosphorous and ammonia, there does not seem to be any dependency on discharge. Therefore, average values were calculated and used to predict organic nitrogen concentrations (ammonia concentrations subtracted from TKN concentrations). The average TKN concentrations and the predicted and measured concentrations of organic nitrogen are shown in Table 3.7. The prediction of organic nitrogen is not significantly different than the direct organic nitrogen measurements taken by the USGS.

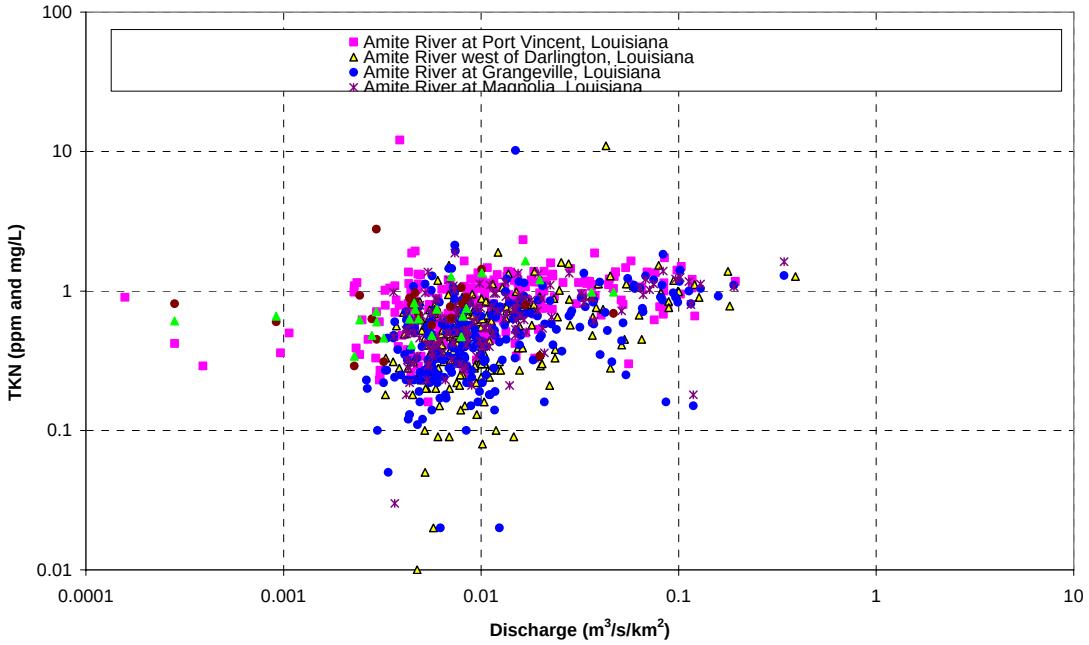

Figure 3.13 Relationship between TKN concentration and discharge for the Amite River.

Table 3.7 Average TKN and organic nitrogen concentrations around the Pontchartrain Estuary basin.

River	Average LADEQ TKN Concentration (mg/L)	Predicted Organic Nitrogen Concentrations (TKN-NH4) (mg/L)	Average USGS Organic Nitrogen Concentrations (mg/L)	Percent Error for Organic Nitrogen (%)
Amite	0.71037	0.60072	0.75635	20.6
Bogue Chitto	0.59744	0.52938	0.58414	9.4
Pearl	0.74454	0.64829	0.75051	13.6
Tangipahoa	0.68370	0.59664	0.58524	1.9
Tchefuncte	0.72160	0.65466	0.65254	0.3
Comite		0.59642		
Natalbany		0.73298		
Tickfaw		0.66960		

The predicted organic nitrogen concentrations were used to develop a long-term loading estimate into the Pontchartrain Estuary (Figure 3.14). Organic nitrogen concentrations are unknown on the Natalbany, Tickfaw and Comite Rivers and were instead predicted from the long-term loading results. The pink, square points in Figure 3.14 represent the estimates for these rivers. Average annual long-term organic nitrogen loading was estimated to be 0.8494 kg/day/km^2 or 10,340 kg/day for a 12,174 km^2 watershed.

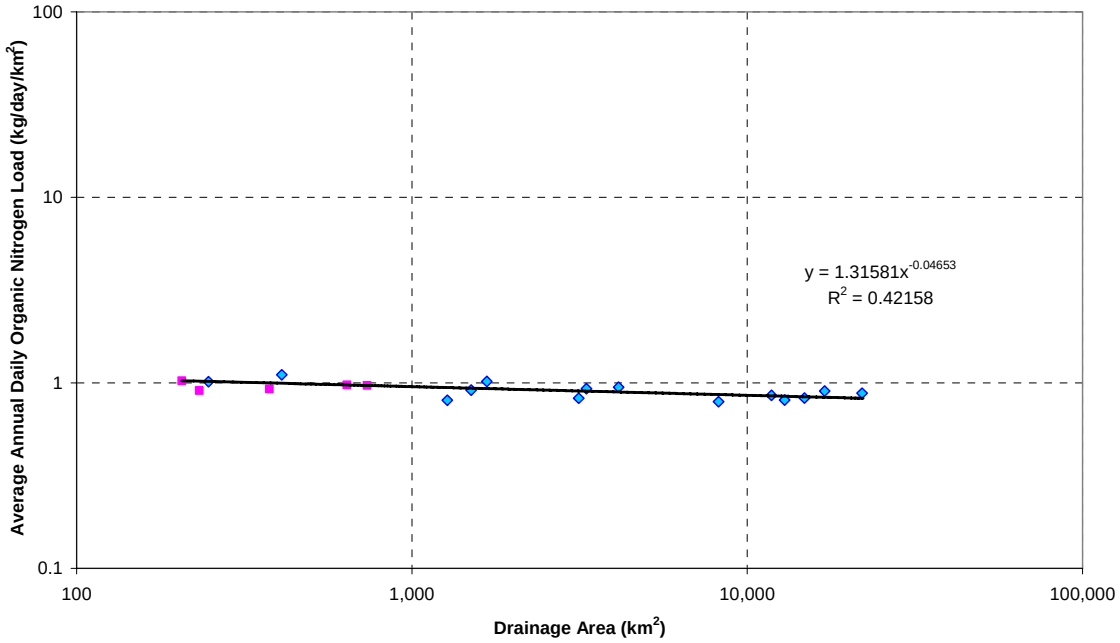

Figure 3.14 Relationship between average annual daily organic Nitrogen load and drainage area.

3.2.6 Tributary sediment load analysis

There are a few types of measurements that can be used to develop sediment loading curves: suspended sediment concentrations, total suspended solid concentrations and turbidity measurements. The USGS periodically measures both suspended sediment concentrations and turbidity in the tributaries around the Pontchartrain Estuary basin while the LADEQ only regularly measures turbidity. Twelve USGS stations had limited suspended sediment concentrations. Turbidity was measured at 13 USGS sites and 23 LADEQ sites.

Suspended sediment concentrations are a superior measure of sediment load in tributaries (Glysson et. al., 2002). Uhrich (2002) showed that regression equations between suspended sediment concentrations and turbidity measurements can be used to accurately predict suspended sediment concentrations. Since turbidity measurements are plentiful and suspended sediment concentrations are scarce in the Pontchartrain Estuary basin, relationships between these two parameters were developed and used to extend the data. Figure 3.15 below shows this relationship for the Amite River. The observation that turbidity increases with increasing suspended sediment concentrations was observed on the Amite, Tangipahoa, Bogue Chitto, Tangipahoa and Tchefuncte Rivers (see Table 3.8 and Appendix A). Suspended sediment data was not available on the Natalbany, Tickfaw or Comite Rivers and was instead borrowed from the Tchefuncte River since the drainage areas are similar.

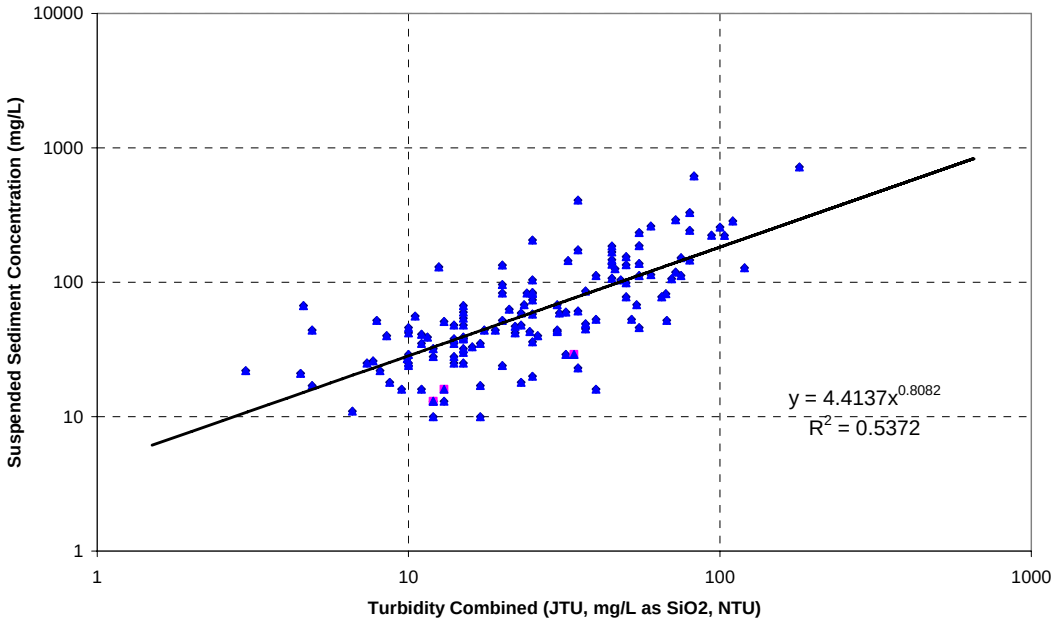

Figure 3.15 Relationship between suspended sediment concentration and turbidity on the Amite River.

Table 3.8 Relationships between suspended sediment concentration, turbidity and discharge.

River	Suspended Sediment Concentration (mg/L) vs. Turbidity (JTU, NTU, mg/L as SiO2)	Suspended Sediment Concentration (mg/L) vs. Discharge ($m^3/s/km^2$)
Amite	$SSC = 4.4137*T^{0.8082}$	$SSC = 454.6143*Q^{0.4605}$
Bogue Chitto	$SSC = 12.9710*T^{0.4772}$	$SSC = 176.8691*Q^{0.3070}$
Tangipahoa	$SSC = 9.9394*T^{0.6300}$	$SSC = 384.6485*Q^{0.4753}$
Pearl	$SSC = 18.7612*T^{0.4013}$	$SSC = 127.9681*Q^{0.1455}$
Tchefuncte	$SSC = 7.4201*T^{0.5175}$	$SSC = 95.8189*Q^{0.2678}$
Tickfaw	$SSC = 7.4201*T^{0.5175}$	$SSC = 96.2056*Q^{0.2403}$
Natalbany	$SSC = 7.4201*T^{0.5175}$	$SSC = 74.7192*Q^{0.1334}$
Comite	$SSC = 7.4201*T^{0.5175}$	$SSC = 152.1685*Q^{0.2710}$

The turbidity data was converted to suspended sediment concentrations and related to discharge to use in the loading calculations. The result for the Amite River is shown in Figure 3.16 and shows increasing suspended sediment load with increasing discharge. All of the other rivers showed a similar trend (Table 3.8). These loadings were used to calculate long-term sediment loadings into the Pontchartrain Estuary (Figure 3.17). Average annual long-term daily sediment loading was estimated to be 116 kg/day/km^2 or 1.4 million kg/day for a 12,174 km^2 drainage basin.

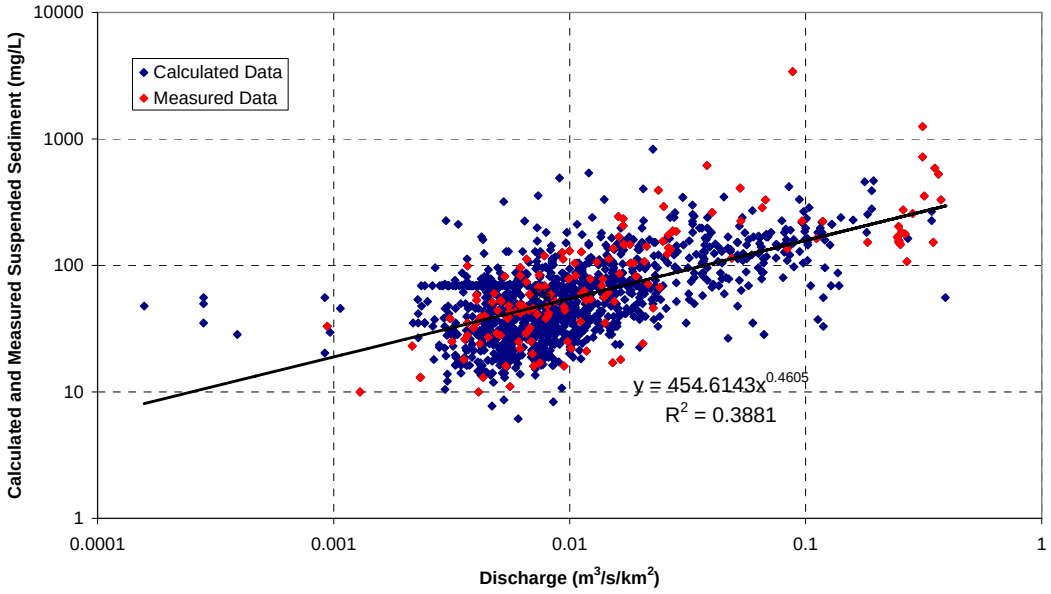

Figure 3.16 Relationship between suspended sediment concentration and discharge on the Amite River.

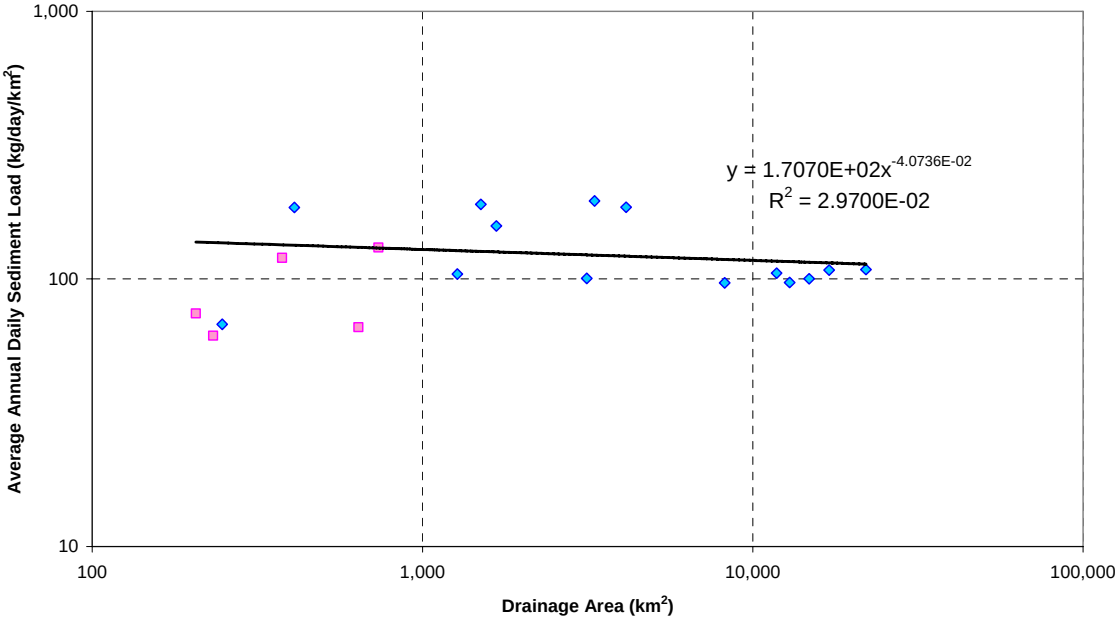

Figure 3.17 Relationship between average annual daily sediment load and discharge.

3.3 Bonnet Carré Spillway analysis

3.3.1 Bonnet Carré Spillway discharge analysis

As the Bonnet Carré Spillway is only opened intermittently, flow is not continuously monitored. However, during opening events, flow is monitored in the spillway by the USGS. Recorded flows during the 1994 and 1997 openings are listed below in Table 3.9.

Table 3.9. Measured flows during 1994 and 1997 Bonnet Carré Spillway openings.

1994 Date	1994 Measured Flow (m^3/s)	1997 Date	1997 Measured Flow (m^3/s)
April 20	24.86	March 17	424.75
May 11	247.49	March 25	6199.01
May 15	206.71	March 31	6133.17
May 17	247.49	April 8	45119.20
May 18	244.37	April 14	2170.18
May 20	238.14	April 21	141.58
May 23	283.17		
May 25	396.44		
May 31	0.32		

When the Mississippi River stage gets high, water can leak into the Spillway by either flowing through or over the base of the weir. Cruise et al. (2007) present the following equation for calculating flow over a spillway:

$$Q = 2.19LH_d^{\frac{3}{2}} \qquad 3.1$$

where Q is flow in m^3/s, L is the length of the spillway, and H_d is the head above the spillway crest. This equation was used to calculate flow over the Bonnet Carré Spillway during high river stages. The base elevation of the weir located along the entrance to the Bonnet Carré Spillway is 4.57 m for 174 bays (or 1,060 m) and is 5.18m for 176 bays (1075 m) with respect to NAVD88 (Brantley, 2008, personal communication). USACE gage 1280 at the Bonnet Carré Spillway was used to determine when flows exceeded the height of the weir. The result was then reduced by 95% since the water only flows between the spaces between each creosote timber.

3.3.2 Mississippi River nutrient and sediment load analysis

The USGS has two stations located in the vicinity of the Bonnet Carré Spillway where water quality measurements were taken: USGS 07373420 Mississippi River near St. Francisville, LA; and USGS 7374400 Mississippi River at Luling, LA. The St. Francisville station is located approximately 233 km upstream from the Bonnet Carré and the Luling station

is located roughly 12 km downstream. The two datasets were combined to make the nutrient and sediment analyses more robust.

Long-term monthly averages of nitrite + nitrate as nitrogen, ammonia, phosphorous, organic nitrogen and suspended sediment concentrations were made from the St. Francisville and Luling datasets. At the Luling (downstream) gage, monthly averages for nitrite + nitrate as nitrogen and phosphorous concentrations were 3.2% and 20% higher, while ammonia, organic nitrogen and suspended sediment concentrations were 62%, 72% and 65% lower than those at St. Francisville. However, phosphorous, organic nitrogen and suspended sediment data was sparse at Luling and may not accurately represent the change from upstream concentrations.

Non-weighted averages were taken between the two stations to develop a long-term monthly concentration for each nutrient. The suspended sediment concentrations at St. Francisville were used for the suspended sediment concentrations since the Luling dataset was insufficient. The resulting concentrations were used to develop the loadings into the Bonnet Carré Spillway and are shown below in Table 3.10.

Table 3.10 Average monthly nutrient concentrations on the Mississippi River (average of USGS St. Francisville and Luling gages).

Month	Nitrite + Nitrate as Nitrogen (mg/L)	Ammonia as Nitrogen (mg/L)	Phosphorous unfiltered (mg/L)	Organic Nitrogen unfiltered (mg/L)	Suspended Sediment[1] (mg/L)
1	1.2332	0.0648	0.2491	0.5932	231.7692
2	1.3189	0.0775	0.2584	0.7510	285.0370
3	1.4292	0.0657	0.2358	0.5787	239.3667
4	1.6365	0.0340	0.2301	0.7468	219.2667
5	1.8329	0.0356	0.2325	0.6296	202.5152
6	1.6459	0.0379	0.2357	0.7547	221.8378
7	2.1236	0.0364	0.2560	0.8636	209.7308
8	1.2893	0.0390	0.2140	0.7367	172.3704
9	0.8984	0.0277	0.2172	0.8092	131.7917
10	0.9161	0.0287	0.2207	0.5233	140.0526
11	1.1925	0.0322	0.2112	0.7155	223.7619
12	1.2499	0.0518	0.2360	0.6039	242.8800

[1]Suspended concentrations measured at USGS St. Francisville station only.

3.4 Atmospheric input analysis

Khariy (2000) found that atmospheric nitrogen contributes significant loads of nitrate and ammonia to the Tangipahoa watershed through rainfall. Atmospheric loadings were calculated from Wang (2003). He found from August 1999 to June 2003: ammonia nitrogen deposition ranged from 6-39 kg/km^2-mo with a mean of 17 kg/km^2-mo; nitrate nitrogen deposition ranged from 9-56 kg/km^2-mo with a mean of 21 kg/km^2-mo; TKN deposition ranged from 30-139 kg/km^2-mo with a mean of 54 kg/km^2-mo; and TP deposition ranged from 2-16 kg/km^2-mo with a mean of 6 kg/km^2-mo. The mean values were used and applied over the entire 1632 km^2 area of Lake Pontchartrain for each month. Organic nitrogen values were calculated by subtracting

ammonia loads from TKN loads. A nitrogen fixation rate of 1 g/m^2/year (Smith, 1990) was also considered in the atmospheric loading analysis. Nitrogen fixation varies throughout the year with higher fixation rates in the spring and summer and lower fixation rates in the fall and winter. The following annual distribution was applied to the fixation rate (equation 3.2):

$$1+\sin(2\pi\left(\frac{day}{365}-\frac{1}{4}\right) \qquad 3.2$$

Half of the distributed nitrogen fixation value was added to the atmospheric ammonia input while the other half was added to the atmospheric organic nitrogen contribution. The atmospheric loadings around Lake Pontchartrain are shown in Table 3.11.

Table 3.11 Atmospheric loading for Lake Pontchartrain (Wang, 2003).

Atmospheric Input	Contribution to Lake Pontchartrain (kg/day)
Nitrate nitrogen	1127
Ammonia nitrogen	912 + 2,236 = 3,148
Total Phosphorous	322
TKN	2,897
Organic nitrogen	1,985 + 2,236 = 4,221
Nitrogen Fixation (Smith, 1990)	4,471

3.5 Meteorological analysis

3.5.1 Precipitation

Five stations were used to assess precipitation over the Pontchartrain Estuary: the LUMCON site and four NCDC sites located at the New Orleans International airport, Lakefront airport (2 stations) and Slidell. Monthly totals were calculated at each station and then averaged between all of the stations to determine the average monthly rainfall over the Estuary. The five wettest and driest months between 1990 and 2006 are listed below in Table 3.12. Long-term monthly precipitation is shown in Figure 3.18. On an annual basis, there is approximately 1.54 m of rainfall around the basin.

Table 3.12 Wettest and driest months on the Pontchartrain Estuary between 1990-2006.

Wettest months (cm/month)	Driest months (cm/month)
May 1995 (62.74)	October 2005 (0.13)
January 1991 (57.35)	May 2000 (0.19)
January 1998 (51.28)	April 1999 (0.33)
June 2001 (46.92)	May 2006 (0.49)
November 1992 (43.36)	November 1999 (0.98)

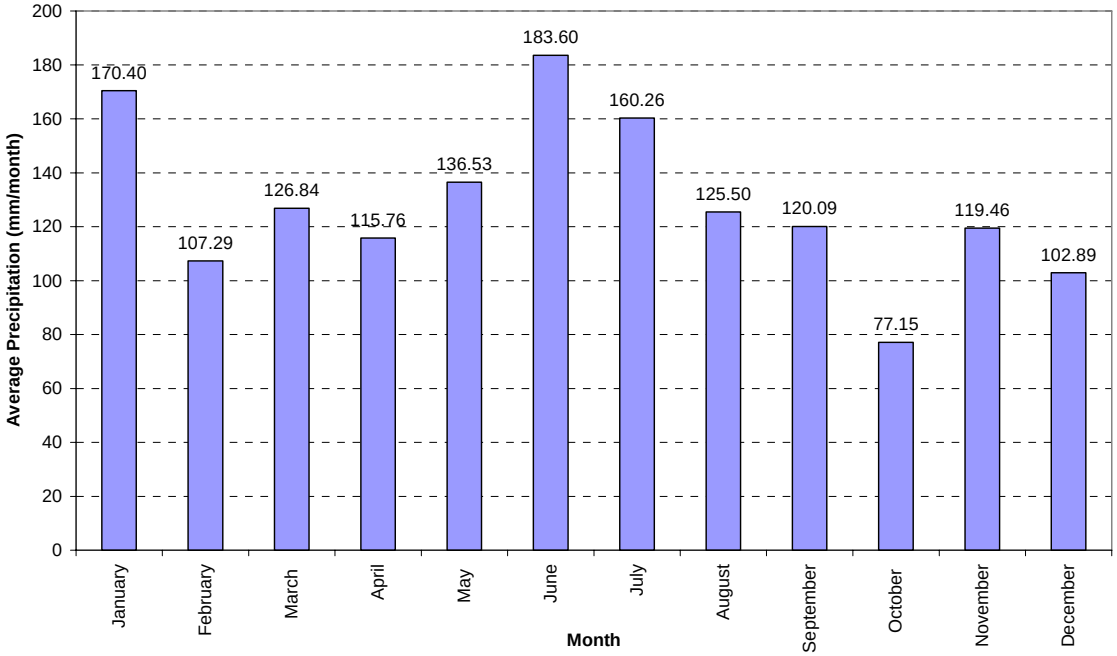

Figure 3.18 Long-term monthly precipitation around the Pontchartrain Estuary.

3.5.2 Evapotranspiration

Daily evapotranspiration values were estimated using Fontenot's (2004) composite coastal monthly dataset. This dataset was created using results from the Food and Agriculture Organization (FAO) Penman-Monteith model using data between December 2002 and November 2003 at five sites: Ben Hur, Hammond, Houma, Rice, and Southeast. Figure 3.19 below shows the monthly variation of evapotranspiration.

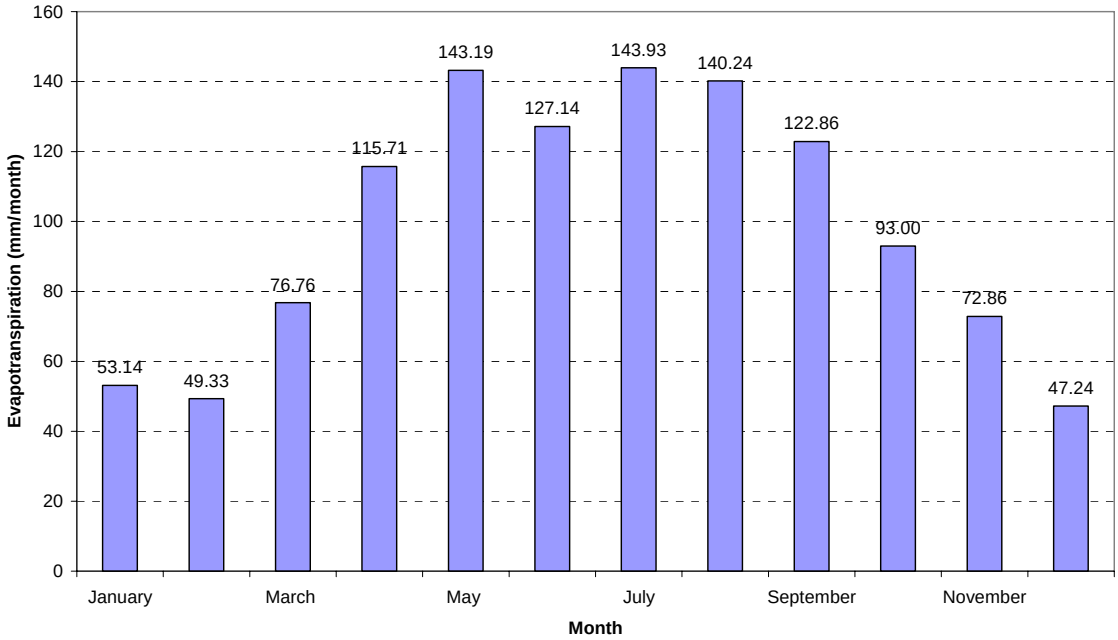

Figure 3.19 Long-term monthly evapotranspiration around the Pontchartrain Estuary (from Fontenot, 2004).

3.5.3 Air and water temperature

Air temperature was calculated by averaging the daily values at four NCDC sites (New Orleans International airport, 2 Lakefront airport stations and Slidell). Table 3.13 below shows the monthly average, maximum and minimum air temperature measured between 1990 and 2006.

Table 3.13 Monthly air temperatures around the Pontchartrain Estuary.

Month	Average Air Temp. (° C)	Max. Air Temp. (° C)	Min. Air Temp. (° C)
1	12.40	23.44	-0.74
2	14.09	23.46	-3.44
3	17.05	25.30	2.03
4	20.77	26.87	10.80
5	24.77	29.91	17.61
6	27.28	30.76	22.67
7	28.21	32.26	23.75
8	28.25	31.86	22.37
9	26.51	31.89	17.69
10	21.91	28.58	5.97
11	16.63	25.89	4.44
12	13.02	24.69	0.35

Water temperature is not monitored continuously in the Pontchartrain Estuary. Therefore all of the available daily data was averaged (LUMCON, 5 USGS Stations, and 95 LADEQ sites). The resultant averages were correlated to air temperature so a continuous record could be generated. Figure 3.20 below shows this relationship. Once the long-term water temperature record was generated, a 14 day average was taken over the entire record to smooth out any irregular values. The resulting monthly average, maximum and minimum water temperatures between 1990 and 2006 are listed in Table 3.14.

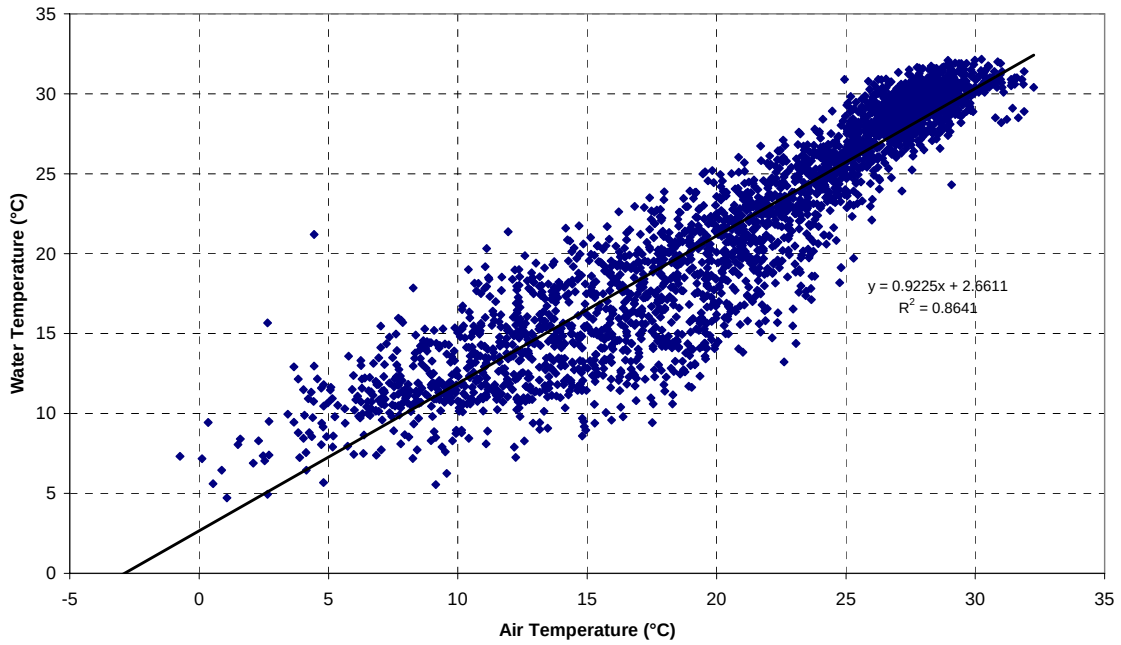

Figure 3.20 Correlation between air and water temperature in the Pontchartrain Estuary.

Table 3.14 Monthly water temperatures around the Pontchartrain Estuary.

Month	Average Water Temp. (° C)	Max. Water Temp. (° C)	Min. Water Temp. (° C)
1	13.14	21.90	4.72
2	14.99	20.60	9.70
3	18.02	22.70	9.50
4	21.87	27.22	16.01
5	25.72	29.20	20.18
6	28.30	31.04	25.30
7	29.27	32.09	26.34
8	29.35	32.17	25.85
9	27.44	31.40	18.98
10	22.96	28.92	16.35
11	18.06	25.90	12.30
12	14.22	22.00	6.45

3.5.4 Wind speed

Wind speed was calculated by averaging the daily values at LUMCON and four NCDC sites (New Orleans International airport, 2 Lakefront airport stations and Slidell). The average, maximum and minimum daily wind speed over Lake Pontchartrain between 1990 and 2006 was found to be 3.87 m/s, 15.05 m/s and 0.62 m/s respectively.

4.0 Model description

4.1 Introduction

Water quality modeling involves the assessment of many factors within a watershed or estuary. Typically water quality modeling includes: analyses of the hydrological and meteorological factors of the area; determination of the hydrodynamics of the receiving body; quantification of nutrient and sediment load inputs from both point and non-point sources; in addition to ecological and biological interactions (McCorquodale, 2006).

4.2 General overview

It is essential to understand how the proposed freshwater diversions will affect the water quality in the Pontchartrain Estuary. The effect of freshwater diversions on water quality in the Pontchartrain Estuary has been assessed previously. Dortch et al. (2007) used a water quality model to look at the effects of a freshwater diversion at the Bonnet Carré Spillway on Mississippi Sound. They used the Curvilinear-grid Hydrodynamics 3D model (CH3D) that linked to the finite volume eutrophication model (CE-QUAL-ICM). Their model looked at the changes in Mississippi Sound resulting from an opening between March and October 1999 with moderate flows. McCorquodale et al. (2004) used the 3-D hydrodynamic and contaminant transport model Estuarine, Coastal and Ocean Modeling System with Sediments (ECOMSED) with a simplified algal bloom model that they developed based on research by Ismail (1999), Haralampides (2000) and Dortch (1999, 2001). They successfully predicted the algal bloom potential on Lake Pontchartrain due to the opening and leakage events from the Bonnet Carré Spillway in 1993, 1994 and 1997. Other researchers have looked at the effects of freshwater diversions on Lake Pontchartrain water quality in a more general, qualitative way (USACE, 2004 in cooperation with the USGS, the Louisiana Department of Natural Resources (LADNR), the National Marine Fisheries Service (NMFS), U.S. Fish and Wildlife (USFW), and the Environmental Protection Agency (EPA)).

The models that were previously used to assess the effects of freshwater diversions on the Pontchartrain Estuary have a number of limitations associated with them. Both CH3D with CE-QUAL-ICM and ECOMSED are complex hydrodynamic and water quality models that can only simulate relatively short time-periods (on the order of one year) due to the extensive computing requirements that are required. When complex, multi-dimensional models are pushed to simulate longer periods, the solutions may have a tendency to "drift". The tendency of solutions to "drift" can cause unnatural responses to occur. When the ECOMSED model was applied to the Pontchartrain Estuary over a longer period of time, the solution "drift" caused the system to freshen with time. Barotropic rather than baroclinic treatment of the salinity flux at the pen bundary was found to cause some of this unnatural effect (Retana,2008, personal communication).

There is a need to develop a simplistic model that can be run quickly over long time periods to determine the general effects freshwater diversions might have on the water quality in the Pontchartrain Estuary. The simplistic model can then be used as a screening tool to focus more complex hydrodynamic and water quality modeling studies.

A 1-D tidal, salinity and water quality model that analyzes the general effects freshwater diversions have on the water quality of the Pontchartrain Estuary over a 17-year period is presented here. This model is computationally efficient and can easily assess the effects of

different timing, duration and quantity of flow scenarios over long time periods. The 17-year period from 1990 to 2006 was selected since adequate data records are present in the Estuary for calibration and validation of the model and shell dredging in the Pontchartrain Estuary was banned beginning in 1990.

4.3 Model description

4.3.1 General model description

The 1-D tidal, salinity and water quality model developed in this study was adapted from the model used in the 2007 sediment budget study of the Chenier Plain by McCorquodale et al. (2007). The 1-D model uses a similar link-cell structure and connectivity matrix to that used in the EPA EXTRAN model (the hydrodynamic part of the EPA Storm Water Management Model (SWMM) 5.0) for urban hydraulics. In this model, the Pontchartrain Estuary is divided up into a series of storage elements (cells) that are connected to one another via channels (links). The model is driven by the evaluation of the differential stages between each cell (equation 4.1) through the connecting links (equation 4.2). Wetland areas are incorporated into the model by assigning a hydraulically connected area to each cell. The open water area and the runoff contribution from the wetlands are also considered as per equation 4.3.

$$\frac{d\eta_j}{dt} = n_j' = \left(\frac{\sum Q_{i,trib,div} + P_j - ET_j}{As_j} \right) + \frac{Run_j}{As_j} \qquad 4.1$$

$$Q_i = A_i \left\{ \frac{2g\left|\eta_j - \eta_{j+1}\right|}{\left(\sum k_{im} + 2gn_i^{\,2} \frac{L_i}{R_i^{\frac{2}{3}}} \right)} \right\}^{\frac{1}{2}} sign(\eta_j - \eta_{j+1}) \qquad 4.2$$

$$Run_j = A_{dj} \left\{ P_j - k_{ow} \times ET_j - (1 - k_{ow}) k_{crop} \times ET_j \right\} \qquad 4.3$$

where j = number of cells in model; i = number of links in model; η_j = stage in each cell; $Q_{i,trib,div}$ = inflow to each storage cell from links (i), tributaries (trib) and diversions (div); P_j = precipitation rate on each cell; ET_j = evapotranspiration rate on each cell; As_j = surface area of each storage cell; Run_j = runoff contribution for each cell; A_i = cross-sectional area of each link; k_{im} = eddy loss coefficients in each link; n_i = Manning's roughness coefficient for each link; L_i = length of each link; R_i = hydraulic radius of each link; the function *sign* assigns a negative or

positive value to 1 depending on the value in the brackets; A_{dj} = hydraulically connected area for each cell; k_{ow}= fraction of open water in A_{dj}; and k_{crop} = crop factor (0.1 to 1).

The mass balance equations for salinity and suspended solids are shown below in equations 4.4 and 4.5.

$$\frac{dCS_j}{dt} = \frac{\sum CS_{i,trib} Q_{i,trib}}{y_j As_j} - k_{dis} k_{diff} \left(\frac{A_i}{L_i} \right) \left(\frac{CS_j - CS_{j,nb}}{y_j As_j} \right) - \frac{CS_j \eta_j'}{y_j} \tag{4.4}$$

$$\frac{dCSS_j}{dt} = \frac{\sum CSS_{i,trib,div} Q_{i,trib,div}}{y_j A_j} - \frac{k_{set} VsCSS_j}{y_j} + \frac{k_{rs} k_{rsc} d_{ref} Vw^2 - k_{ls} CSS_j y_j}{2 y_j{}^2 T_{res}} - \frac{CSS_j \eta_j'}{y_j} - k_{dis} k_{diff} \left(\frac{A_i}{L_i} \right) \left(\frac{CSS_j - CSS_{j,nb}}{y_j As_j} \right) + G_s \tag{4.5}$$

where CS_j = salinity concentration in each cell; $CS_{i,trib}$ = salinity concentration from each link and tributary; y_j = depth in each storage cell; k_{dis} = dispersion coefficient; k_{diff} = diffusion coefficient; A_i = area of each link; L_i = length of each link; $CS_{j,nb}$ = salinity concentration in neighbouring cells; η_j' = rate of rise of stage in each cell; CSS_j = suspended sediment concentration in each cell; $CSS_{i,trib,div}$ = suspended sediment concentration from each link, tributary and diversion; k_{set} =settling velocity calibration factor; Vs = settling velocity; k_{rs} = wind resuspension coefficient; k_{rsc} = wind resuspension calibration factor; d_{ref} = reference depth; Vw = wind speed; k_{ls} = suspended sediments boundary calibration factor; T_{res} = residence time; $CSS_{j,nb}$ = suspended sediment concentration in neighbouring cells; and G_s = area based internal source generation rate.

The Euler method was used for numerical integration of the time-step in the model. A hybrid upwinding and central differencing numerical integration solution scheme was used to solve the advective transport of salinity, suspended sediment and chemical equations. A central difference/upwinding calibration factor was used to determine the weighting between each solution method where 1 = pure upwinding and 0.5 = central differencing. The diffusive fluxes were computed using central differencing.

4.3.2 General chemical description

The chemical concentrations are calculated in a manner similar to salinity. The general equation for the chemical concentrations is shown below (adapted from Thomann and Mueller, 1987; Chapra, 1997; and McCutcheon, 1989):

$$\frac{dCC(n)_j}{dt} = \frac{\sum CC(n)_{i,trib,div} Q_{i,trib,div}}{y_j As_j} + \frac{\sum Q_{atm}'(n)_j As_j}{y_j As_j} - \frac{CC(n)_j \eta_j'}{y_j}$$
$$- k_{dis} k_{diff} \left(\frac{A_i}{L_i} \right) \left(\frac{CC(n)_j - CC(n)_{j,nb}}{y_j As_j} \right) + R(n)_j \qquad 4.6$$

where $CC(n)_j$ = concentration of chemical (n) in each cell; $CC(n)_{i,trib,div}$ = concentration of chemical (n) from each link, tributary and diversion; $Q_{i,trib,div}$ = inflow to each storage cell from links, tributaries and diversions; As_j = surface area of each storage cell; y_j = depth in each storage cell; $Q_{atm}'(n)_j$ = atmospheric loading of each chemical (n) on each cell; η_j' = rate of rise of stage in each cell; k_{dis} = dispersion coefficient; k_{diff} = diffusion coefficient; A_i = area of each link; L_i = length of each link; $CC(n)_{j,nb}$ = chemical concentration in neighbouring cells; and $R(n)_j$ = reaction equations for each chemical (n).

Nine chemicals are evaluated in this model: nitrite + nitrate as nitrogen (NO2+NO3), ammonia (NH4), dissolved inorganic nitrogen (DIN), organic nitrogen (ON), phosphorous (P), carbon (C), dissolved oxygen (DO), live algae as chlorophyll a (LA), and dead algae (DA). Figure 4.1 shows a schematic of the chemical interactions considered in this model. The first order reaction equations for each chemical are described in the sections below.

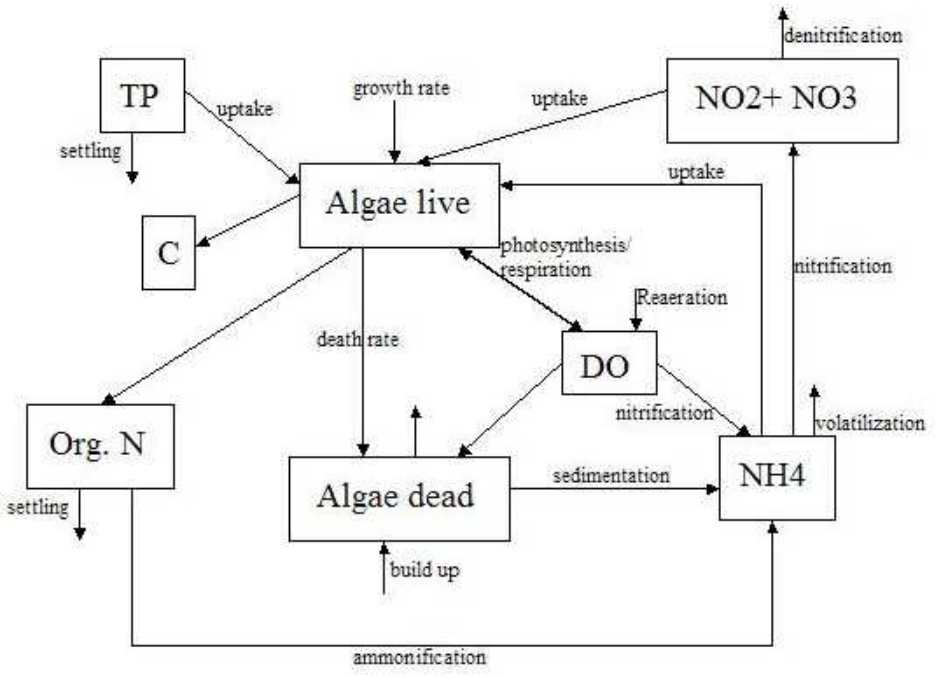

Figure 4.1 Diagram showing chemical interactions considered in the Pontchartrain Estuary model.

4.3.3 Live algae as chlorophyll a chemical description

The live algae concentrations calculated by the model are equivalent to chlorophyll a concentrations. Live algae growth in the model is limited by: light, suspended sediment concentrations, salinity concentrations, dead algae concentrations, nutrient concentrations (DIN and P), water temperature, and death and growth rates. The limiting equations for live algae are shown below (equations 4.7 to 4.11). The definitive live algae concentration equation is shown in equation 4.12. Equation 4.7 is adapted from Thomann and Mueller.

$$f(L) = 0.3 + 0.2\sin\left(2\pi\left(\frac{day}{365.25} - 0.25\right)\right) \quad 4.7$$

$$f\left(CSS_j, CS_j, CC(DA)_j\right) = \sqrt{\left(1 - \frac{CSS_j + CC(DA)_j}{k_{SS} + CSS_j + CC(DA)_j}\right)\left(1 - \frac{CS_j}{k_S + CS_j}\right)} \quad 4.8$$

$$f\left(CC(DIN)_j, CC(P)_j\right) = MIN\left(1, \frac{CC(DIN)_j}{k_{DIN} + CC(DIN)_j}, \frac{CC(P)_j}{k_P + CC(P)_j}\right) \quad 4.9$$

$$f(T) = 1.07^{T-20} \quad 4.10$$

$$k_{g,LA} = k_{g0,LA} \times f(L) \times f(CSS_j, CS_j, CC(DA)_j) \times f(CC(DIN)_j, CC(P)_j) \times f(T) \quad 4.11$$

$$R(LA)_j = k_{g,LA} \times CC(LA)_j + \left(\frac{k_{LA\rightarrow DA} \times CC(LA)_j \times CC(DA)_j}{CC(LA)_j + CC(DA)_j + sm}\right) \quad 4.12$$

where f(L) = light limitation function; day = number of day in the year; $f(CCS_j,CS_j,CC(DA)_j)$ = suspended sediment, salinity and dead algae concentration limitation in each cell; $CC(DA)_j$ = chemical concentration of dead algae in each cell; k_{ss} = suspended sediment Michaelis constant; k_s = salinity Michaelis constant; f(CC(DIN)j,CC(P)j) = DIN and P limitation function; $CC(DIN)_j$ = chemical concentration of DIN in each cell; $CC(P)_j$ = chemical concentration of P in each cell; k_{DIN} = DIN Michaelis constant; k_P = P Michaelis constant; f(T) = water temperature limitation; T = water temperature; $k_{g,LA}$ = growth limitation for live algae; $k_{g0,LA}$ = maximum potential growth rate for live algae; $CC(LA)_j$ = chemical concentration of live algae in each cell; $k_{LA\rightarrow DA}$ = first order reaction constant between live and dead algae; and sm = a small number to prevent division by zero.

4.3.4 Dead algae chemical description

The dead algae growth rate in the model is limited by gains from live algae and losses from anaerobic respiration and volatilization. Equation 4.13 shows how the dead algae concentration is calculated in the model.

$$R(DA)_j = k_{g0,DA}\left(\frac{CC(DA)_j \times CC(LA)_j}{CC(DA)_j + CC(LA)_j + sm}\right) + 2\left(k_{DA\rightarrow NH4} \times CC(DA)_j\right) + k_{DA\rightarrow DO} CC(DA)_j \quad 4.13$$

where $k_{g0,DA}$ = dead algae growth rate; $k_{DA\rightarrow NH4}$ = volatilization rate; and $k_{DA\rightarrow DO}$ = aerobic decomposition of dead algae.

4.3.5 Nitrite + nitrate as nitrogen chemical description

The nitrite + nitrate as nitrogen growth rate in the model is limited by gains from nitrification and losses by denitrification and uptake rates from live algae (that are further limited by the Redfield ratio for N:C). Equation 4.14 shows the limitation imposed by live algae on the growth rate of NO3. Equation 4.15 illustrates how nitrite + nitrate as nitrogen is calculated in the model

$$k_{NO3\rightarrow LA} = k_{g,LA} \times \left(\frac{CC(NO3)_j}{CC(DIN)_j + sm}\right) \times \left(\frac{1}{5.68}\right) \quad 4.14$$

$$R(NO3)_j = k_{g0,NO3} \times CC(NO3)_j + k_{NH4\rightarrow NO3} \times CC(NH4)_j + k_{NO3\rightarrow LA} CC(LA)_j \quad 4.15$$

where $k_{NO3\rightarrow LA}$ = growth limitation on NO3 imposed by live algae and the Redfield ratio; $k_{g0,NO3}$ = denitrification rate; and $k_{NH4\rightarrow NO3}$ = nitrification rate.

4.3.6 Ammonia chemical description

The ammonia growth rate in the model is limited by gains from ammonification and losses due to volatilization, nitrification, and uptake rates from live algae (that are further limited by the Redfield ratio for N:C). Equation 4.16 shows the growth rate limitation of live algae applied to NH4. Equation 4.17 illustrates how ammonia is calculated in the model.

$$k_{NH4\to LA} = k_{g,LA} \times \left(1 - \frac{CC(NO3)_j}{CC(DIN)_j + sm}\right) \times \left(\frac{1}{5.68}\right) \quad 4.16$$

$$R(NH4)_j = k_{g0,NH4} \times CC(NH4)_j + k_{ON\to NH4} \times CC(ON)_j + k_{NH4\to LA} CC(LA)_j \quad 4.17$$

where $k_{NH4\to LA}$ = growth limitation on NH4 imposed by live algae and the Redfield ratio; $k_{g0,NH4}$ = nitrification and volatilization rate; and $k_{ON\to NH4}$ = ammonification rate.

4.3.7 Organic nitrogen chemical description

The organic nitrogen growth rate in the model is limited by losses due to ammonification and settling and gains from live algae inputs (that are further limited by the Redfield ratio for N:C). Equation 4.18 shows the growth rate limitation of live algae applied to ON. Equation 4.19 illustrates how organic nitrogen is calculated in the model.

$$k_{LA\to ON} = k_{g,LA} \times \left(\frac{1}{5.68}\right) \quad 4.18$$

$$R(ON)_j = k_{g0,ON} \times CC(ON)_j + k_{ON\to NH4} \times CC(ON)_j + k_{LA\to ON} CC(LA)_j \quad 4.19$$

where $k_{LA\to ON}$ = growth rate of ON from live algae inputs limited by the Redfield ratio; $k_{g0,ON}$ = settling rate of ON; and $k_{ON\to NH4}$ = ammonification rate.

4.3.8 Phosphorous chemical description

The phosphorous growth rate in the model is limited by losses due to settling and uptake rates from live algae (that are further limited by the Redfield ratio for P:C). Equation 4.20 shows the growth rate limitation of live algae applied to P. Equation 4.21 illustrates how phosphorous is calculated in the model.

$$k_{P\to LA} = k_{g,LA} \times \left(\frac{1}{41.10}\right) \quad 4.20$$

$$R(P)_j = k_{g0,P} \times CC(P)_j + k_{P\to LA} CC(LA)_j \quad 4.21$$

where $k_{P\rightarrow LA}$ = growth limitation on NH4 imposed by live algae and the Redfield ratio; and $k_{g0,P}$ = settling rate of P.

4.3.9 Carbon chemical description

The carbon growth rate in the model is limited by uptake rates from live algae Equation 4.22 shows how carbon is calculated in the model.

$$R(C)_j = k_{LA\rightarrow C} \times k_{g,LA} \times CC(LA)_j \qquad 4.22$$

where $k_{LA\rightarrow C}$ = live algae growth contribution to carbon.

4.3.10 Dissolved oxygen chemical description

The dissolved oxygen growth rate in the model is limited by gains from photosynthesis and reaeration and losses from respiration and nitrification. The reaeration function is shown in equation in 4.23. Equation 4.24 shows how dissolved oxygen concentrations are calculated in the model.

$$Ra = O2Sat(day) - CC(DO)_j \qquad 4.23$$

$$\begin{aligned} R(DO)_j &= k_{g0,DO} \times Vw^2 Ra + 4k_{DO\rightarrow NH4} CC(NH4)_j \\ &+ k_{LA\rightarrow DO} CC(LA)_j + 2.28k_{DO\rightarrow DA} CC(DA)_j \end{aligned} \qquad 4.24$$

where $kg_{0,DO}$ = growth rate for dissolved oxygen, $k_{DO\rightarrow NH4}$ = nitrification rate; $k_{LA\rightarrow DO}$ = photosynthetic rate; and $k_{DO\rightarrow DA}$ = respiration rate.

4.3.11 Algal bloom probability model description

The simplified algal bloom probability model developed by McCorquodale et al. (2007) was also incorporated into the code. The algal bloom probability model was developed based on research by Ismail (1999), Haralampides (2000) and Dortch (1999, 2001) and is shown below (equation 4.25):

$$p_{HAB,j} = \left(p_T\, p_{CSS}\, p_{CS}\, p_{CC(DIN)}\right)_j^{\frac{1}{4}} \qquad 4.25$$

where $p_{HAB,j}$ = probability of a harmful algal bloom occurring in each cell; $p_{T,j}$ is the index of suitable water temperature and light in each cell; $p_{CSS,j}$ is the index of suitable suspended sediment concentration in each cell; $p_{CS,j}$ is the index of acceptable salinity concentration in each cell; and $p_{CC(DIN)j}$ is the index of available nitrogen concentration in each cell. These indices are defined below in equations 4.26 to 4.29:

$$p_{T,j} = \frac{1}{2}\left(1 + \tanh\left(\alpha_T \left(T_j - T_{cr}\right)\right)\right)\left(\frac{T_j}{T_{cr}}\right)^{\frac{1}{4}} \quad 4.26$$

$$p_{CSS,j} = \frac{1}{2}\left(1 - \tanh\left(\alpha_{CSS} \left(CSS_j - CSS_{cr}\right)\right)\right) \quad 4.27$$

$$p_{CS,j} = \frac{1}{2}\left(1 - \tanh\left(\alpha_{CS} \left(CS_j - CS_{cr}\right)\right)\right) \quad 4.28$$

$$p_{CC(DIN)} = \frac{1}{2}\left(1 + \tanh\left(\alpha_{CC(DIN)} \left(CC(DIN)_j - CC(DIN)_{cr}\right)\right)\right)\left(\frac{CC(DIN)_j}{CC(DIN)_{cr}}\right)^{\frac{1}{2}} \quad 4.29$$

where T_j = the temperature in each cell (°C); CSS_j = the concentration of suspended sediment (mg/L); CS_j = the salinity in each cell (ppt); $CC(DIN)_j$ = the concentration of DIN in each cell (ug/L). The parameters with the subscript 'cr' are the critical parameters and were defined by McCorquodale et al (2007) to be: T_{cr} = 20°C; CSS_{cr} = 25 mg/L; CS_{cr} = 2.6 ppt; and $CC(DIN)_{cr}$ = 400 ug/L. The α parameters are spreading factors that are defined as α_T = 0.75; α_{CSS} = 0.3; α_{CS} = 8; and $\alpha_{CC(DIN)}$ = 0.005.

5.0 Model inputs

5.1 General inputs

The 1-D tidal, salinity and water quality model requires extensive input datasets. The inputs include hydrological, meteorological, physical, ecological, biological and water quality factors. The inputs developed from the analyses in section 3.0 are described in this chapter.

The cell-link configuration for the 1-D tidal, salinity and water quality model is illustrated in Figure 5.1. The dimensions of each cell and link as well as other preliminary data assignments are listed below in Tables 5.1 and 5.2. The constants k_m, k_{en} and k_{ex} represent the minor loss coefficient due to structures, the entrance loss coefficient and the exit loss coefficient in each link respectively.

A few other general parameters were input into the model: the reference depth (d_{ref}) = 4.0m; settling velocity (Vs) = 8 m/s (Miller et al., 2005, Chilmakuri, 2005); and the area based internal source generation rate (G_s) = 0.63 m^3/year/m (CERC, 1984).

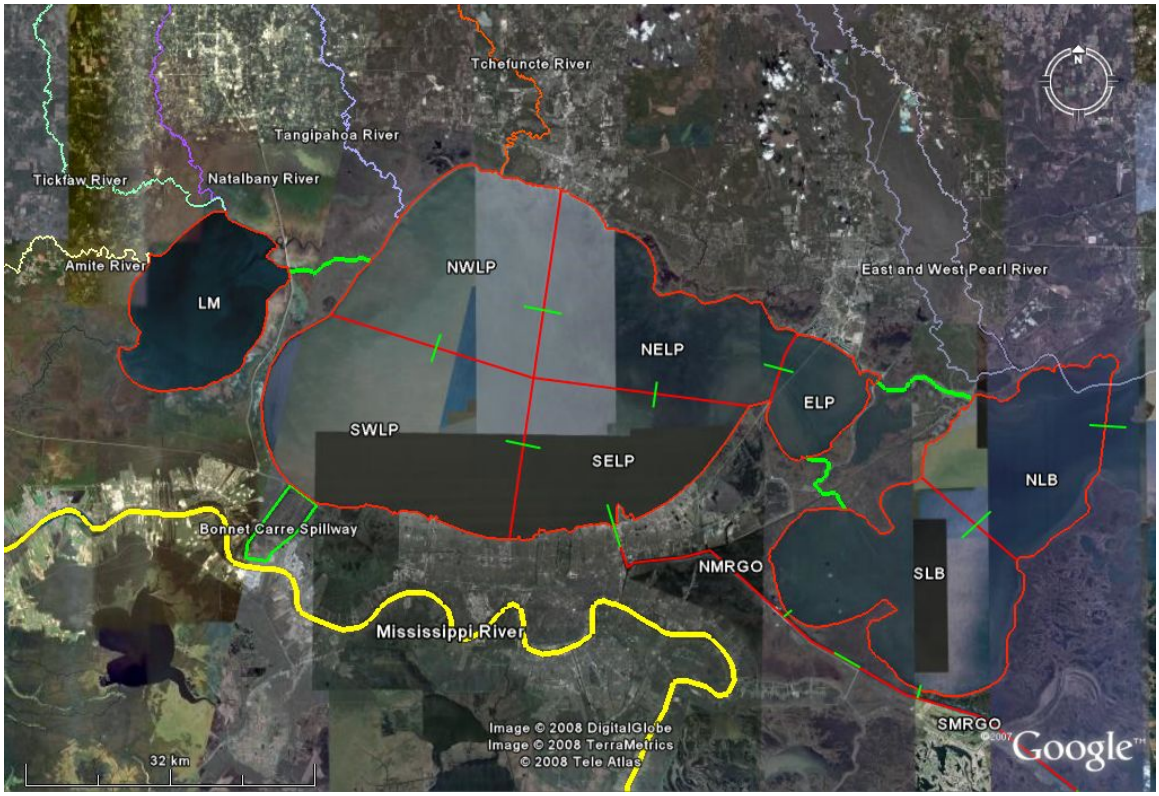

Figure 5.1 Cell-link model structure for Pontchartrain Estuary model.

Table 5.1 Pontchartrain Estuary model cell inputs.

Cell No. (j)	Cell name	Surface Area (As_j in km^2)	Depth (y_j in m)	Hydraulically Connected Area (A_{dj} in km^2), Percent Open Water (k_{ow} in %)	Initial Salinity (CS_j in ppt)	E-W Fetch (km)	N-S Fetch (km)
1	North Lake Borgne	650	-5	50 (15%)	10	20	20
2	South Lake Borgne	550	-5	50 (15%)	12	20	20
3	E Lake Pontchartrain	380	-2.8	150 (15%)	6	40	20
4	SE Lake Pontchartrain	180	-3.8	10 (10%)	5	50	30
5	NE Lake Pontchartrain	350	-4	150 (20%)	2	30	40
6	NW Lake Pontchartrain	350	-3.5	150 (20%)	2	30	40
7	Lake Maurepas	350	-3.5	250 (20%)	0.2	25	25
8	South MRGO	150	-6	100 (20%)	19	5	5
9	North MRGO	100	-6	100 (20%)	15	5	5
10	SW Lake Pontchartrain	350	-3	250 (20%)	2	30	40

Table 5.2 Pontchartrain Estuary model link inputs.

Link No. (i)	From Cell (j)	To Cell (j)	From Cell Name	To Cell Name	Depth (y_i in m)	Length (L_i in m)	Width (W_i in m)	Manning's n	K_m	K_{en}	K_{ex}
1	1	101	N.LB	G.O.M	-6	5,000	10,000	0.025	0	0.05	0.5
2	3	1	E.LP	N.LB	-10	10,500	1,000	0.025	0	0.5	1
3	2	1	S.LB	N.LB	-5	15,000	15,000	0.025	0	0.1	1
4	3	2	E.LP	S.LB	-8.5	7,800,	375	0.025	0	0.5	0.5
5	8	102	S.MR GO	G.O.M	-5	70,420	400	0.025	0	0.5	0.5
6	9	8	N.MR GO	S.MR GO	-5	10,000	250	0.025	0	0.5	1
7	9	2	N.MR GO	S.LB	-5	20,000	150	0.025	0	0.5	1
8	4	9	SE.LP	N.MR GO	-10	15,000	100	0.025	0	0.5	1
9	5	3	NE.LP	E.LP	-3.5	20,000	40,000	0.025	0	0.02	0.25
10	5	4	NE.LP	SE.LP	-3.5	40,000	40,000	0.025	0	0.02	0.25
11	6	5	NW.LP	NE.LP	-5	10,000	10,000	0.025	0	0.5	1
12	7	6	LM	NW.LP	-6.6	9,200	375	0.025	0	0.5	1
13	8	2	S.MR GO	S.LB	-5	1,000	1,000	0.025	0	0.5	1
14	10	6	SW.LP	NW.LP	-3	20,000	20,000	0.025	0	0.02	0.25
15	10	4	SW.LP	SE.LP	-3	20,000	20,000	0.025	0	0.02	0.25

5.2 Tributary inputs

There are seven rivers that flow into the Pontchartrain Estuary. The rivers drainage areas cover a total area of 6,900 km^2. The Pearl, Bogue Chitto and Comite Rivers drainage areas are not included in this total since the Comite River flows into the Amite River, the Bogue Chitto River flows into the Pearl River and the Pearl River flows into the Gulf of Mexico. The remaining drainage area (5,274 km^2) in the Pontchartrain Estuary is ungaged. The tributary contributions are assigned to a cell, affecting the mass balance equations in the model. The drainage area of each river and their relative contribution to each cell is described in Table 5.3 below. The Comite River was used as a surrogate of storm water runoff from the metropolitan New Orleans area.

Table 5.3 Tributary contributions to each cell in the Pontchartrain Estuary model.

Cell No.	Cell Name	Drainage Area (km^2)	Percentage (%) of Tributary Contribution to Cell (Cell No.)
1	Amite River	4,134	100% Lake Maurepas (Cell 7)
2	Bogue Chitto River	3,142	None
3	Comite River	736	25% SELP (Cell 4); 25% SWLP (Cell 10)
4	Natalbany River	206	100% Lake Maurepas (Cell 7)
5	Tangipahoa River	1,673	100% NWLP (Cell 6)
6	Tchefuncte River	247	100% NWLP (Cell 6)
7	Tickfaw River	640	100% Lake Maurepas (Cell 7)
8	Pearl River	21,999	100% NLB (Cell 1)
9	Ungaged Areas	5,274	10% NLB (Cell 1); 20% ELP (Cell 3); 20% NELP (Cell 5); 10% NWLP (Cell 6); 20% Lake Maurepas (Cell 7); 20% SWLP (Cell 10)

The 1-D tidal, salinity and water quality requires daily inputs from the tributaries between 1990 and 2006. Daily discharge was input using the starred gages in Table 3.1. If data was missing, it was either calculated using the relationships from other gages on the tributary in Table 3.2 or related to another river. The Tchefuncte River was the only river with daily discharge values missing (January 1993 to September 1997) and no alternate gage. The Tchefuncte River was related to the Robert gage on the Tangiphoa River instead ($Q_{\text{Tchefuncte at Folsom}} = 0.8797 * Q_{\text{Tangipahoa at Robert}}^{1.0294}$, see Appendix A for Figure) to replace these missing values. The daily discharge from the ungaged rivers was calculated using the long-term daily discharge relationship presented in Figure 3.3 and was found to be 83.81 m^3/s/day. This value was varied throughout the year by multiplying it by the normalized discharge values on the Tangipahoa River. The final discharge data input into the model is shown below in Figure 5.2.

Daily tributary nutrient and sediment loadings were all calculated in the same manner. First, daily concentrations were calculated from the equations and average values presented in Section 3.2.2 to 3.2.6. These concentrations were then multiplied by the daily river discharges above to generate the daily loading. Figures 5.3 to 5.7 show the nitrite+nitrate as nitrogen, phosphorous, ammonia, organic nitrogen and sediment loadings from the tributaries. The daily nitrite+nitrate as nitrogen, phosphorous, ammonia, organic nitrogen and sediment loadings for the ungaged areas were calculated using the long-term loading relationships presented in section 3.2 and were found to be 1,275 kg/day; 840 kg/day; 1,250 kg/day and 4,650 kg/day respectively. These values were varied throughout the year by multiplying it by the normalized loading values on the Tangipahoa River. Salinity concentrations from the tributaries were assumed to be constant at 0.25 ppt.

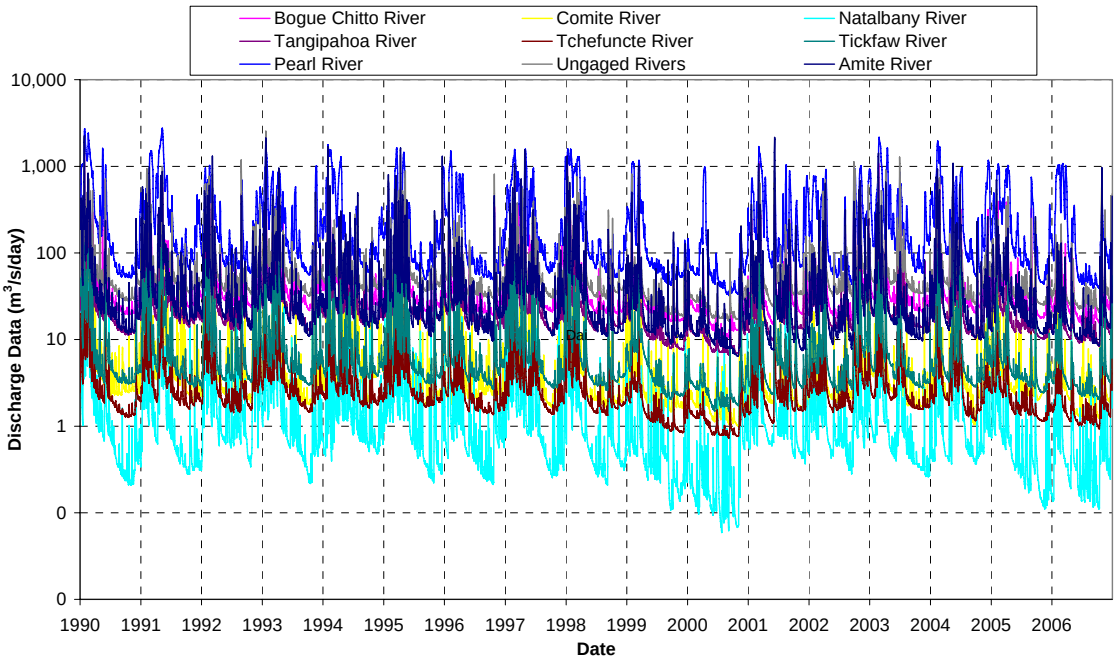

Figure 5.2 Daily tributary discharge input for the Pontchartrain Estuary model.

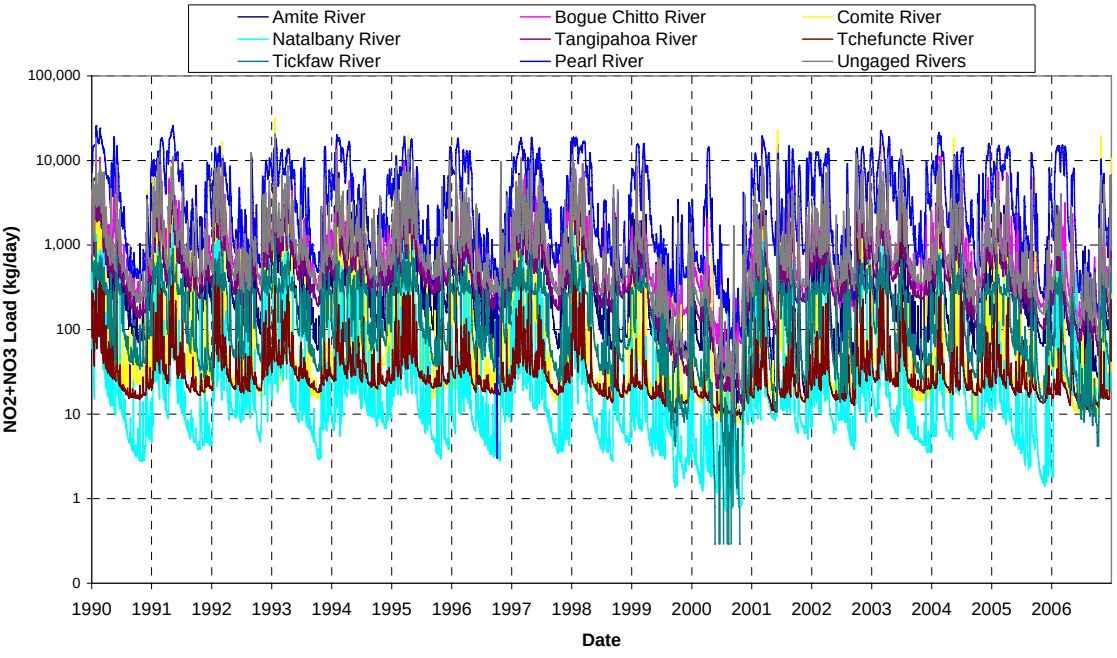

Figure 5.3 Daily tributary nitrite + nitrate as nitrogen loading for input into the Pontchartrain Estuary model.

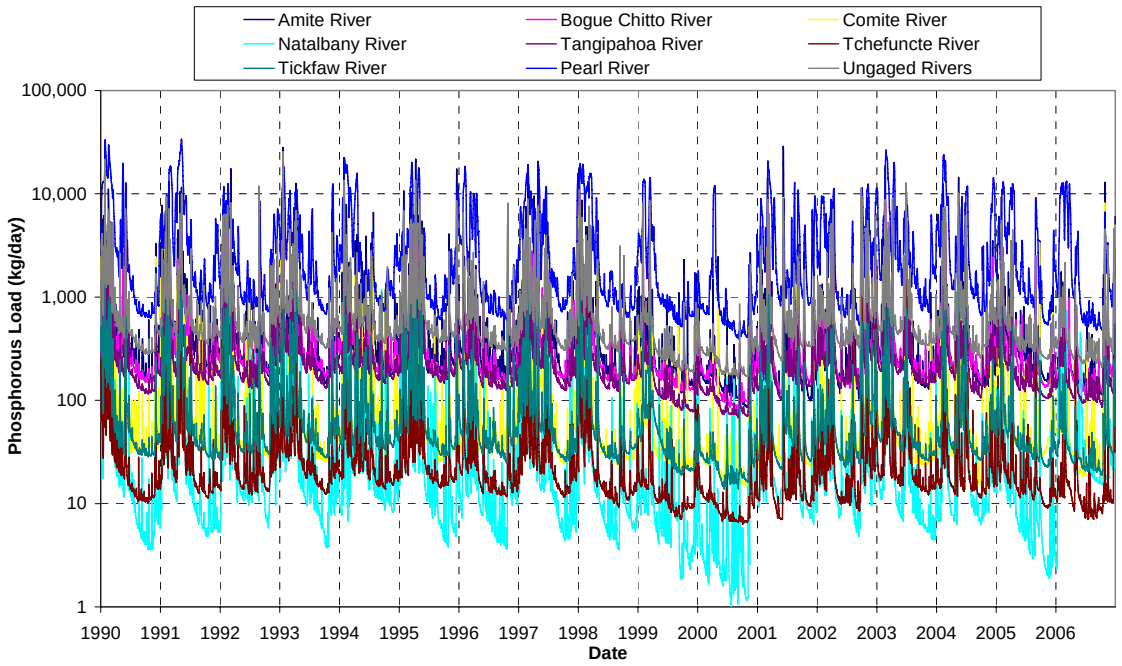

Figure 5.4 Daily tributary phosphorous loading for input into Pontchartrain Estuary model.

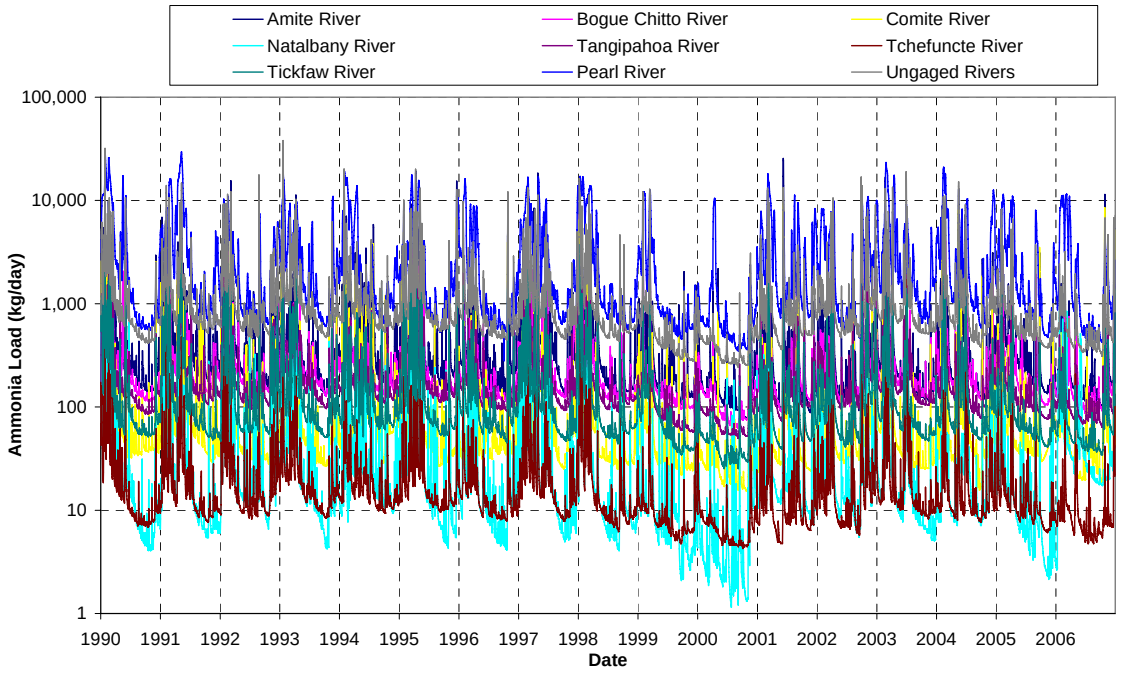

Figure 5.5 Daily tributary ammonia loading for input into the Pontchartrain Estuary model.

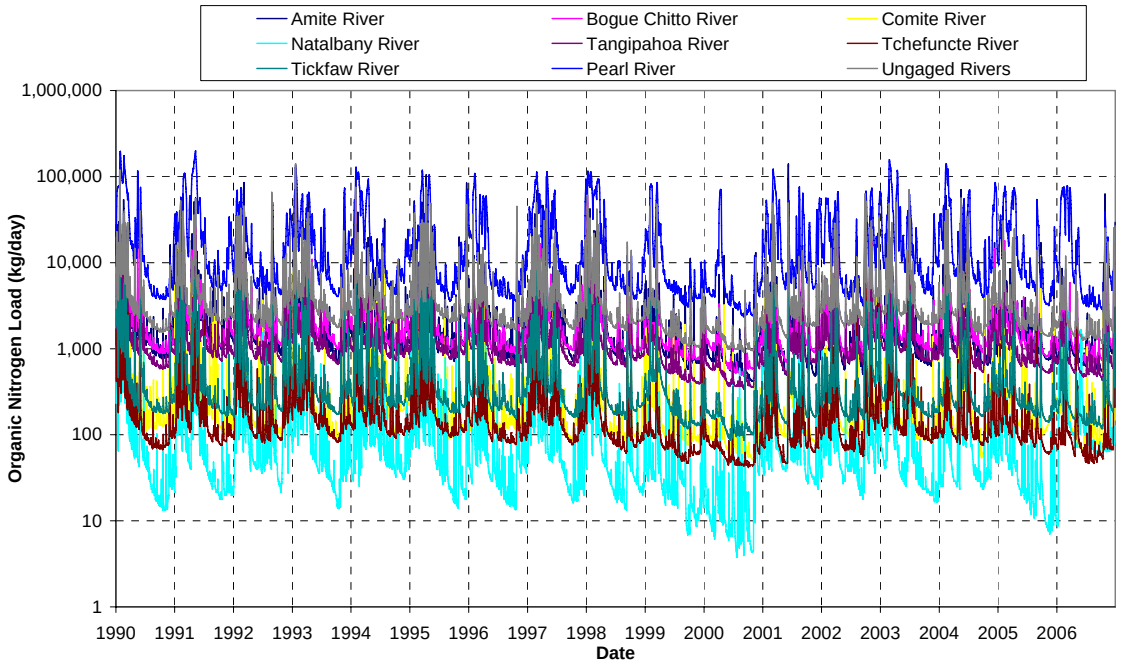

Figure 5.6 Daily tributary organic nitrogen loading for input into the Pontchartrain Estuary model.

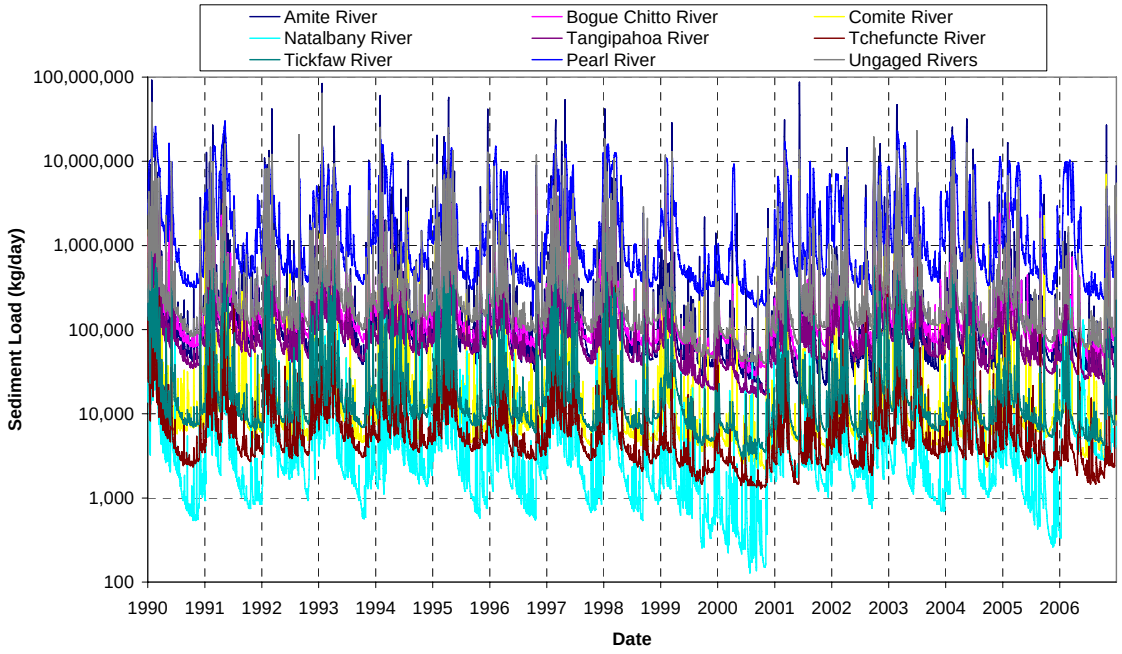

Figure 5.7 Daily tributary sediment loading for input into the Pontchartrain Estuary model.

5.3 Bonnet Carré Spillway Inputs

Daily inputs were also required from the Bonnet Carré Spillway. As mentioned in Section 3.3, flow was measured in the Bonnet Carré Spillway when it was opened in 1994 and 1997. A daily discharge record was developed by linearly interpolating between the different measurement dates. Leakage events were also added to the time-series using equation 3.1 reduced by 95% since flow only occurred through the creosote timber pins. This equation yielded a total of 853 days where leakage occurred from 1990 to 2006. All of the leakage events and the 1994 opening had discharges of less than 500 m^3/s. The opening and leakage events are shown in Figure 5.8. The large opening in 1997 (pink) is the associated with the right hand y-axis since flows were an order of magnitude higher than the 1994 and leakage flows. The data from the Bonnet Carré Spillway was input into the southwest cell in Lake Pontchartrain (Cell 10). Figure 5.9 shows the yearly distribution of the Bonnet Carré Spillway events (the large opening in 1997 is the only year associated with the right-hand y-axis).

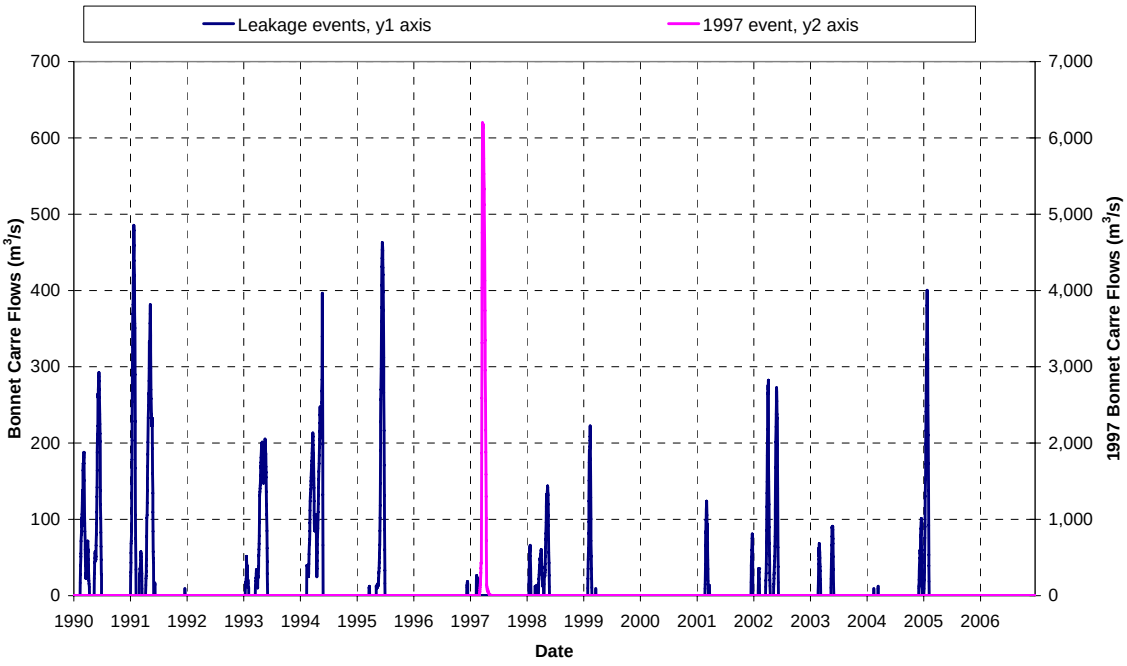

Figure 5.8 Daily Bonnet Carré Spillway flows input into the Pontchartrain Estuary model (1997 event, y2 axis).

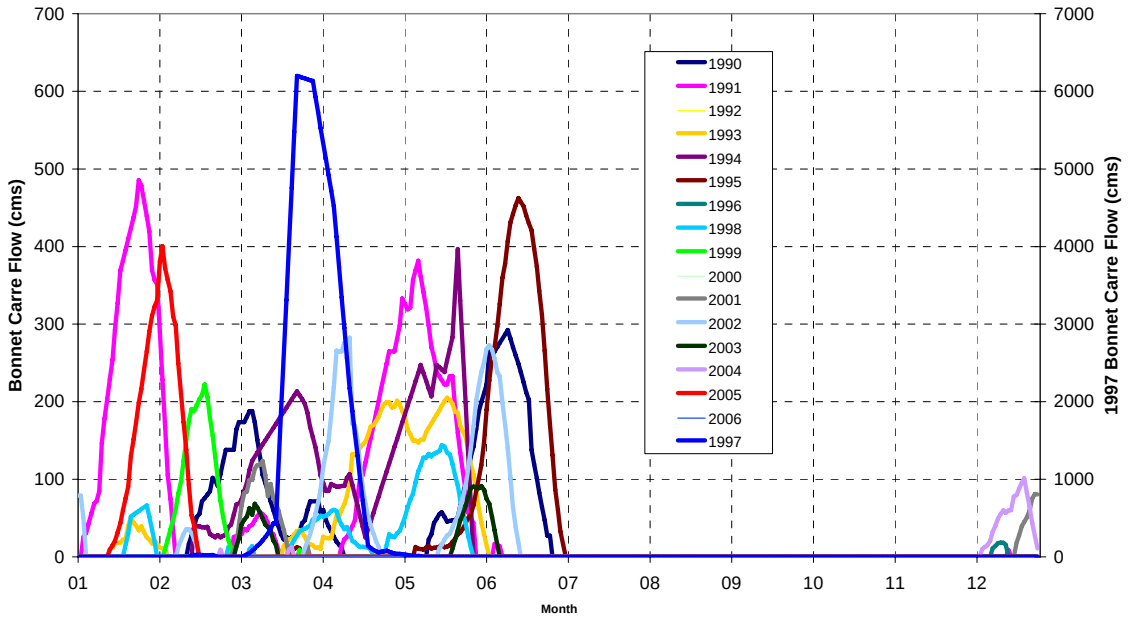

Figure 5.9 Annual distribution of the Bonnet Carré Spillway flows input into the Pontchartrain Estuary model (1997 event, y2 axis).

Daily nutrient and sediment concentrations from the Mississippi River were input into the model instead of loadings. Concentrations were entered so that information would not be lost during zero flow conditions (at no flow conditions, loadings would be equal to zero). Daily concentrations were produced from the measured records at the USGS St. Francisville and Luling gages. If daily data was missing from the record, the average values presented in Table 3.10 were used. The resultant concentrations input to the model are shown in Figure 5.10 and 5.11. If the flows were less than 500 m^3/s, then the concentrations were reduced according to the amounts found by Lane et al. (2001): suspended sediment concentrations decreased by 85%, nitrite + nitrate as nitrogen concentrations decreased by 17.5% (half of that recommended by Lane et al., 2001), ammonia and organic nitrogen concentrations decreased by 28% and total phosphorous concentrations decreased by 25% (half of that recommended by Lane et al., 2001) throughout the length of the spillway.

The daily nutrient and sediment concentrations from the Mississippi River developed here were also used as input for the proposed diversion scenarios. The same nutrient reductions discussed above were also applied. The flow conditions for the proposed scenarios differed from those used in the Bonnet Carré Spillway and will be discussed in section 8.0.

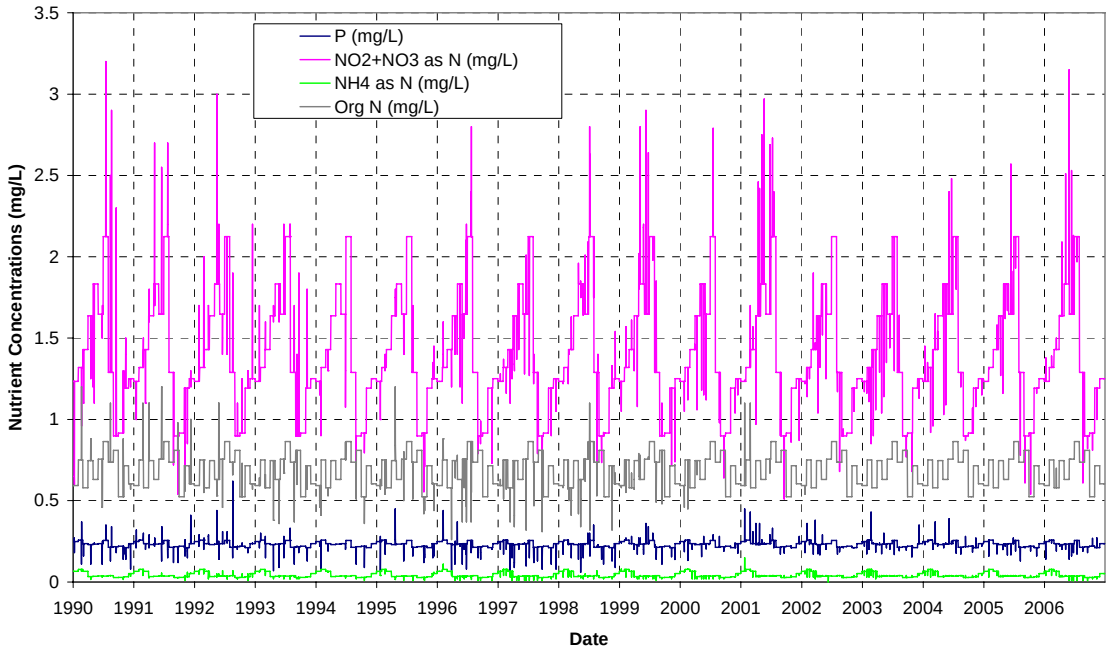

Figure 5.10 Daily Bonnet Carré Spillway nutrient concentrations input into the Pontchartrain Estuary model (does not include reductions).

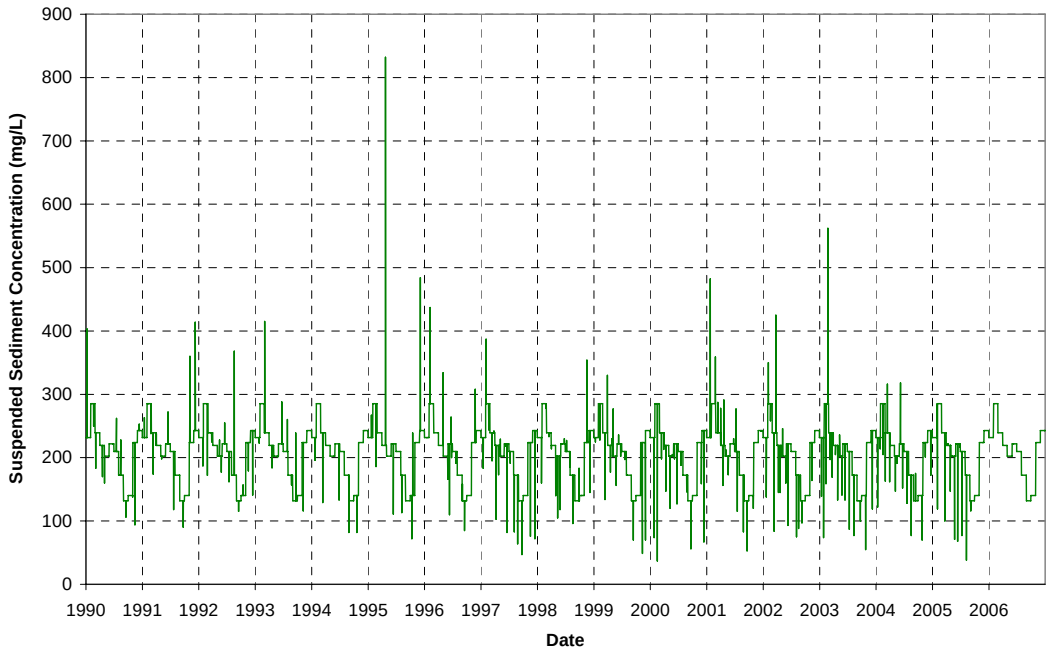

Figure 5.11 Daily Bonnet Carré Spillway suspended sediment concentrations input into the Pontchartrain Estuary model (does not include reductions).

5.4 *Atmospheric Inputs*

Atmospheric loadings were entered into the model as described in section 3.4. Figure 5.12 below shows the daily atmospheric loading variation from 1990 to 2006.

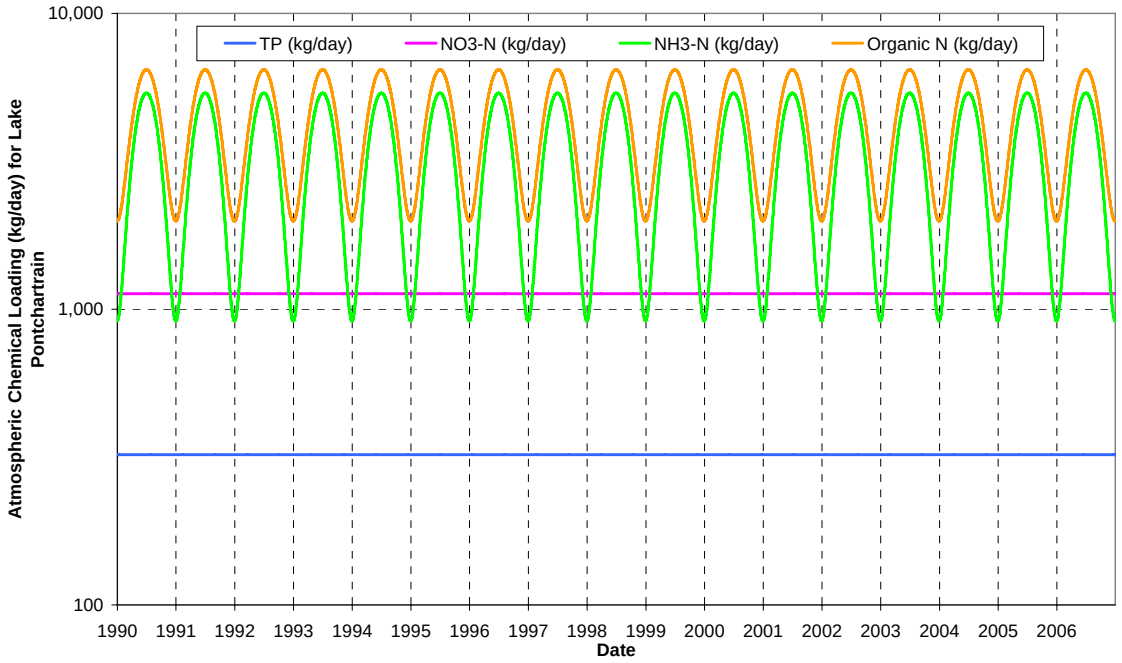

Figure 5.12 Daily atmospheric loadings input to the Lake Pontchartrain model.

5.5 *Meteorological Inputs*

Daily precipitation, evapotranspiration, air temperature, water temperature and wind speed were all input to the Lake Pontchartrain model as described above in section 3.5. Figure 5.13 to 5.15 below show the values input into the Pontchartrain Estuary model. Wind direction data was insufficient and was not included in the model.

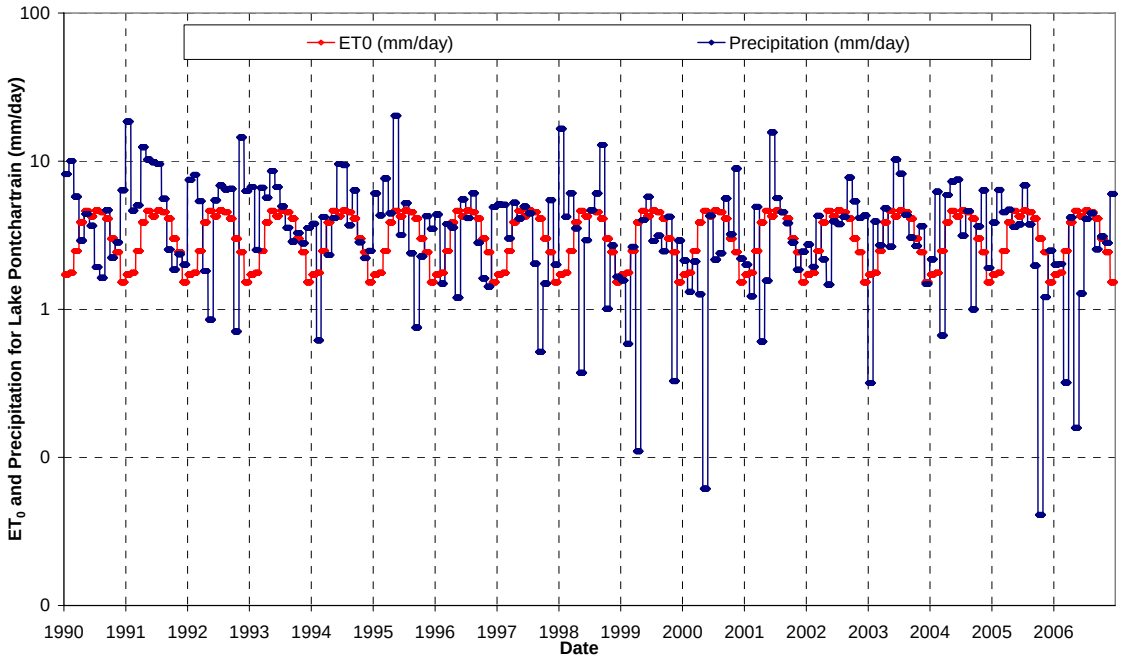

Figure 5.13 Daily precipitation and evapotranspiration rates input into the Pontchartrain Estuary model.

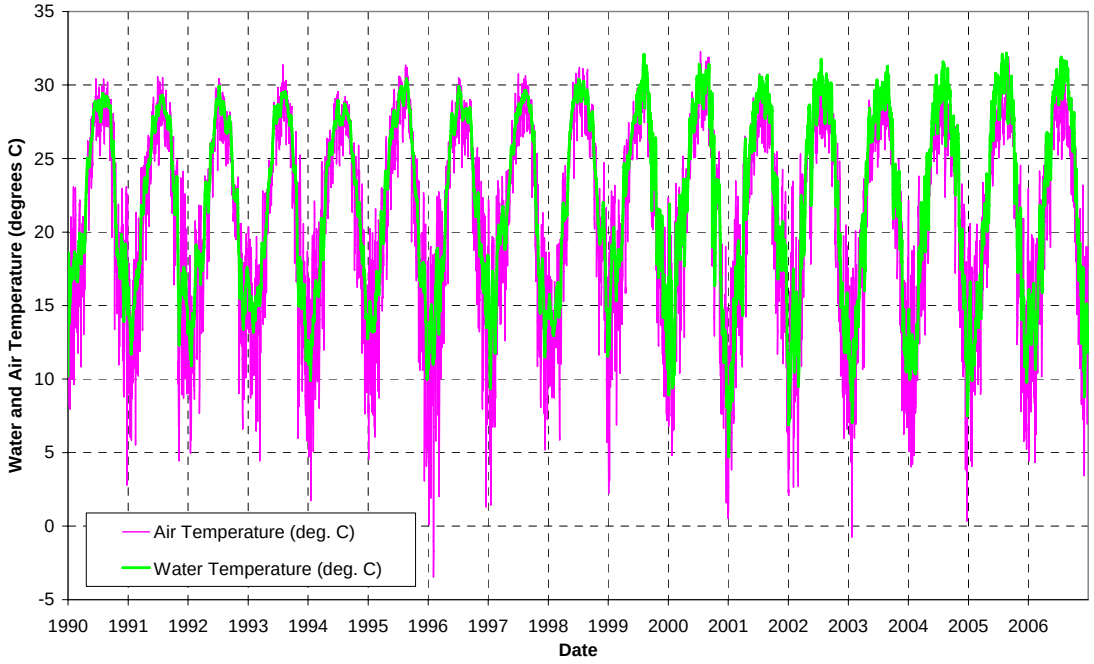

Figure 5.14 Daily air and water temperatures input into the Pontchartrain Estuary model.

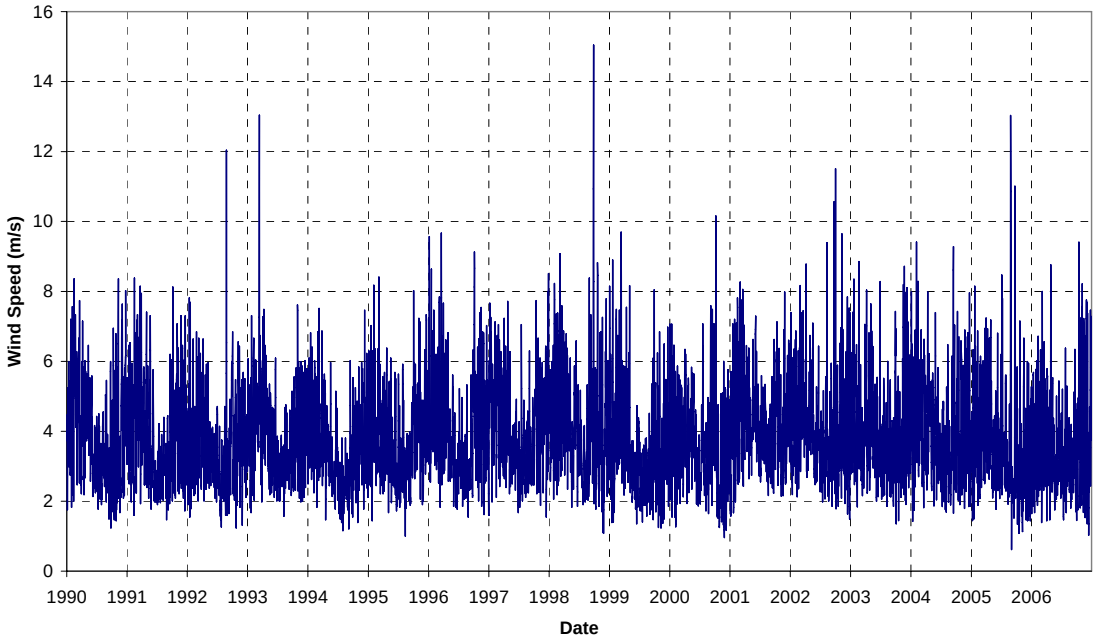

Figure 5.15 Average daily wind speed input into the Pontchartrain Estuary model.

6.0 Model calibration

6.1 Introduction

The model was calibrated to data that was measured in the Pontchartrain Estuary between January 1990 and December 1994. Only a few parameters are measured regularly enough in the Pontchartrain Estuary to be used in the calibration of the model. The measured datasets include salinity, nitrate + nitrite as nitrogen; phosphorous; total organic carbon; and TKN concentrations which are measured by the USGS, LADEQ, LUMCON and other researchers. The calibration of salinity is described in section 6.3. The nutrient calibrations are described in section 6.4. The tidal calibration is described in section 6.5 and the algal bloom probability model is interpreted in section 6.6.

It should be noted that these measured datasets are not extensive (spatially or temporally) and can only provide an approximation of the ambient conditions present in the Pontchartrain Estuary. It should also be noted that the regression equations (described in section 3.0) that were used to estimate the nutrient and sediment loadings in the tributaries and the spillway are also only approximations. Actual loadings may differ significantly from the regression estimates at specific times. Due to these inherent errors, the results produced from the model are only expected to capture general trends.

6.2 General calibration

The following general parameters were assigned during the calibration process: crop factor (k_{crop}) = 0.1; initial suspended solids concentration = 22 mg/L; resuspension coefficient (k_{rs}) = 1.0; resuspension calibration factor (k_{rsc}) = 1.3; settling velocity calibration factor (k_{set}) = 1.0; boundary suspended sediment calibration factor (k_{ls}) = 1.0; central difference/upwinding calibration factor = 0.54; dispersion calibration factor (k_{dis}) = 0.9 and the residence time (T_{res}) = 3600 s. The factors that were calibrated for each link are shown in Table 6.1. Of these parameters, the resuspension calibration factor, central difference/upwinding calibration factor and the dispersion calibration factor are the most important.

Table 6.1. Lake Pontchartrain link calibration factors.

Link No. (i)	From Cell Name	To Cell Name	Manning's n (n_i)	K_m (minor loss coefficient due to structures)	Diffusion calibration factor (k_{diff})
1	N.LB	G.O.M	0.025	0.00075	8
2	E.LP	N.LB	0.033	0.075	50
3	S.LB	N.LB	0.02	0.00075	5
4	E.LP	S.LB	0.02	0.75	50
5	S.MRGO	G.O.M	0.035	0	15,000
6	N.MRGO	S.MRGO	0.035	0	15,000
7	N.MRGO	S.LB	0.027	0	18,000
8	SE.LP	N.MRGO	0.025	0.1	500
9	NE.LP	E.LP	0.02	0	2.75
10	NE.LP	SE.LP	0.02	0	1.55
11	NW.LP	NE.LP	0.02	0	1.55
12	LM	NW.LP	0.02	0	80
13	S.MRGO	S.LB	0.05	0	8,000
14	SW.LP	NW.LP	0.02	0	1.55
15	SW.LP	SE.LP	0.02	0	1.55

6.3 Salinity calibration

Salinity was calibrated based on both quantitative and qualitative observations. The qualitative analysis will be discussed first. The calculated salinity output for all of the cells in the Pontchartrain Estuary model is shown below in Figure 6.1. The calculated relative salinity gradation is accurate: the highest concentrations are predicted near the Gulf of Mexico (in the MRGO and Lake Borgne) while the lowest concentrations are predicted in Lake Maurepas. Salinity decreases from east to west across Lake Pontchartrain with the highest values occurring near the Rigolets (east Lake Pontchartrain) and the IHNC (southeast Lake Pontchartrain). The vertical black dashed lines in the figure indicate the months where high rainfall occurred (2nd and 5th wettest years between 1990 and 2006). The model captures the freshening effect that increased rainfall would have on the Pontchartrain Estuary.

Large flows from the tributaries and openings of the Bonnet Carré Spillway will also have a freshening effect on the Pontchartrain Estuary. Leakage events occurred on the Bonnet Carré Spillway in March and June of 1990, January and May of 1991 and 1993, and March and May of 1994 over the calibration period (see Figure 5.8). The model salinity decreased in the areas near the Bonnet Carré Spillway in response to these events. The freshening in 1992 is likely due to high rainfall. The range of salinity concentrations is much higher for north Lake Borgne and east Lake Pontchartrain due to the contribution of freshwater from the Pearl River and the proximity to the Gulf of Mexico. During high flows, freshwater from the Pearl River can enter Lake Pontchartrain on flood tides and significantly effect the lake's salinity regime.

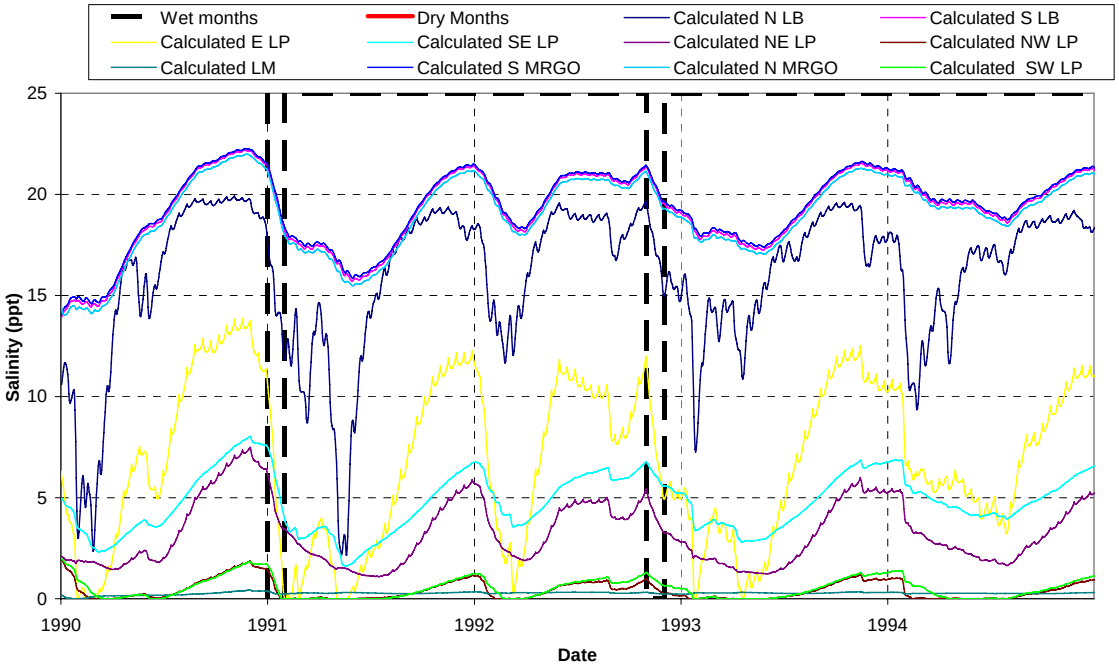

Figure 6.1 Calculated salinity for each cell in the Lake Pontchartrain model (1990-1995).

Salinity was measured by both the LADEQ and the USGS in the Pontchartrain Estuary. Figure 6.2. shows the predicted results for the Pontchartrain Estuary cells (solid lines) with the measured data (points). The dotted bars associated with the measured data points show the standard deviation of the dataset. As can be seen, all of the measured data falls within the predicted results. In particular, the LADEQ data measured in the north part of Lake Pontchartrain (causeway at Covington and causeway south of Mandeville) lies between the predicted NW and NE Lake Pontchartrain results and the LADEQ data measured in the southern part of Lake Pontchartrain (causeway near Metairie and causeway north of Metairie) lies between the results for the SE and SW cells of Lake Pontchartrain. Since the causeway is located at the boundary between the east and west cells, the model is corresponding accurately to the measured data. All of the USGS measurements were taken during the 1994 experimental opening and also all lie within the predicted results. Figure 6.3. shows the results for the calibration period in Lake Borgne. The eastern cell of Lake Pontchartrain corresponds very well to the measured USGS and LADEQ data on the Rigolets and Chef Menteur Passes (located on the eastern boundary of the cell). No salinity measurements were available on Lake Maurepas for the calibration period.

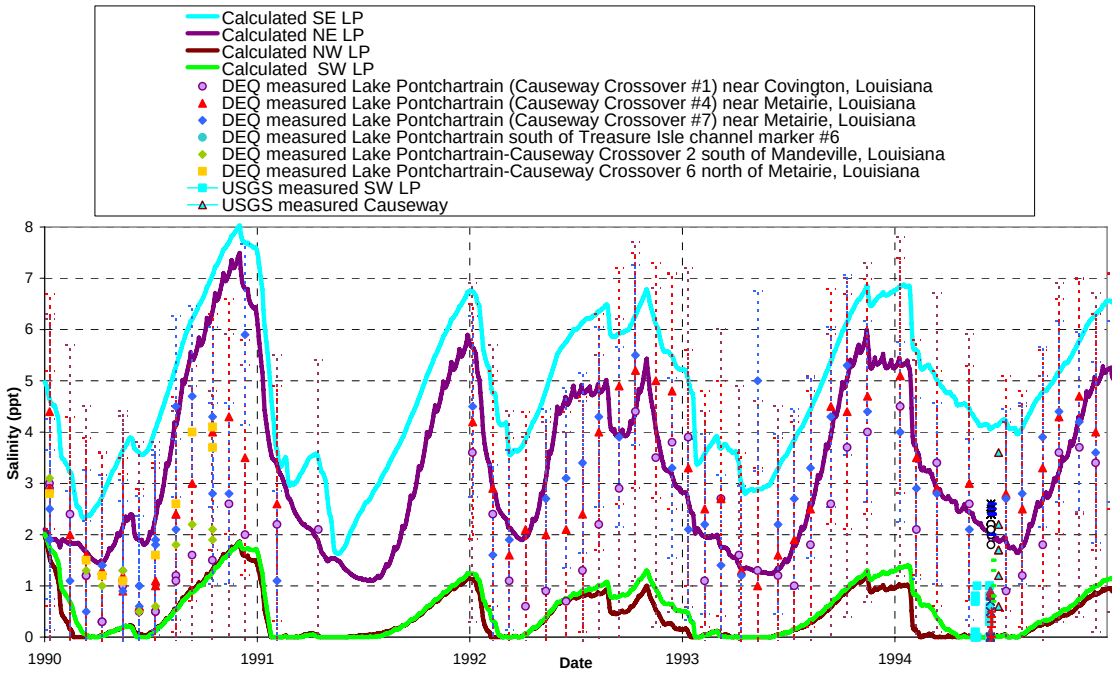

Figure 6.2 Salinity calibration on Lake Pontchartrain (1990-1995).

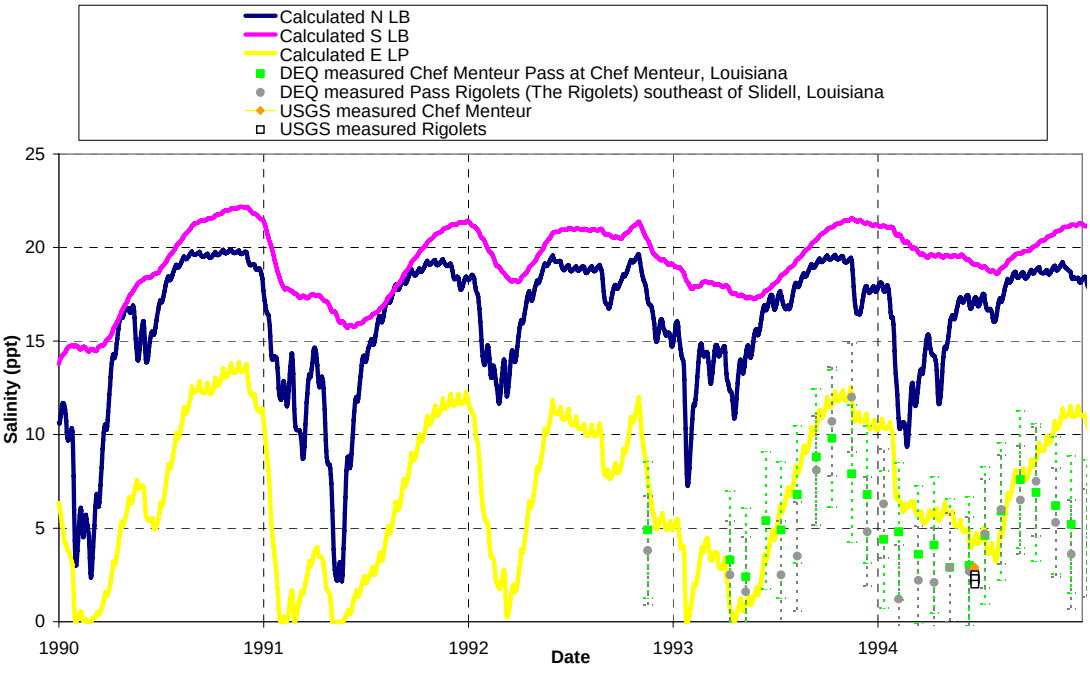

Figure 6.3 Salinity calibration on Lake Borgne (1990-1995).

6.4 Nutrient calibration

The model was calibrated to measured nitrate + nitrite as nitrogen, phosphorous, TKN and total organic carbon concentration measurements between January 1990 and December 1994 on the Pontchartrain Estuary. The rate constants determined during the calibration process are described in section 6.4.1. Comparisons between the measured data and the calculated results are shown in sections 6.4.2 to 6.4.5.

6.4.1 Calibration constants

The rate constants defined during the calibration period are listed in Table 6.2 below.

Table 6.2 Rate constants defined in the Pontchartrain Estuary model (table continued).

Process name	Parameter	Value	Reference
Nitrite + nitrate as nitrogen			
Denitrification	$k_{g0,NO3}$	-0.045	Jenkins (1984)
Nitrification	$k_{NH4\rightarrow NO3}$	+0.1 to 0.2	
Uptake	$k_{NO3\rightarrow LA}$	-1.0	
Ammonia			
Volatilization/Nitrification	$k_{g0,NH4}$	-0.01 to -0.21	
Ammonification	$k_{ON\rightarrow NH4}$	+0.004	
Uptake	$k_{NH4\rightarrow LA}$	-1.0	
DIN			
DIN Michaelis constant	k_{DIN}	20	Thomann (1987)
Organic Nitrogen			
Settling	$k_{g0,ON}$	-0.000001	
Ammonification	$k_{ON\rightarrow NH4}$	-0.00001	
Death rate	$k_{LA\rightarrow ON}$	+1.0	
Phosphorous			
Settling	$k_{g0,P}$	-0.002	
Uptake	$k_{P\rightarrow LA}$	-1.0	
P Michaelis constant	k_P	3.0	Thomann (1987)
Carbon			
Death rate	$k_{LA\rightarrow C}$	+0.015	
Dissolved Oxygen			
Reaeration	$k_{g0,DO}$	+1.0	Chapra (2003)
Nitrification	$k_{DO\rightarrow NH4}$	-0.2	Chapra (1997)
Photosynthesis	$k_{LA\rightarrow DO}$	+0.05	
Respiration	$k_{DO\rightarrow DA}$	-0.1	
Dead Algae			
Build up	$k_{g0,DA}$	+0.05	
Ammonification	$k_{DA\rightarrow NH4}$	-0.0005	
Anaerobic respiration	$k_{DA\rightarrow DO}$	-0.005	
Live Algae			

Maximum growth rate	$k_{g0,LA}$	+0.25	Thomann (1987)
Death rate	$k_{LA \rightarrow DA}$	-0.0005	Thomann (1987)
Other			
SS Michaelis constant	k_{SS}	30	Thomann (1987)
S Michaelis constant	k_s	4.0	Thomann (1987)

6.4.2 Nitrite + nitrate as nitrogen calibration

The model was calibrated to data measured by the LADEQ on the Pontchartrain Estuary between January 1990 and December 1994. Nitrite + nitrate as nitrogen concentrations were reduced by 17.5% (half of that recommended by Lane et al., 2001) when the corresponding flows on the Bonnet Carré Spillway were less than 500 m^3/s. When the flows were greater than 500 m^3/s , the loads were not reduced. Nitrite + nitrate as nitrogen concentrations increased as a result of nitrification (conversion of ammonia) and decreased as a result of denitrification (loss to the atmosphere) and uptake from algae.

The comparisons between the predicted results and the data measured by the LADEQ are shown below for Lakes Maurepas, Pontchartrain and Borgne in Figures 6.4 to 6.6. The solid lines in the figures represent the model output for each cell, the points represent the measured data, and the dotted bars associated with the measured data represent the standard deviation of the data.

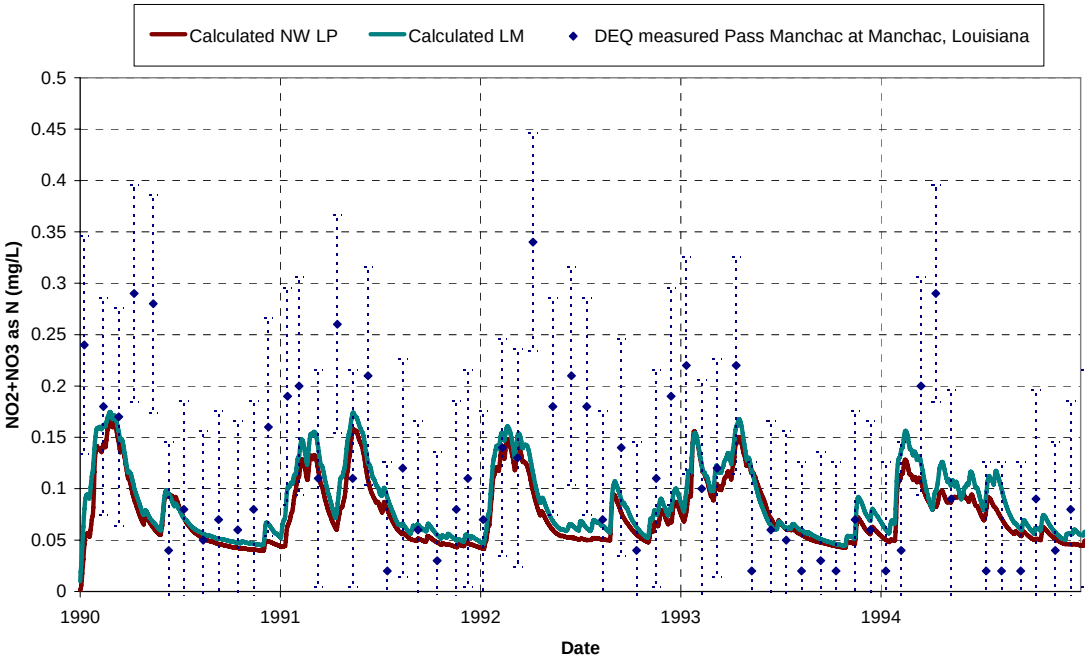

Figure 6.4 Nitrite + nitrate as nitrogen calibration on Lake Maurepas (1990-1995).

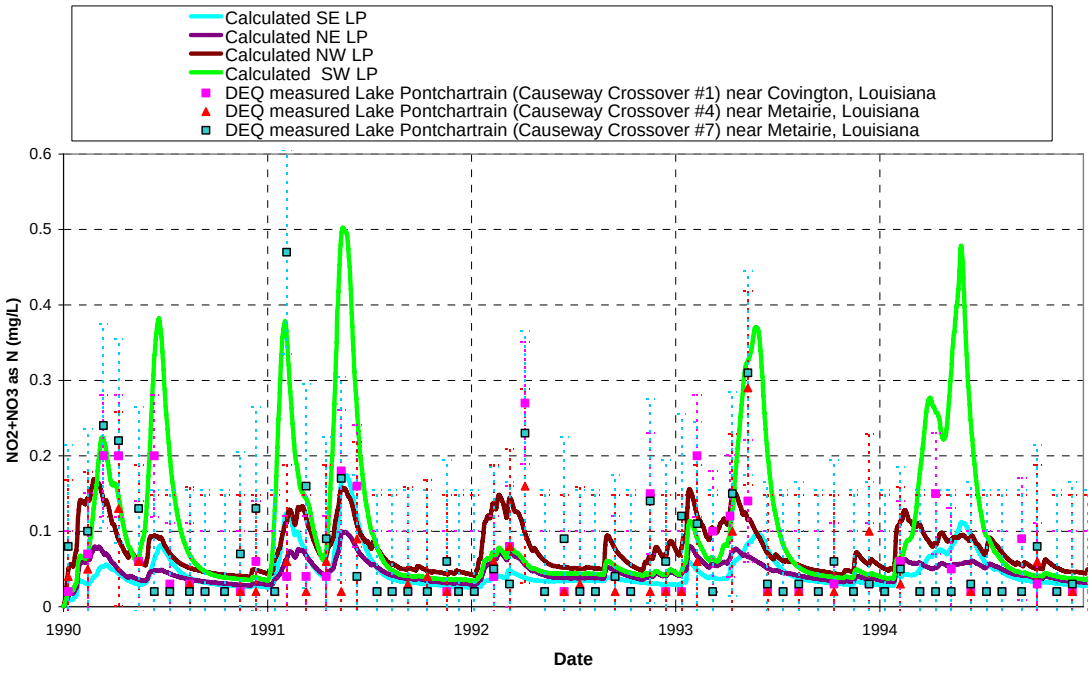

Figure 6.5 Nitrite + nitrate as nitrogen calibration on Lake Pontchartrain (1990-1995).

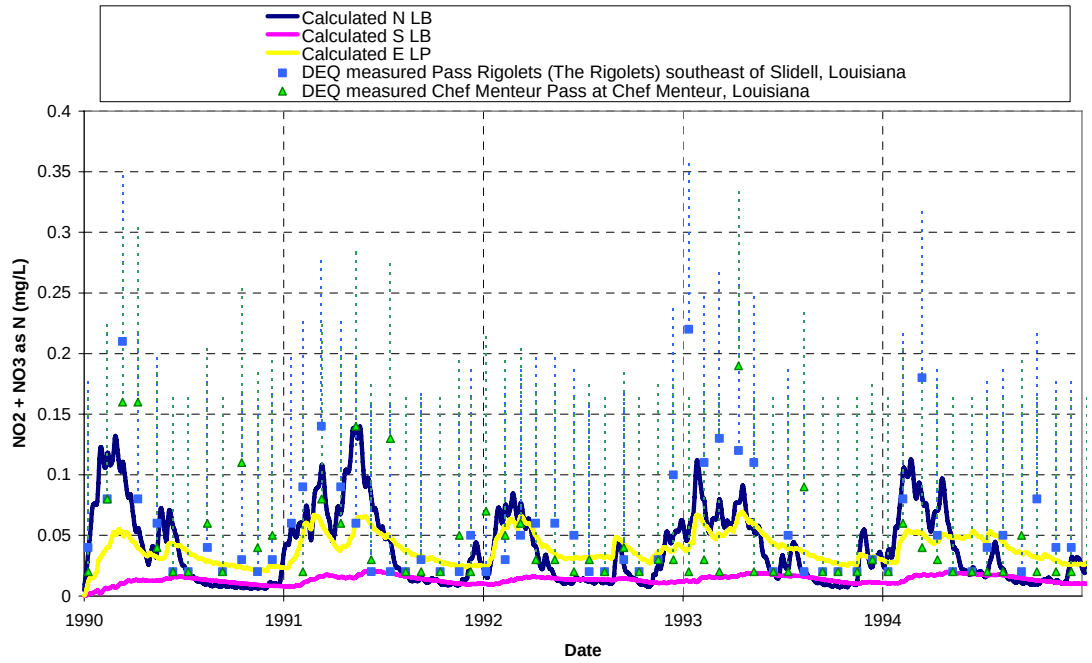

Figure 6.6 Nitrite + nitrate as nitrogen calibration on Lake Borgne (1990-1995).

During the calibration period, leakage events from the Bonnet Carré Spillway occurred in March and June of 1990, January and May of 1991 and 1993, and March and May of 1994 (see Figure 5.8). The effect of the Bonnet Carré Spillway leakage events on the modeled nitrite +nitrate as nitrogen concentrations can be observed in the plots above. During each of the leakage events, the predicted concentrations increased above the background nitrite + nitrate as nitrogen concentrations of approximately 0.04 to 0.05 mg/L (closer to 0.02 mg/L for Lake Borgne). The closer the cell was to the Bonnet Carré Spillway, the higher the concentrations increased. For example, southwest Lake Pontchartrain concentrations increased the most (above 0.2 mg/L) and south Lake Borgne concentrations increased the least. The peak in 1992 is not explained from leakage in the Bonnet Carré Spillway and may be due to increased precipitation during that period.

The modeled data generally corresponds well to the measured data. Concentrations are over-predicted in some areas, and under-predicted in other areas but the modeled concentrations generally fall within the standard deviation of the datasets. Considering the limited extent of the measured data (both spatially and temporally), the modeled results seem to behave satisfactorily. However, the model underestimates the concentrations in Lake Borgne. The cause of the underestimation will be discussed in section 9.0.

The modeled results for dissolved inorganic nitrogen (DIN) are shown in Figure 6.7 below. DIN is equivalent to the summation of nitrite + nitrate as nitrogen and ammonia concentrations and behaves similarly to the nitrite + nitrate as nitrogen modeled results described above.

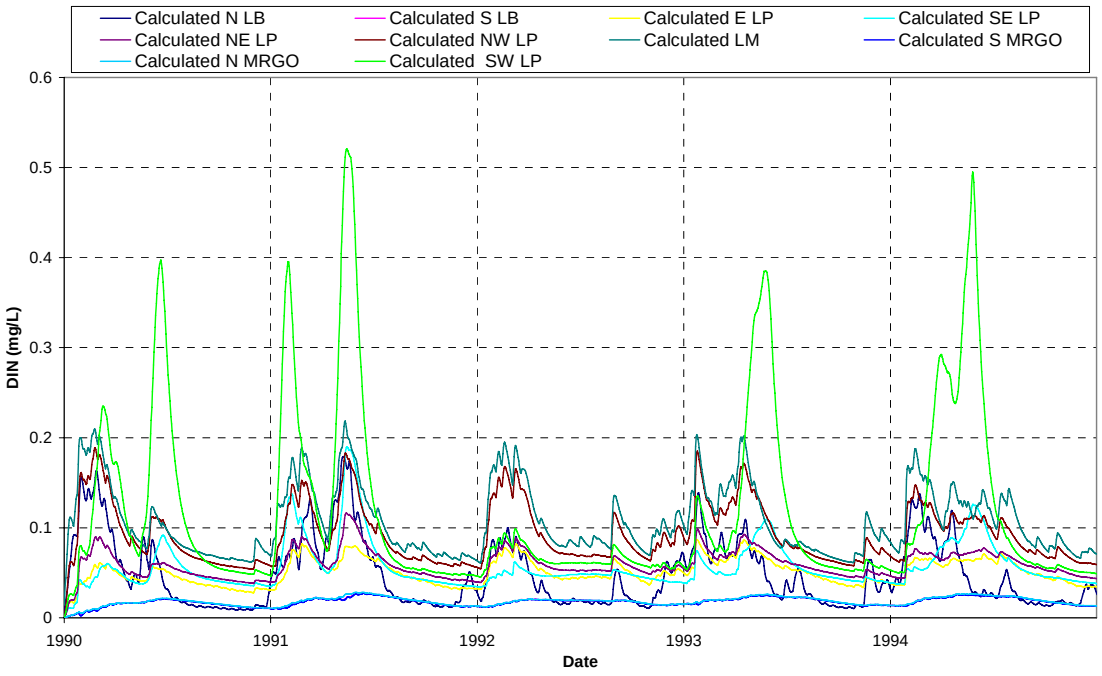

Figure 6.7 Calculated DIN concentrations (1990-1995).

6.4.3 Phosphorous calibration

The model was calibrated to data measured by the LADEQ and the USGS in the Pontchartrain Estuary from January 1990 to December 1994. Total phosphorous concentrations were reduced by 25% (half of that recommended by Lane et al., 2001) when the corresponding flows into the Bonnet Carré Spillway were less than 500 m^3/s. Concentrations were not reduced for flows greater than 500 m^3/s. Phosphorous concentrations were reduced by uptake from algae and settling processes.

Comparisons between the predicted phosphorous concentrations and the measured data are shown below for Lakes Maurepas, Pontchartrain and Borgne (Figures 6.8 to 6.10). The solid lines in the figures represent the model output for each cell, the points represent the measured data, and the dotted bars associated with the measured data represent the standard deviation of the data.

The increases as a result of the Bonnet Carré Spillway leakage events are less pronounced for the phosphorous concentrations than the nitrite + nitrate as nitrogen concentrations. The modeled data in Lake Maurepas and northwest Lake Pontchartrain corresponds well to the measured data at Pass Manchac, which lies between them (Figure 6.8). The modeled data in eastern Lake Pontchartrain also corresponds well to the measured data on the Rigolets and Chef Menteur Passes located on the eastern edge of the cell (Figure 6.10). The model underestimates the concentrations in Lake Borgne. The cause of the underestimation will be discussed in section 9.0. The modeled data around Lake Pontchartrain produces slightly higher values than the measured results along the causeway, but generally falls within the error bars and follows the seasonal pattern.

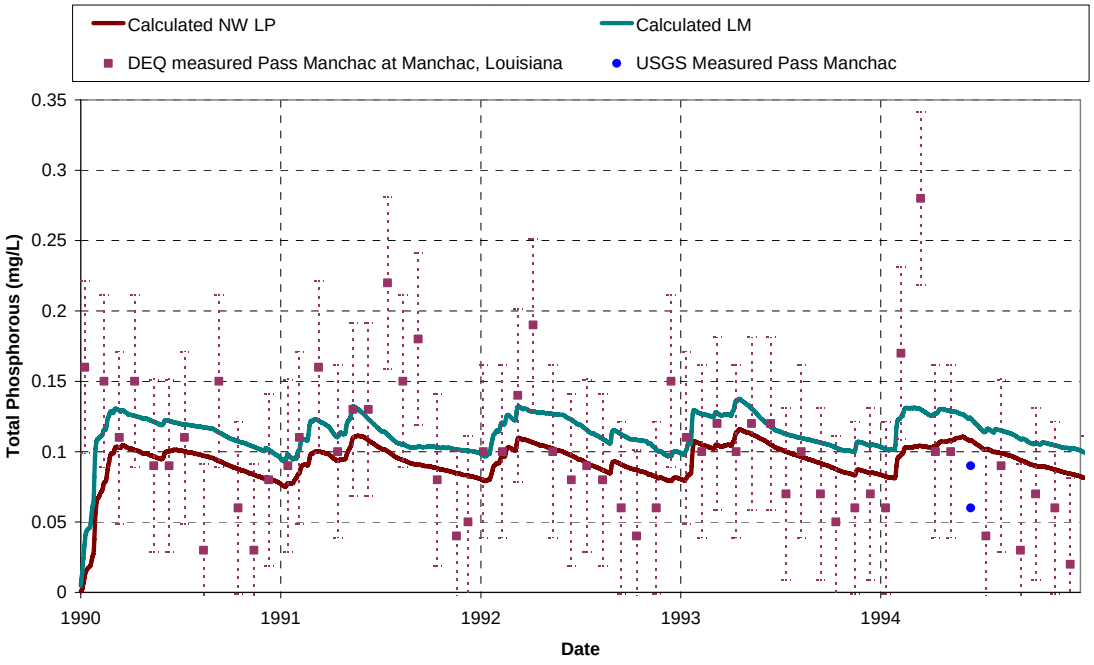

Figure 6.8 Total phosphorous calibration on Lake Maurepas (1990-1995).

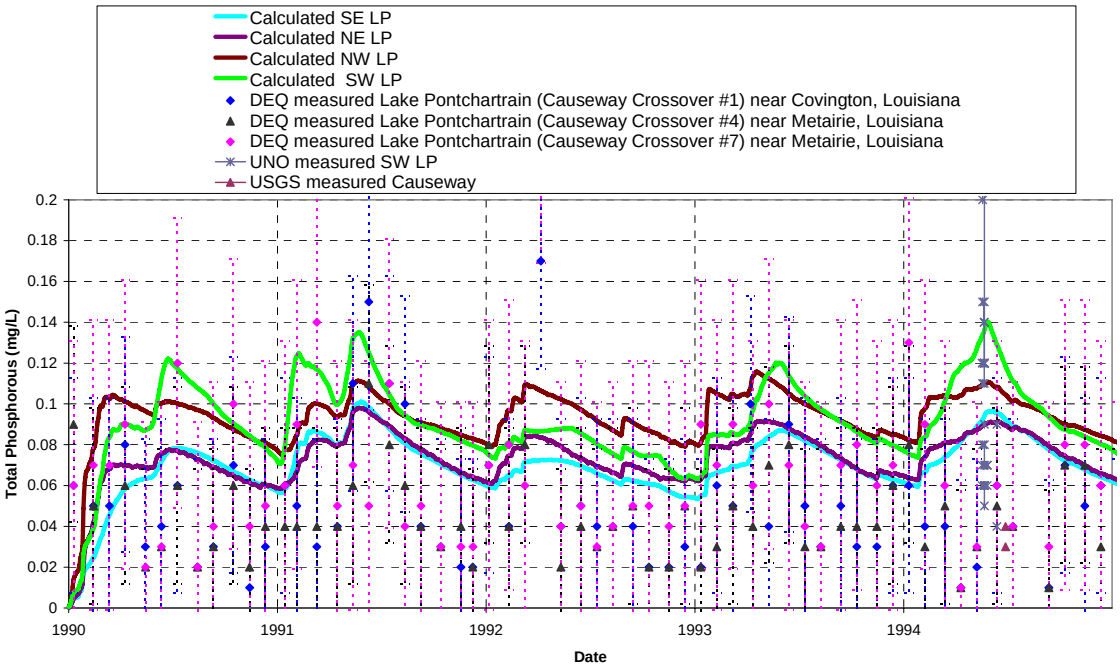

Figure 6.9 Total phosphorous calibration on Lake Pontchartrain (1990-1995).

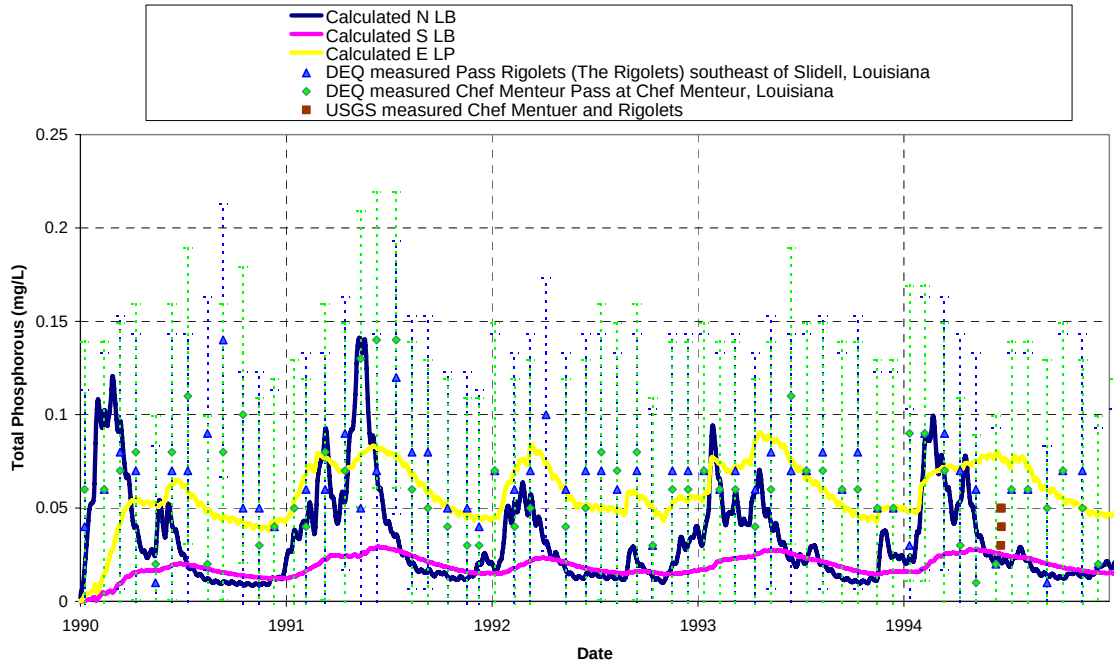

Figure 6.10 Total phosphorous calibration on Lake Borgne (1990-1995).

6.4.4 Total kjeldahl nitrogen (TKN) calibration

The model was calibrated to TKN data measured by the LADEQ and USGS in the Pontchartrain Estuary between January 1990 and December 1994. TKN measurements are equivalent to the summation of organic nitrogen and ammonia concentrations. Ammonia and organic nitrogen concentrations from the Bonnet Carré Spillway were decreased by 28% for flows less than 500 m^3/s. Concentrations were not reduced for flows above 500 m^3/s. Ammonia concentrations decrease as a result of volatilization, nitrification (conversion to nitrite and nitrate), and uptake from algae; and increase due to ammonification (from organic nitrogen), and sedimentation (from dead algae). Organic nitrogen concentrations decrease by ammonification and settling; and increase due to inputs from live algae.

Comparisons between the predicted TKN concentrations and the measured data are shown below for Lakes Maurepas, Pontchartrain and Borgne (Figures 6.11 to 6.13). The solid lines in the figures represent the model output for each cell, the points represent the measured data, and the dotted bars associated with the measured data represent the standard deviation of the data. The predicted results for ammonia and organic nitrogen are shown separately in Figures 6.14 and 6.15.

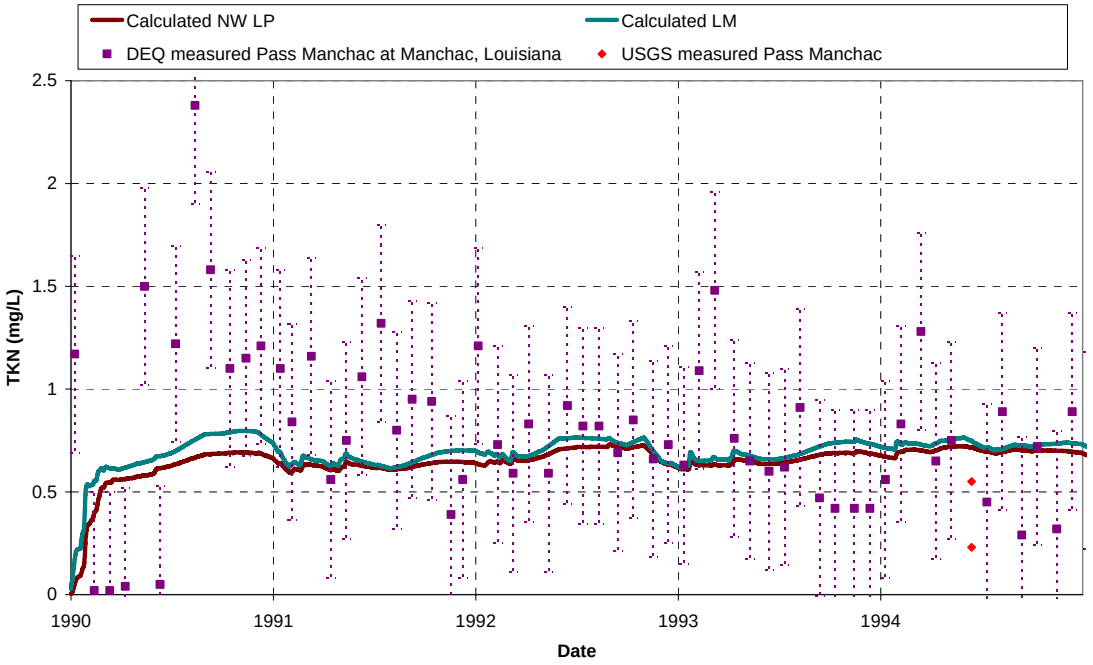

Figure 6.11 TKN calibration on Lake Maurepas (1990-1995).

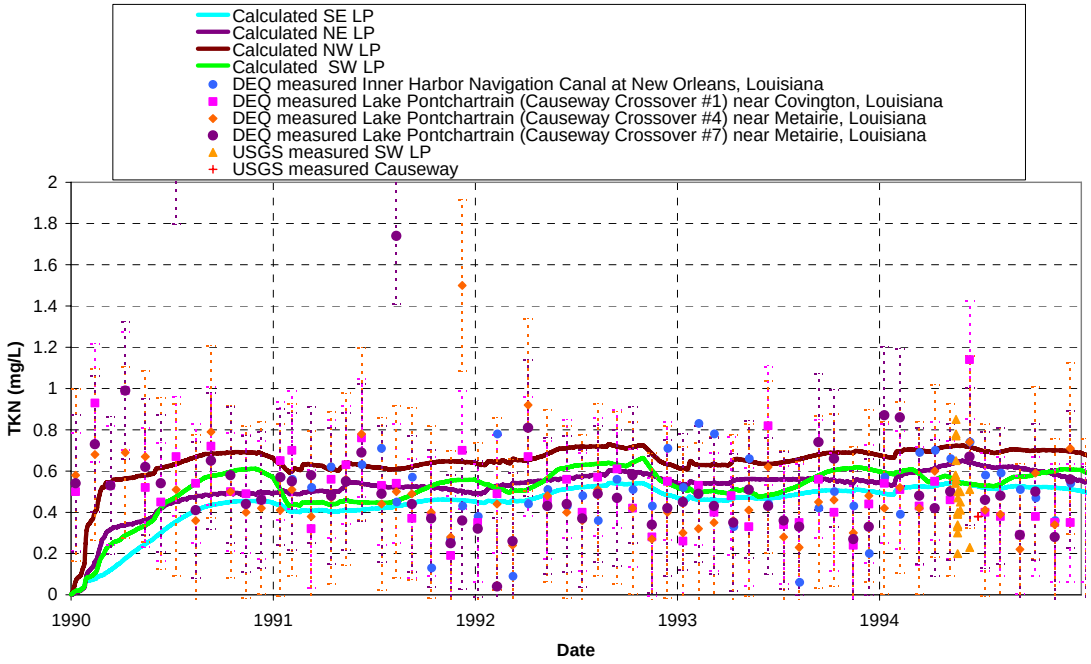

Figure 6.12 TKN calibration on Lake Pontchartrain (1990-1995).

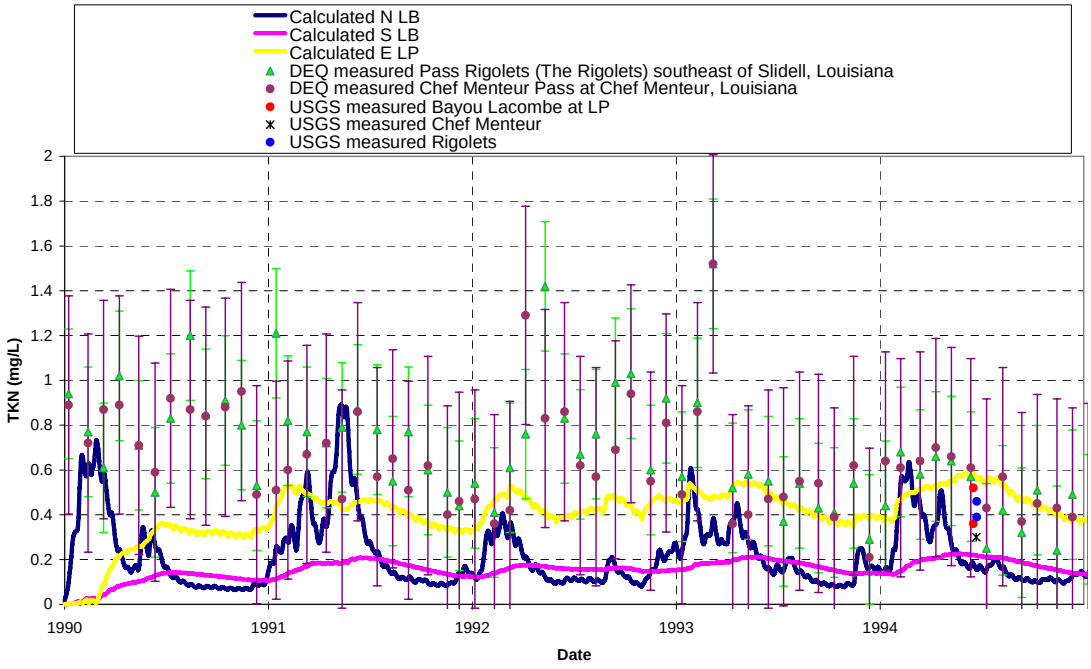

Figure 6.13 TKN calibration on Lake Borgne (1990-1995).

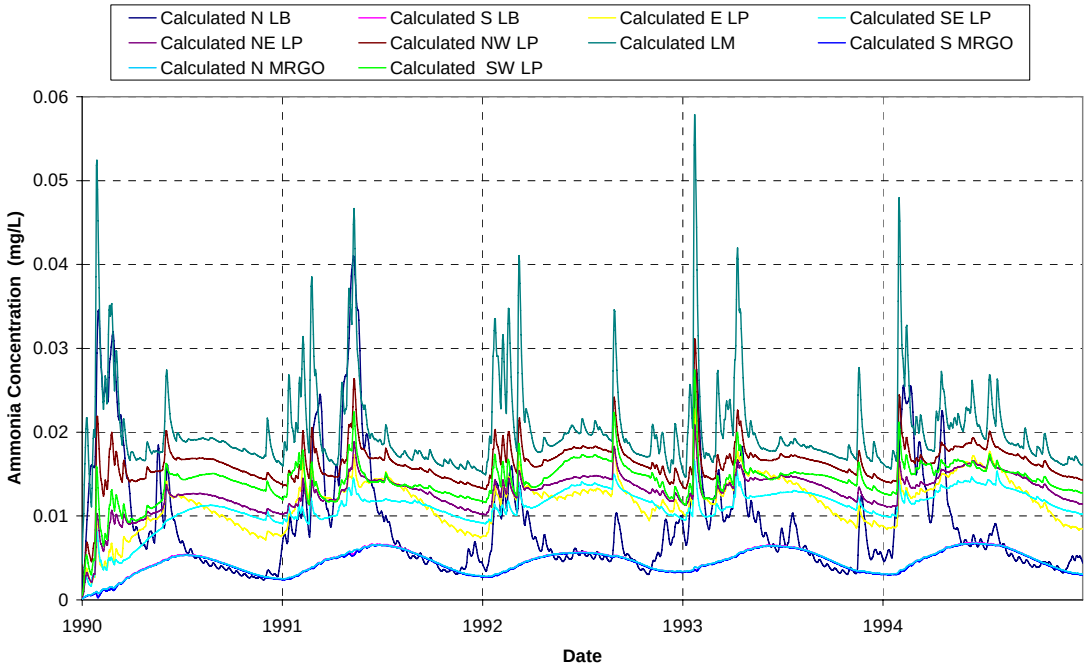

Figure 6.14 Calculated ammonia concentrations (1990-1995).

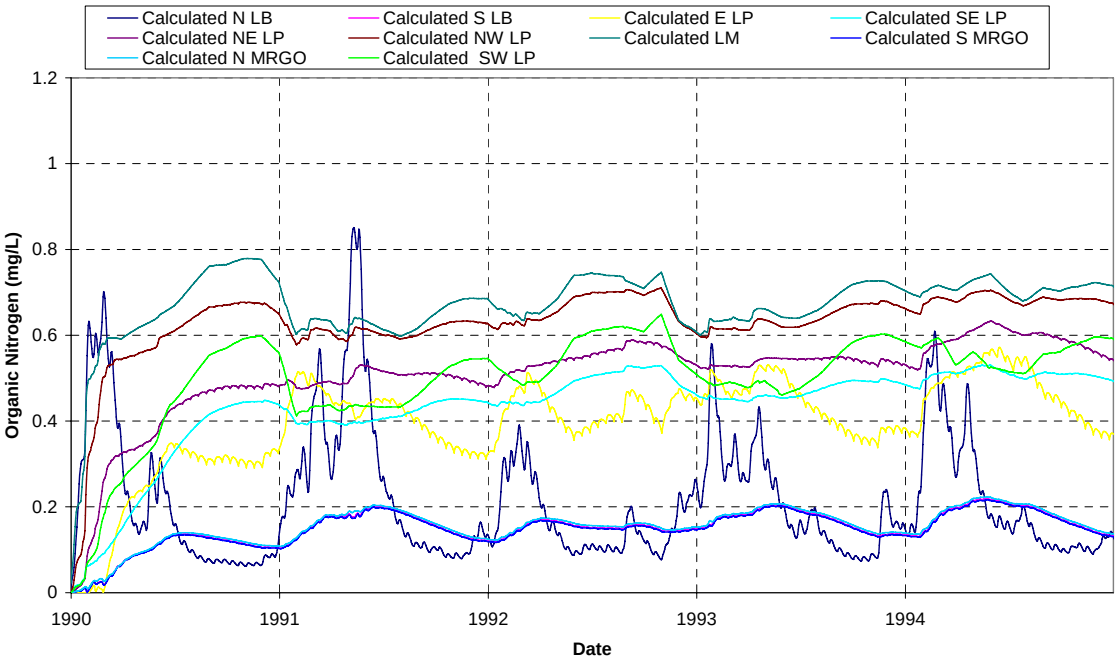

Figure 6.15 Calculated organic nitrogen concentrations (1990-1995).

The measured results indicate that TKN concentrations do not vary significantly with time around the Pontchartrain Estuary. As mentioned earlier, TKN is equivalent to the summation of organic nitrogen and ammonia concentrations. Looking at the results presented in Figures 6.14 and 6.15, it is clear that the modeled organic nitrogen concentrations are dominant over the modeled ammonia concentrations. The modeled ammonia concentrations behave similarly to the nitrite + nitrogen as nitrogen results (the concentrations are influenced by Bonnet Carré Spillway openings). The organic nitrogen and predicted TKN results are not influenced by the Spillway and do not vary significantly with time.

The modeled TKN data agrees with the measured data on Lake Pontchartrain and Lake Maurepas sufficiently between 1991 and 1995. The modeled data are not accurate for the first year (1990) since it took about six months to ramp up to the appropriate background concentrations. The modeled TKN data in east Lake Pontchartrain agree sufficiently with the measured data from the Rigolets and Chef Menteur in 1991, 1993 and 1994. The predicted results are under-predicted in 1992 but still fall within the measured error bars. The model underestimates the concentrations in Lake Borgne. The cause of the underestimation will be discussed in section 9.0.

6.4.5 Total organic carbon (TOC) calibration

The model was calibrated to total organic carbon (TOC) data measured by the LADEQ in the Pontchartrain Estuary between January 1990 and December 1994. TOC concentrations were assumed to be equivalent to the summation of live algae, dead algae, carbon and 7% of the suspended sediment concentrations output by the model. Suspended sediment concentrations decreased by 85% (Lane et al., 2001) for corresponding flows from the Bonnet Carré Spillway of less than 500 m^3/s. Concentrations were not reduced when flows exceeded 500 m^3/s. The interactions that affect live algae, dead algae, carbon and suspended sediment concentrations are discussed in section 4.0.

Comparisons between the predicted TOC concentrations and the measured LADEQ data are shown below for Lakes Maurepas, Pontchartrain and Borgne (Figures 6.16 to 6.18). The solid lines in the figures represent the model output for each cell, the points represent the measured data, and the dotted bars associated with the measured data represent the standard deviation of the data. The predicted results for live algae, dead algae, carbon and suspended sediment concentrations are shown separately in Figures 6.19 to 6.22.

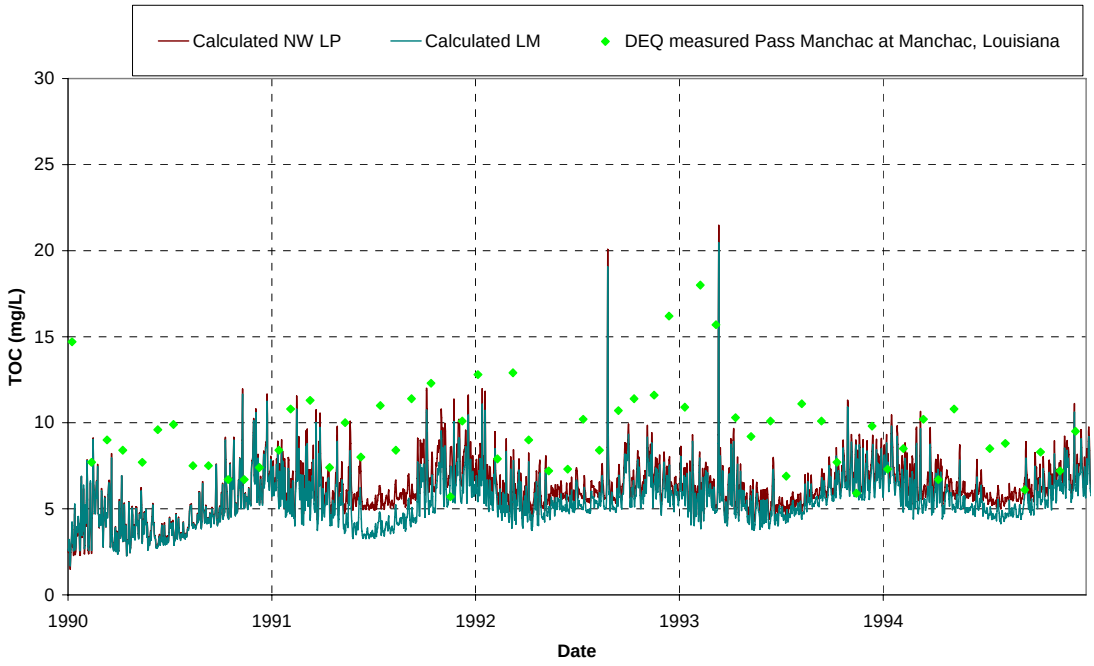

Figure 6.16 TOC calibration on Lake Maurepas (1990-1995).

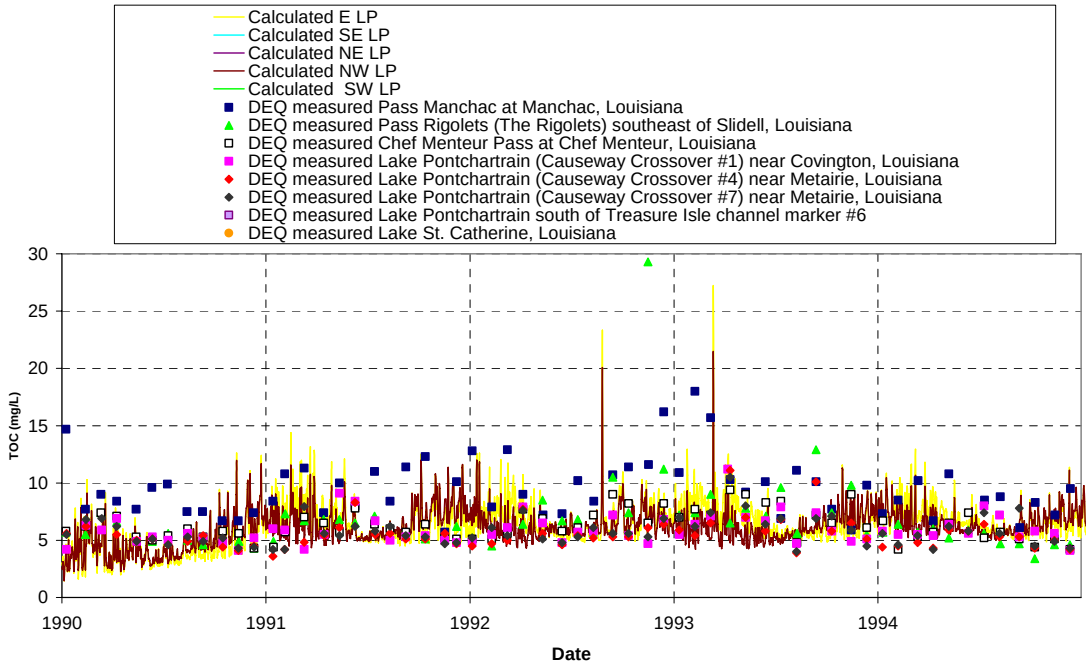

Figure 6.17 TOC calibration on Lake Pontchartrain (1990-1995).

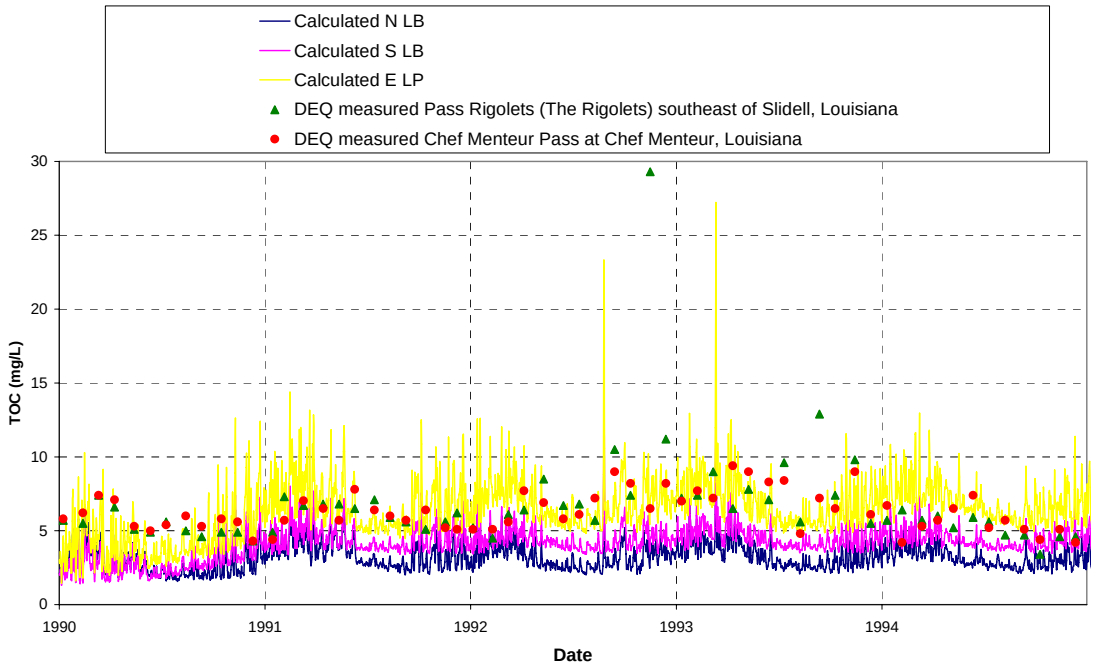

Figure 6.18 TOC calibration on Lake Borgne (1990-1995).

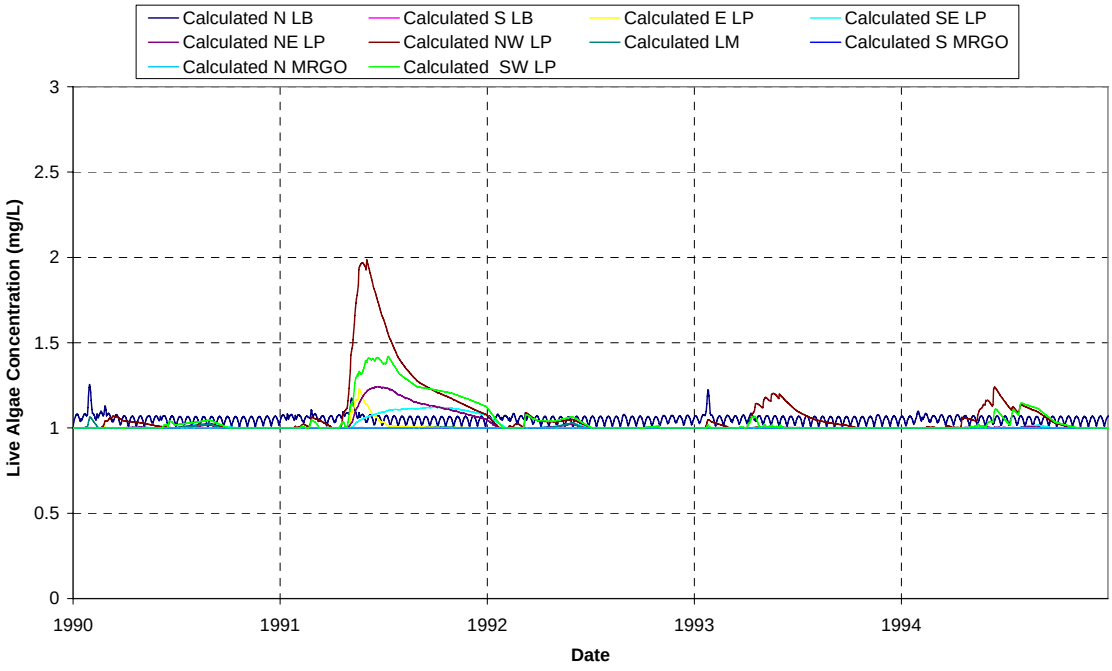

Figure 6.19 Calculated live algae concentrations (1990-1995).

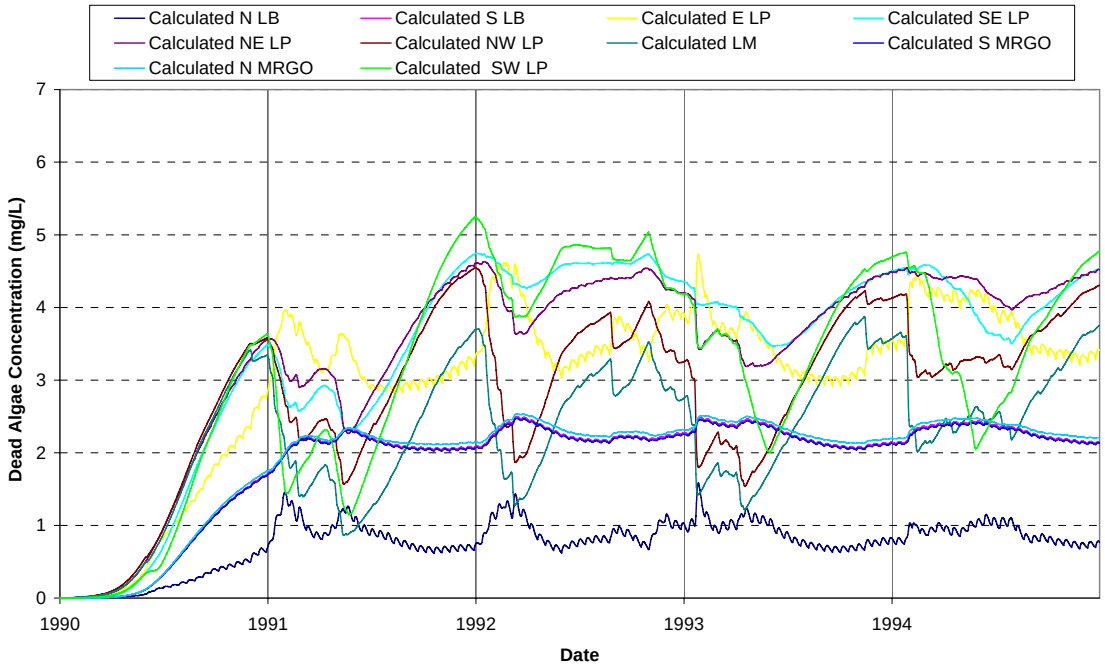

Figure 6.20 Calculated dead algae concentrations (1990-1995).

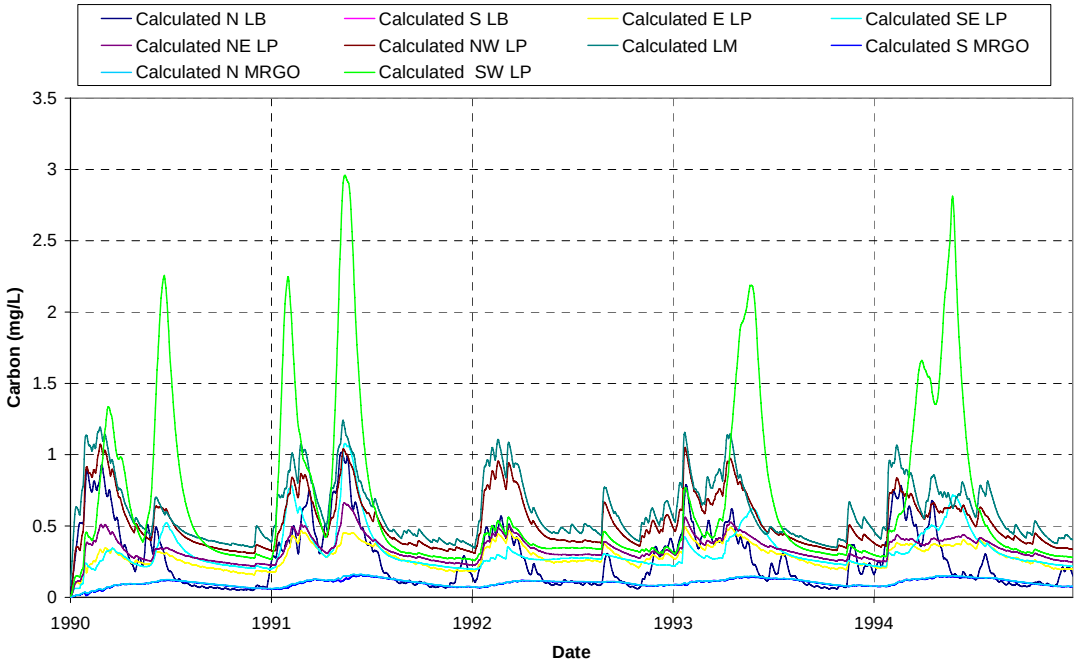

Figure 6.21 Calculated carbon concentrations (1990-1995).

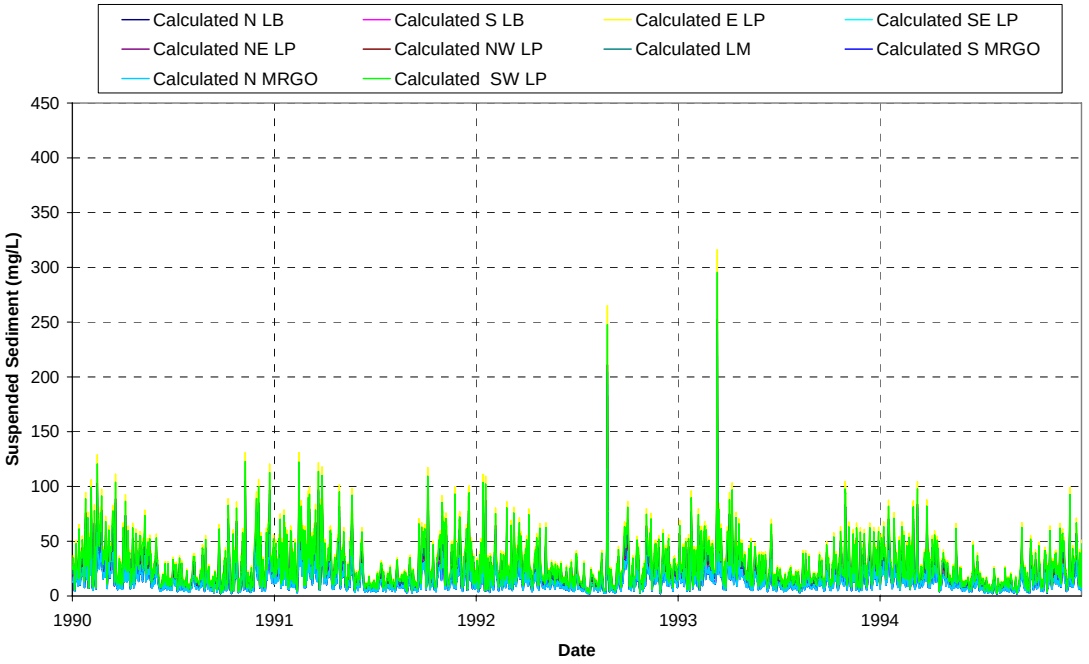

Figure 6.22 Calculated suspended sediment concentrations (1990-1995).

The predicted TOC concentrations match up well with the measured LADEQ data in Lake Pontchartrain. The modeled data is a little lower than the measured results in Lake Maurepas. However, considering the limited (spatial and temporal) extent of the measured data, the results are acceptable. Generally, TOC concentrations seem to follow a seasonal pattern with low values occurring in the summer and higher concentrations occurring in the winter months. The model underestimates the concentrations in Lake Borgne. This underestimation will be discussed in section 9.0.

The modeled results for live algae correspond to the observations made by Poirrier et al. (1998). Poirrier et al. (1998) observed a small bloom of the blue green algae *Anabaena circinalis* near Mandeville in June of 1993. The model shows a small increase in live algae in northwest Lake Pontchartrain right around this time. Poirrier et al. (1998) also observed a more extensive surface bloom in late June 1994. The modeled results again show a spike in live algae concentrations in both southwest and northwest Lake Pontchartrain. The increased concentrations of live algae in 1991 have not been documented by any groups and cannot be verified at this time.

Dead algae concentrations and carbon concentrations are highest in western Lake Pontchartrain. Both dead algae and carbon concentrations respond to the leakage events of the Bonnet Carré Spillway, dead algae concentrations decrease and carbon concentrations increase. The suspended sediment concentrations are consistent around Lake Pontchartrain and follow a seasonal pattern with low concentrations in the summer and high concentrations in the winter. The suspended sediment concentrations were calibrated to total suspended sediment concentration data measured by the LADEQ. Since daily suspended sediment concentrations vary greatly around the Estuary, the modeled data was calibrated to the long-term average value of the suspended sediment data of 22.3 mg/L. The resuspension calibration factor was adjusted

until the average of all of the modeled data approached this value. The resuspension calibration factor was found to equal 1.3.

6.5 *Tidal calibration*

The spring tidal range in Lake Pontchartrain is approximately 0.15 m, while the mean tidal range is 0.11 m. The peak exchange flows on the spring ebb and flood tides through all of the passes (IHNC, Chef Menteur, Rigolets and Pass Manchac) are approximately 8,800 m^3/s (McCorquodale et al., 2007). The predicted tides for the Pontchartrain Estuary model are shown below in Figure 6.23 for Lake Borgne and eastern Lake Pontchartrain between May and August 1992. The variation in the Lake Pontchartrain tides is approximately 0.12m, which corresponds well to the observed tidal range.

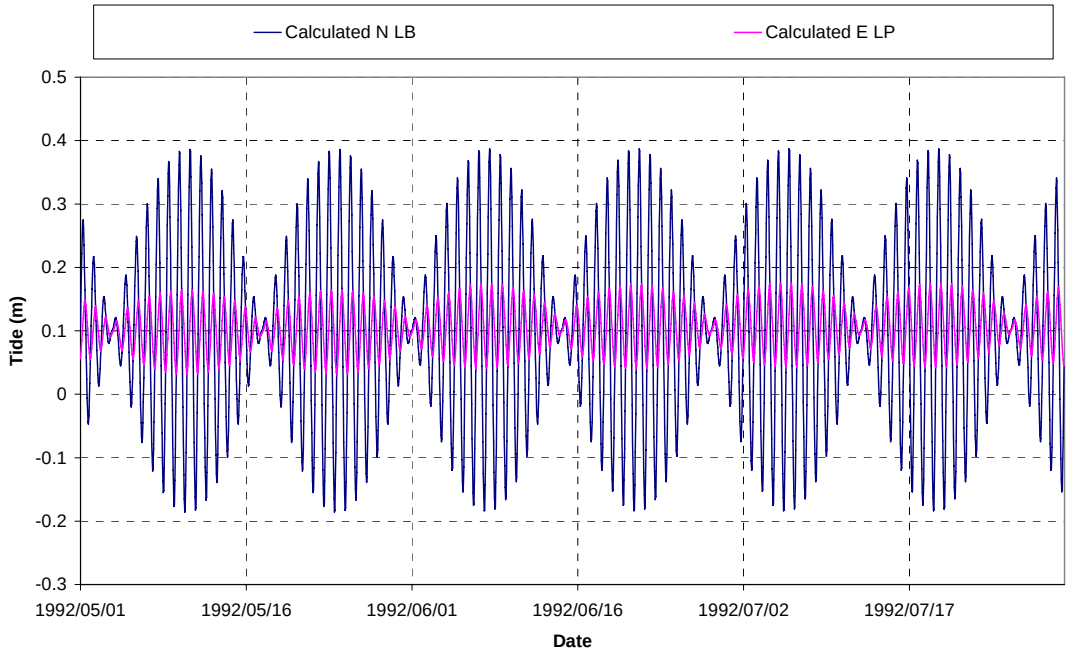

Figure 6.23 Calculated tidal fluctuation around the Pontchartrain Estuary (1990-1995).

6.6 *Algal bloom probability model interpretation*

The predicted output from the algal bloom probability model described in section 4.3.11 is shown below in Figures 6.24 to 6.30. The occurrence of algal blooms around the Pontchartrain Estuary can be predicted when the output from the algal bloom probability model is used in conjunction with the modeled live algae concentrations. The algal bloom probability model fluctuates a lot since it assesses the likelihood of algal blooms occurring on a daily basis. The live algae concentrations are produced from averaged results that depend on the conditions preceding it and do not have a tendency to fluctuate. When the live algae concentrations are heightened and the probability from the algal bloom model is high, algal blooms will be assumed

to occur. The live algae concentrations calculated by the model are shown in Figures 6.24 to 6.30 above the algal bloom probability model results.

The algal bloom probability model shows high probabilities in 1991 in Lake Borgne (Figure 6.24). However, a corresponding increase in live algae concentrations is not predicted during this period. From these results, it can be concluded that an algal bloom did not occur on Lake Borgne in 1991.

In Figure 6.25, the results show that there is a high probability of an algal bloom occurring in eastern Lake Pontchartrain in both 1991 and 1993. However, live algae concentrations only show an increase in 1991. Therefore, an algal bloom may have occurred in eastern Lake Pontchartrain in 1991. This result has not been documented with observations

Figures 6.26 and 6.27 show a high probability of an algal bloom and increases in live algae concentrations in 1991 for northeast and southeast Lake Pontchartrain. Therefore, an algal bloom may have occurred in northeast and southeast Lake Pontchartrain in 1991. This result has not been documented with observations. No algal blooms occurred in northeast Lake Pontchartrain in 1993 or 1994 despite high probabilities since a corresponding increase was not seen in the live algae concentrations.

Figure 6.28 shows both high probabilities and increased live algae concentrations in 1991 and 1994 in southwest Lake Pontchartrain. The latter occurrence can be corroborated by observations by Poirrier et al. (1998) who observed a surface bloom of *Anabaena circinalis* in late June 1994 that could have been present in southwest Lake Pontchartrain. The predicted bloom in 1991 has not been documented in the literature.

Figure 6.29 shows both high probabilities and increased live algae concentrations in 1991, 1993 and 1994 in northwest Lake Pontchartrain. The latter two predicted algal blooms correspond to the observations made by Poirrier et al. (1998). Poirrier et al. (1998) observed a small bloom of the blue green algae *Anabaena circinalis* near Mandeville in June of 1993 and a more extensive surface bloom in late June 1994. The predicted bloom in 1991 has not been documented in the literature.

Figure 6.30 indicates that there is a high probability of an algal bloom occurring in Lake Maurepas in most years. This is likely due to the high concentrations of nutrients flowing into Lake Maurepas from the tributaries. The modeled live algae concentrations do not show any increases in Lake Maurepas over the calibration period. No algal blooms have been documented on Lake Maurepas in the literature during the calibration period.

The calibration indicates that the occurrence of algal blooms around the Pontchartrain Estuary can be predicted when the output from the algal bloom probability model is used in conjunction with the modeled live algae concentrations. The events that were observed by Poirrier et al. (1998) in northwest Lake Pontchartrain in 1993 are captured in the model. The more extensive surface bloom in 1994 is also predicted to occur in northwest and southwest Lake Pontchartrain. The predicted algal bloom in Lake Pontchartrain in 1991 cannot be disproved since no observations were documented.

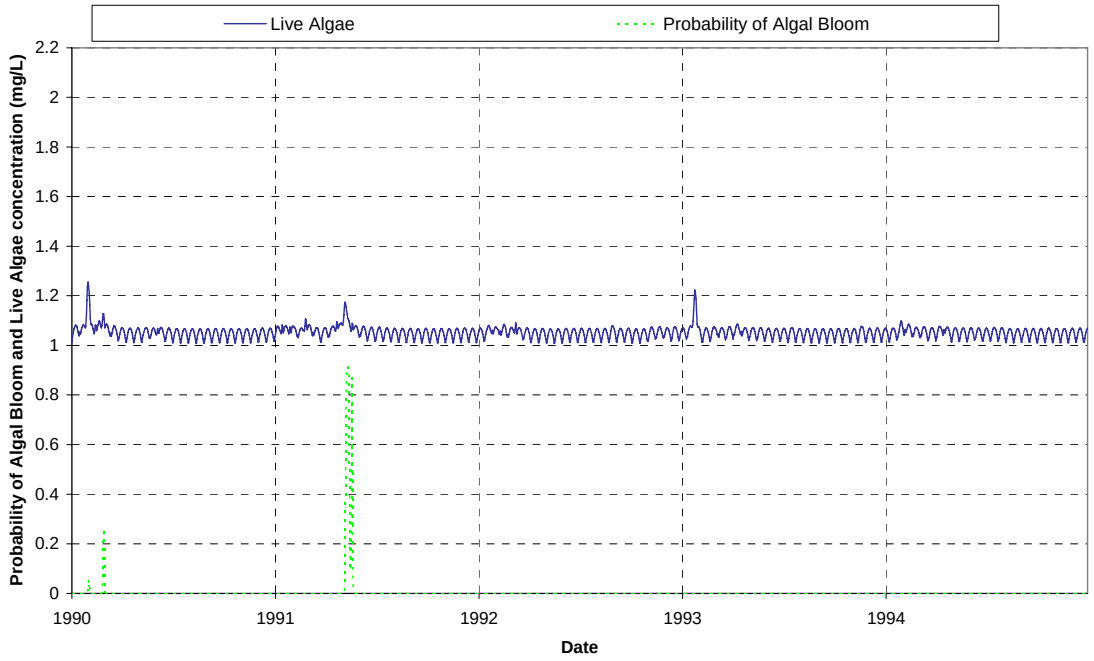

Figure 6.24 Predicted probability of algal bloom on Lake Borgne with predicted live algae concentrations.

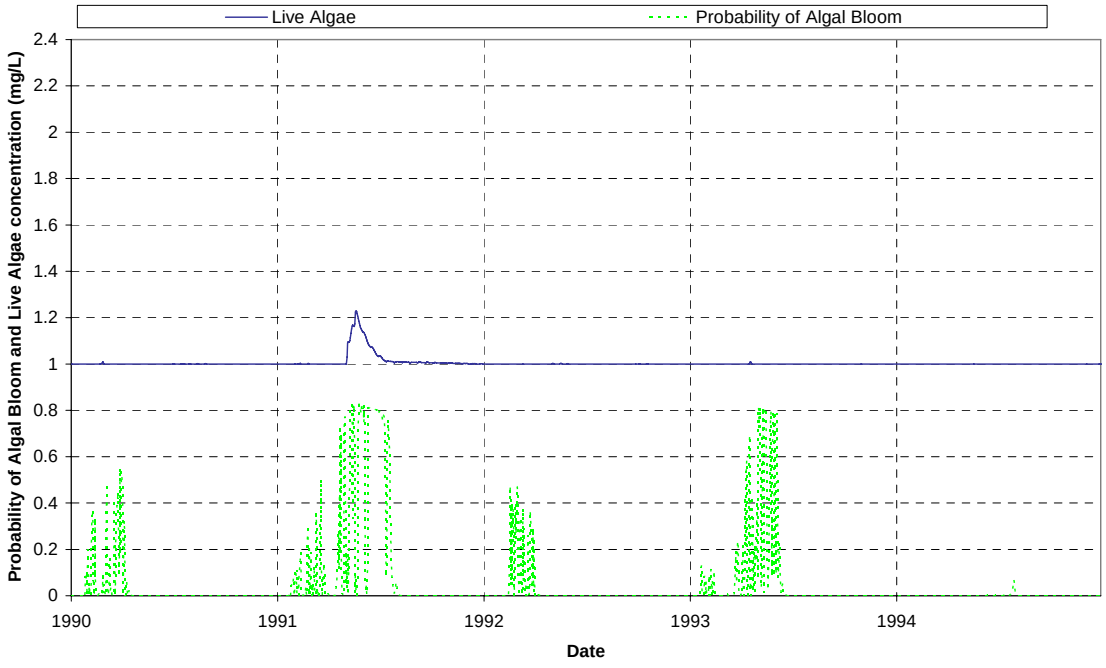

Figure 6.25 Predicted probability of algal bloom on eastern Lake Pontchartrain with predicted live algae concentrations.

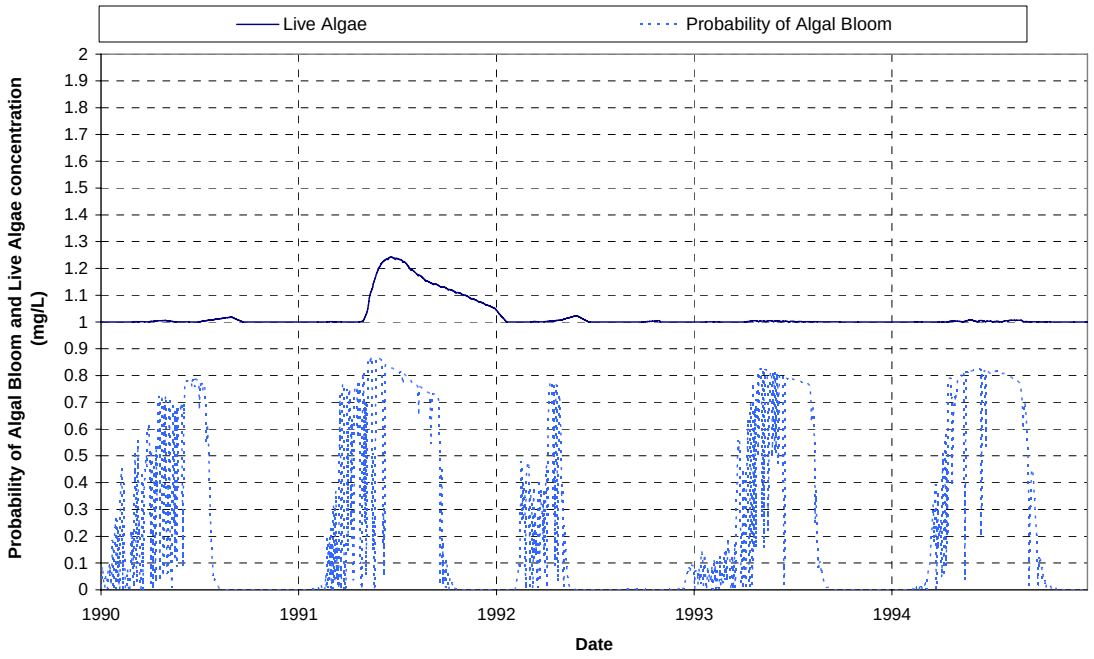

Figure 6.26 Predicted probability of algal bloom on northeast Lake Pontchartrain with predicted live algae concentrations.

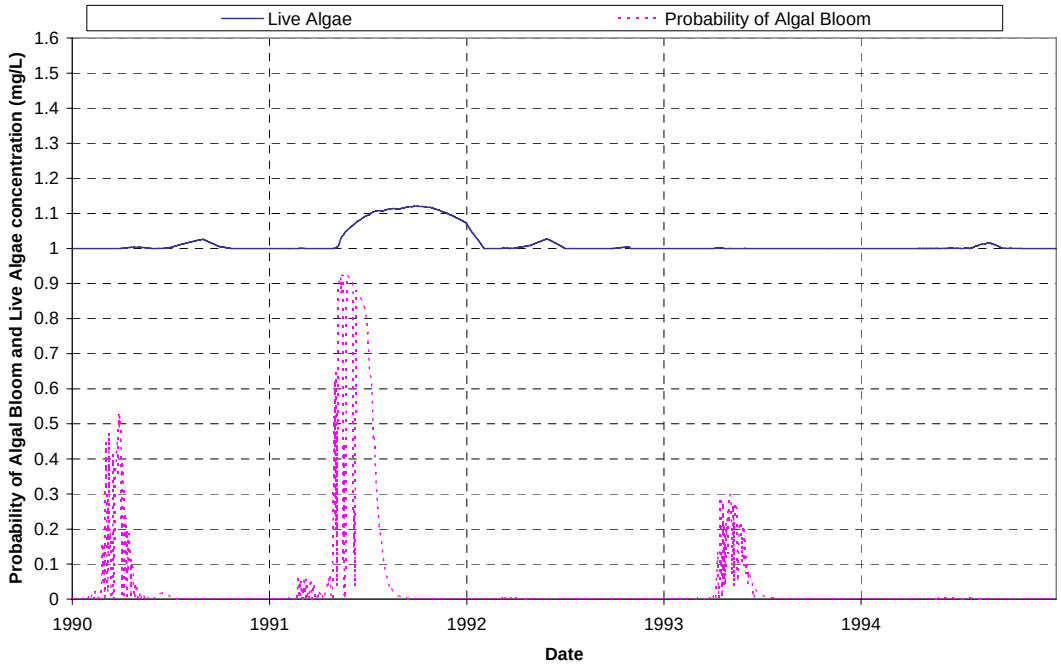

Figure 6.27 Predicted probability of algal bloom on southeast Lake Pontchartrain with predicted live algae concentrations.

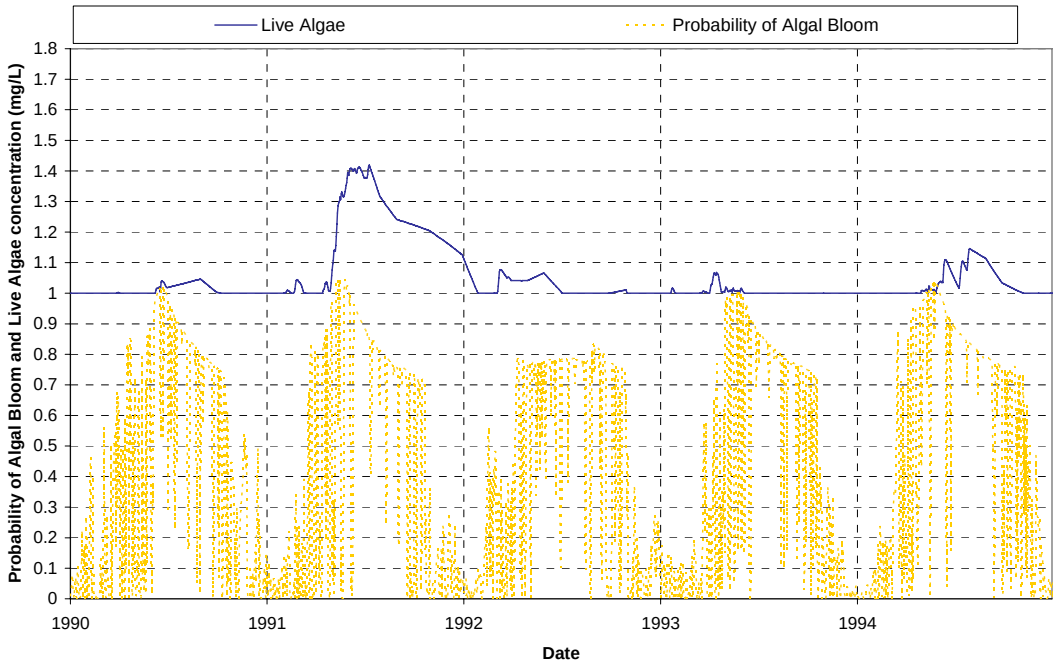

Figure 6.28 Predicted probability of algal bloom on southwest Lake Pontchartrain with predicted live algae concentrations.

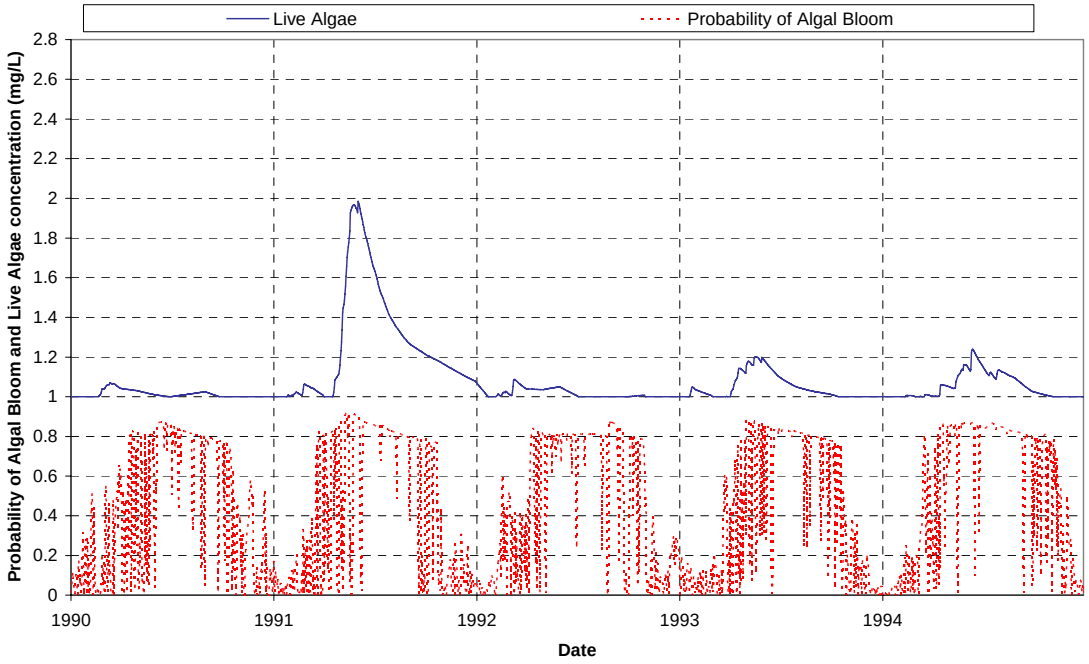

Figure 6.29 Predicted probability of algal bloom on northwest Lake Pontchartrain with predicted live algae concentrations.

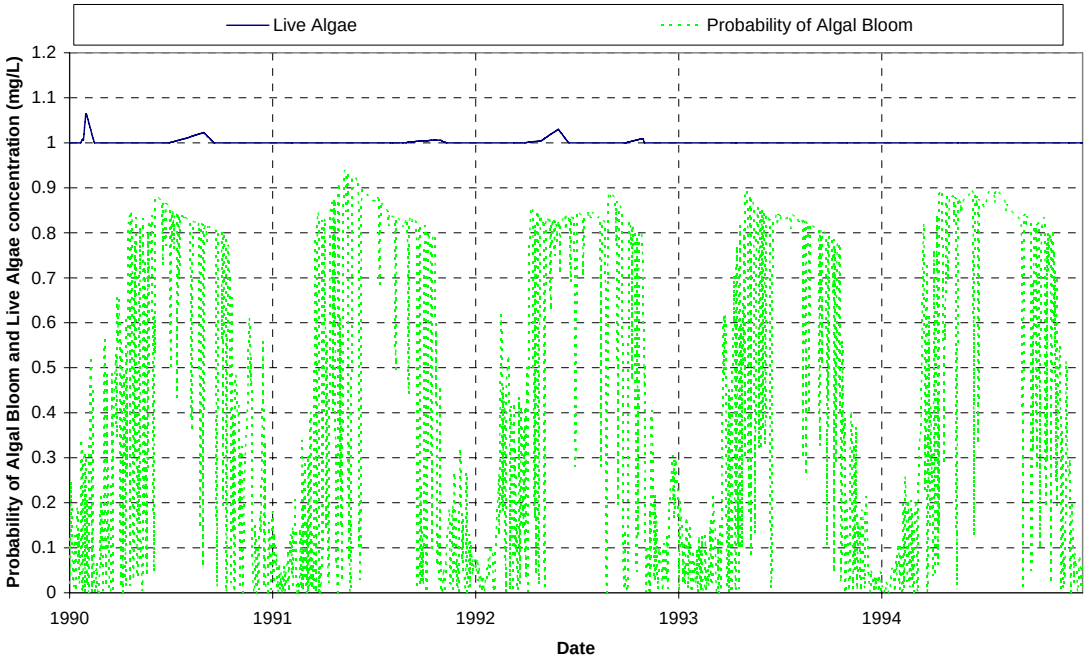

Figure 6.30 Predicted probability of algal bloom on Lake Maurepas with predicted live algae concentrations.

7.0 Model validation

7.1 General validation

The model was validated with measured salinity, nitrate + nitrite as nitrogen, phosphorous, TKN and total organic carbon concentration measurements taken between January 1995 and December 2006. All of the calibration parameters (coefficients and rate constants, etc.) that were assigned during the calibration process were held constant during the validation run. The validation of salinity is described in section 7.2. The nutrient validations are described in section 7.3. The tidal validation is described in section 7.4 and the algal bloom probability model is interpreted in section 7.5. Appendix B shows all of the modeled results that did not have measured data associated with them (DIN, ammonia, organic nitrogen, carbon, live algae, dead algae and suspended sediment concentrations).

7.2 Salinity validation

The calculated salinity output (solid lines) for all of the cells in the Pontchartrain Estuary model is shown below in Figures 7.1 and 7.2. The calculated relative salinity gradation is the same as that described in the calibration section: the highest salinities occur in Lake Borgne and the lowest salinities occur in Lake Maurepas. The vertical black dashed lines in the figures indicate the months where high rainfall occurred while the vertical red dashed lines indicate the months where the lowest rainfall occurred. The model again captures the freshening effect that increased rainfall would have on Lake Pontchartrain. It also mimics the increases in salinity that would occur during dry conditions.

Between 1995 and 2006, one major opening and 11 leakage events occurred on the Bonnet Carré Spillway. The major opening occurred in March to April 1997; and the leakage events occurred: in June 1995; January and mid-April/May 1998; February 1999; March 2001; January, April and June 2002; March and June 2003, and late January/February 2006 (Figure 5.8). As indicated by the figures, the major opening and the leakage events all have a freshening effect on the modeled Pontchartrain Estuary salinity regime. There are a few other instances where Lake Pontchartrain freshens as a result of high rainfall events. For example, the freshening in September 1998 is associated with the 6th largest rainfall between 1990 and 2006 of 38 cm/month. Again, the range of salinity concentrations is much higher for north Lake Borgne and east Lake Pontchartrain due to the contribution of freshwater from the Pearl River and the proximity to the Gulf of Mexico.

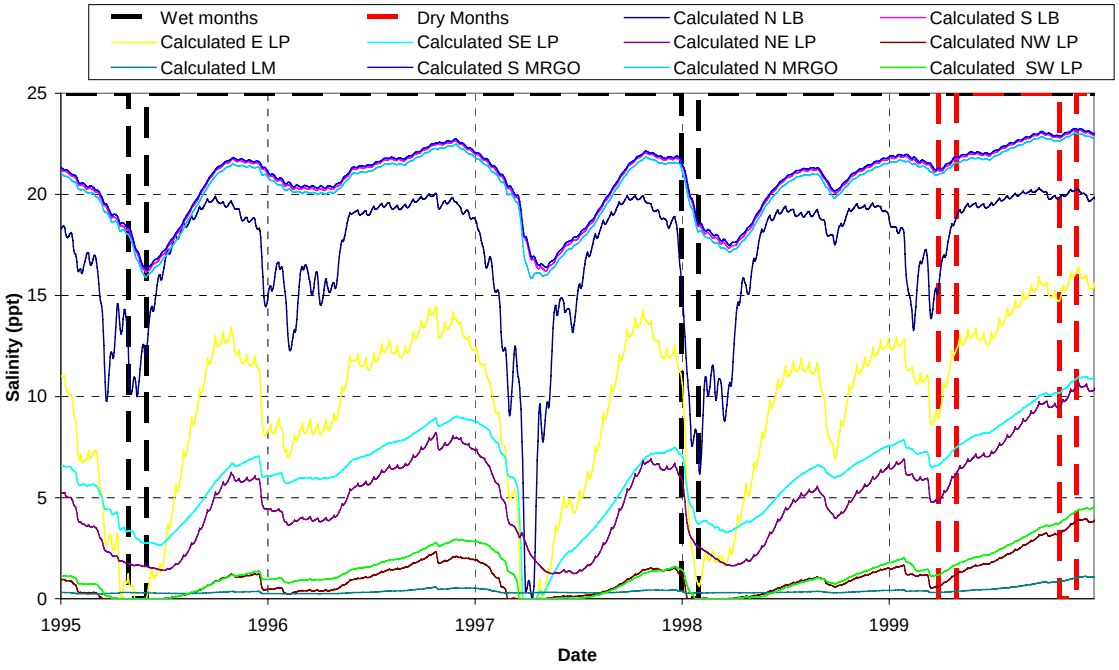

Figure 7.1 Calculated salinity from the Pontchartrain Estuary model (1995-2000).

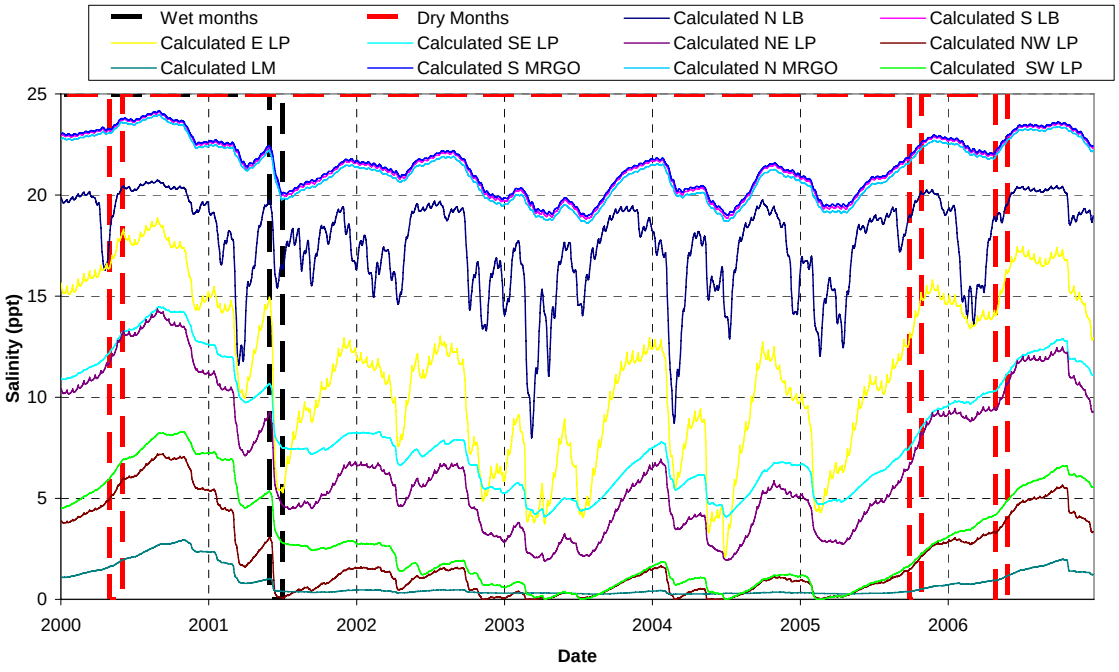

Figure 7.2 Calculated salinity from the Pontchartrain Estuary model (2000-2007).

Salinity was measured much more extensively during the validation period (January 1995 to December 2006) than during the calibration period. The LADEQ, the USGS, LUMCON, and UNO researchers all took salinity measurements at various locations around the Estuary. The comparison between the predicted and measured data is shown in Figures 7.3 and 7.4 for Lake Maurepas, Figures 7.5 and 7.6 for Lake Pontchartrain and Figures 7.7 and 7.8 for Lake Borgne. The solid lines in the figures represent the model output for each cell, the points represent the measured data, and the dotted bars associated with the measured data represent the standard deviation of the data.

The modeled salinity on Lake Maurepas (Figure 7.3 and 7.4) captured the freshening effect due to the 1997 Bonnet Carré Spillway opening as well as the increases in salinity concentrations due to the drought in 1999 and 2000. The predicted northwest Lake Pontchartrain salinity concentrations correspond well to the USGS measured salinities in Pass Manchac that have been continuously measured since 2004.

All of the measured salinity on Lake Pontchartrain falls within the limits of the modeled data around the lake. Between 1997 and 2000 UNO undertook an extensive monitoring program on Lake Pontchartrain to look at the effects of the Bonnet Carré Spillway. The locations where they took measurements around Lake Pontchartrain are shown in Appendix B. Except during a short period in 1998, the UNO data measured falls within the modeled limits around the lake. The LADEQ and LUMCON data, which were measured near the causeway, fall within the modeled eastern and western salinity results. The modeled salinity values in each cell around Lake Pontchartrain are predicting salinity values accurately.

The salinities in eastern Lake Pontchartrain follow the LADEQ measurements in the Rigolets and Chef Menteur quite well. The USGS dataset that measures salinity in the Rigolets shows a freshening effect in eastern Lake Pontchartrain in 2006 that is not captured in the model. This may be due to either an under estimation of the discharges in the Pearl River for that period (due to the regression equations), or a miscalculation of the percent connection between the Pearl River and eastern Lake Pontchartrain (i.e. the pearl river could contribute more than 5-10% of its loads and discharges to the system). Our model has a lower salinity range than the data measured at the USGS gage in Mississippi Sound which is probably due to the effect of cell averaging.

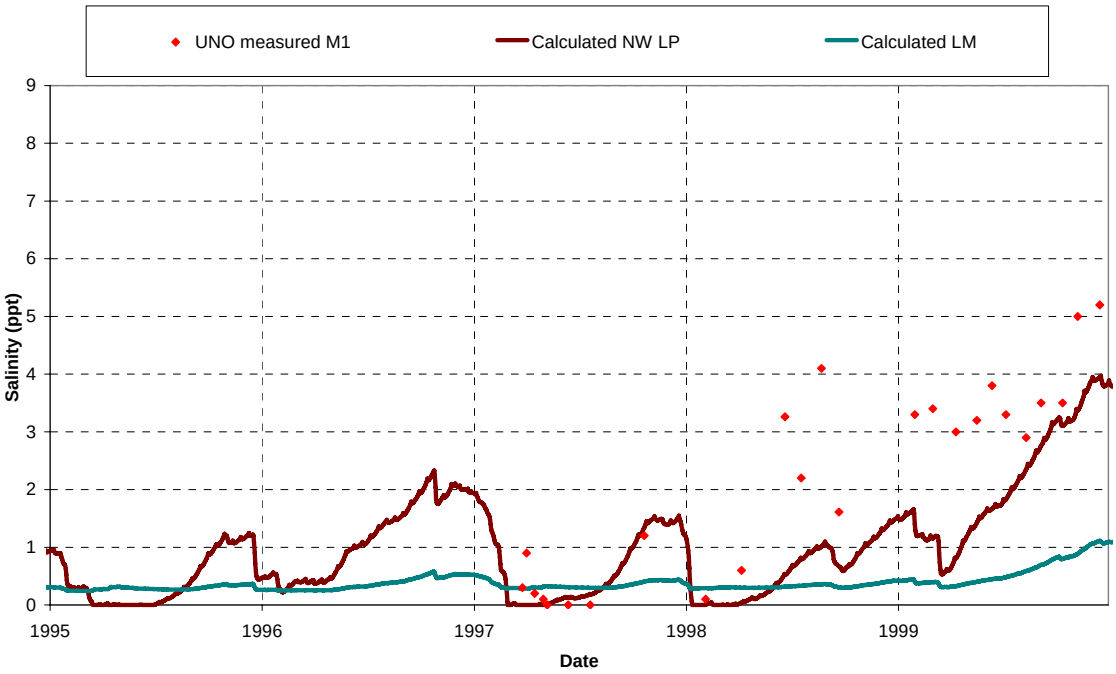

Figure 7.3 Salinity validation on Lake Maurepas (1995-2000).

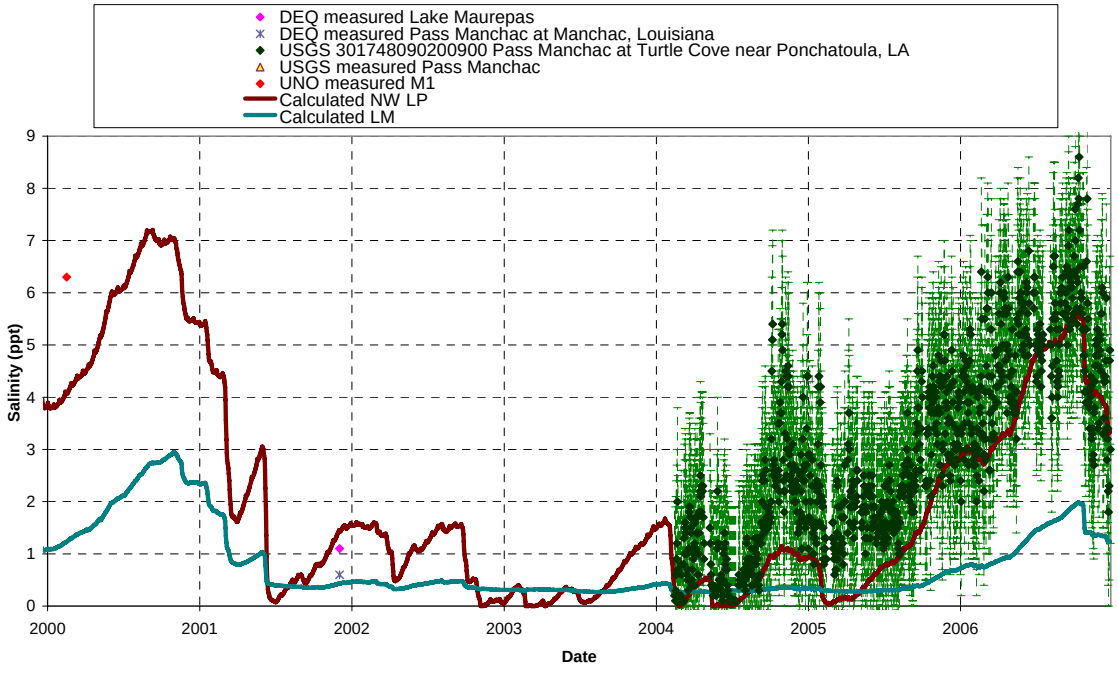

Figure 7.4 Salinity validation on Lake Maurepas (2000-2007).

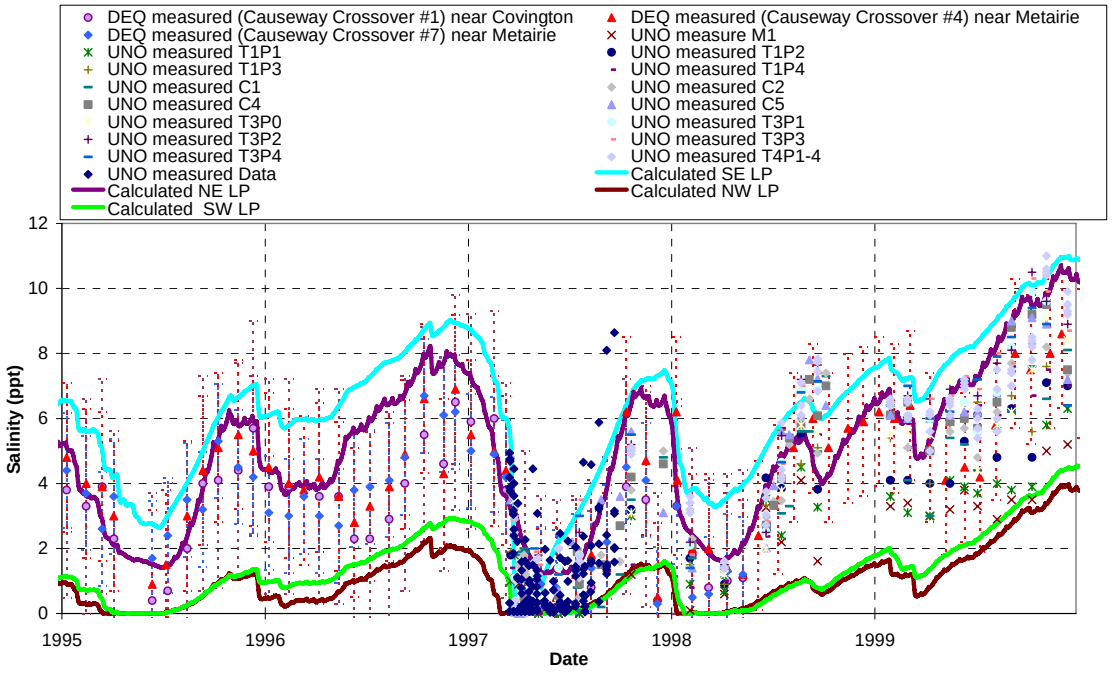

Figure 7.5 Salinity validation on Lake Pontchartrain (1995-2000).

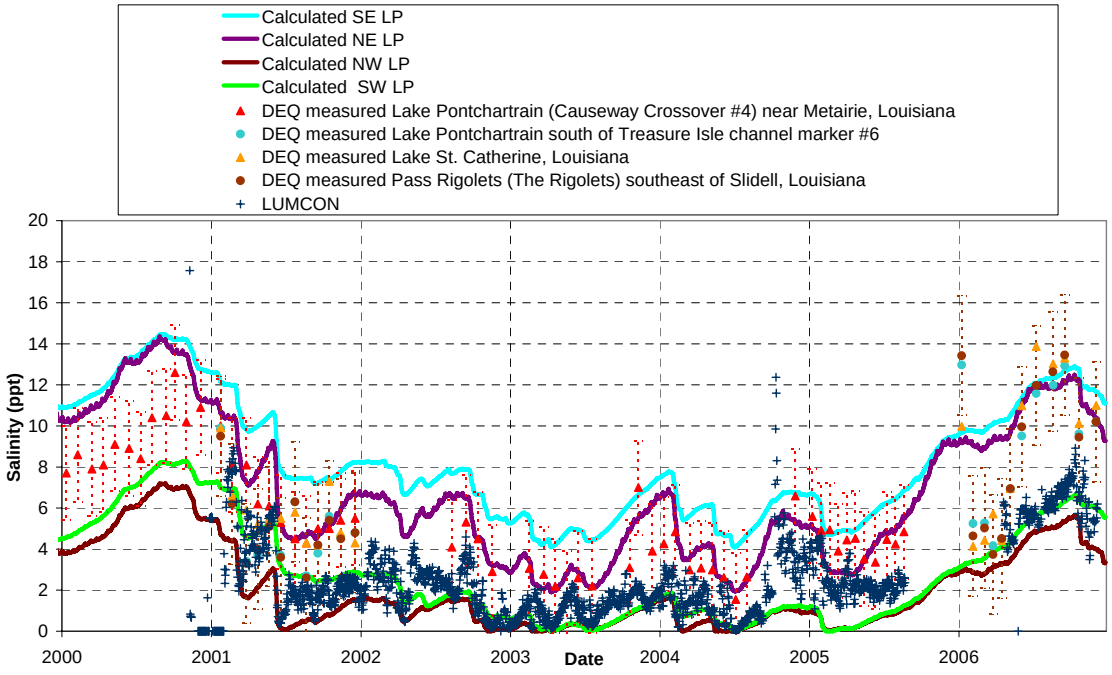

Figure 7.6 Salinity validation on Lake Pontchartrain (2000-2007).

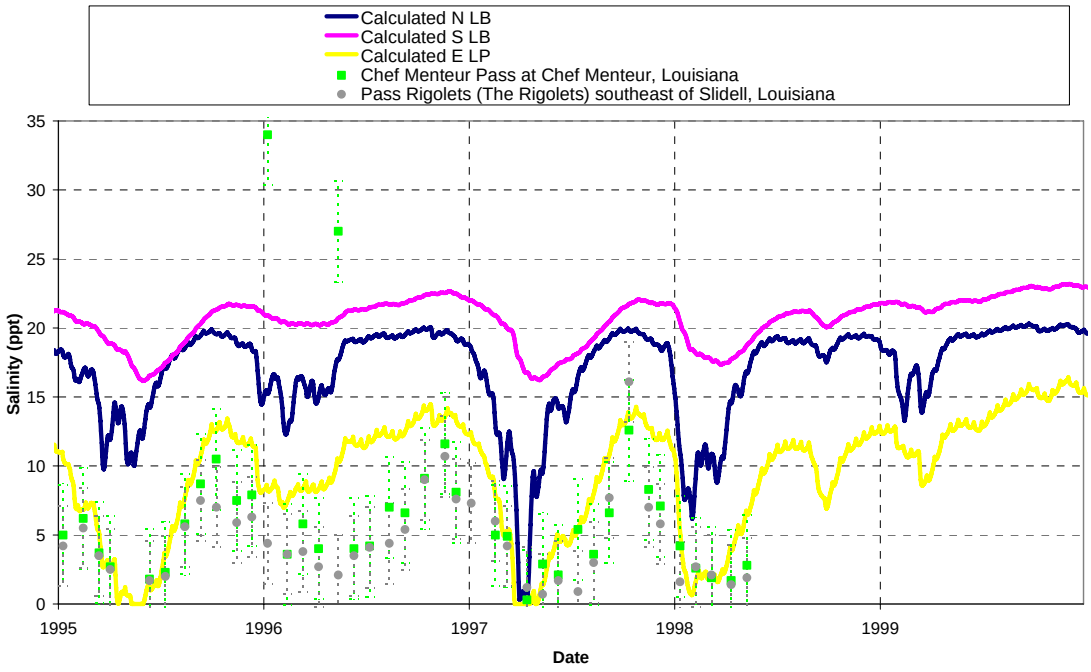

Figure 7.7 Salinity validation on Lake Borgne (1995-2000).

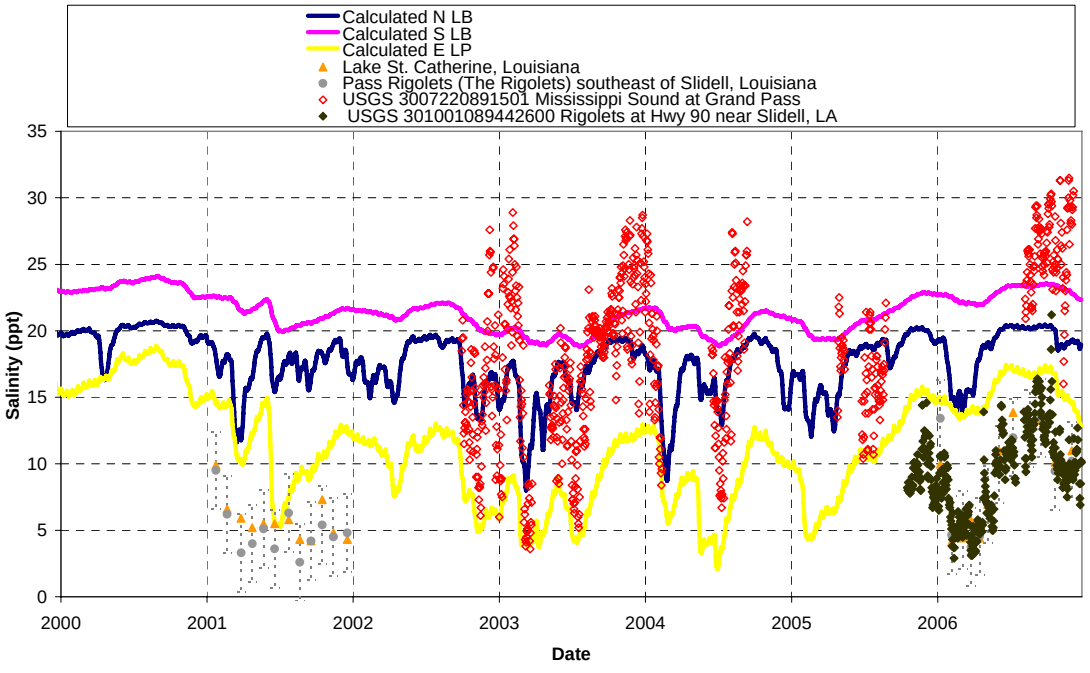

Figure 7.8 Salinity validation on Lake Borgne (2000-2007).

7.3 Nutrient validation

Nitrate + nitrite as nitrogen, phosphorous, TKN and total organic carbon concentration measurements were available in the Pontchartrain Estuary for validation of the model between January 1995 and December 2006. Comparisons between the measured data and the calculated results are shown in sections 7.3.1. to 7.3.4. Appendix B. shows the calculated results that did not have measured data associated with them (DIN, ammonia, organic nitrogen, carbon, live algae, dead algae and suspended sediment concentrations).

7.3.1 Nitrite + nitrate as nitrogen validation

The model was validated using data measured by the LADEQ from January 1995 to December 2006. Figure 7.9 to 7.14 show the predicted versus measured results on Lake Maurepas, Lake Pontchartrain and Lake Borgne. The solid lines in the figures represent the model output for each cell, the points represent the measured data, and the dotted bars associated with the measured data represent the standard deviation of the data.

As with the calibrated results, the modeled results follow the general trends of the dataset between 1995 and 2006 for both Lake Maurepas and Lake Pontchartrain. The Lake Borgne modeled results are a little lower than the measured data. Again, it is clear that the Bonnet Carré Spillway leakage events influence the concentrations in the cells nearest the spillway (southwest and northwest Lake Pontchartrain). The 1997 Bonnet Carré Spillway opening had a profound effect on nitrite + nitrate as nitrogen in the Estuary. Concentrations were increased by an order of magnitude around the entire Estuary. The model is calculating the nitrite + nitrate concentrations in the Pontchartrain Estuary sufficiently.

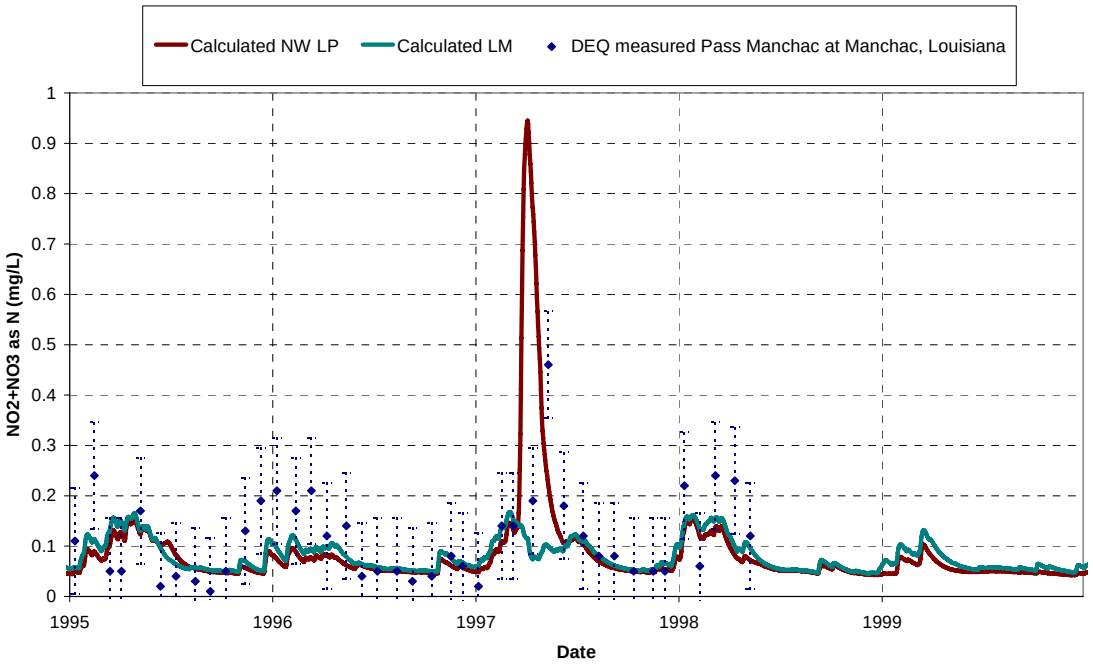

Figure 7.9 Nitrite + nitrate as nitrogen validation on Lake Maurepas (1995-2000).

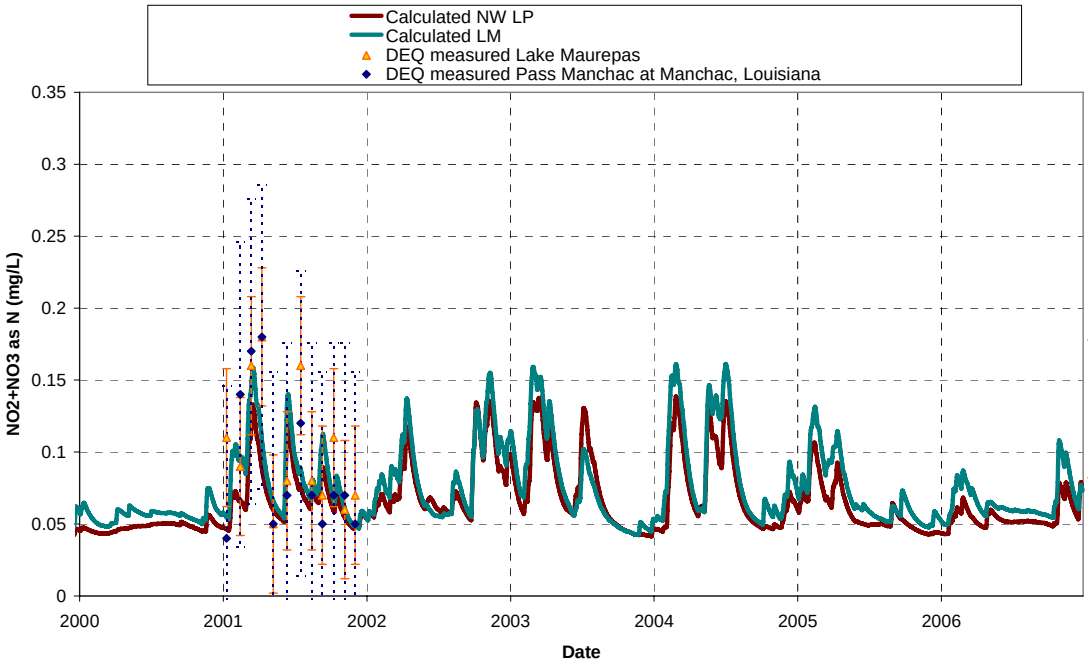

Figure 7.10 Nitrite + nitrate as nitrogen validation on Lake Maurepas (2000-2007).

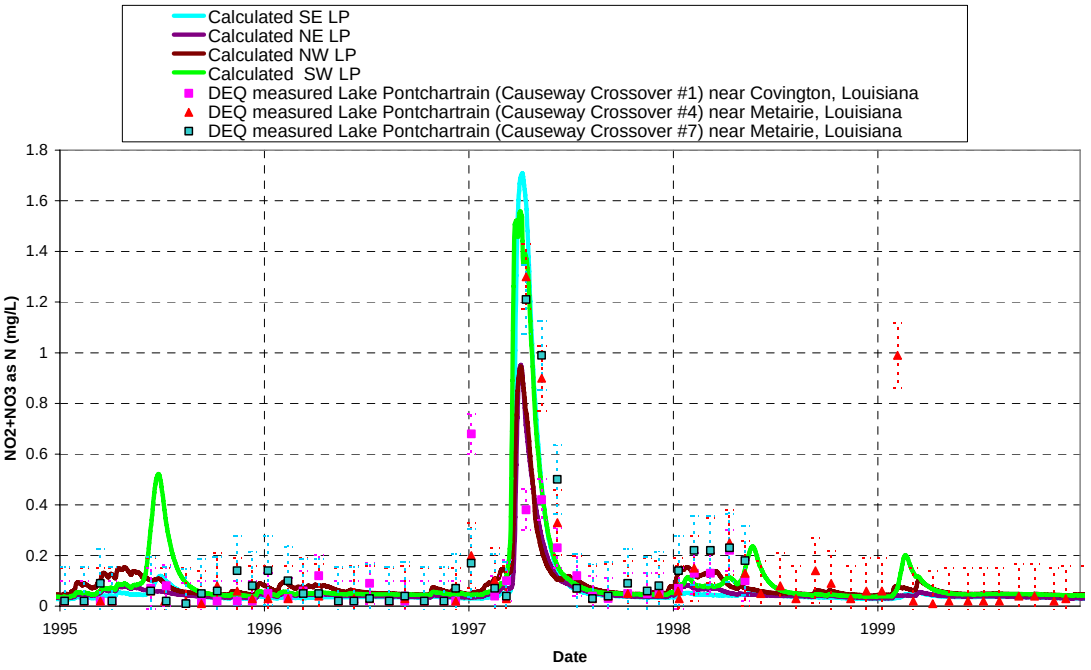

Figure 7.11 Nitrite + nitrate as nitrogen validation on Lake Pontchartrain (1995-2000).

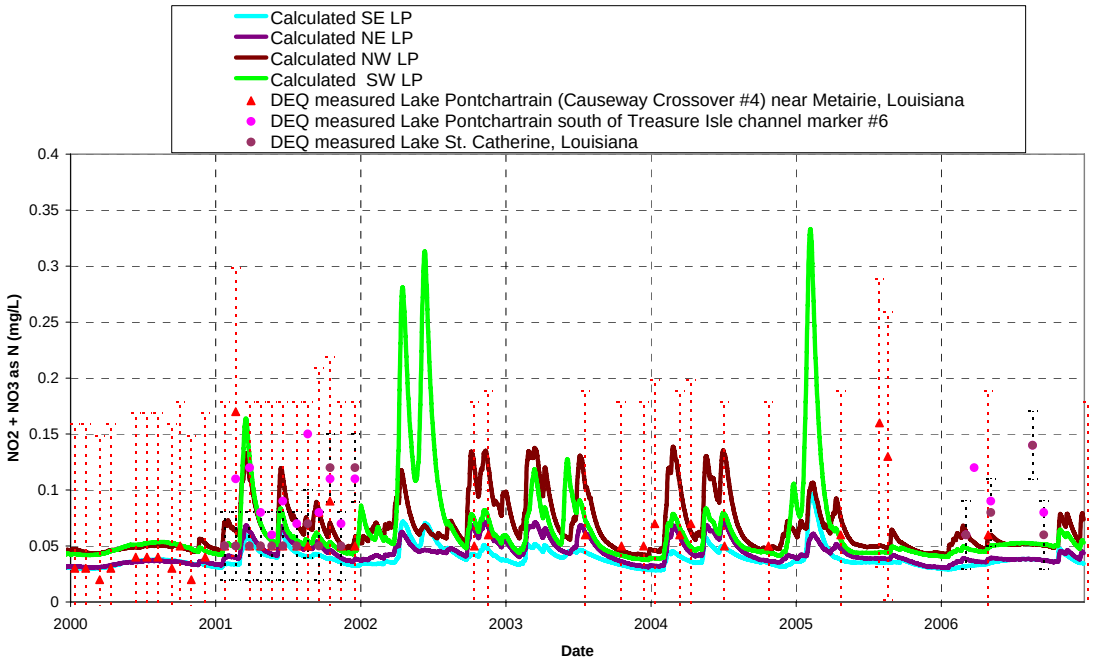

Figure 7.12 Nitrite + nitrate as nitrogen validation on Lake Pontchartrain (2000-2007).

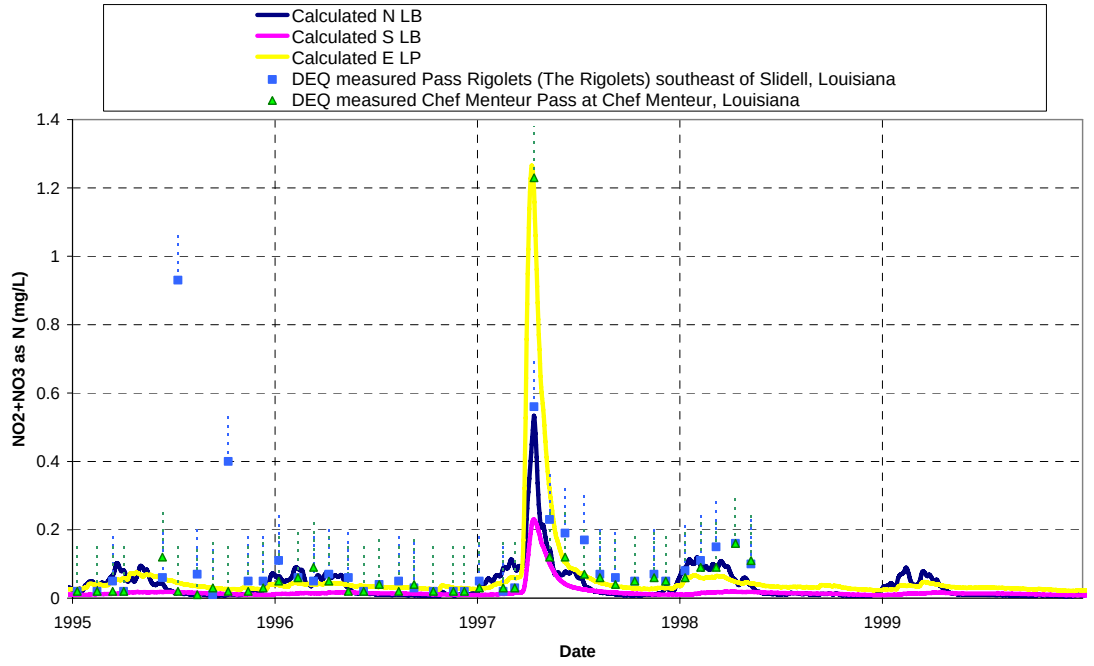

Figure 7.13 Nitrite + nitrate as nitrogen validation on Lake Borgne (1995-2000).

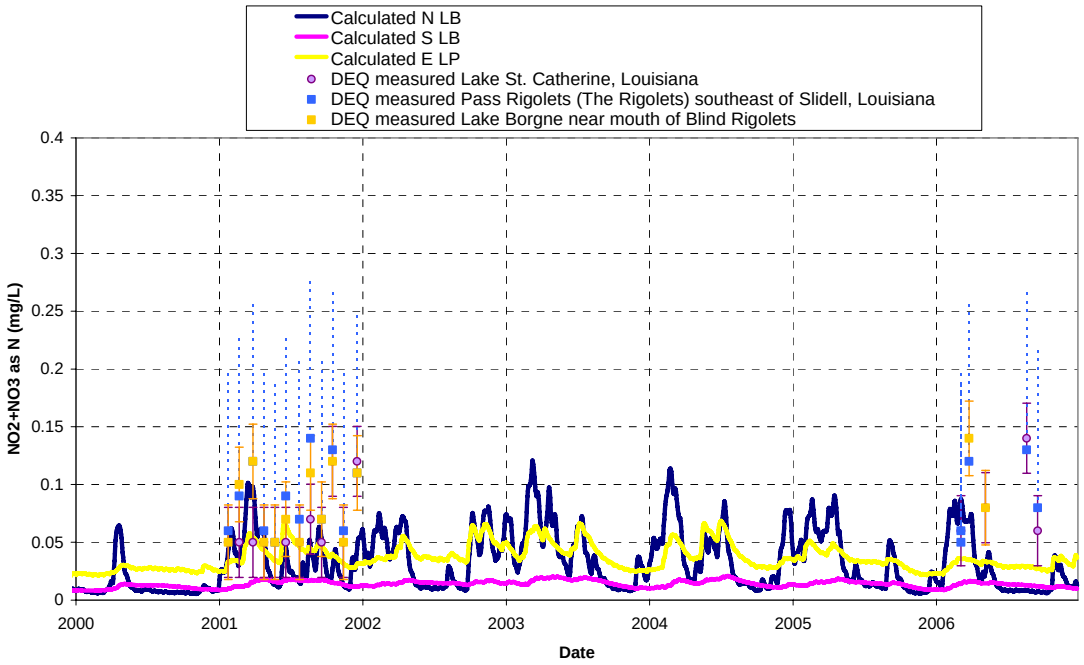

Figure 7.14 Nitrite + nitrate as nitrogen validation on Lake Borgne (1995-2000).

7.3.2 Phosphorous validation

The model was validated using data measured by the LADEQ from January 1995 to December 2006. Comparisons between the predicted phosphorous concentrations and the measured data are shown below for Lakes Maurepas, Pontchartrain and Borgne (Figures 7.15. to 7.20.). The solid lines in the figures represent the model output for each cell, the points represent the measured data, and the dotted bars associated with the measured data represent the standard deviation of the data.

The modeled data on all of the lakes corresponds well to the measured data (perhaps more so than during the calibration period). The increases as a result of the Bonnet Carré Spillway leakage events are again less pronounced for the phosphorous concentrations than the nitrite + nitrate as nitrogen concentrations. However, the 1997 opening had a significant effect on the phosphorous concentrations. The modeled concentrations on Lake Borgne and Lake Pontchartrain showed a two-fold increase in 1997 over the background concentrations. In 2000, the modeled results on Lake Pontchartrain under-predict the measured results on Lake Pontchartrain. This is expected since average phosphorous concentrations were assumed which do not capture the effect of seasonal variations or droughts. The phosphorous concentrations predicted by the model are sufficiently accurate to represent any phosphorous limit on algal growth.

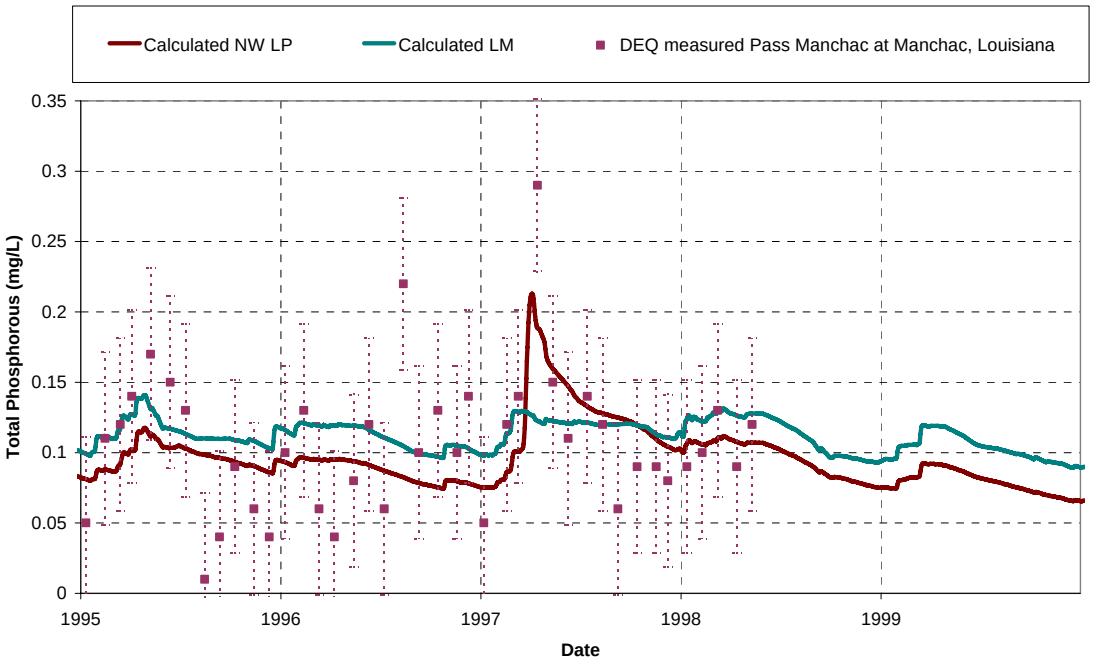

Figure 7.15 Total phosphorous validation on Lake Maurepas (1995-2000).

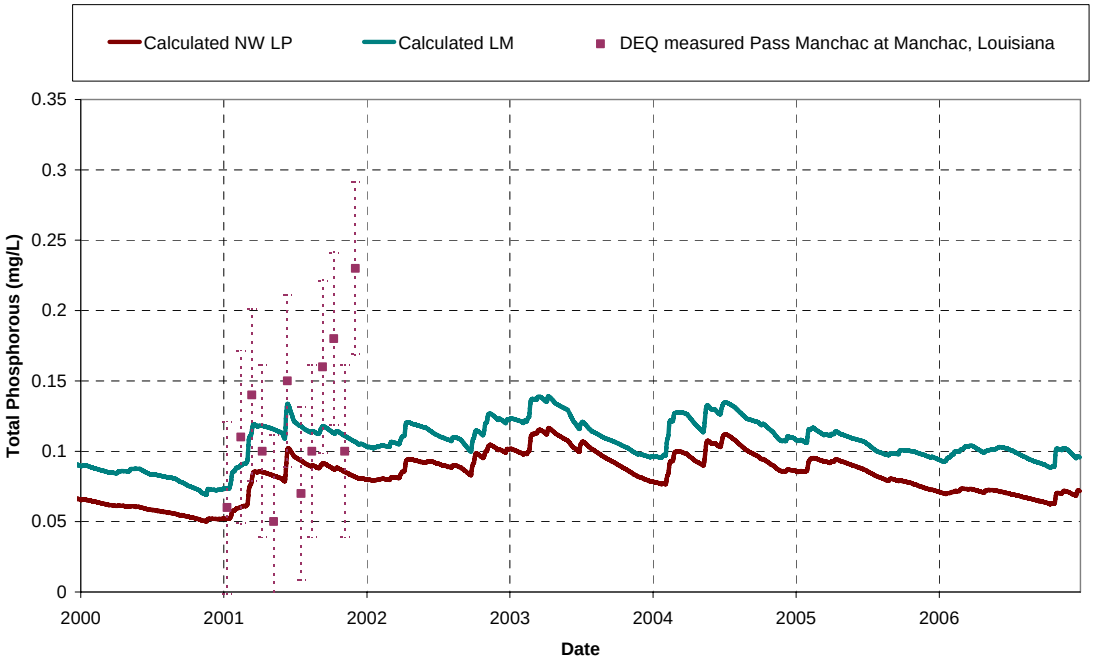

Figure 7.16 Total phosphorous validation on Lake Maurepas (2000-2007).

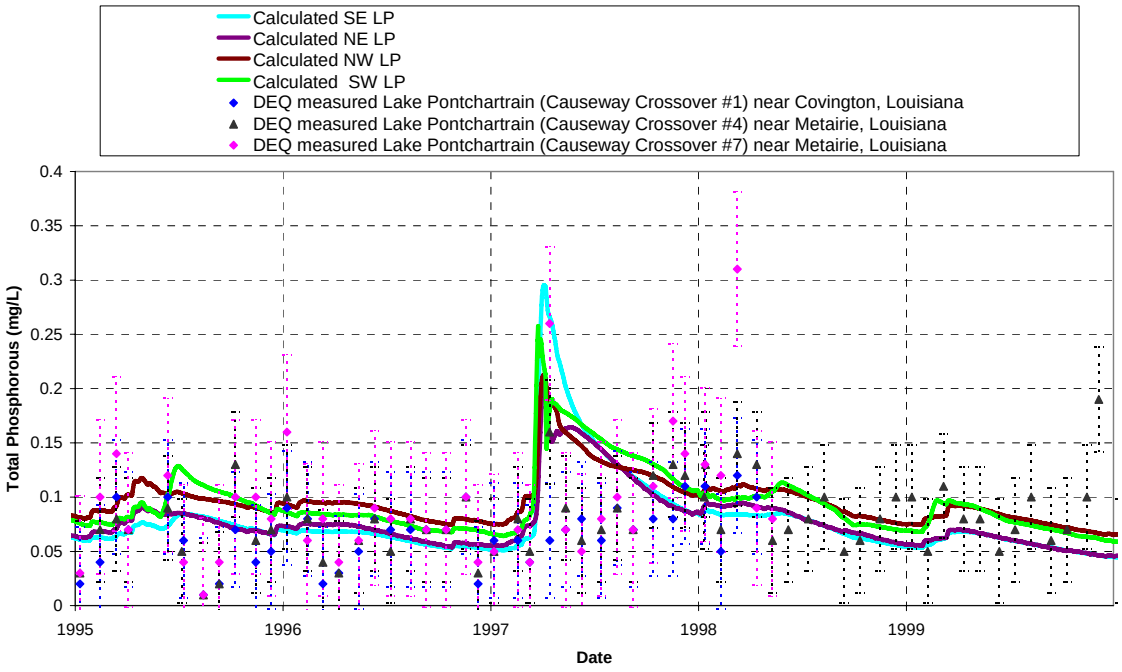

Figure 7.17 Total phosphorous validation on Lake Pontchartrain (1995-2000).

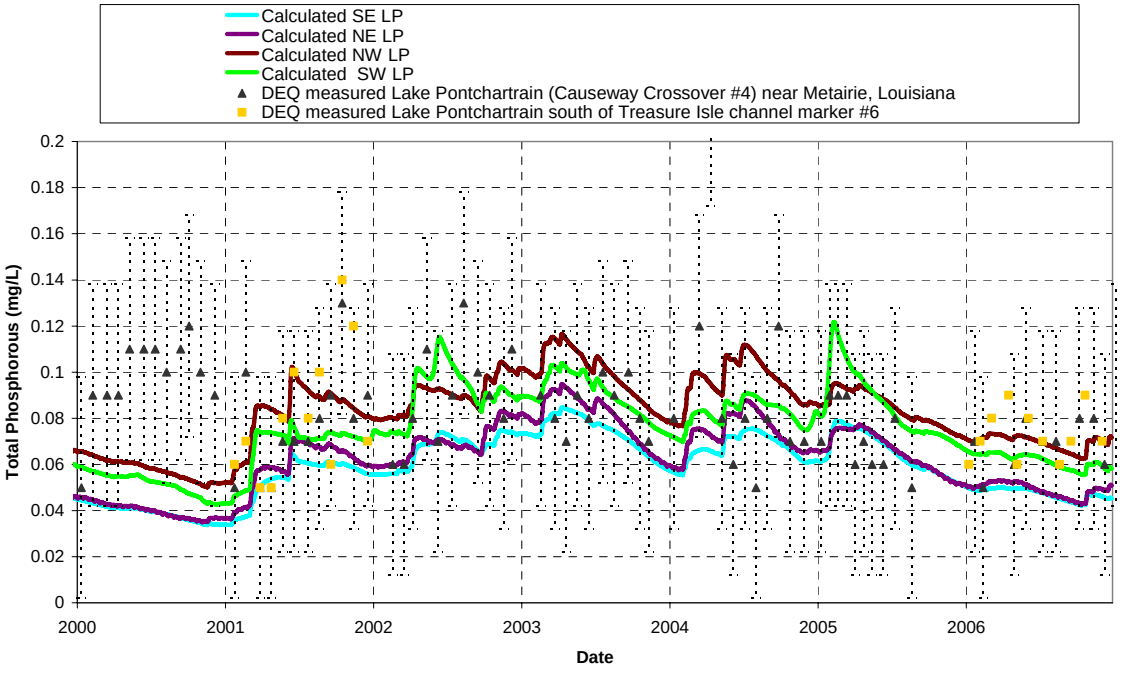

Figure 7.18 Total phosphorous validation on Lake Pontchartrain (2000-2007).

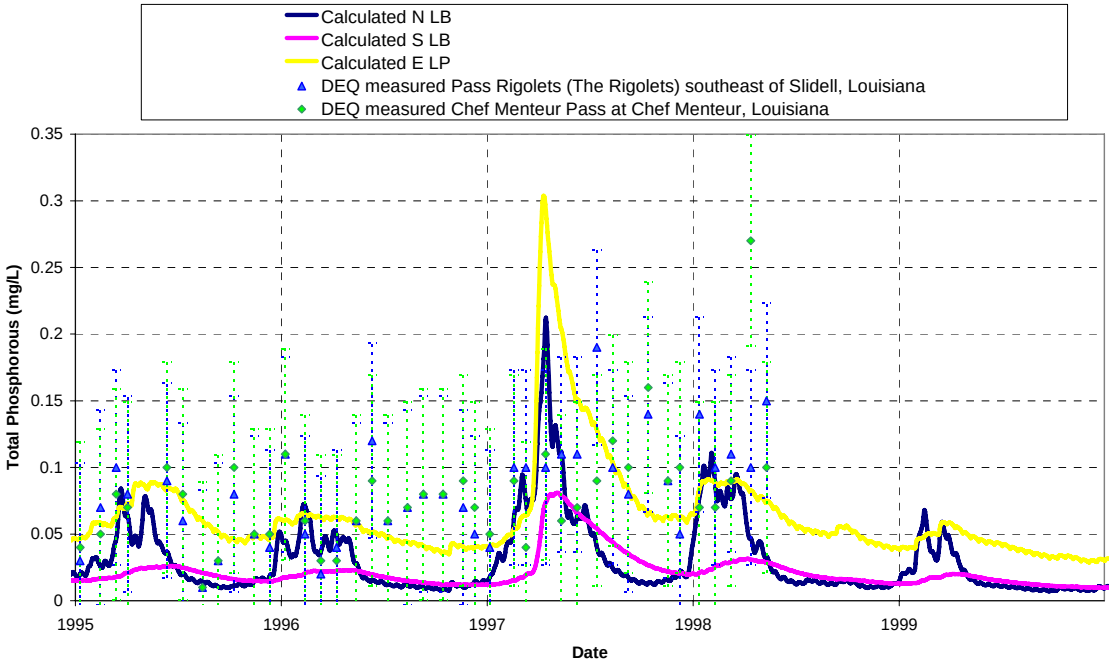

Figure 7.19 Total phosphorous validation on Lake Borgne (1995-2000).

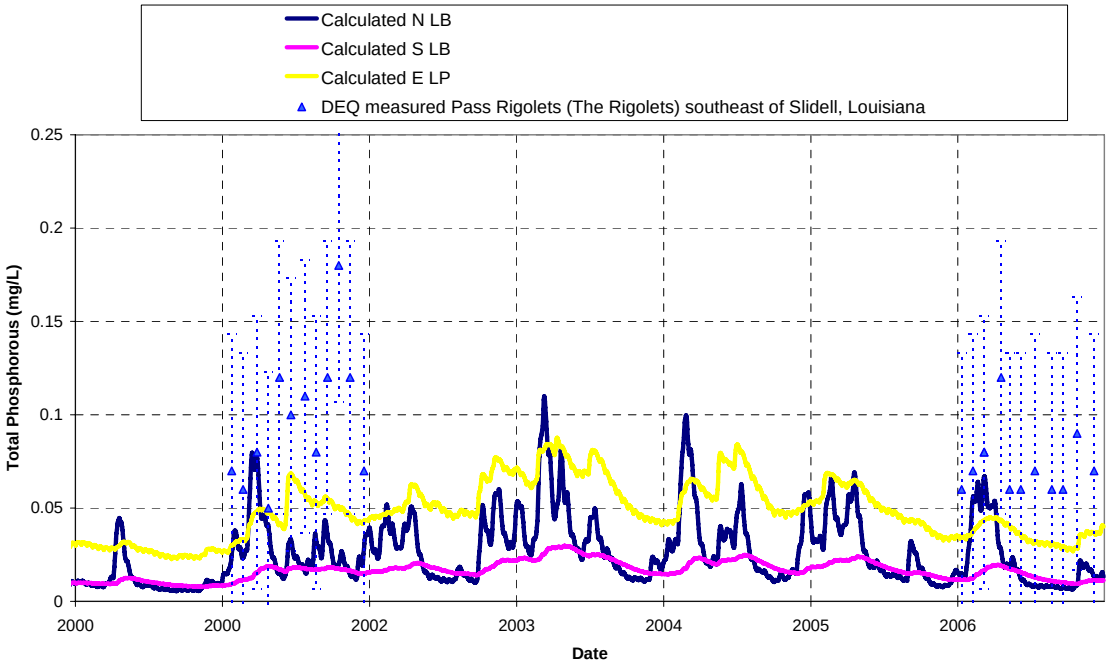

Figure 7.20 Total phosphorous validation on Lake Borgne (2000-2007).

7.3.3 Total Kjeldahl Nitrogen (TKN) validation

The model was validated using TKN data measured by the LADEQ in the Pontchartrain Estuary between January 1995 and December 2006. TKN measurements are equivalent to the summation of organic nitrogen and ammonia concentrations. Comparisons between the predicted TKN concentrations and the measured data are shown below for Lakes Maurepas, Pontchartrain and Borgne (Figures 7.21 to 7.26). The solid lines in the figures represent the model output for each cell, the points represent the measured data, and the dotted bars associated with the measured data represent the standard deviation of the data. The predicted results for organic nitrogen and ammonia are shown separately in Appendix B.

Again, the TKN concentration measurements show that TKN concentrations do not vary significantly with time around the Pontchartrain Estuary. The modeled data matches up with the measured data well on Lake Maurepas. The predicted eastern Lake Pontchartrain concentrations match up well with the measured results in the Chef Menteur Pass in Figure 7.25. The predicted data seems to over-predict the measured results from 1998 onward in Lake Pontchartrain. However, the measured data from 1998 onward is consistently lower (average of 0.47 mg/L) than the measured data between 1990 and 1998 (average value of 0.59 mg/L). It is unclear whether this change in measured concentrations is due to a change in condition of the Lake or if the measurement or analysis technique used by the LADEQ changed. However, the modeled TKN concentrations were considered adequate since the results fall within the standard deviation of the datasets.

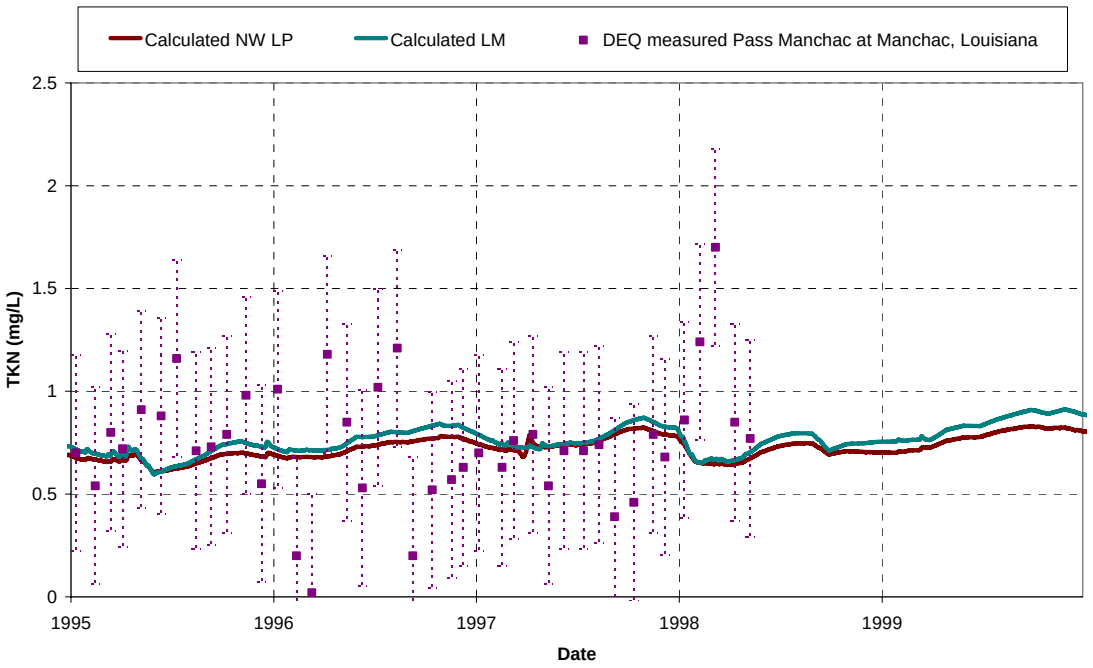

Figure 7.21 TKN validation on Lake Maurepas (1995-2000).

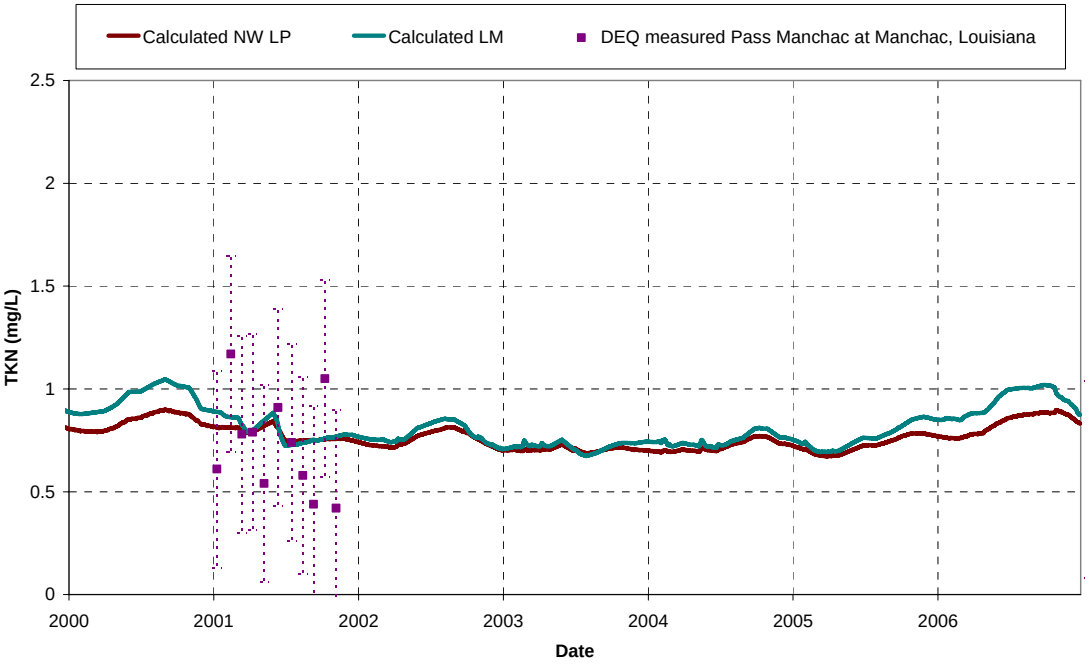

Figure 7.22 TKN validation on Lake Maurepas (2000-2007).

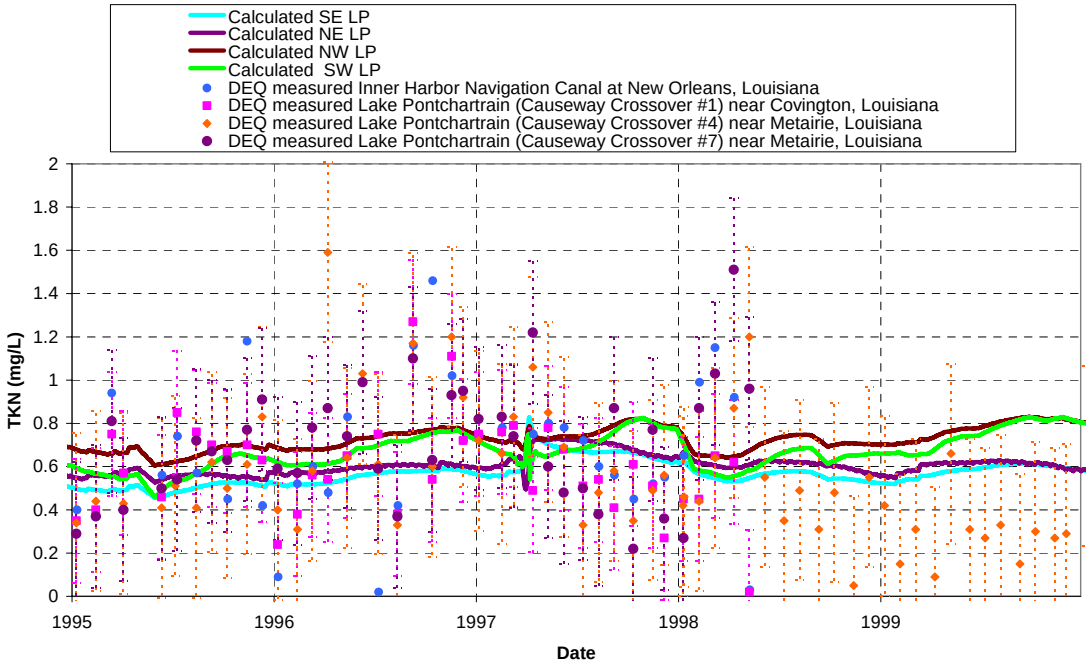

Figure 7.23 TKN validation on Lake Pontchartrain (1995-2000).

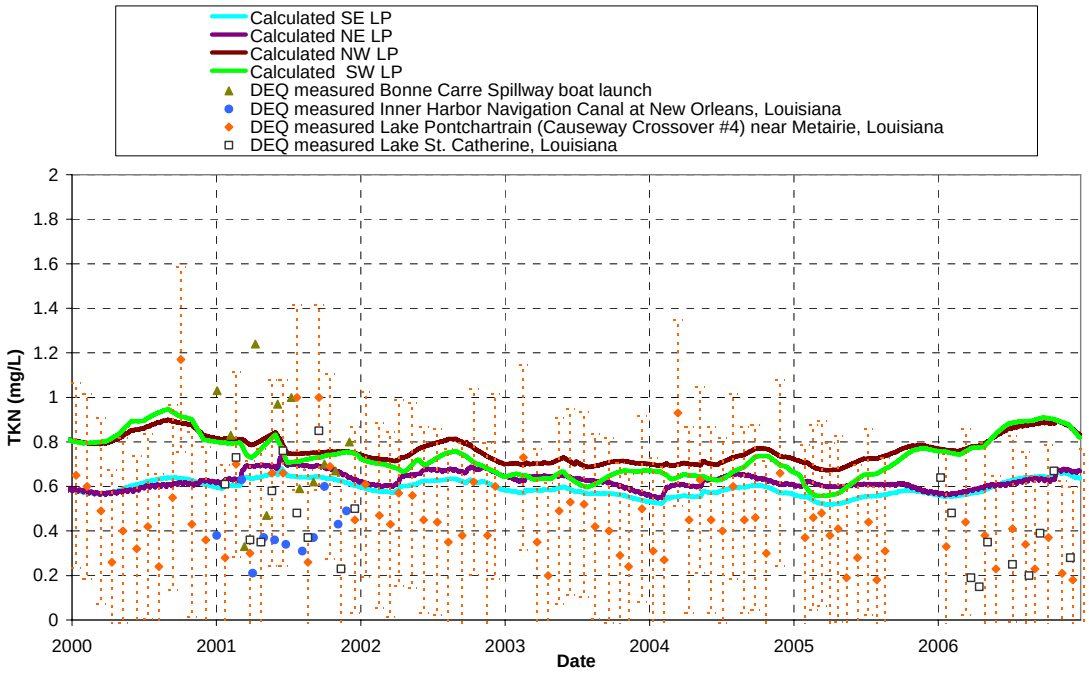

Figure 7.24. TKN validation on Lake Pontchartrain (2000-2007).

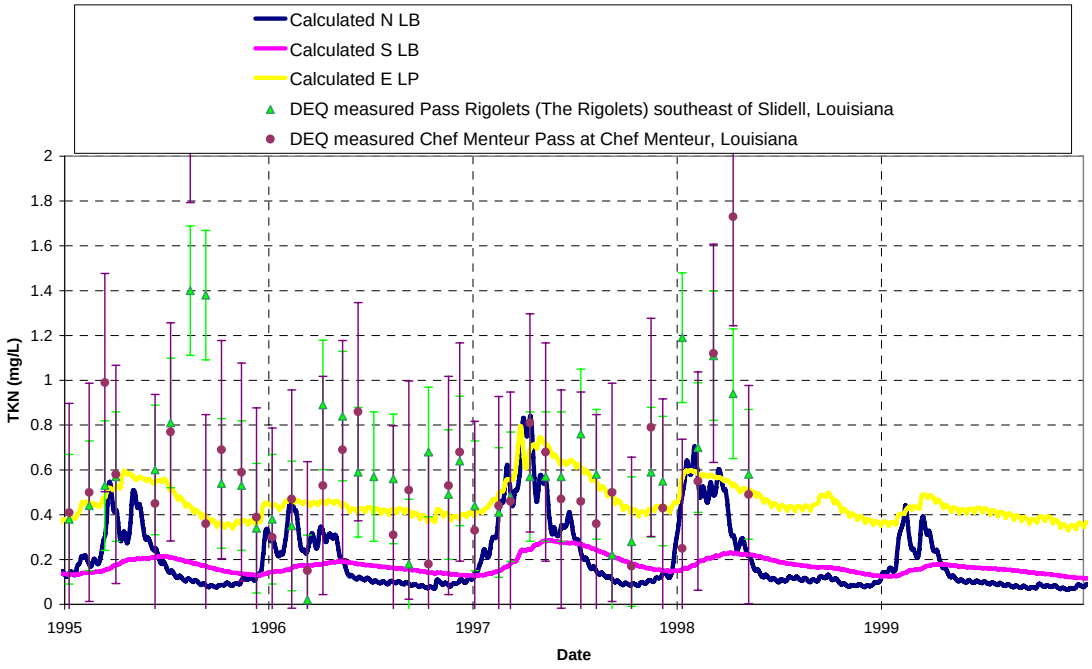

Figure 7.25 TKN validation on Lake Borgne (1995-2000).

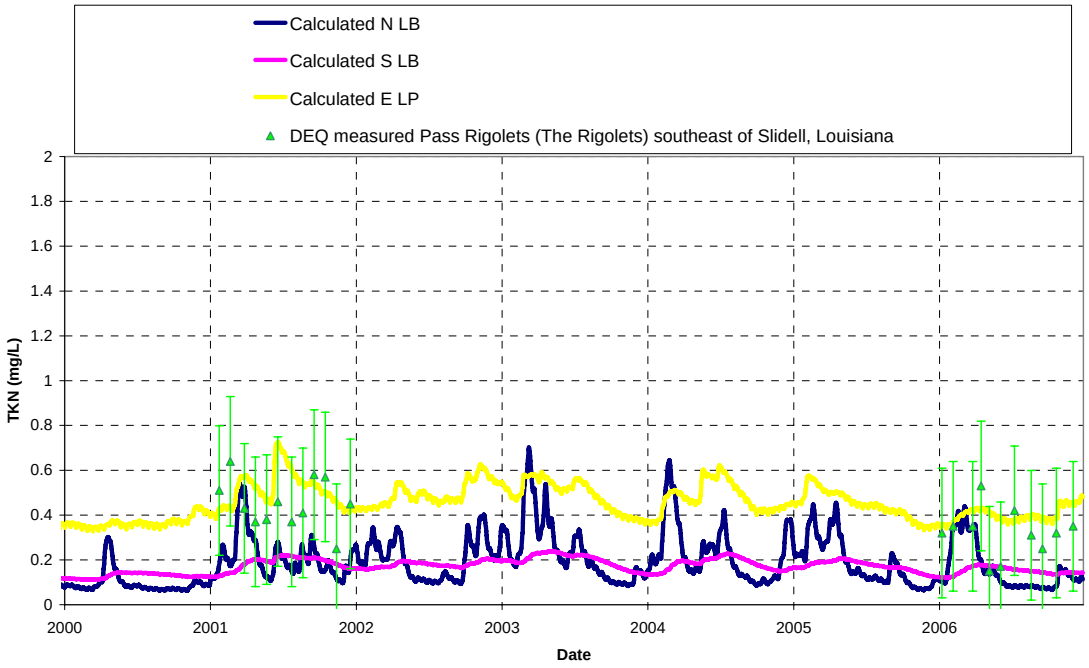

Figure 7.26 TKN validation on Lake Borgne (2000-2007).

7.3.4 Total organic carbon (TOC) validation

The model was validated with TOC data measured by the LADEQ between January 1995 and December 2006. TOC measurements are equivalent to the summation of live algae, dead algae, carbon and 7% of the suspended sediment concentrations output by the model. Comparisons between the predicted TOC concentrations and the measured data are shown below for Lakes Maurepas, Pontchartrain and Borgne (Figures 7.27 to 7.32). The solid lines in the figures represent the model output for each cell, the points represent the measured data, and the dotted bars associated with the measured data represent the standard deviation of the data. The predicted results for live algae are shown in Figures 7.33 and 7.34. The modeled results for dead algae, carbon and suspended sediment are shown separately in Appendix B.

The modeled data actually approaches the measured data better for the validation period (January 1995 to December 2006) than it did during the calibration run (January 1990 to December 1994). Again the TOC concentrations seem to follow a seasonal pattern with low values occurring in the summer and higher concentrations occurring in the winter months.

The modeled results for live algae correspond to the observations made by Poirrier et al. (1998). Poirrier et al. (1998) observed a major bloom of *Anabaena circinalis* from mid June to the end of July in 1995. The modeled live algae concentrations show an increase in concentrations during this time for all of the Lake Pontchartrain cells. The modeled live algae concentrations also increased around the entire Lake Pontchartrain basin in 1997 (including north Lake Borgne) agreeing with the well-documented algal bloom occurring after the 1997 Bonnet Carré Spillway opening. The increased concentrations in 2004 on northwest Lake Pontchartrain have not been verified with any observations.

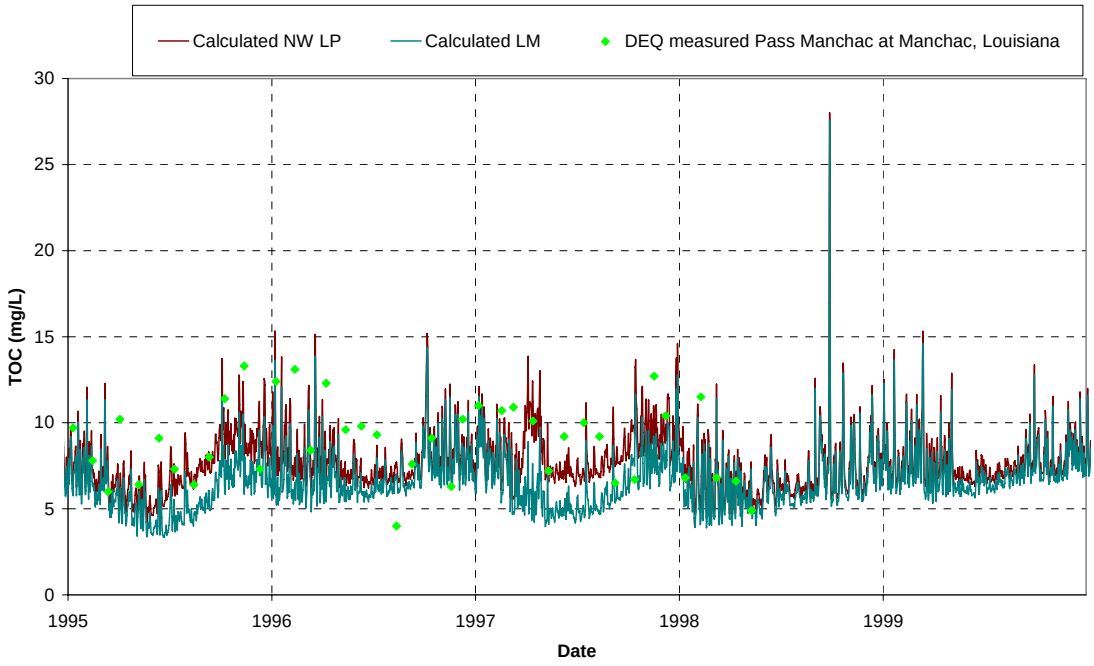

Figure 7.27 TOC validation on Lake Maurepas (1995-2000).

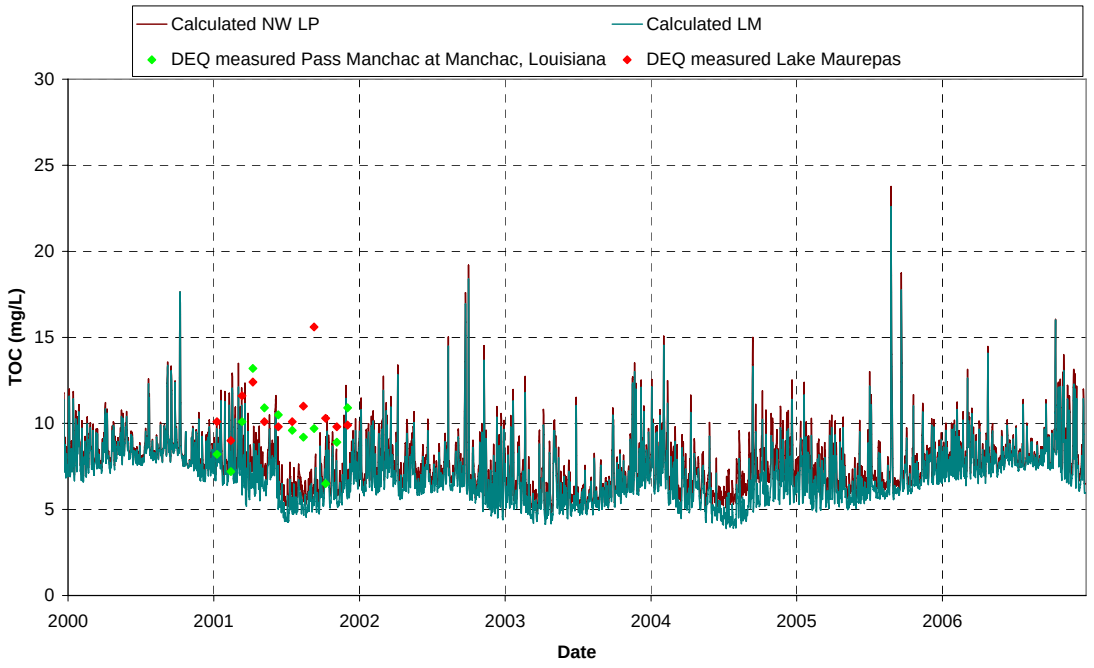

Figure 7.28 TOC validation on Lake Maurepas (2000-2007).

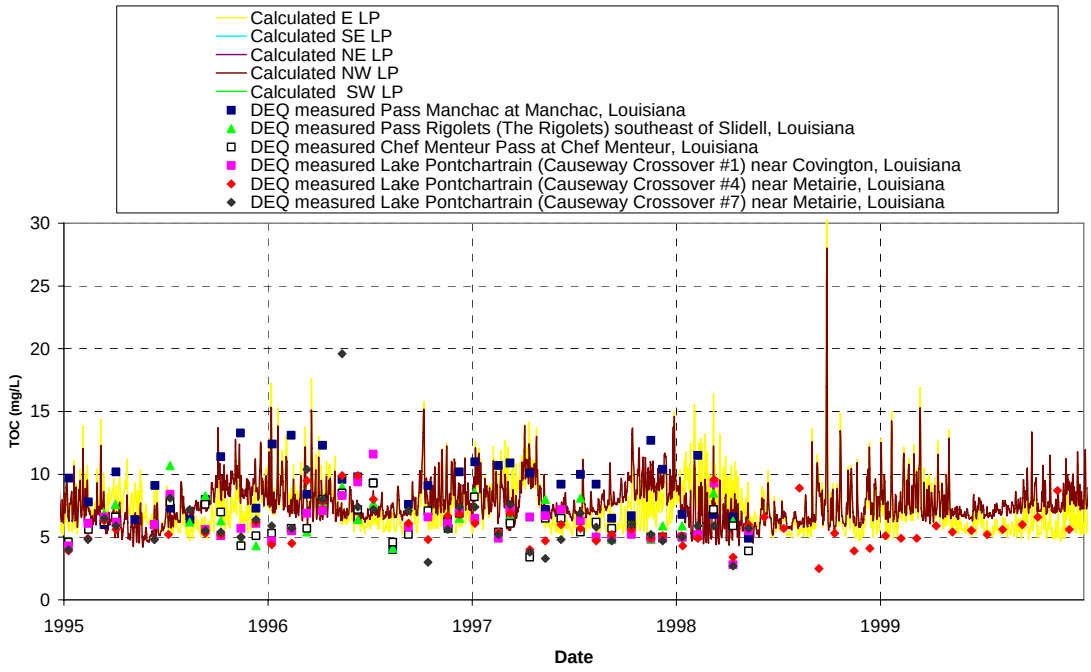

Figure 7.29 TOC validation on Lake Pontchartrain (1995-2000).

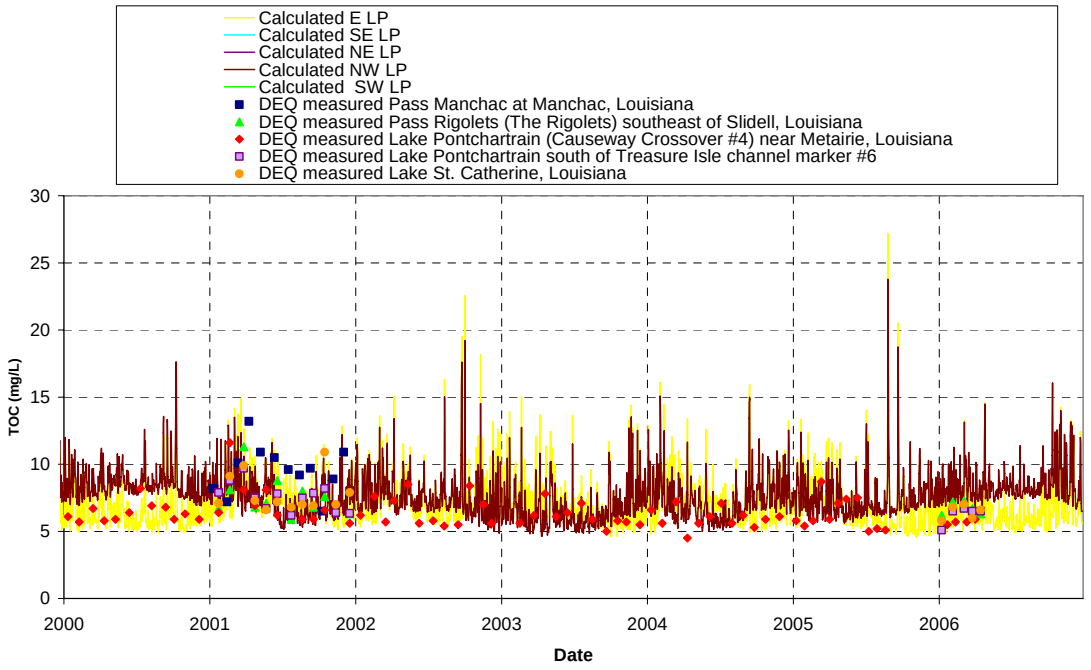

Figure 7.30 TOC validation on Lake Pontchartrain (2000-2007).

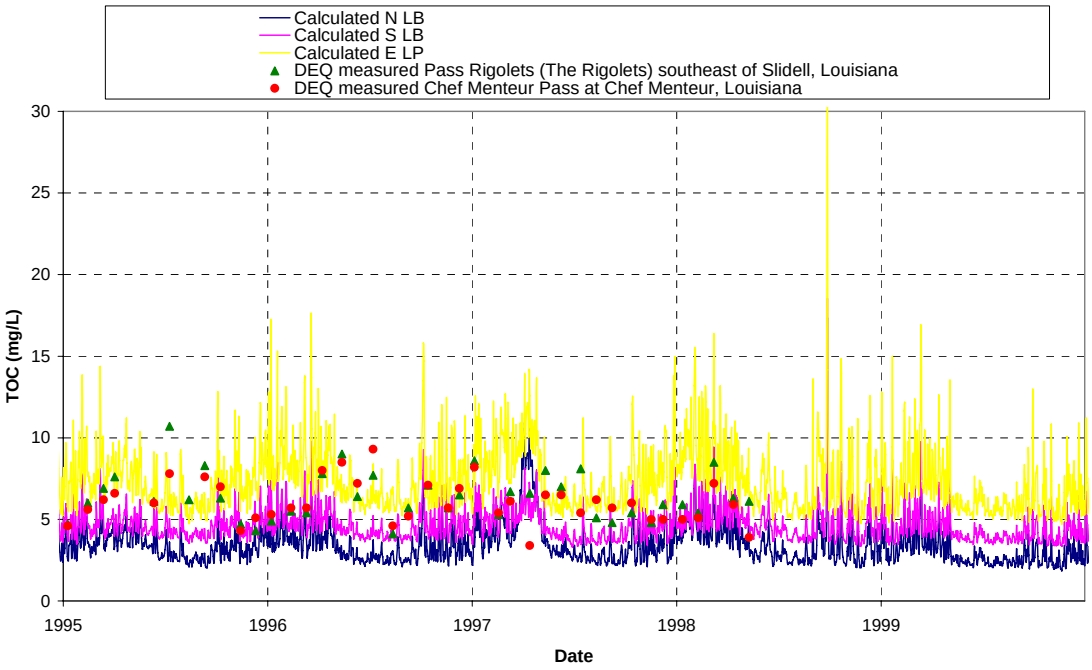

Figure 7.31 TOC validation on Lake Borgne (1995-2000).

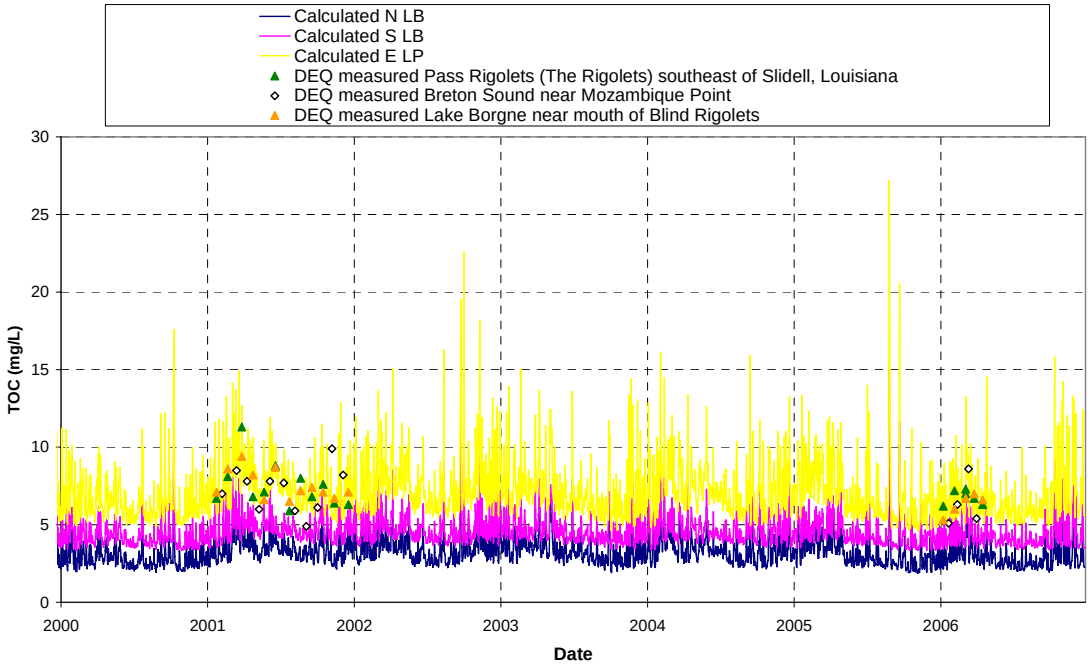

Figure 7.32 TOC Validation on Lake Borgne (2000-2007).

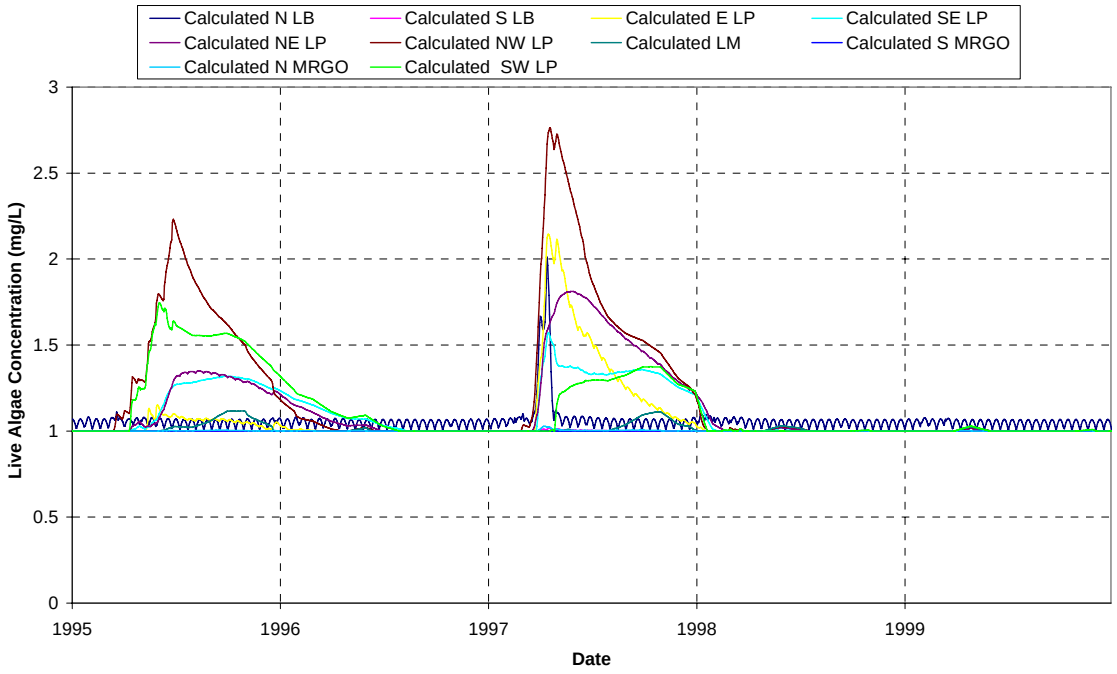

Figure 7.33 Calculated live algae concentrations (1995-2000).

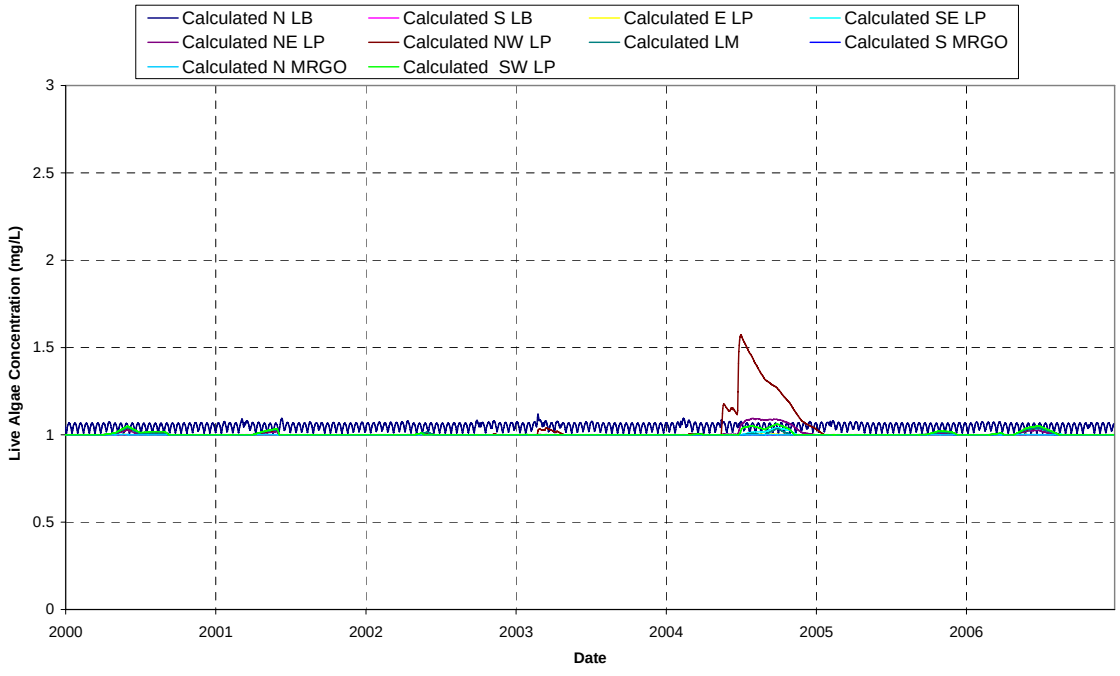

Figure 7.34 Calculated live algae concentrations (2000-2007).

7.4 Tidal validation

The tidal properties are the same during the validation period: the spring tidal range in Lake Pontchartrain is approximately 0.15 m, the mean tidal range is approximately 0.11 m and the peak exchange flows on the spring ebb and flood tides through all of the passes (IHNC, Chef Menteur, Rigolets and Pass Manchac) are approximately 8,800 m^3/s (McCorquodale et al., 2007). The predicted tides for the Pontchartrain Estuary model between June and August 1997 and 2003 are shown below in Figure 7.35 and 7.36 for north Lake Borgne and east Lake Pontchartrain. The tides in Lake Pontchartrain are in the mean range of 0.11m.

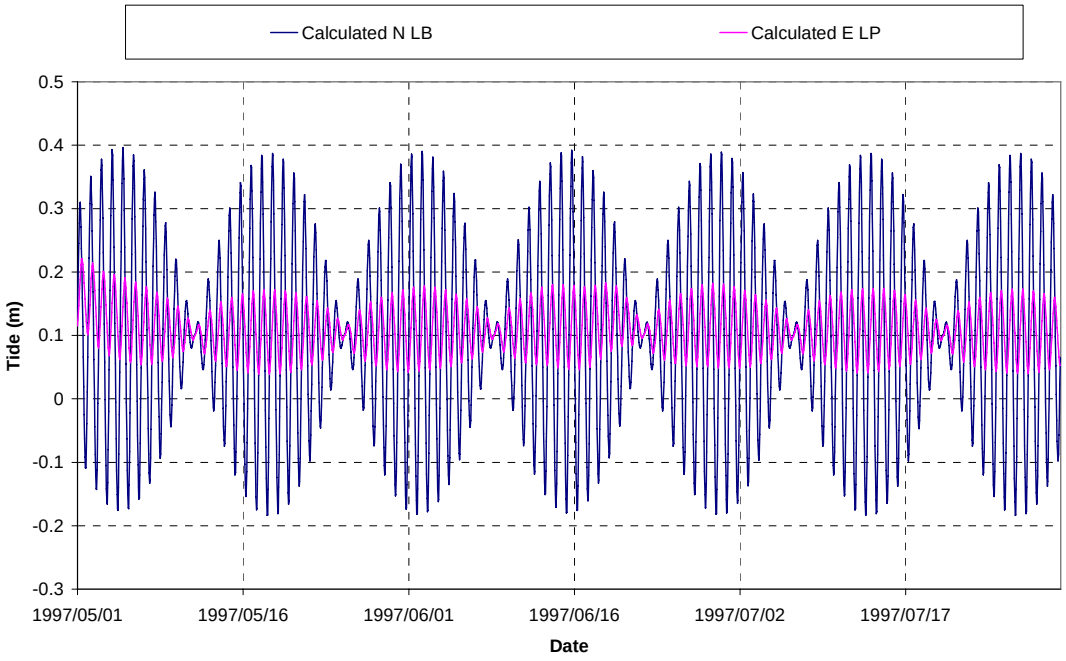

Figure 7.35 Calculated tidal fluctuations (1995-2000).

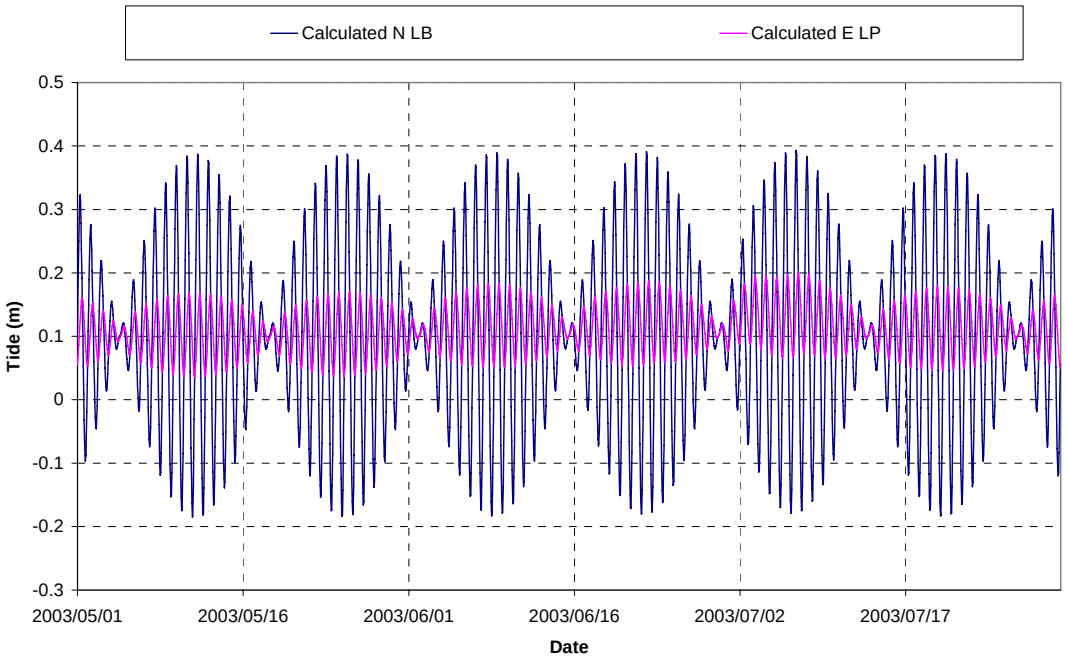

Figure 7.36 Calculated tidal fluctuations (2000-2007).

7.5 Algal bloom probability model interpretation

The predicted output from the algal bloom probability model described in section 4.3.11 is shown below in Figures 7.37 to 7.43. The occurrence of algal blooms around the Pontchartrain Estuary can be predicted when the output from the algal bloom probability model is used in conjunction with the modeled live algae concentrations. The algal bloom probability model fluctuates a lot since it assesses the likelihood of algal blooms occurring on a daily basis. The live algae concentrations are produced from averaged results that depend on the conditions preceding it and do not have a tendency to fluctuate. When the live algae concentrations are heightened and the probability from the algal bloom model is high, algal blooms will be assumed to occur. The live algae concentrations calculated by the model are shown in Figures 7.37 to 7.43 above the algal bloom probability model results.

In Figure 7.37, there is only a high probability of an algal bloom occurring in Lake Borgne in 1997. Live algae concentrations are also high during this period indicating that an algal bloom likely occurred in Lake Borgne in 1997. This corresponds to observations made during the 1997 algal bloom in the Pontchartrain Estuary.

In Figure 7.38 and 7.40, there is a high probability of an algal bloom occurring in 1995 and 1997 in eastern and southeastern Lake Pontchartrain. Live algae concentrations are also high during these periods. These observations correspond to the statements made by Poirrier et al. (1998) regarding the extensive 1995 bloom and the large bloom that occurred after the 1997 Bonnet Carré Spillway opening.

In Figure 7.39 for northeastern Lake Pontchartrain, high probabilities of an algal bloom and increases in live algae concentrations occur in 1995, 1997 and 2004. The two observations in 1995 and 1997 can be confirmed by the observations made by Poirrier et al. (1998) but the 2004 occurrence cannot. It could be that the increase in live algae concentrations was not large enough to have caused a bloom in northeast Lake Pontchartrain in 2004.

Figure 7.41 shows the results for southwest Lake Pontchartrain. High probabilities of an algal bloom and increases in live algae concentrations occur in 1995, 1997 and 2004. Again, the two observations in 1995 and 1997 can be confirmed with observational data (Poirrier et al., 1998) but the 2004 occurrence cannot. An algal bloom may not have occurred in 2004 since the increase in live algae concentration and algal bloom probability are lower than the 1995 and 1997 results where blooms were documented. Interestingly, the live algae concentrations are significantly higher in 1995 than in 1997 in southwest Lake Pontchartrain.

Figure 7.42 shows the results for northwest Lake Pontchartrain. High probabilities of an algal bloom and increases in live algae concentrations occur in 1995, 1997 and 2004. Again, the two observations in 1995 and 1997 can be confirmed with observational data (Poirrier et al., 1998) but the 2004 occurrence cannot. An algal bloom may actually have occurred in northwest Lake Pontchartrain in 2004 since the increases in live algae concentration and algal bloom probability are higher than the modeled results for southwest and northeast Lake Pontchartrain.

Figure 7.43 again shows that there is a high probability of an algal bloom occurring in Lake Maurepas in most years. This is likely due to the high concentrations of nutrients flowing into Lake Maurepas from the tributaries. However, during the validation period the modeled live algae concentrations show an increase in 1995 and 1997 indicating the occurrence of a potential algal bloom. Poirrier et al. (1998) documented a major bloom of *Anabaena circinalis* from mid June to the end of July in 1995 that could have occurred in Lake Maurepas. Other researchers also documented the extensive bloom that occurred around the entire Lake Pontchartrain basin in 1997.

The validation of the model again indicates that the occurrence of algal blooms around the Pontchartrain Estuary can be predicted when the output from the algal bloom probability model is used in conjunction with the modeled live algae concentrations. The model accurately predicted the bloom events that were observed by Poirrier et al. (1998) around Lake Pontchartrain in 1995 and the entire Pontchartrain Estuary in 1997. The predicted algal bloom in northwest, northeast and southwest Lake Pontchartrain in 2004 cannot be disproved since no observations were documented.

The model accurately predicts the spatial extent of algal blooms in the Pontchartrain Estuary and can be used to assess how new diversions will effect the potential for algae blooms around the Estuary.

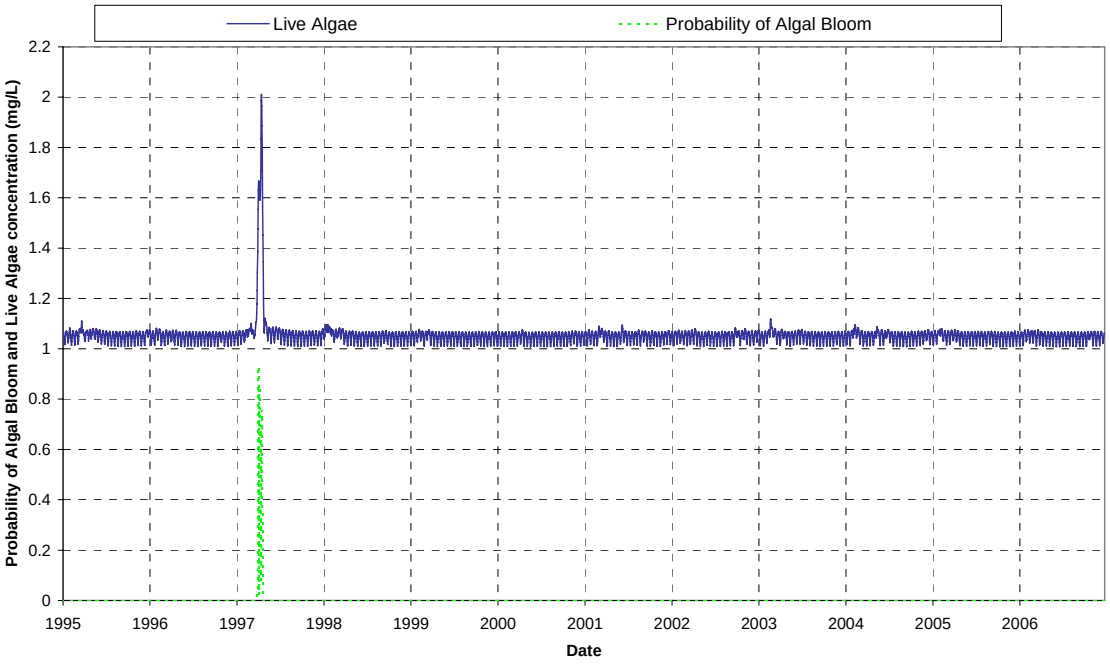

Figure 7.37 Predicted probability of algal bloom on Lake Borgne with predicted live algae concentrations (1995-2007).

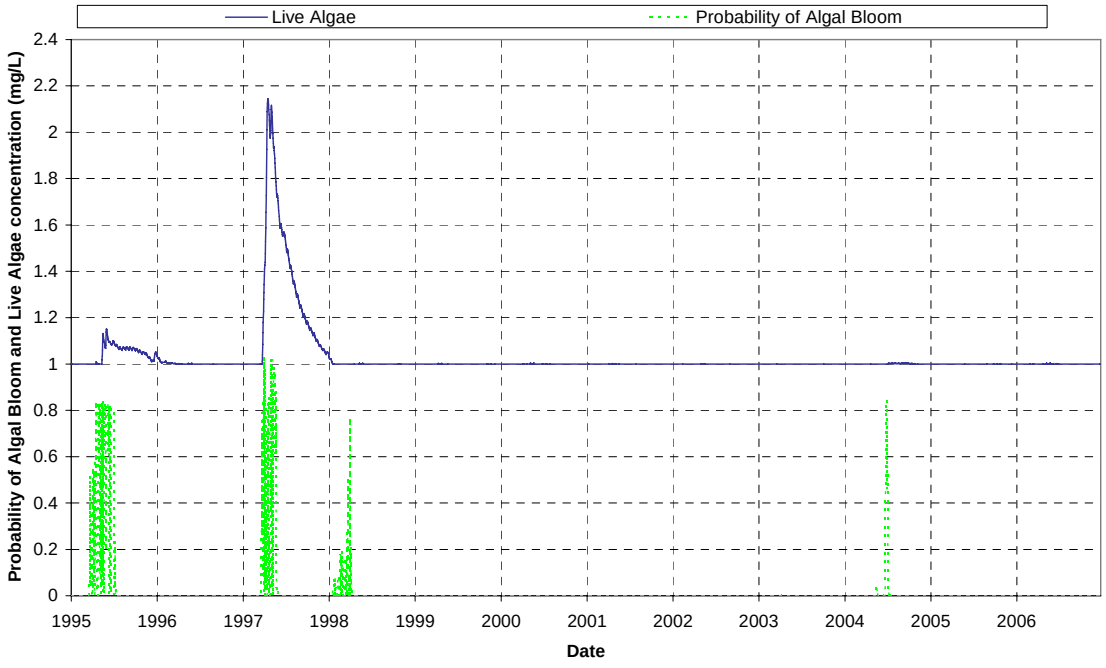

Figure 7.38 Predicted probability of algal bloom on eastern Lake Pontchartrain with predicted live algae concentrations (1995-2007).

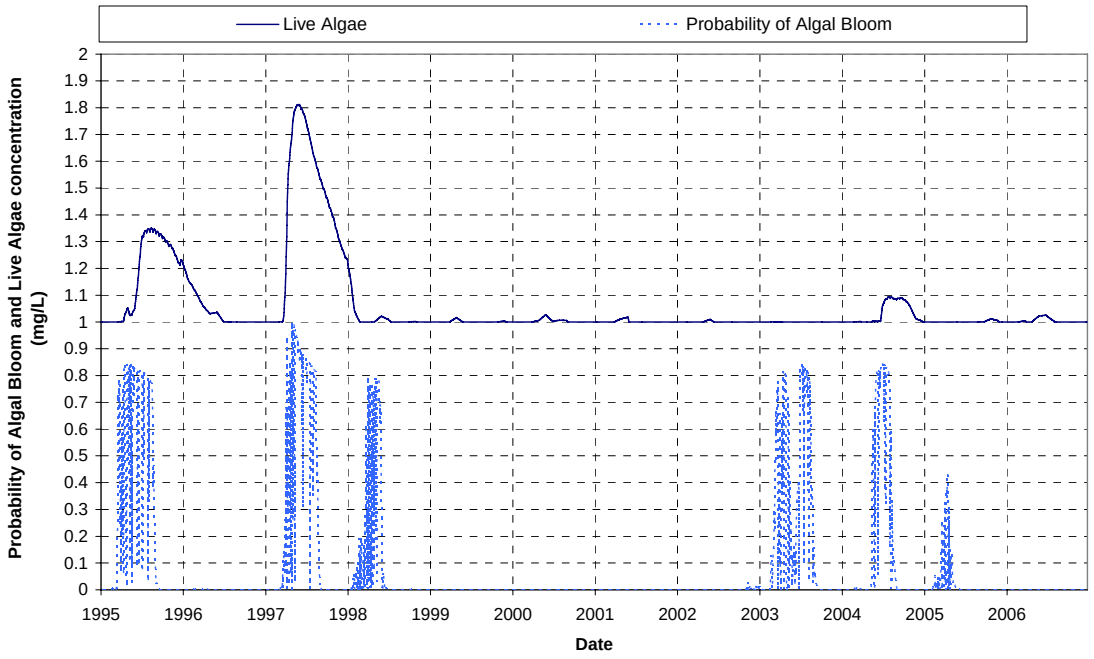

Figure 7.39 Predicted probability of algal bloom on northeast Lake Pontchartrain with predicted live algae concentrations (1995-2007).

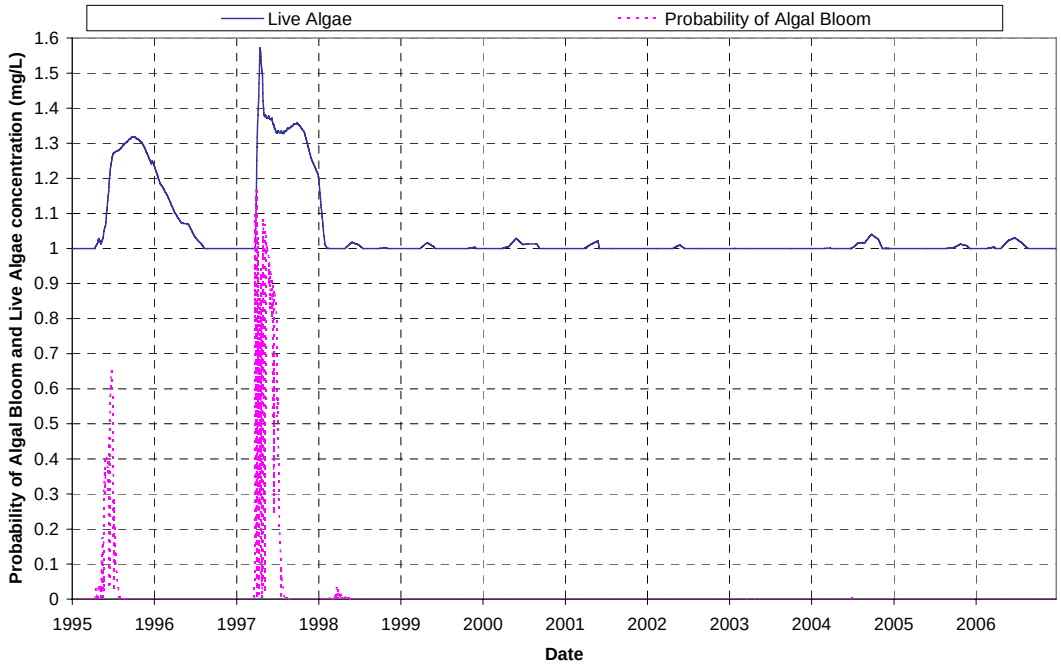

Figure 7.40 Predicted probability of algal bloom on southeast Lake Pontchartrain with predicted live algae concentrations (1995-2007).

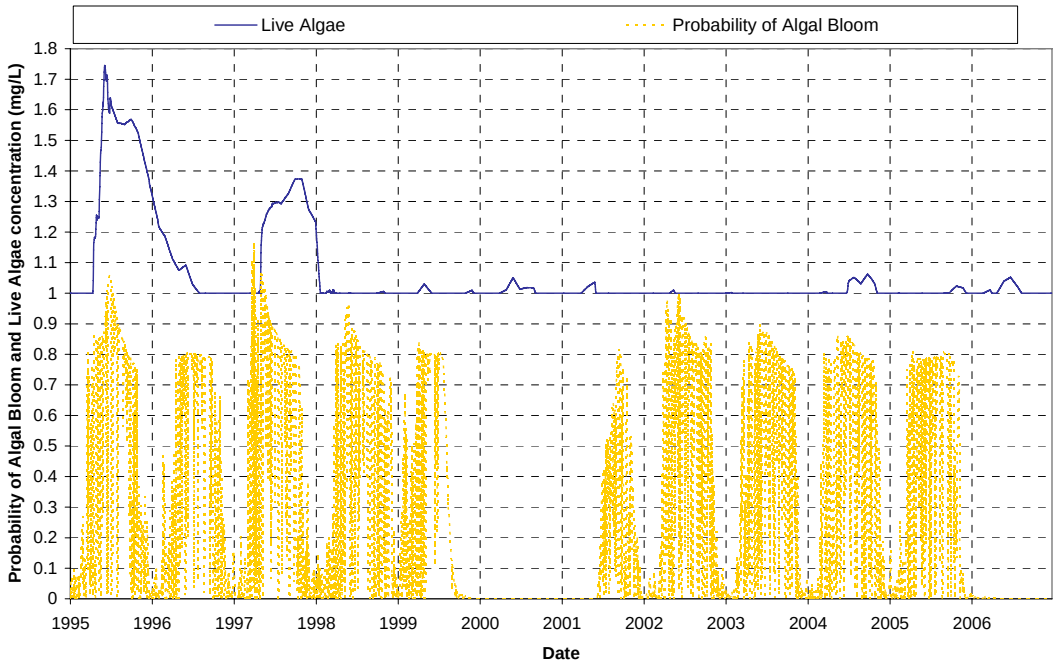

Figure 7.41 Predicted probability of algal bloom on southwest Lake Pontchartrain with predicted live algae concentrations (1995-2007).

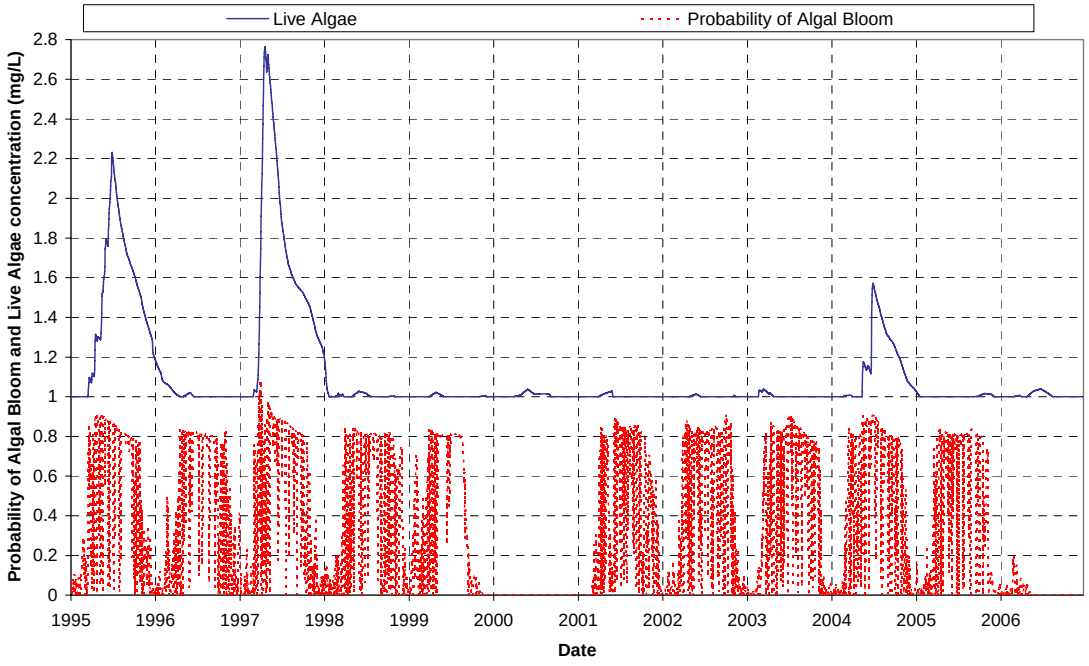

Figure 7.42 Predicted probability of algal bloom on northwest Lake Pontchartrain with predicted live algae concentrations (1995-2007).

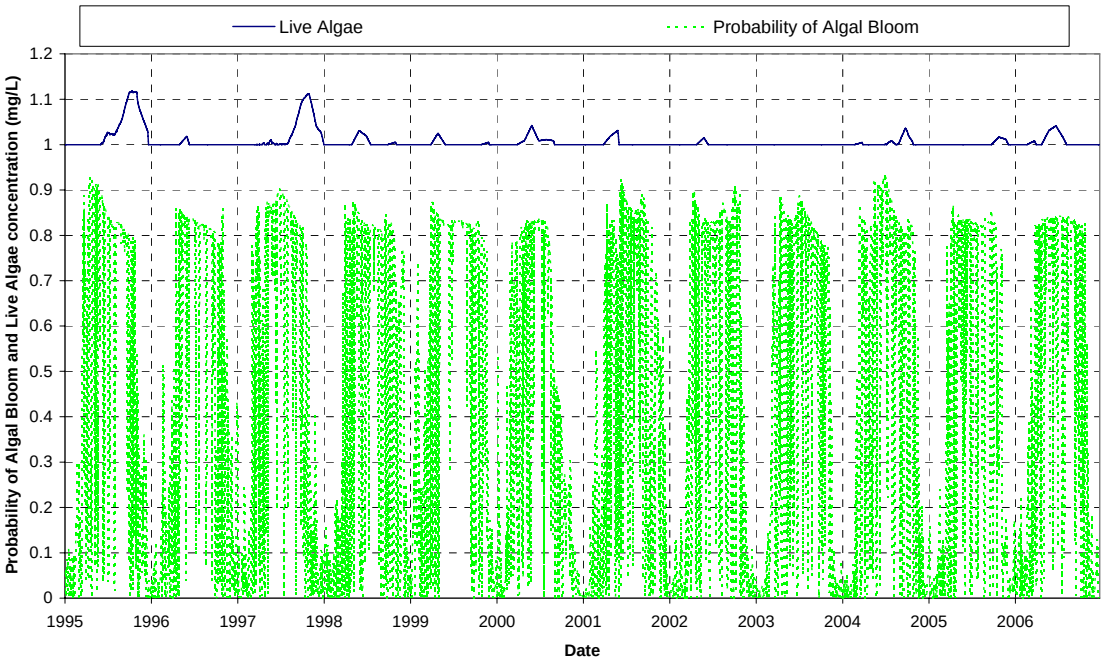

Figure 7.43 Predicted probability of algal bloom on Lake Maurepas with predicted live algae concentrations (1995-2007).

8.0 Management scenarios

8.1 General

As outlined in section 1.5, one of the main purposes of this research is to investigate the long-term effects of different management scenarios on the water quality of the Upper Pontchartrain Estuary. The 1-D tidal, salinity and water quality model accurately predicts the occurrence of algal blooms in the Estuary between January 1990 and December 2006. This model can now be used to assess how different management scenarios will change the probability of algal blooms around the Estuary. Three management scenarios have been considered and involve looking at the:

- Effect of the proposed freshwater diversions into Maurepas Swamp on water quality in the Pontchartrain Estuary,
- Effect of increased leakage events from the Bonnet Carré Spillway on water quality in the Pontchartrain Estuary, and
- Effect of timing of complete Bonnet Carré Spillway openings on Pontchartrain Estuary water quality.

The management scenarios were run from January 1990 to December 2006 using the calibrated and validated 1-D tidal, salinity and water quality model described above in sections 4.0 to 6.0. All of the inputs, constants, and coefficients that were used in the model for calibration and validation were held constant. The same nutrient concentrations and reductions as those used for Mississippi River water in the calibration and validation runs were used in the scenarios. If the diversion flows were less than 500 m^3/s, then the concentrations were reduced according to the amounts found by Lane et al. (2001): suspended sediment concentrations decreased by 85%, nitrite + nitrate as nitrogen concentrations decreased by 17.5% (half of that recommended by Lane et al., 2001), ammonia and organic nitrogen concentrations decreased by 28% and total phosphorous concentrations decreased by 25% (half of that recommended by Lane et al., 2001) throughout the length of the spillway. If the flows were greater than 500 m^3/s, no reductions took place. The three management scenarios and the changes observed in the algal bloom probability model will be discussed below.

8.2 Proposed diversions on Lake Maurepas

8.2.1 Lake Maurepas diversion scenario description

As mentioned earlier, the State Master Plan has proposed three freshwater diversions projects in the Pontchartrain Estuary basin area. Two new small diversions (flows between 30 m^3/s to 140 m^3/s) connecting the Mississippi River to Maurepas Swamp are anticipated at Hope Canal and Convent/Blind River near Gramercy, LA. These diversions will be adding sediment and nutrient rich Mississippi River water to Maurepas Swamp, which drains into Lake Maurepas and eventually Lake Pontchartrain. The third proposed freshwater diversion project involves redistributing flow along the Amite River and does not involve the introduction of a new source of freshwater. Therefore, only the first two diversions will be considered in our first management scenario.

Two flow scenarios were simulated to capture the full range of proposed diversion flows. The first scenario run assumed only one diversion was actively discharging into Lake Maurepas while the second scenario run assumed two diversions were actively discharging into Lake Maurepas. For the one diversion scenario, the minimum flow of 30 m^3/s was assumed, while for the two diversion scenario, the maximum flow of 280 m^3/s was considered.

To emulate the natural fluctuations of the Mississippi River, the hydrograph that was developed for the leakage and flow events on the Bonnet Carré Spillway (section 5.3) was used as a basis for the Lake Maurepas diversion hydrographs. The diversion hydrographs used the Bonnet Carré Spillway hydrograph for flows that were less than their assumed flows (30 m^3/s or 280 m^3/s) and assigned the assumed flows to any areas where the Bonnet Carré Spillway hydrograph exceeded the assumed flows. Figure 8.1 shows the hydrographs used in the analysis.

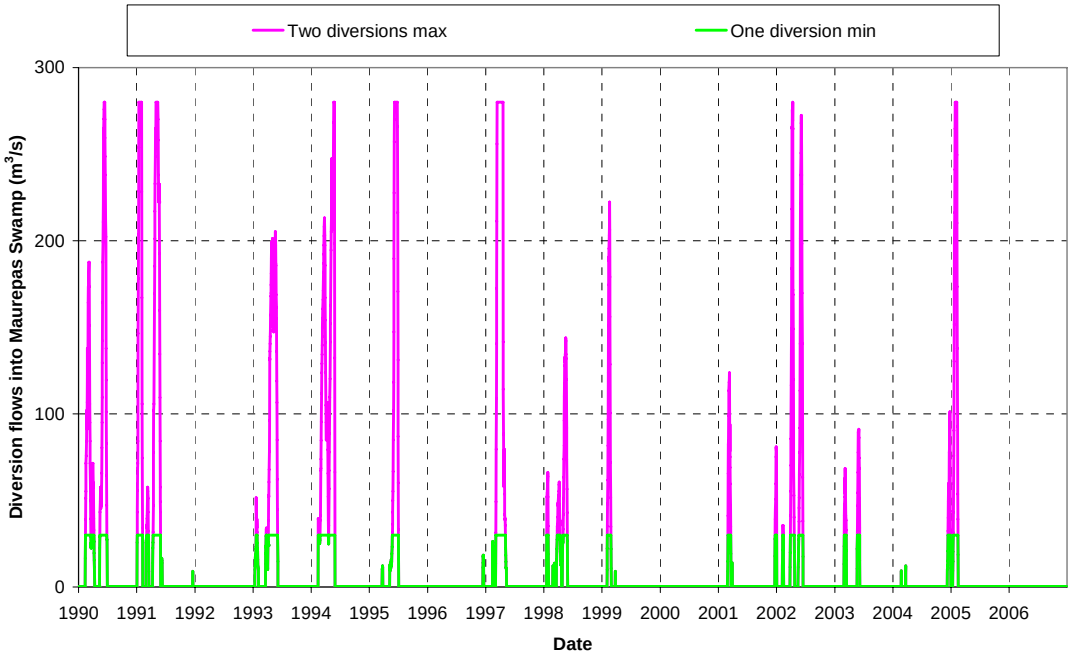

Figure 8.1 Maurepas Swamp diversion scenario hydrographs.

The proposed Lake Maurepas diversions were assumed to contribute 100% of their flow and loading to the Lake Maurepas cell (cell 7). As discussed above, the same loadings and reductions of Mississippi River water were applied to these diversions as those in the Bonnet Carré Spillway in the calibration and validation runs. This is a conservative assumption since reductions will likely be higher for diversions entering Maurepas Swamp then those entering the Bonnet Carré Spillway due to the longer length and denser vegetation present. The same Bonnet Carré Spillway opening and leakage events were input into the model as those in the calibration and validation run.

8.2.2 Algal bloom probability model interpretation

The probability of an algal bloom results for the two diversion scenario (maximum flow of 280 m^3/s) are shown below in Figures 8.2 to 8.8. The live algae concentrations are shown above the probabilities on all of the plots. As discussed in the calibration and validation sections, algal blooms can be accurately predicted around the Pontchartrain Estuary when the probability model results are combined with the live algae concentrations. When the probabilities and live algae concentrations are high, it is likely that an algal bloom will occur in the Estuary. The results for the one diversion scenario (minimum flow of 30 m^3/s) into Lake Maurepas are shown in Appendix C.

If a diversion flow of 280 m^3/s entered Lake Maurepas through Maurepas Swamp between 1990 and 2006, algal blooms around the Pontchartrain Estuary would have been more frequent and intense. The predicted algal blooms that occur in response to the new diversions are documented in Table 8.1 (the change from the initial condition is documented). The table shows that if a diversion of 280 m^3/s was flowing into Lake Maurepas between 1990 and 2006, the blooms in 1993 and 1994 would have extended into eastern Lake Pontchartrain and another bloom would have occurred around most of Lake Pontchartrain in 1990 in addition to those that occurred in 1991, 1995, 1997 and 2004. Small diversions (30 m^3/s) into Maurepas Swamp do not have a significant impact on the water quality around the Pontchartrain Estuary. Each plot and how the predicted algal blooms were derived for each area in the Pontchartrain Estuary are discussed below.

Table 8.1 Changes in algal bloom occurrence around the Pontchartrain Estuary as a result of the new diversions into Lake Maurepas.

Year	Calibrated and Validated model (initial conditions)	One diversion, minimum flow scenario 30 m^3/s	Two diversion, maximum flow scenario 280 m^3/s	Timing of Bonnet Carré flow Event
1990		LM	SELP, NELP, NWLP, SWLP, LM	March and June
1991	ELP, SELP, NELP, NWLP, SWLP			January and May
1993	NWLP		SELP, NELP, SWLP	January and May
1994	NWLP, SWLP		NELP	March and May
1995	ELP, SELP, NELP, NWLP, SWLP, LM			June
1997	LB, ELP, SELP, NELP, NWLP, SWLP, LM			March and April
2004	NELP, NWLP, SWLP			

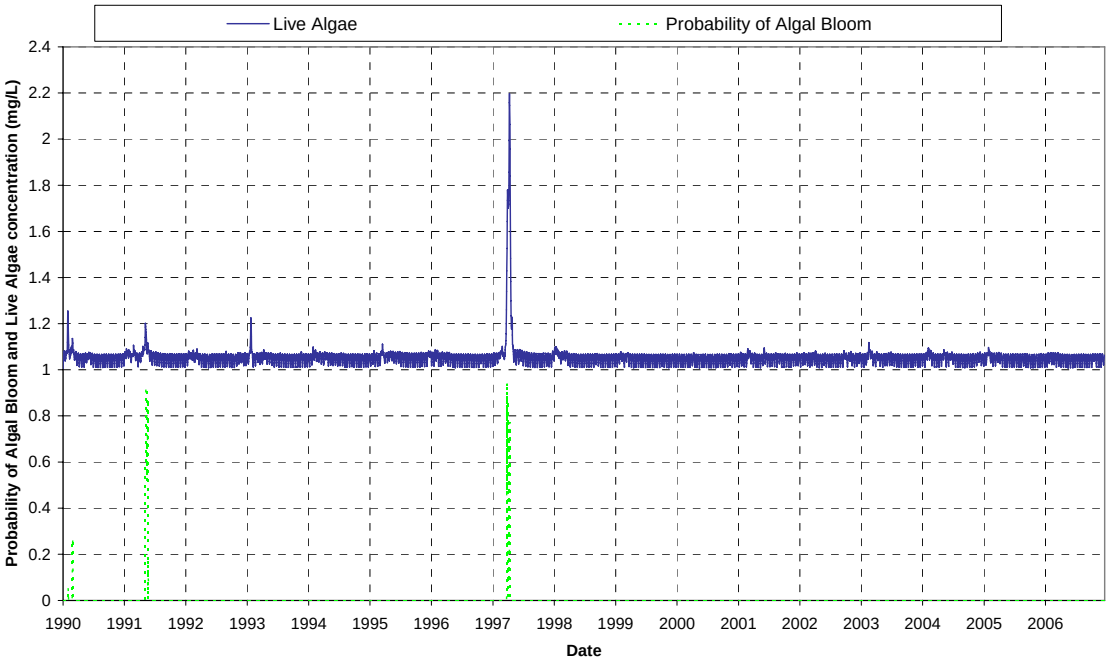

Figure 8.2 Probability of an algal bloom on Lake Borgne with live algae concentrations (two diversions, flow of 280 m^3/s).

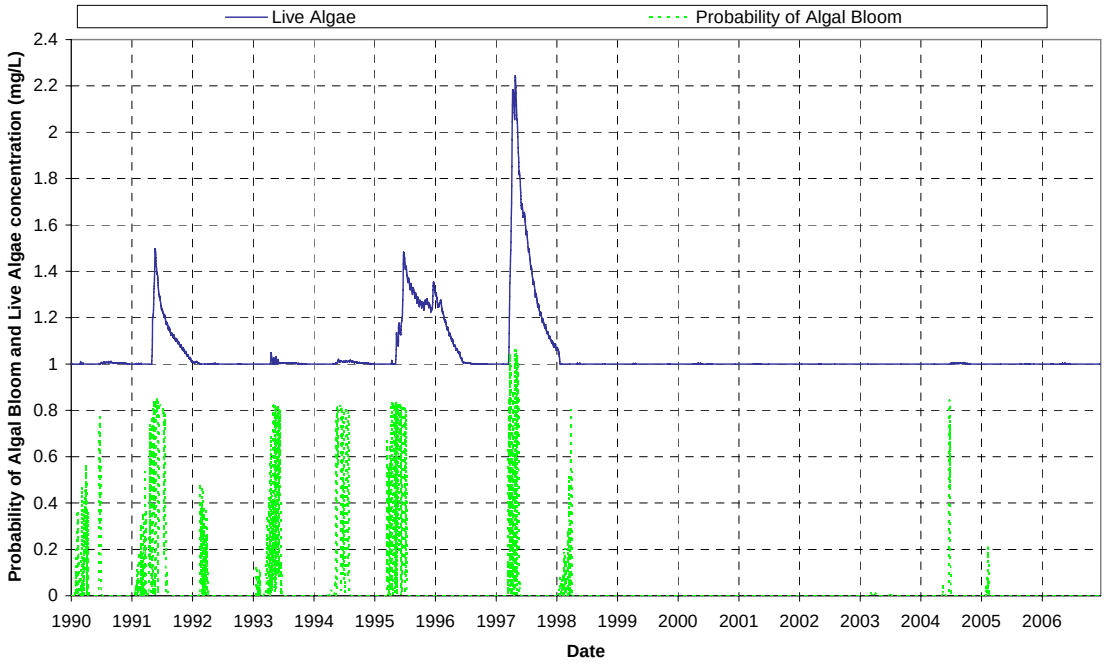

Figure 8.3 Probability of an algal bloom on east Lake Pontchartrain with live algae concentrations (two diversions, flow of 280 m^3/s).

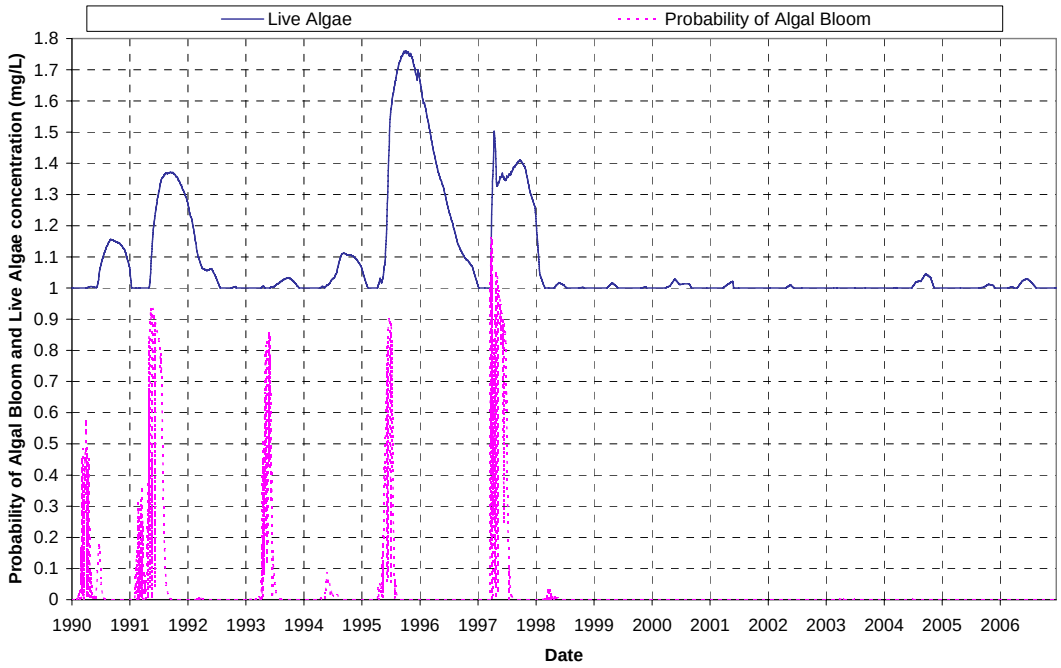

Figure 8.4 Probability of an algal bloom on southeast Lake Pontchartrain with live algae concentrations (two diversions, flow of 280 m^3/s).

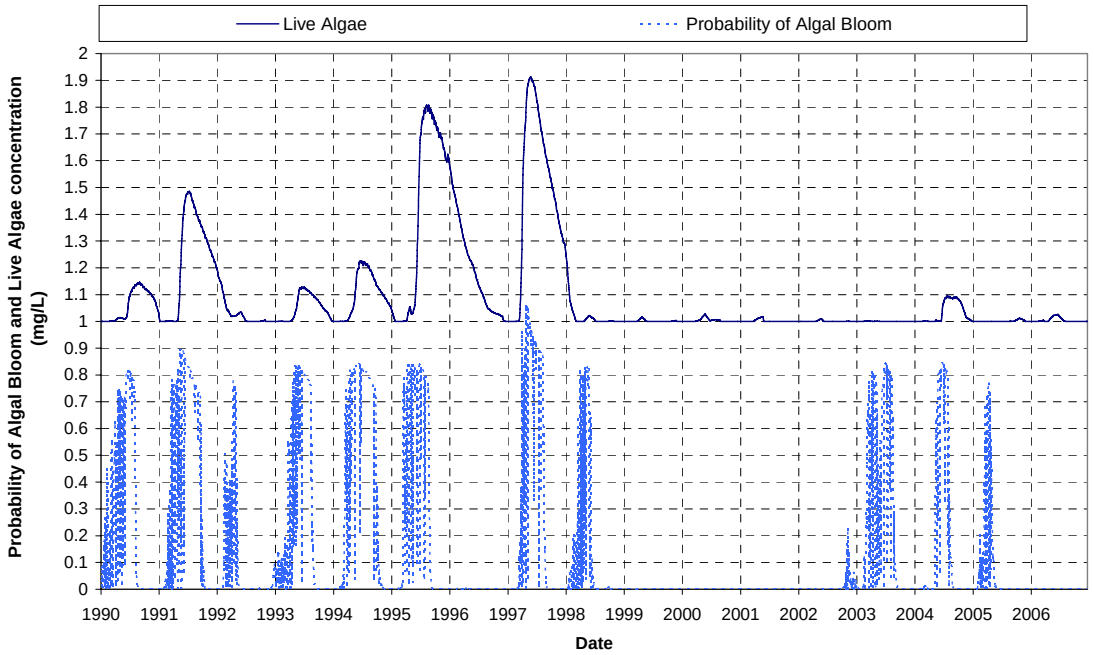

Figure 8.5 Probability of an algal bloom on northeast Lake Pontchartrain with live algae concentrations (two diversions, flow of 280 m^3/s).

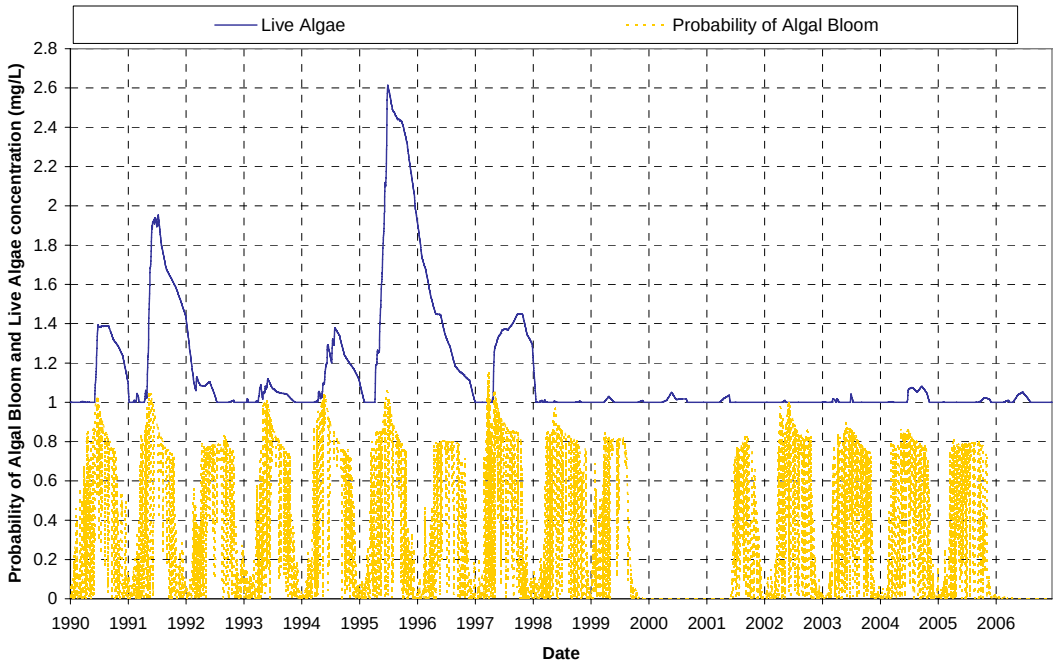

Figure 8.6 Probability of an algal bloom on southwest Lake Pontchartrain with live algae concentrations (two diversions, flow of 280 m^3/s).

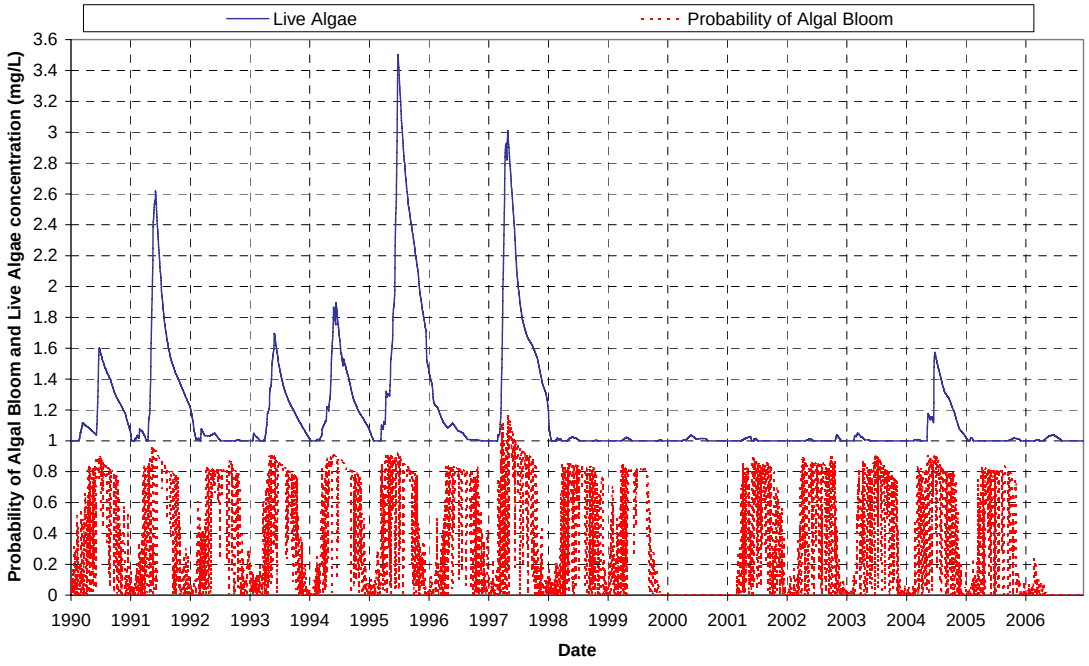

Figure 8.7 Probability of an algal bloom on northwest Lake Pontchartrain with live algae concentrations (two diversions, flow of 280 m^3/s).

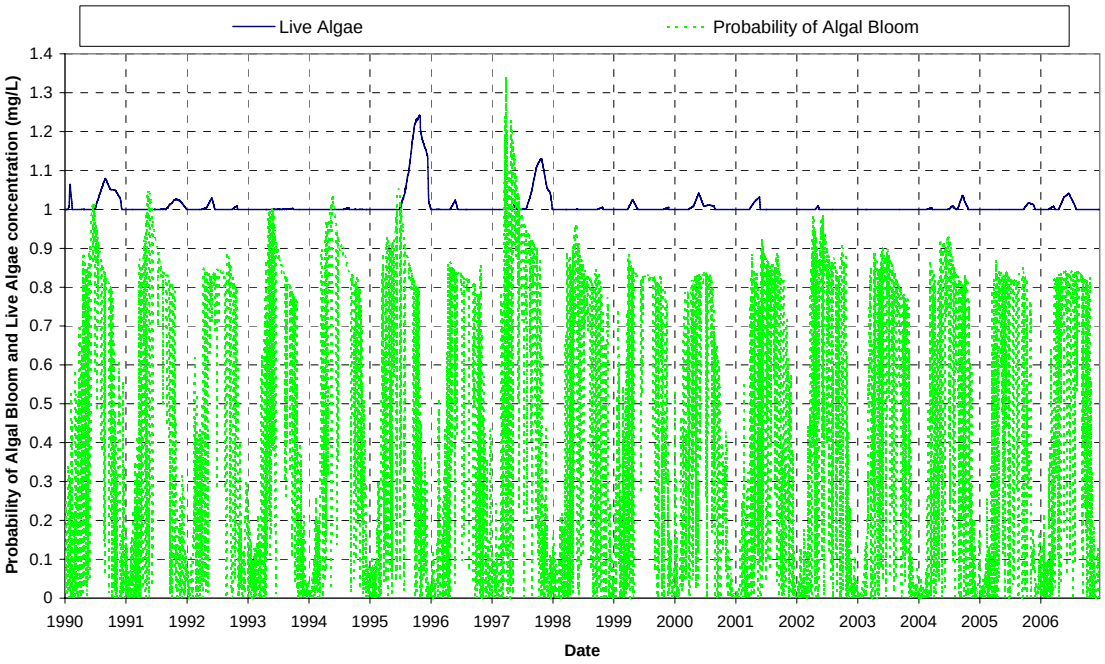

Figure 8.8. Probability of an algal bloom on Lake Maurepas with live algae concentrations (two diversions, flow of 280 m^3/s).

The proposed diversions did not have a significant effect on the occurrence of algal blooms in Lake Borgne (Figure 8.2). The proposed diversions also did not have a significant effect on algal blooms in east Lake Pontchartrain (Figure 8.3). The live algae concentrations increased as a result of the new diversions, but no additional blooms outside of those previously predicted in 1991, 1995 and 1997 were predicted to occur. There is little difference between the magnitude of live algae concentrations between the two diversion maximum flow scenario and the one diversion minimum flow scenario.

This is not the case in southeast Lake Pontchartrain (Figure 8.4). The two diversion, maximum flow scenario, causes both live algae concentrations and the probabilities of an algal bloom to increase in 1990 and 1993. Therefore the new diversion into Lake Maurepas (two diversions maximum flow scenario) could have caused algal blooms to occur in 1990 and 1993 in addition to the previously predicted blooms that occurred in 1991, 1995 and 1997. The one diversion, minimum flow scenario does not predict the occurrence of any algal blooms in southeast Lake Pontchartrain apart from those that were predicted in the calibrated and validated model.

In northeast Lake Pontchartrain (Figure 8.5), the probabilities do not increase significantly for either scenario (except a small increase in 2005). However, the two diversion, maximum flow scenario, causes the live algae concentrations to increase in the years 1990, 1991, 1993, 1994, 1995, 1997, and 2004. These increases indicate that three new algal blooms could have occurred in northeast Lake Pontchartrain in 1990, 1993 and 1994 as a result of the new diversion into Lake Maurepas (two diversion, maximum flow scenario) in addition to the previously predicted blooms that occurred in 1991, 1995, 1997 and 2004. The one diversion scenario with minimum flow did not predict the formation of any new blooms in northeast Lake Pontchartrain apart from those that were predicted in the calibrated and validated model.

In southwest Lake Pontchartrain (Figure 8.6), the probabilities do not increase significantly for either scenario. However, for the two diversion, maximum flow scenario, the live algae concentrations increase in the years 1990, 1991, 1993, 1994, 1997, and 2004. There is a significant increase in live algae concentrations in 1995. These increases in live algae concentrations indicate that two new algal blooms could have occurred in 1990 and 1993 as a result of the new diversion into Lake Maurepas (two diversion scenario at maximum flow) in addition to the previously predicted blooms that occurred in 1991, 1994, 1995, 1997 and 2004. The significant increase in live algae concentrations could also have caused an additional bloom to occur in 1996. The one diversion scenario with minimum flow did not predict the formation of any new algal blooms on southwest Lake Pontchartrain apart from those that were predicted in the calibrated and validated model.

In northwest Lake Pontchartrain (Figure 8.7), the probabilities do not increase significantly for either scenario. However, for the two diversion, maximum flow scenario, the live algae concentrations increase in the years 1990, 1991, 1993, 1994, 1997, and 2004. Similar to southwest Lake Pontchartrain, there is a significant increase in live algae concentrations in 1995. These increases indicate that an additional algal bloom could have occurred in 1990 in addition to the previously predicted blooms that occurred in 1991, 1993, 1994, 1995, 1997 and 2004. The one diversion scenario with minimum flow did not predict the formation of any new blooms in northwest Lake Pontchartrain apart from those that were predicted in the calibrated and validated model.

In Lake Maurepas (Figure 8.8) the two diversion, maximum flow scenario causes both live algae concentrations and probabilities to increase. The probabilities are increased for the years 1990, 1991, 1993, 1994, 1995, 1997, 1998 and 2002. The live algae concentrations increase in the years 1990, 1991, 1995 and 1997. These increases indicate that a new algal bloom could have occurred in 1990 as a result of the new diversions (for both scenarios), in addition to the already predicted blooms that occurred in 1995 and 1997. There is the potential that a new bloom could have occurred in 1991, however the timing is a little out of phase with light and water temperatures for optimum algal growth and the likelihood that a bloom would have occurred is low.

8.3 Bonnet Carré Spillway increased flows

8.3.1 Increased flow scenario descriptions

Leakage through the weir located at the Bonnet Carré Spillway is currently not measured. The leakage flows used to calibrate and validate the model were estimated using an equation for flow over a weir (equation 3.1). The head above the base of the weir was estimated using stage data from the Mississippi River gage located at the Bonnet Carré Spillway. The calculated flows were reduced by 95% since the water only flows through the small spaces between each creosote timber pin. The validity of these assumptions cannot be validated since measurements of leakage do not currently exist. Therefore, the calculated flows were increased to determine how they affected the water quality in the Estuary.

The calculated flows from the Bonnet Carré Spillway were increased 1.5 (50%) and 4 (200%) times their calculated values to determine how the water quality and potential for algal blooms would change in the Estuary. Flows during the 1997 opening were held constant since they correspond to measured data. Figure 8.9 shows the increases that were applied to the

hydrograph between 1990 and 1992. The 1997 event (dotted line) is associated with the right-hand y-axis.

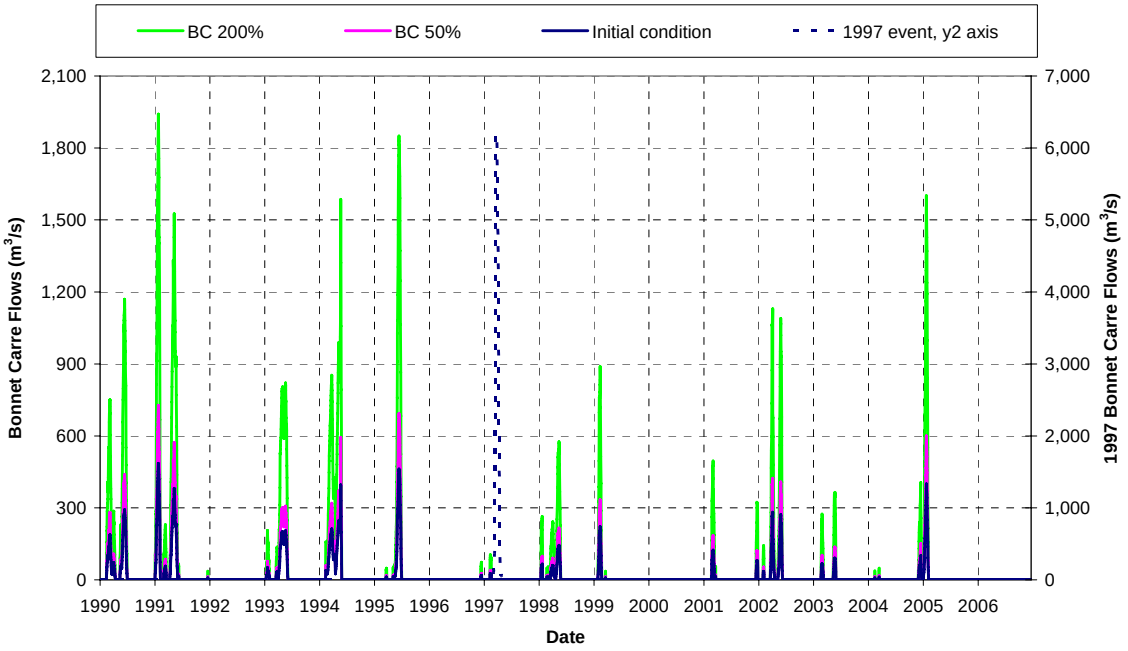

Figure 8.9. Bonnet Carré Spillway scenario hydrographs (1997 event, y2 axis).

8.3.2 Algal bloom probability model interpretation

The probability of an algal bloom results for the case when the Bonnet Carré Spillway flows were increased by 200% are shown below in Figures 8.10 to 8.16. The live algae concentrations are also shown above the probabilities on all of the plots. As discussed in the calibration and validation sections, algal blooms can be accurately predicted around the Pontchartrain Estuary when the probability model results are combined with the live algae concentrations. When the probabilities and live algae concentrations are high, it is likely that an algal bloom will occur in the Estuary. The results for the case when the Bonnet Carré Spillway flows were increased by 50% are shown in Appendix C.

If the flows from the Bonnet Carré Spillway were increased between 1990 and 2006, algal blooms around the Pontchartrain Estuary would have been more frequent and intense. The predicted algal blooms that occur in response to the higher flows are documented in Table 8.2 (the change from the initial condition is documented). The table shows that if the Bonnet Carré Spillway flows were increased by 50-200% between 1990 and 2006, the blooms in 1993 and 1994 would have extended into eastern Lake Pontchartrain and another bloom would have occurred around most of Lake Pontchartrain in 1990 in addition to those that occurred in 1991, 1995, 1997 and 2004. If the Bonnet Carré Spillway flows were increased by 200%, small blooms would also have occurred in 2002 and 2003. Each plot and how the predicted algal blooms were derived for each area in the Pontchartrain Estuary are discussed below.

Table 8.2 Changes in algal bloom occurrence around the Pontchartrain Estuary as a result of increased Bonnet Carré Spillway flows.

Year	Calibrated and Validated model	50% increase to Bonnet Carré flows	200% increase to Bonnet Carré flows	Timing of Bonnet Carré flow Event
1990		NELP, NWLP SWLP,	ELP, SELP, NELP, NWLP, SWLP, LM	March and June
1991	ELP, SELP, NELP, NWLP, SWLP		LB	January and May
1993	NWLP	NELP	ELP, SELP, NELP, SWLP	January and May
1994	NWLP, SWLP	NELP	ELP, SELP, NELP	March and May
1995	ELP, SELP, NELP, NWLP, SWLP, LM			June
1997	LB, ELP, SELP, NELP, NWLP, SWLP, LM			March and April
2002			NELP, NWLP	Jan, April, and June
2003			SWLP	March and June
2004	NELP, NWLP, SWLP			N/A

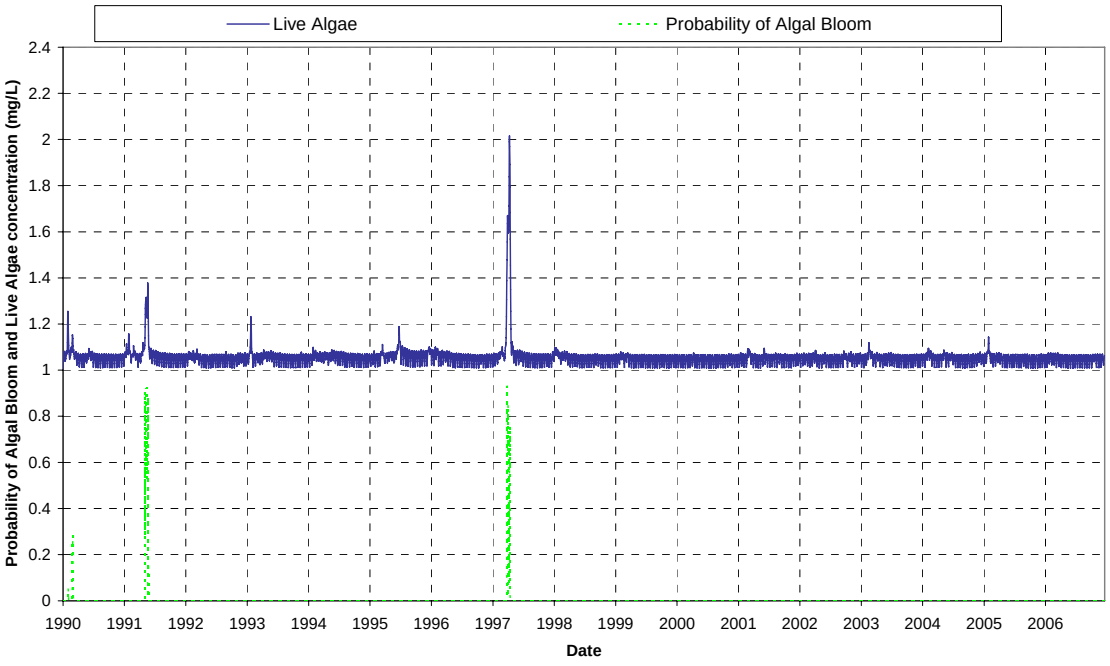

Figure 8.10 Probability of an algal bloom on Lake Borgne with predicted live algae concentrations (200% increase to Bonnet Carré Spillway flows).

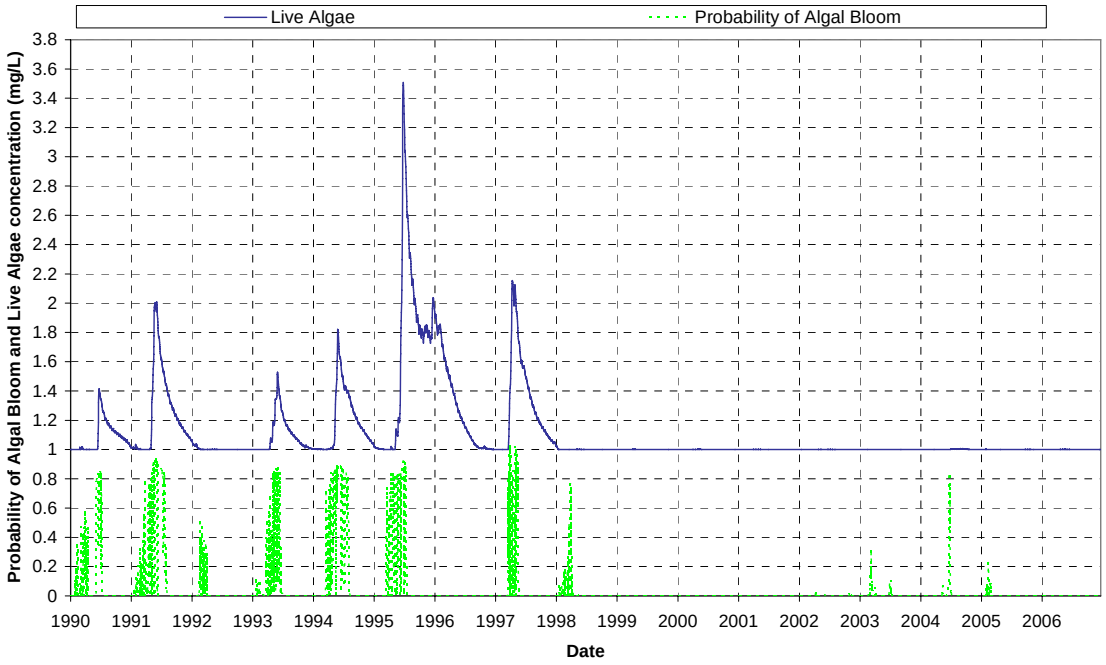

Figure 8.11 Probability of an algal bloom on east Lake Pontchartrain with predicted live algae concentrations (200% increase to Bonnet Carré Spillway flows).

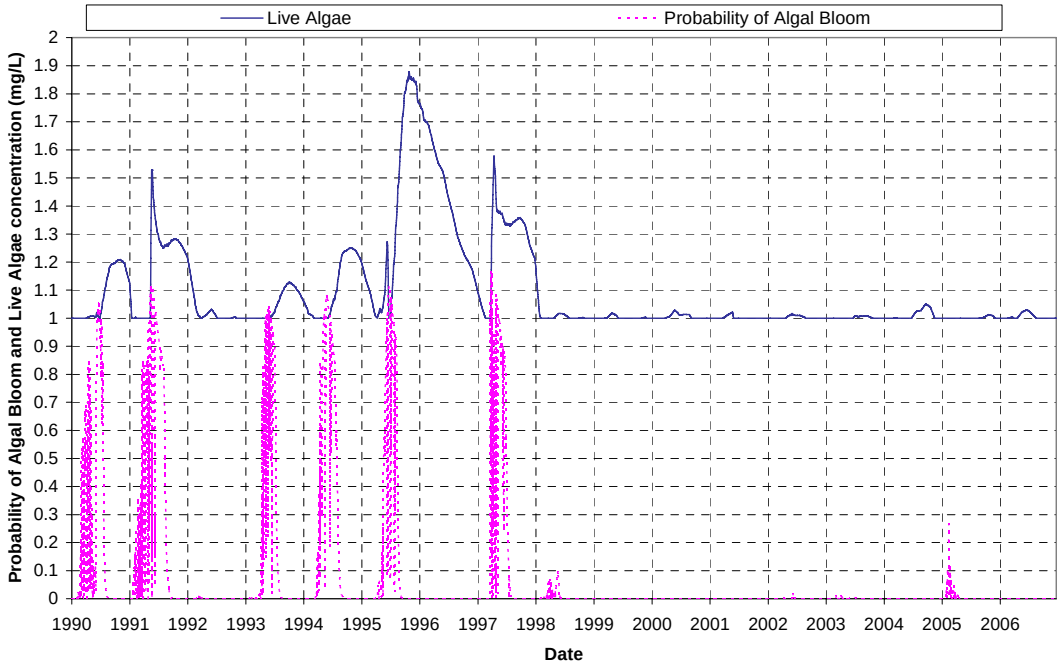

Figure 8.12 Probability of an algal bloom on southeast Lake Pontchartrain with predicted live algae concentrations (200% increase to Bonnet Carré Spillway flows).

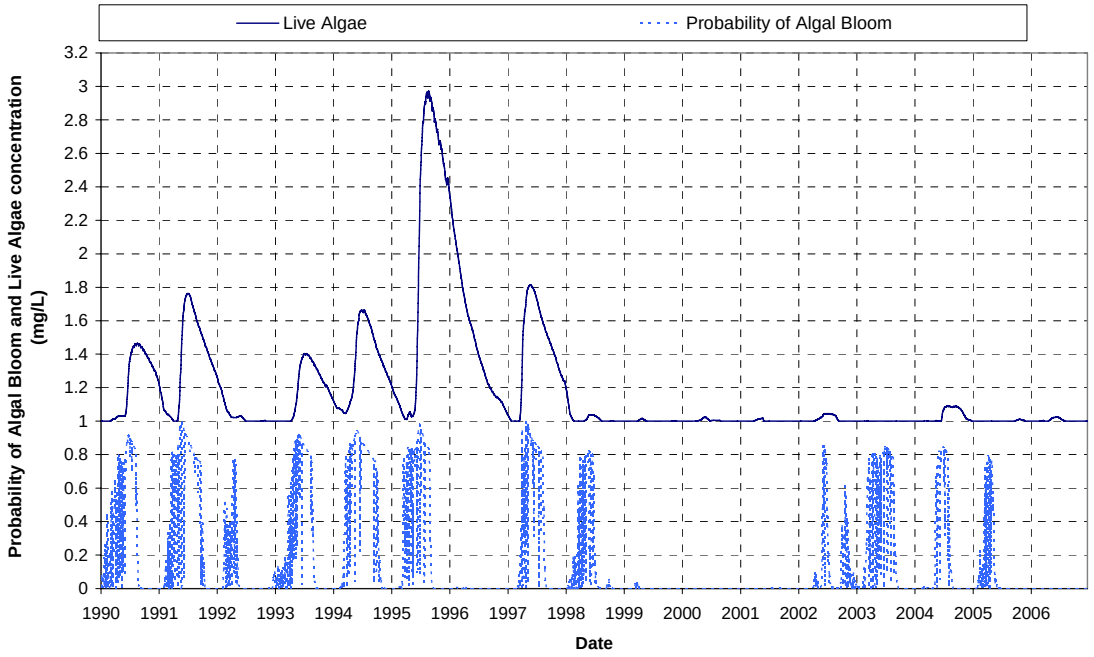

Figure 8.13 Probability of an algal bloom on northeast Lake Pontchartrain with predicted live algae concentrations (200% increase to Bonnet Carré Spillway flows).

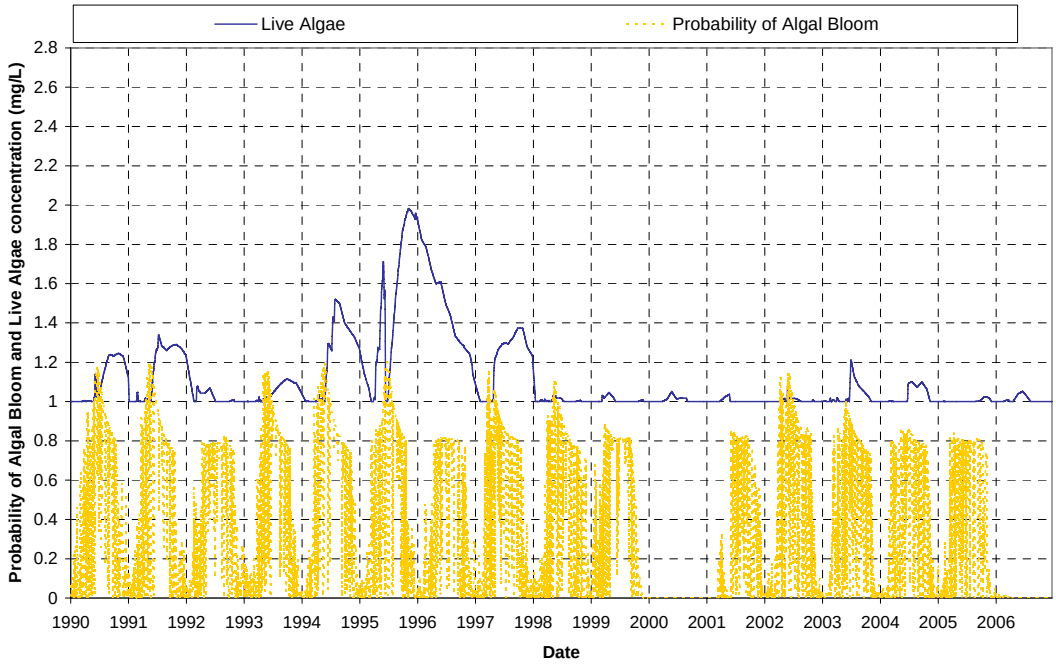

Figure 8.14 Probability of an algal bloom on southwest Lake Pontchartrain with predicted live algae concentrations (200% increase to Bonnet Carré Spillway flows).

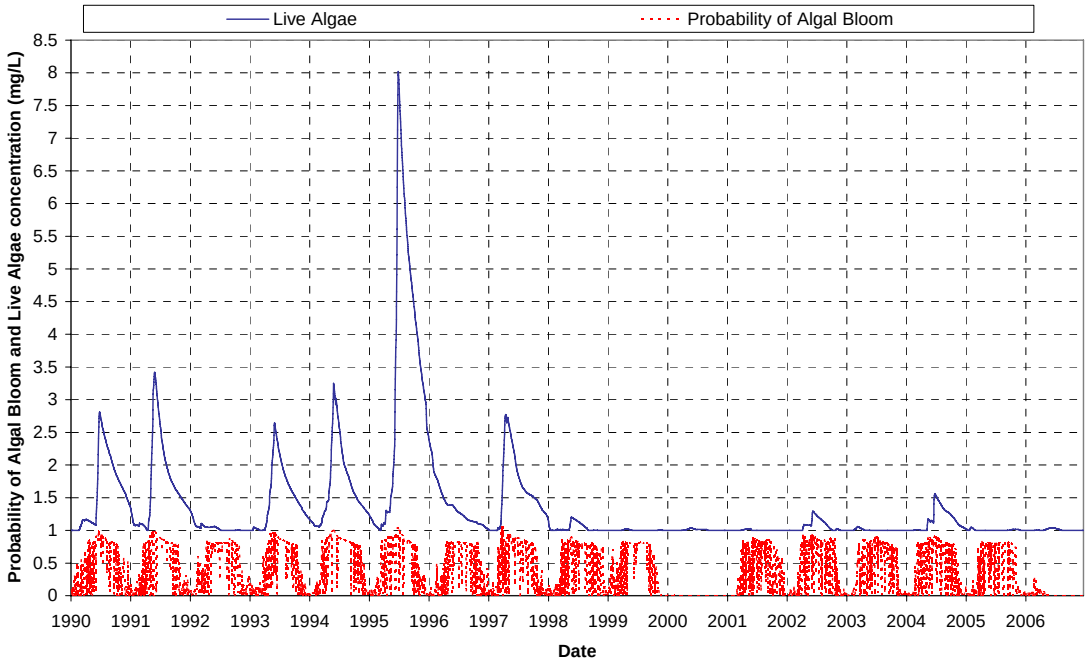

Figure 8.15 Probability of an algal bloom on northwest Lake Pontchartrain with predicted live algae concentrations (200% increase to Bonnet Carré Spillway flows).

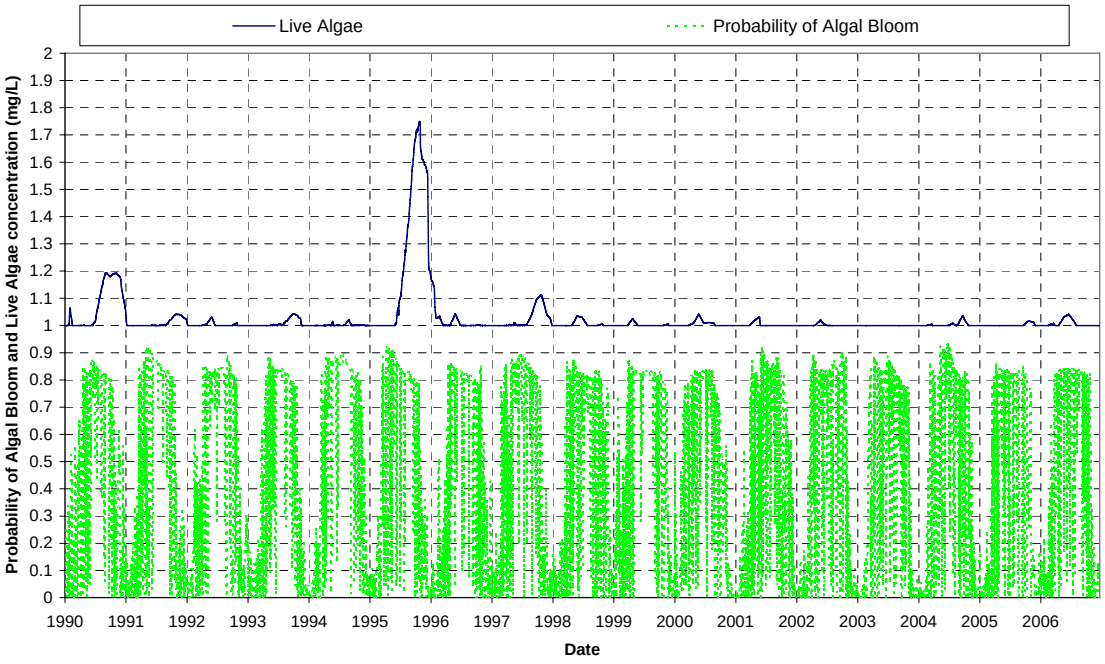

Figure 8.16. Probability of an algal bloom on Lake Maurepas with predicted live algae concentrations (200% increase to Bonnet Carré Spillway flows).

The 200% increase in flow in the Bonnet Carré Spillway could have caused a new algal bloom to occur in Lake Borgne in 1991 (Figure 8.10). The 200% increase to Bonnet Carré Spillway flows could also have caused the algal bloom in 1993 and 1994 to extend into the east Lake Pontchartrain cell (Figure 8.11) and could have caused an entirely new bloom to occur in 1990 in addition to those previously predicted in 1991, 1995 and 1997. The 50% increase in flows slightly increased the probabilities in 1991 and 1994 but no new blooms are predicted to occur in either Lake Borgne or east Lake Pontchartrain.

In southeast Lake Pontchartrain (Figure 8.12) the 50% increase in flows increases the probabilities in 1990, 1993, 1994 and 1995. However, there is not a corresponding increase in the live algae concentrations and no new algal blooms are predicted to occur in southeast Lake Pontchartrain apart from those that were predicted in the calibrated and validated model. However, the live algae concentrations increased in response to the 200% increase in Bonnet Carré Spillway flows and new algal blooms could have occurred in southeast Lake Pontchartrain in 1990, 1993 and 1994 in addition to the previously predicted blooms in 1991, 1995 and 1997.

In northeast Lake Pontchartrain (Figure 8.13) both scenarios predict an increase live algae and algal bloom occurrence probabilities. As a result of the increases in flow, new algal blooms could have occurred in 1990, 1993 and 1994 in northeast Lake Pontchartrain in addition to the previously predicted blooms in 1991, 1995, 1997 and 2004. Both the live algae concentrations and probability increases are higher for the 200% increase scenario. A small bloom could also have occurred in 2002 for the 200% increase in flow.

In southwest Lake Pontchartrain (Figure 8.14), the probabilities increase due to the 200% increase in Bonnet Carré flow in almost all of the years except 1996. Three new small algal blooms could have occurred in southwest Lake Pontchartrain in 1990, 1993 and 2003 as a result of the 200% increase to Bonnet Carré flows in addition to those that occurred in 1991, 1994, 1995, 1997 and 2004. The 50% increase in flows yielded similar results to the calibrated and validated model. However, the 50% increase in flows could have caused a new algal bloom to occur in 1990.

The probabilities increase for most years in northwest Lake Pontchartrain (Figure 8.15). The live algae concentrations increase significantly in the 200% increased flow scenario but do not increase dramatically in the 50% increased flow scenario. The 50% increased flow scenario could have caused a small bloom to occur in 1990 in northwest Lake Pontchartrain in addition to those observed in the calibrated and validated model. New blooms could have occurred in 1990 and 2002 in northwest Lake Pontchartrain in response to the 200% increase in Bonnet Carré flows in addition to those in 1991, 1993, 1994, 1995, 1997 and 2004. With the increased Bonnet Carré flow (200%), the bloom in 1995 is predicted to be much more severe than it was initially.

The proposed increases in flow in the Bonnet Carré Spillway do not have a significant effect on the potential for algal blooms in Lake Maurepas (Figure 8.16). A new bloom could have occurred in 1990 due to the 200% flow increase, and the 1995 bloom would likely have been more severe.

8.4 Shift timing of 1997 Bonnet Carré Spillway opening event

8.4.1 Shifted 1997 Bonnet Carré Spillway opening scenario descriptions

To assess the effects of timing on water quality in the Pontchartrain Estuary, the 1997 Bonnet Carré Spillway opening event was shifted: The first scenario that was considered shifted

the hydrograph back so that the peak flow occurred at the end of January/beginning of February. The second scenario considered shifting the peak of the hydrograph forward by one month to reflect the opening of the Spillway that occurred in 2008 due to high levels in the Mississippi River. The flows that correspond to the 1997 opening are higher than those that occurred in 2008, but the effect of timing will be illustrated. The shifted hydrographs are shown below in Figure 8.17.

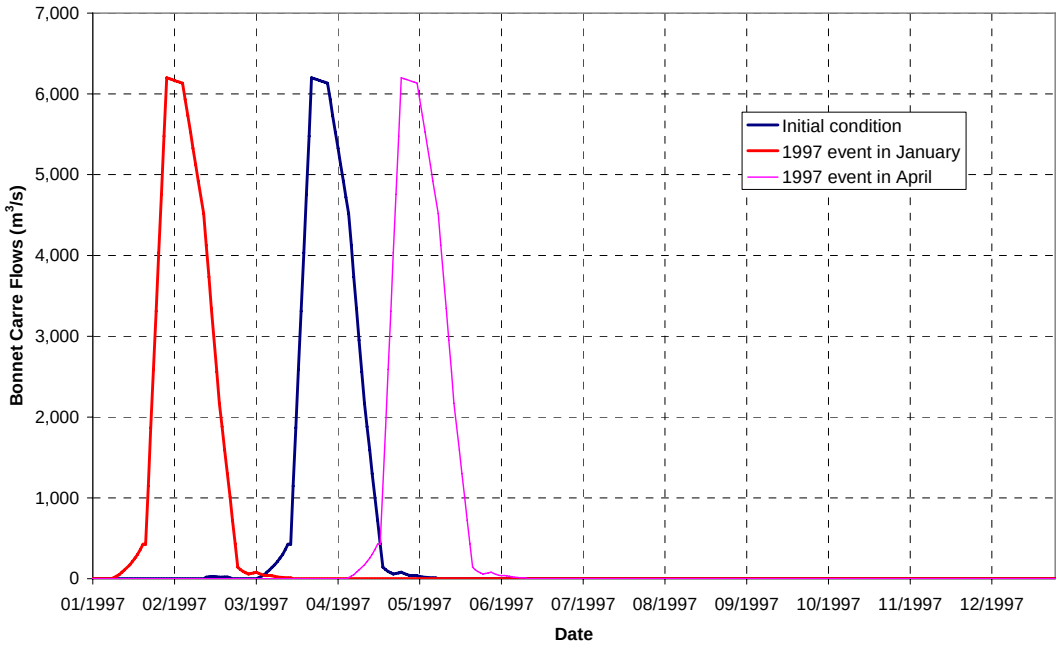

Figure 8.17 Shifted Bonnet Carré Spillway 1997 hydrograph to end of January.

8.4.2 Algal bloom probability model interpretation

The probability of an algal bloom for the Bonnet Carré Spillway 1997 peak flow shifted to late January/early February is shown below in Figures 8.18 to 8.24. The results from the initial condition where the 1997 peak flow occurred at the end of March (baseline condition) are also shown on the Figures. The live algae concentrations are shown above the probabilities on all of the plots. As discussed in the calibration and validation sections, algal blooms can be accurately predicted around the Pontchartrain Estuary when the probability model results are combined with the live algae concentrations. When the probabilities and live algae concentrations are high, it is likely that an algal bloom will occur in the Estuary. The results for Bonnet Carré Spillway peak 1997 flow shifted to April are shown in Appendix C.

The predicted algal blooms that occur in response to the shifted 1997 Bonnet Carré Spillway event are documented in Table 8.3 below. Each plot and how the new algal blooms were derived are discussed below.

By shifting the large flows so that the peak occurs at the end of January/beginning of February, the likelihood of an algal bloom is greatly reduced in all areas of the Estuary. As a result of the shift, a small bloom is predicted to occur in northwest, southwest, northeast and southeast Lake Pontchartrain with a small chance that it may extend into east Lake Pontchartrain.

The duration and degree of the algal bloom will be much shorter and less severe than the algal bloom that occurred in response to the March flows from the Bonnet Carré Spillway. When flows are released into Lake Pontchartrain earlier, there is more time for assimilation to occur and less opportunity for high nutrient levels to be present during elevated temperatures that are required for blooms to occur.

Shifting the large flows so that the 1997 peak occurs at the end of April instead of March changes the likelihood of an algal bloom occurring in all areas of the Estuary. As a result of the shift, live algae concentrations and probabilities increase for all areas. However, the duration of the algal bloom can be both increased and decreased. Algal bloom growth is limited by light intensity, water temperature and salinity in addition to nutrient inputs. These limitations bound the period where algal growth can occur (late spring to early fall). When nutrient inputs are added to the system at the beginning of the growth period, the duration of the algal blooms will be longer than if the nutrient inputs were added after the growth period started. Sufficient nutrients were available after the March 1997 opening to stimulate an algal bloom over the entire growth period. When the opening event was shifted to April, nutrients entered the system after the start of the growth period, and the duration of the algal bloom was decreased around most of the Lake Pontchartrain. However, the algal bloom duration increased in response to the April 1997 event in areas on Lake Pontchartrain that had growth periods limited by salinity (east Lake Pontchartrain and southeast Lake Pontchartrain). The input of freshwater extends the optimum growth period and potential period for an algal bloom to occur in these areas.

Table 8.3 Predicted algal blooms occurrence from increased Bonnet Carré Spillway flows.

Cell	Calibrated and Validated model (1997 Peak at the end of March)	1997 peak shifted to late January/early February	1997 peak shifted to end of April
LB	Yes	No	Yes
ELP	Yes	No	Yes
NELP	Yes	Small	Yes
SELP	Yes	Small	Yes
NWLP	Yes	Small	Yes
SWLP	Yes	Small	Yes
LM	Yes	No	Yes

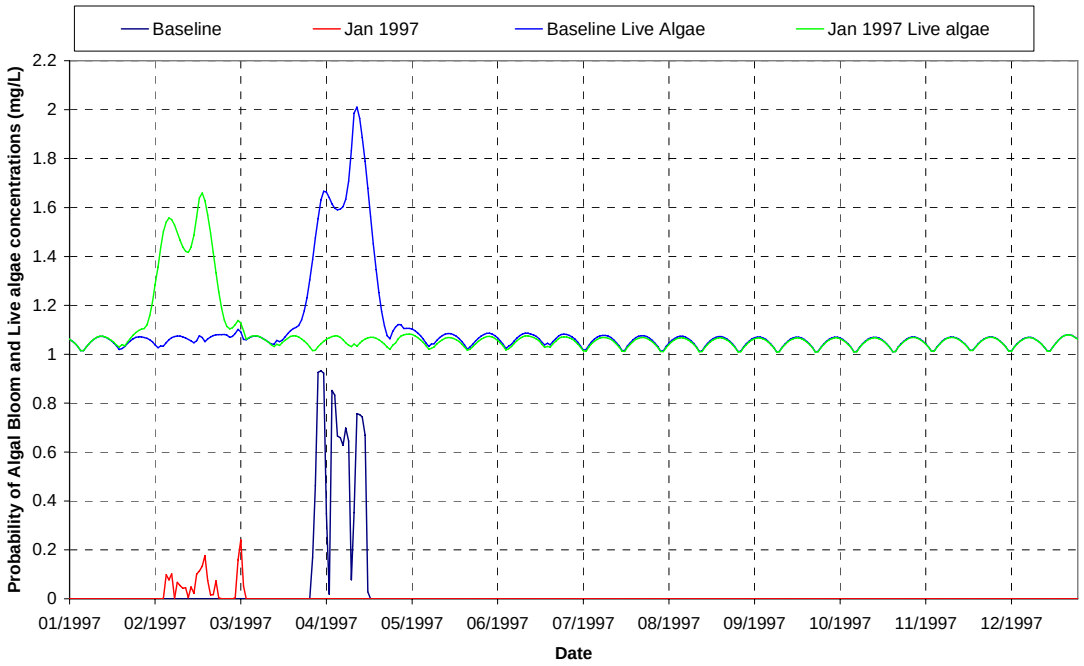

Figure 8.18 Probability of an algal bloom on Lake Borgne with live algae concentrations (January and March 1997 opening).

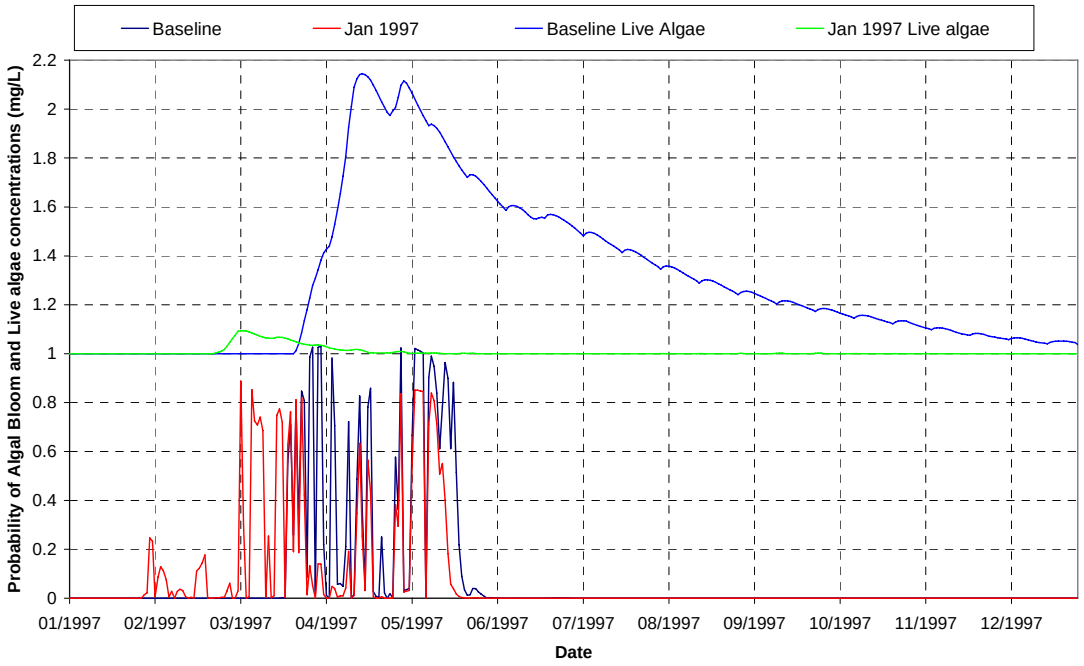

Figure 8.19 Probability of an algal bloom on east Lake Pontchartrain with live algae concentrations (January and March 1997 opening).

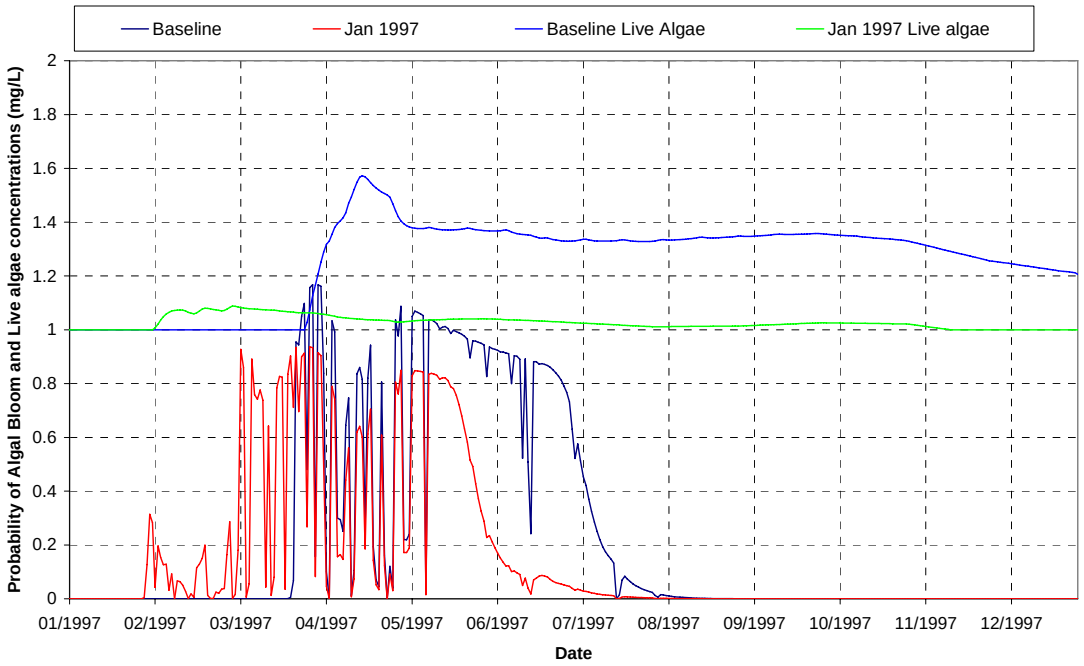

Figure 8.20 Probability of an algal bloom on southeast Lake Pontchartrain with live algae concentrations (January and March 1997 opening).

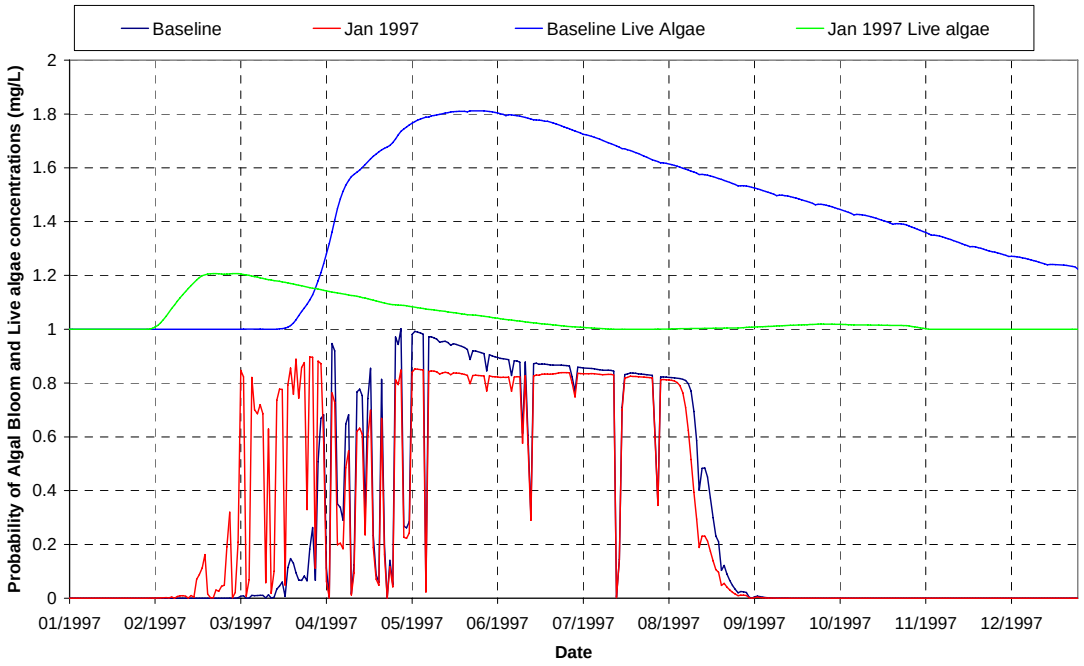

Figure 8.21 Probability of an algal bloom on northeast Lake Pontchartrain with live algae concentrations (January and March 1997 opening).

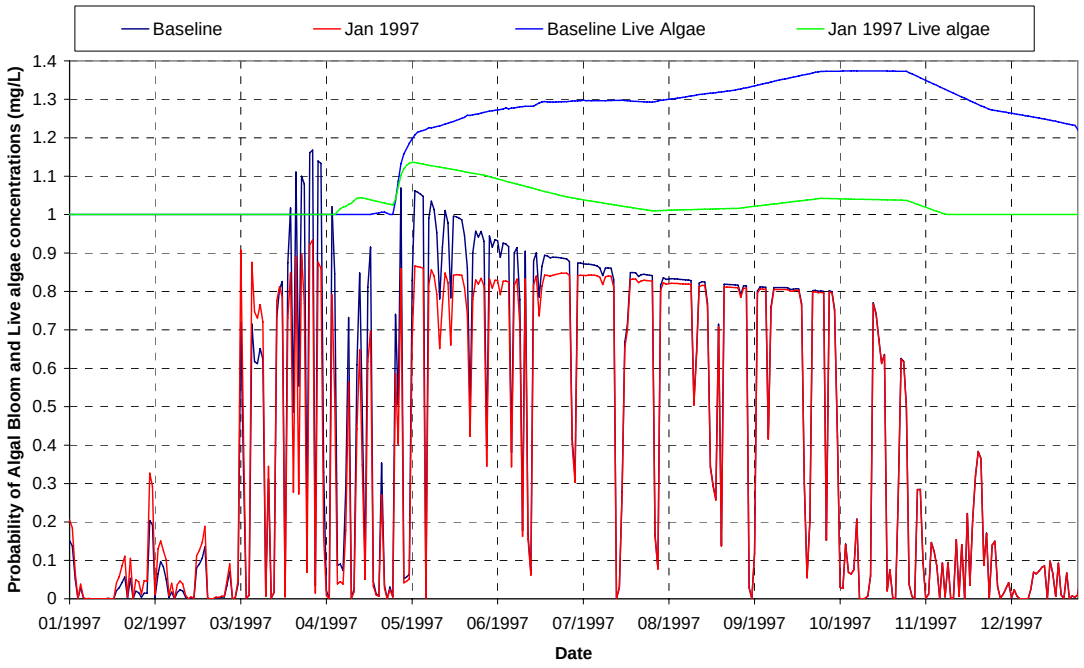

Figure 8.22 Probability of an algal bloom on southwest Lake Pontchartrain with live algae concentrations (January and March 1997 opening).

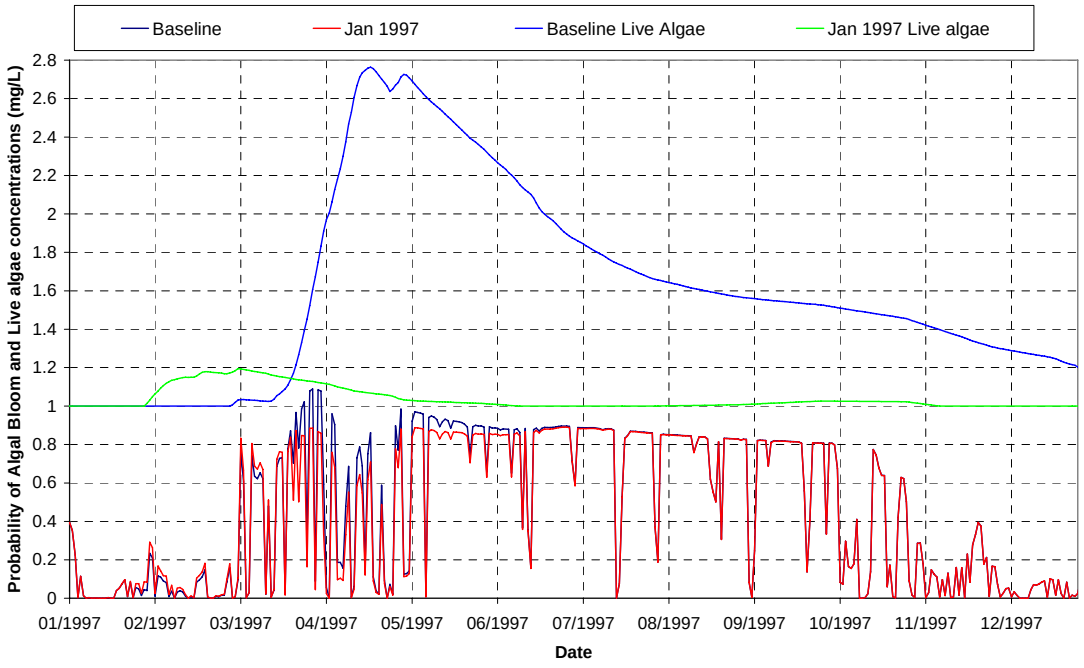

Figure 8.23 Probability of an algal bloom on northwest Lake Pontchartrain with live algae concentrations (January and March 1997 opening).

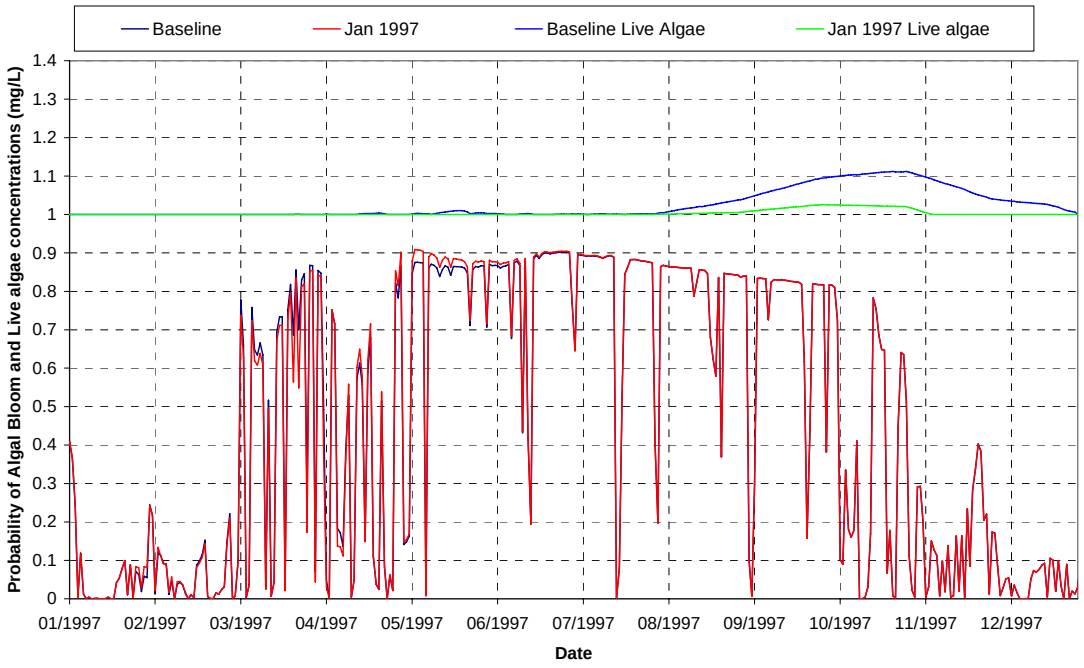

Figure 8.24 Probability of an algal bloom on Lake Maurepas with live algae concentrations (January and March 1997 opening).

9.0 Results and Discussion

9.1 Quantification of annual load summary

9.1.1 Annual nutrient loading rates

The long-term annual loadings calculated in section 3.0 are summarized in Table 9.1 below.

Table 9.1. Long-term loading rates per unit area and for the Pontchartrain Estuary basin area (12,174 km^2).

Parameter	Loading ($kg/day/km^2$)	Total loading (kg/day)	Annual loading (metric tonnes/year)
Nitrite + nitrate as nitrogen	0.2530	3,080	1,125
Phosphorous	0.1800	2,200	800
Ammonia	0.2110	2,560	940
Organic Nitrogen	0.8980	10,930	4,000

These totals result in a total nitrogen input of 6,050 metric tonnes per year and a total phosphorous input of 800 metric tonnes per year (a ratio of 8.1). The average long-term daily discharge into Lake Pontchartrain can be calculated as 0.0150 $m^3/s/km^2$ (or 183 m^3/s using a drainage area of 12,173 km^2).

Waldon and Bryan (1999) created a salinity and nutrient budget for Lake Pontchartrain. In their analysis, they found that 8,380 metric tons of total nitrogen and 1,370 metric tons of total phosphorous enter Lake Pontchartrain through the tributaries and urban stormwater runoff each year. These estimates are 1.4 and 1.7 times greater than the annual average loadings calculated in this study. The loading analysis performed by Waldon and Bryan (1999) likely over-predicts the loads because they used monthly estimates of flow in their calculations. Their reported average annual flow was 227 m^3/s (1.25 times higher than the average annual flow calculated in this analysis). The flow is likely higher since they used monthly estimates of flow. Turner et al.(2002) estimated that 7,800 metric tonnes of nitrogen enter Lake Pontchartrain from the Pontchartrain Estuary watershed, which is 1.3 times higher than our estimate. The estimates made by Waldon and Bryon (1999) and Turner et al. (2002) are based on shorter records of data than those used in this analysis, which could also account for the discrepancy. However, the difference in this estimate could also be a result of the uncertainty in the estimate of the watershed yield for nitrogen. There are currently insufficient measurements of nutrient concentrations at high flows in the tributaries. As a result, the regression equations could be underestimating the loads at higher discharges.

Turner et al. (2002) also estimated that 1,000 metric tonnes of nitrogen and 1,300 metric tonnes of nitrogen enter the Pontchartrain Estuary from urban and atmospheric inputs respectively. In our model, we found that 812 metric tonnes of nitrogen and 3,100 metric tonnes of nitrogen enter the Pontchartrain Estuary from urban and atmospheric inputs respectively. The estimate made by Turner et al. (2002) of urban inputs is 1.2 times higher than the loadings calculated in this study. However, the atmospheric loading in this study is 2.4 times higher than

that found by Turner et al. (2002). The higher atmospheric total nitrogen loading that was used in this study may account for the low input of total nitrogen in the watershed discussed above (6,050 metric tonnes).

As a result of these comparisons, more nutrient concentration data should be collected for periods of high discharge to determine if the regression equations used as input into the model are accurate. The atmospheric loadings should also be further investigated over the Pontchartrain Estuary to ensure that accurate loadings are being applied in the model.

9.1.2 Nitrogen availability in the Pontchartrain Estuary

As discussed in section 2.1.2 above, the Pontchartrain Estuary is a nitrogen-limited system. A ratio of 1.41 to 1 was found when the nitrite + nitrate as nitrogen and phosphorous watershed loadings above were compared. According to the Redfield ratio, ratios below 7.23 indicate nitrogen-limited systems. Figure 9.1 shows the ratios of LADEQ nitrite + nitrate as nitrogen and phosphorous concentration measurements taken in the Pontchartrain Estuary. The pink line shows the average of the measured data (1.14), the black line indicates the ratio from the watershed loadings (1.41), and the blue line indicates the Redfield ratio (7.23). Points below the Redfield ratio indicate a nitrogen-limited system and points above the ratio are indicative of a system where nitrogen is available in excess.

The figure shows that Lake Pontchartrain is usually a nitrogen-limited system. However, at times, the system shifts. A sufficient amount of data occurred above the Redfield ratio during the year 1997. This was the year when the Bonnet Carré Spillway was opened completely and a large algal bloom was observed around the entire Pontchartrain Estuary. The ratios also increase above the background rates in 1990, and 1993-1996. The ratios did not exceed the Redfield ratio but the increased ratios indicate that more nitrogen was available in the system for primary producers during these periods. Poirrier et al. (1998) observed a small bloom near Mandeville in 1993, a more extensive surface bloom in late June 1994 and a major bloom mid June to the end of July in 1995.

Since the observations by Poirrier et al. (1998) correspond to periods where N:P ratios exceed the background rate and approach the Redfield ratio, the Redfield ratio is a good indicator of available nitrogen in the Pontchartrain Estuary.

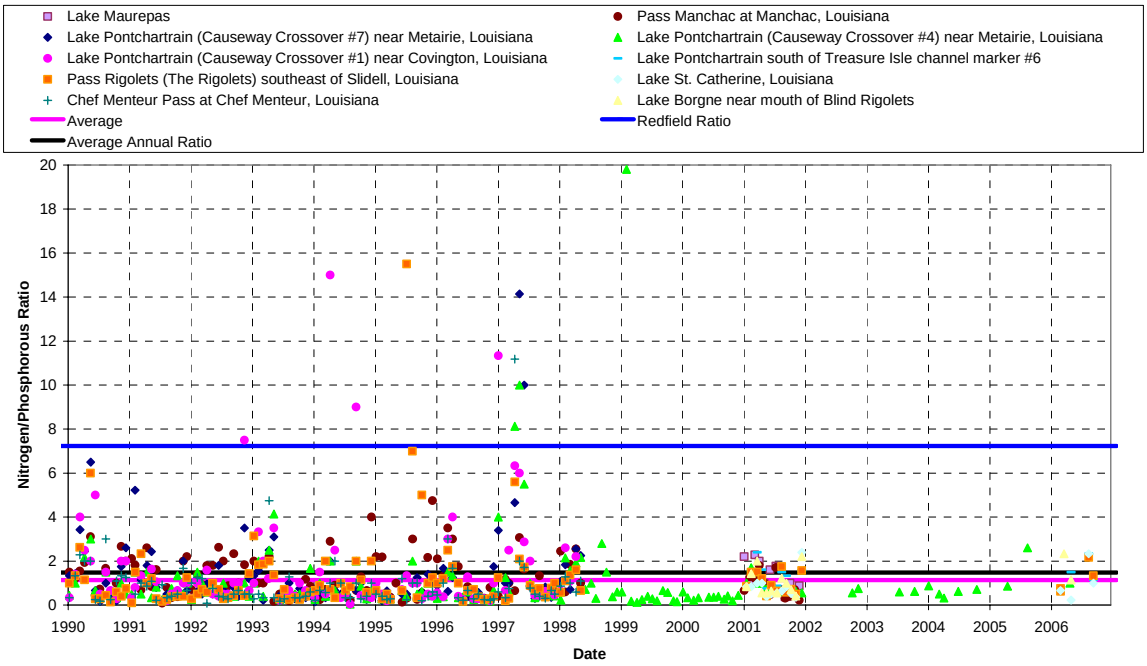

Figure 9.1. Nitrite + nitrate as nitrogen to phosphorous ratios on Lake Pontchartrain.

9.2 Sensitivity Analysis

9.2.1 General discussion

The sensitivity of some parameters was tested on the calibrated and validated 1-D tidal, salinity and water quality model that was created for the Pontchartrain Estuary. During the calibration period, it was determined that the resuspension calibration factor, the central difference/upwinding calibration factor and the dispersion calibration factor affected the results of the model more than the other calibration factors.

9.2.2 Effect of constant evapotranspiration rate

The annually varied evapotranspiration distribution determined by Fontenot 2004) was changed to a uniform distribution to check the sensitivity of the model. Salinity is the main parameter that is affected by the evaporation rate. The testing showed that salinity was not highly sensitive to the distribution of the evapotranspiration rate. Figure 9.2 shows the effects of the uniform evapotranspiration rate on salinity between January 1995 and December 2000. Figure 9.3 shows the effect that the annually varied evapotranspiration rates (Fontenot, 2004) have on salinity between January 1995 and December 2000 (the condition run in the model). No change is noted.

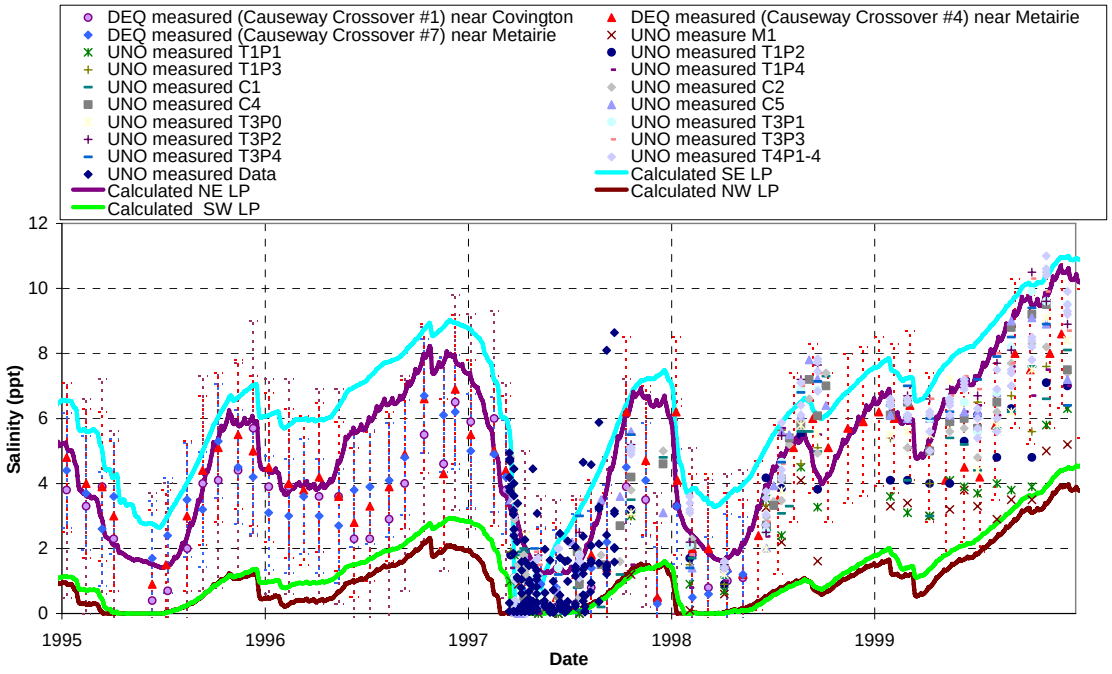

Figure 9.2 Effect of constant evapotranspiration rates on salinity (1995-2000).

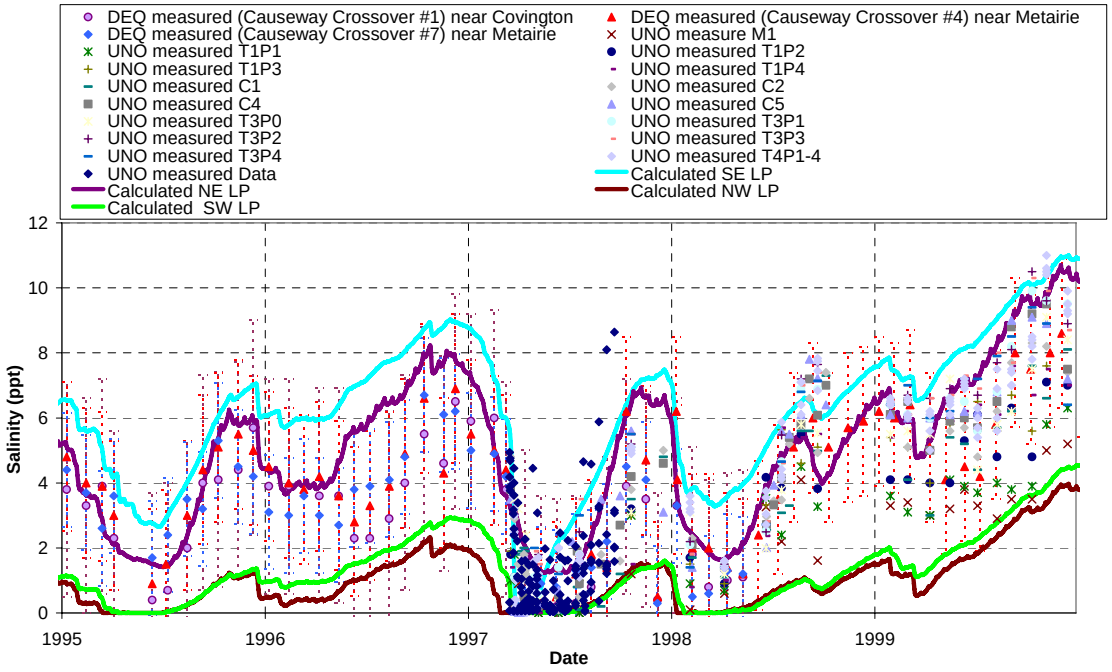

Figure 9.3 Effect of annually varied evapotranspiration rates on salinity (1995-2000).

9.2.3 Application of boundary values at the Gulf of Mexico.

As discussed in the calibration and validation of the model, predicted nutrient concentrations were consistently low in Lake Borgne. No boundary values were assigned to the boundary for cells connected to the Gulf of Mexico. As a result, nutrient concentrations in Lake Borgne were likely underestimated. The model was rerun assigning nutrient values to the Gulf of Mexico boundary. Nitrite + nitrate as nitrogen, phosphorous, and ammonia concentrations in the range of 0.05-0.1 mg/L were applied at the boundary. TKN concentrations and TOC concentrations in the range of 0.5-1 mg/L and 1-5 mg/L were also applied. Figures 9.4 and 9.6 show the modelled results that are produced using these new boundary conditions for nitrite + nitrate as nitrogen and phosphorous concentrations respectively. Figures 9.5 and 9.7 show the previously modelled results where no boundary conditions were applied. The Lake Borgne predicted concentrations approach the measured data better with the boundary conditions applied.

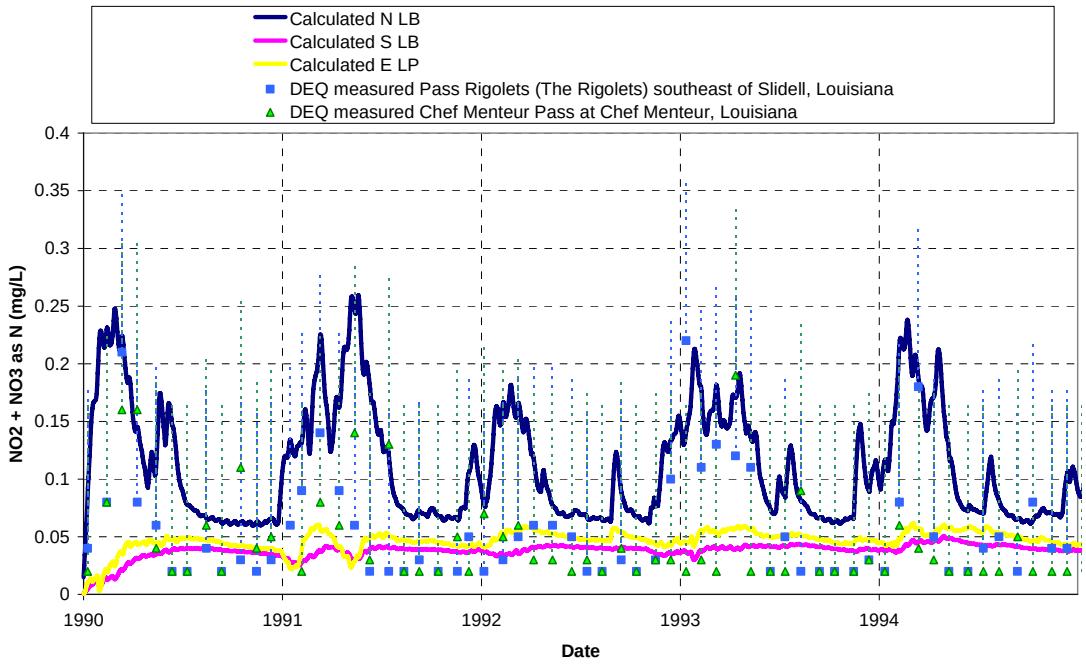

Figure 9.4 Nitrite + nitrate as nitrogen concentrations on Lake Borgne with nutrient concentrations applied at the Gulf of Mexico boundary (1990-1995).

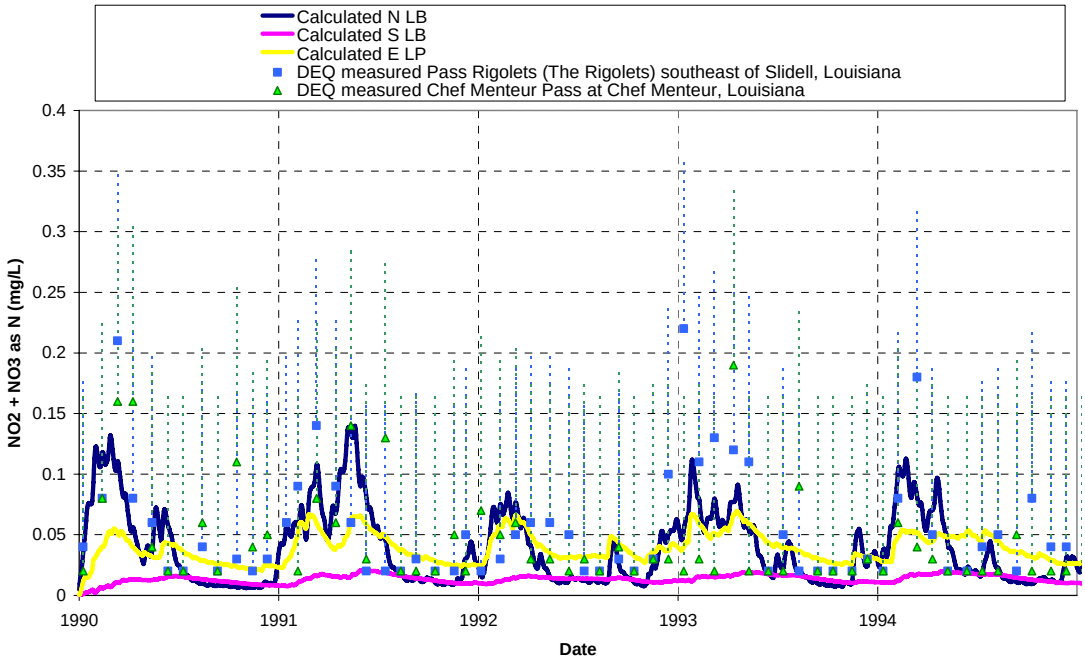

Figure 9.5 Nitrite + nitrate as nitrogen concentrations on Lake Borgne with no nutrient concentrations applied at the Gulf of Mexico boundary (1990-1995).

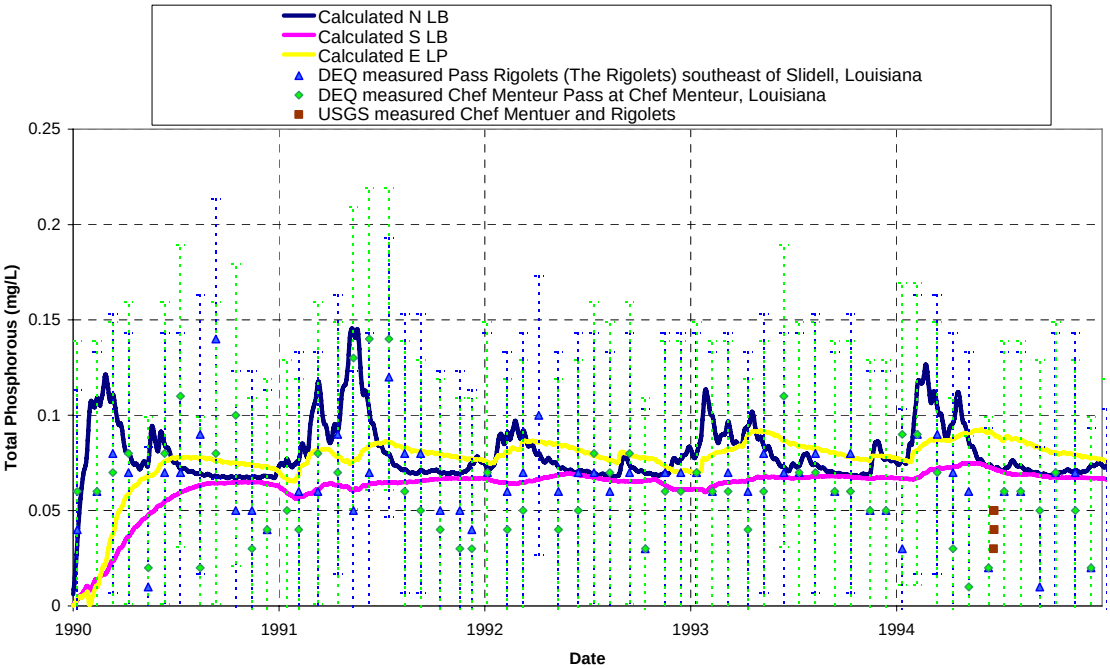

Figure 9.6 Phosphorous concentrations on Lake Borgne with nutrient concentrations applied at the Gulf of Mexico boundary (1990-1995).

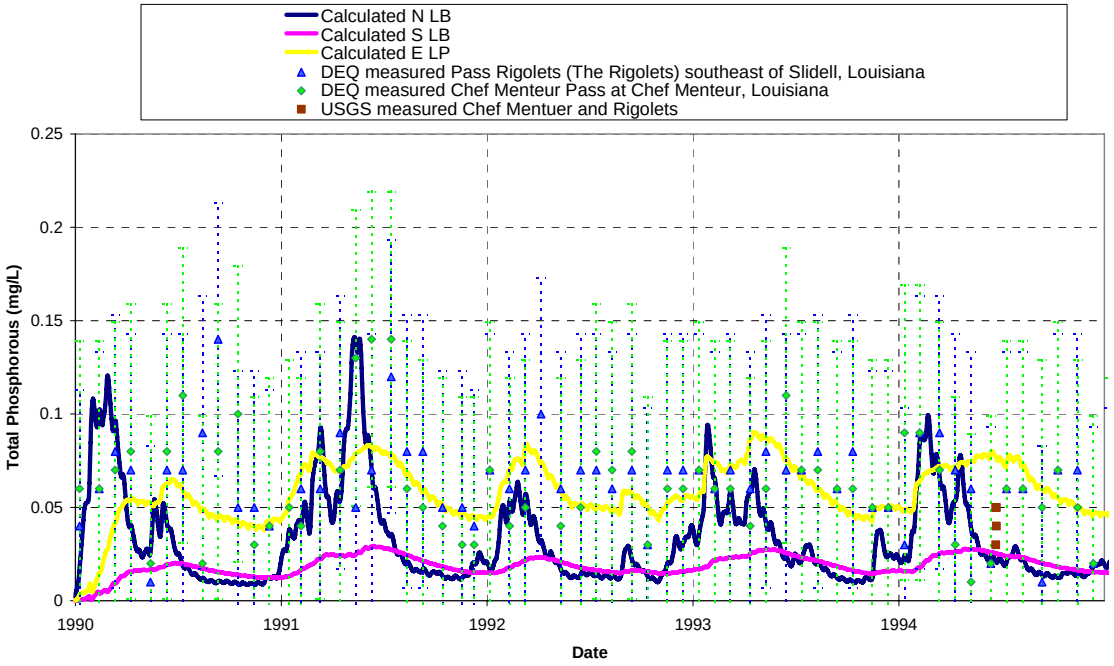

Figure 9.7 Phosphorous concentrations on Lake Borgne with no nutrient concentrations applied at the Gulf of Mexico boundary (1990-1995).

9.2.4 Climate change

The 1-D tidal, salinity and water quality model was not developed with the intention of predicting the effect of extreme events on Pontchartrain Estuary water quality. However, the model is capable of predicting relative changes that could occur to Pontchartrain Estuary water quality over a wide range of hydrologic conditions since the calibrated and validated model included periods (between 1990 and 2006) where extremely wet and extremely dry events occurred, i.e. the model was applied over a drought in 1999 and 2000, extreme rainfall events (63 cm in May 1995 and 57 cm in January1991), and a large opening of the Bonnet Carré Spillway in 1997. The model accurately responded to the effects of these extreme events.

Since the response of water quality in the Pontchartrain Estuary is known for these extreme events, the effects of some climate change scenarios could also be predicted. The response of the system to the extreme dry and wet periods could be used to postulate what could happen if precipitation decreases or increases in the future in response to climate change. The large opening of the Bonnet Carré Spillway could be used to determine how increased runoff events as a result of higher precipitation or increased loading as a result of land use changes in the watershed might impact water quality in the Estuary.

9.3 Algal bloom probability model

9.3.1 Calibrated and validated model

The 1-D tidal, salinity and water quality model created in this research accurately predicts the probability and spatial extent of algal blooms that occurred between January 1990 and December 2006 in the Pontchartrain Estuary. When the algal bloom probability model is used in

conjunction with the predicted live algae concentrations, algal blooms can be predicted well around the Pontchartrain Estuary. The live algae concentration outputs produce an averaged result from the mass balance model that depends on the conditions preceding it. The probability model assesses the conditions required for an algal bloom to occur on a daily basis and does not consider any preceding events. Using the two results together will eliminate any false positives that the algal bloom model might identify on its own.

The results predicted using the calibrated and validated model agree well with observed algal bloom occurrences by Poirrier et al. (1998) around the Pontchartrain Estuary. The predicted algal bloom events from model are compared to the observations made by Poirrier et al. (1998) in Table 9.2.

Table 9.2 Comparison of modeled algal bloom occurrences on Lake Pontchartrain to algal blooms observations made by Poirrier et al. (1998).

Year	Predicted algal blooms from model	Observed Algal Blooms Poirrier et al. (1998)	Bonnet Carré Openings
1991	ELP, SELP, NELP, NWLP, SWLP	Not documented	January and May
1993	NWLP	NWLP	January and May
1994	NWLP, SWLP	NWLP, SWLP	March and May
1995	ELP, SELP, NELP, NWLP, SWLP, LM	ELP, SELP, NELP, NWLP, SWLP	June
1997	LB, ELP, SELP, NELP, NWLP, SWLP, LM	LB, ELP, SELP, NELP, NWLP, SWLP, LM	March
2004	NELP, NWLP, SWLP	Not documented	March

The 1993, 1994 and 1995 results agree well with observations made by Poirrier et at. (1998). In June of 1993, Poirrier et al. (1998) observed a small bloom of the blue green algae *Anabaena circinalis* near Mandeville. A more extensive surface bloom was also observed in late June 1994 as was a major bloom of *Anabaena circinalis* from mid June to the end of July in 1995. The 1995 bloom had surface accumulations covering most of the lake during the peak and fish kills associated with it. The extensive algal bloom that occurred after the 1997 opening of the Bonnet Carré Spillway has been well documented by many different researchers. The 1991 and 2004 blooms predicted by the model cannot be verified with any observations at this time.

9.3.2 Algal bloom probability model response to management scenarios

The 1-D tidal, salinity and water quality model created in this research accurately predicts the probability and spatial extent of algal blooms that occurred between January 1990 and December 2006 on the Pontchartrain Estuary. Three different management scenarios were applied to determine how water quality in the Estuary would respond. The effects of: a new diversion into Maurepas Swamp and Lake Maurepas, increases in the leakage events on the Bonnet Carré Spillway, and different timing of a complete opening of the Bonnet Carré Spillway in 1997 were tested. The results for the first two management scenarios are summarized in Table 9.3.

The first management scenario looked at diverting Mississippi River water into Lake Maurepas as proposed in the State Master Plan. Two runs were simulated: one with a flow of 280 m^3/s and another with a flow of 30 m^3/s, covering the full range of proposed conditions. The second group of management scenarios looked at increased flows from the Bonnet Carré Spillway. A 200% and 50% increase in flows were analyzed. In both cases, the calibrated and validated model parameters were held constant and the same reductions were applied to nutrients and sediments for flows less than 500 m^3/s (see section 8.2.1 for reductions applied).

The two groups of scenarios yielded similar results. The model predicted that if the diversions into Maurepas Swamp or increased Bonnet Carré Spillway flows had been present between 1990 and 2006, more frequent and intense algal blooms could have occurred around the Pontchartrain Estuary (Table 9.2). In each scenario (excluding the small diversion into Maurepas Swamp), the blooms in 1993 and 1994 could have expanded into the east part of Lake Pontchartrain and a new algal bloom could have occurred in 1990 in addition to the blooms that occurred in 1991, 1995, 1997, and 2004. The model also predicted that two small algal blooms could have occurred in 2002 and 2003 in response to the 200% increase to Bonnet Carré flows. The larger diversion into Lake Maurepas and the higher increases to the Bonnet Carré Spillway flows increased the probability and extent of the predicted algal blooms.

It is interesting to note that the algal blooms predicted by the model occur in years where flows or leakage from the Bonnet Carré Spillway entered the Pontchartrain Estuary in May or June (refer back to section 5.3 to review magnitude and timing of Bonnet Carré Spillway leakage events). The exception to this is the algal blooms that were predicted to occur in 1997 and 2004. McCorquodale et al. (1998) observed that salinities on the south shore of Lake Pontchartrain did not return to pre-opening levels until August 29, 1997, indicating that Mississippi River water was still present in Lake Pontchartrain in May and June. The algal bloom in 2004 must be related to inputs from the tributaries instead of inputs from the Bonnet Carré Spillway. The algal blooms that are predicted to occur in response to the management scenarios (Table 9.3) also occur during years where the Bonnet Carré Spillway leaked during either May or June (1990, 2002 and 2003).

During the management scenario model runs, it was noted that when flows were input into the Pontchartrain Estuary earlier in the year (January to March), algal bloom occurrences around the Pontchartrain Estuary did not become more frequent or intense. However, when the flows (even flows that were significantly smaller in magnitude and duration) were input into the Pontchartrain Estuary later in the year (May or June), the predicted live algae concentrations increased significantly resulting in more frequent and intense algal blooms. For example, the leakage event in June 1995 (maximum flow of 460 m^3/s), produced much higher live algae concentrations than those produced in response to the large March 1997 event (maximum flow of 6,200 m^3/s). This observation is important because it indicates that magnitude and timing both greatly influence the probability that an algal bloom will occur.

The effect of timing on the probability of algal blooms was also tested. The peak of the hydrograph from the March 1997 Bonnet Carré Spillway opening was shifted back two months to January/February and forward one month to April. When the large flows were shifted so that the peak occurred at the end of January/beginning of February the likelihood of an algal bloom was greatly reduced in all areas of the Estuary. The duration and degree of the algal bloom events were much shorter and less severe than the algal bloom events that occurred in response to the March flows from the Bonnet Carré Spillway. When flows are released into Lake Pontchartrain earlier, there is more time for assimilation to occur and less opportunity for high

nutrient levels to be present when elevated water temperatures and light intensities, that are required for optimum algal growth, occur.

Shifting the large flows so that the 1997 peak occurs at the end of April instead of March changes the likelihood of an algal bloom occurring in all areas of the Estuary. As a result of the shift, live algae concentrations and probabilities increase for all areas. However, the duration of the algal bloom can be both increased and decreased. Algal bloom growth is limited by light intensity, water temperature and salinity in addition to nutrient inputs. These limitations bound the period where algal growth can occur (late spring to early fall). When nutrient inputs are added to the system at the beginning of the growth period, the duration of the algal blooms will be longer than if the nutrient inputs were added after the growth period started. Sufficient nutrients were available after the March 1997 opening to stimulate an algal bloom over the entire growth period. When the opening event was shifted to April, nutrients entered the system after the start of the growth period, and the duration of the algal bloom was decreased around most of the Lake Pontchartrain. However, the algal bloom duration increased in response to the April 1997 event in areas on Lake Pontchartrain that had growth periods limited by salinity (east Lake Pontchartrain and southeast Lake Pontchartrain). The input of freshwater extends the optimum growth period and potential period for an algal bloom to occur in these areas.

Table 9.3 Changes in algal bloom occurrence around the Pontchartrain Estuary in response to applied management scenarios.

Year	Calibrated and Validated model (initial conditions)	One diversion in LM, minimum flow scenario 30 m^3/s	Two diversions in LM, maximum flow scenario 280 m^3/s	50% increase to Bonnet Carré flows	200% increase to Bonnet Carré flows	Timing of Bonnet Carré flow Event
1990		LM	SELP, NELP, NWLP, SWLP, LM	NELP, NWLP SWLP,	ELP, SELP, NELP, NWLP, SWLP, LM	March and June
1991	ELP, SELP, NELP, NWLP, SWLP				LB	January and May
1993	NWLP		SELP, NELP, SWLP	NELP	ELP, SELP, NELP, SWLP	January and May
1994	NWLP, SWLP		NELP	NELP	ELP, SELP, NELP	March and May
1995	ELP, SELP, NELP, NWLP, SWLP, LM					June
1997	LB, ELP, SELP, NELP, NWLP, SWLP, LM					March and April
2002					NELP, NWLP	Jan, April, and June
2003					SWLP	March and June
2004	NELP, NWLP, SWLP					N/A

10.0 Conclusions

The main conclusions developed from this research are:

- A tidal, salinity and water quality model for the Upper Pontchartrain Estuary was successfully developed, calibrated and applied,
- The long-term effects of different management scenarios on the water quality of the Upper Pontchartrain Estuary were evaluated,
- Long-term physical (hydrological, meteorological, etc.) and water quality data records were collected from stations located within the Pontchartrain Estuary watershed and used to develop long-term daily records of loading for input into the model,
- Long-term average daily loadings were developed based on the collected data. The calculations predict daily long-term loadings of:
    - 183 m^3/s for daily discharge,
    - 3, 080 kg/day for nitrite + nitrate as nitrogen,
    - 2,200 kg/day for phosphorous,
    - 2,560 kg/day for ammonia ,
    - 10,930 kg/day for organic nitrogen, and
    - a total nitrogen input of 6,050 metric tonnes/year and a total phosphorous input of 800 metric tonnes/year.
- Using the modeled live algae concentrations in conjunction with the algal bloom probability model produced accurate predictions of algal bloom occurrences between 1990 and 2006. The model predicted that:
    - Small algal blooms would occur in 1993 and 1994,
    - An intermediate algal bloom would occur in 2004, and
    - Extensive algal blooms would occur in 1991, 1995 and 1997.
    - The 1993, 1994, 1995 and 1997 predictions were verified by observations from Poirrier et al. (1998)
- The model predicted that the addition of freshwater diversions into Maurepas swamp may cause more intense and frequent algal blooms to occur around the Pontchartrain Estuary,
    - The model showed no effect on the probability of algal blooms when a 30 m^3/s diversion was input into Lake Maurepas,
    - For a 280 m^3/s diversion into Lake Maurepas, the model predicted that the 1993 and 1994 algal blooms would expand into the east side of Lake Pontchartrain and that a large bloom would occur in 1990 in addition to those in 1991, 1995, 1997 and 2004.
- The model predicted that increased flows from the Bonnet Carré Spillway into Lake Pontchartrain may cause more intense and frequent algal blooms to occur around the Pontchartrain Estuary
    - For a 50% increase to Bonnet Carré flows, the model predicted that the 1993 and 1994 algal blooms would expand into the east side of Lake Pontchartrain and that a new bloom would occur in 1990 in addition to those in 1991, 1995, 1997 and 2004.
    - For a 200% increase to Bonnet Carré flows, the model predicted that the 1991 algal bloom would expand into Lake Borgne, the 1993 and 1994 algal blooms

would expand into the east side of Lake Pontchartrain and that new blooms would occur in 1990 (large), 2002 (small) and 2003 (small), in addition to those in 1995, 1997 and 2004.

- All of the algal bloom occurrences predicted by the model (except 1997 and 2004) correspond to high nutrient inputs from Bonnet Carré Spillway leakage, opening events or new diversions that occurred in May or June. The flow from the 1997 opening event in March/April was large enough that nutrient rich water still remained in the system until late August. The 2004 algal bloom cannot be explained by input from the Bonnet Carré Spillway but may be a result of high tributary nutrient loadings.
- The model found that high nutrient inputs that entered the system earlier in the year (January/February) did not increase the frequency or intensity of algal blooms even if the magnitude of the event was large. Nitrogen assimilation reduces the nutrient concentrations before the conditions required for an algal bloom are reached.
- The model found that high nutrient inputs that entered the system after the conditions for optimum growth had been reached (optimum growth period is typically late spring to early fall) reduce the duration of algae bloom events in the western area of Lake Pontchartrain and increase the duration of algal bloom events in areas where salinities are higher in Lake Pontchartrain (southeast Lake Pontchartrain and east Lake Pontchartrain).
- Algal bloom occurrences can be avoided if high nutrient inputs are added early (January/February) or late (Fall/Winter) in the year. Diversions (even small ones) that occur in May/June have a high probability of causing an algal bloom event to occur since optimum growth conditions are usually present (when extreme conditions like drought are not present).

Bibliography

Barras, J. A. (2006). *Land area change in coastal Louisiana after the 2005 hurricanes—a series of three maps*. U.S. Geological Survey Open-File Report 06-1274.

Barry, J. M. (1997). *Rising tide: the great Mississippi flood of 1927 and how it changed America*. Touchstone, New York, New York.

Brammer, A. J., Rodriguez del Rey, Z., Spalding, E. A., and Poirrier, M. A. (2007). "Effects of the 1997 Bonnet Carré Spillway opening on infaunal macroinvertebrates in Lake Pontchartrain, Louisiana." *Journal of Coastal Research*, 23(5), 1292-1303.

Brantley, C. (2008). Project Manager, Bonnet Carre Spillway, personal communication.

Chapra, S.C. and Pelletier, G.J. (2003). *QUAL2K: A Modeling Framework for Simulating River and Stream Water Quality: Documentation and Users Manual. Civil and Environmental Engineering, Department.* Tufts University, Medford, MA.

Chapra, S. C. (1997). Surface water quality modeling. WCB/McGraw-Hill, Boston, Massachusetts, USA.

Chilmakuri, C., S. (2005). *Sediment transport and pathogen indicator modeling in Lake Pontchartrain*. A Dissertation for Doctor of Philosophy in Engineering and Applied Science, University of New Orleans, New Orleans, LA.

Coastal Engineering Research Center. (1984). *Shore Protection Manual*. U.S. Army Corps of Engineers, Waterways Experiment Station, Vicksburg Mississippi.

Coastal Protection and Restoration Authority. (2007). *Integrated ecosystem restoration and hurricane protection: Louisiana's comprehensive Master Plan for a sustainable Coast*. Baton Rouge, LA.

Coleman, J. M., Roberts, H. H., and Stone, G. W. (1998). "Mississippi River Delta: an overview." *Journal of Coastal Research*, 14(3): 698-716.

Cruise, J. F., Sherif, M. M., and Singh, V. P. (2007). *Elementary Hydraulics*. Thomson-Nelson, Toronto, Canada.

Day Jr., J. W., and Templet, P. H. (1990). "Consequences of sea level rise: implications from the Mississippi Delta" *Beukema, J. J. et al. (Ed.) (1990). Expected effects of climactic change on marine coastal ecosystems. Developments in Hydrobioloogy*, 57: 155-165.

Day, J. W., Lane, R. R., and Mach, R. F. (1999). "Water chemistry dynamics in Lake Pontchartrain, Louisiana, during the 1997 opening of the Bonnet Carré Spillway." *Recent research in coastal Louisiana: Natural system function and response to human influences*. Louisiana Sea Grant College Program, Baton Rouge, LA.

Day, J. W., Britsch, L. D., Hawes, S. R., Shaffer, G. P., Reed, D. J., and Cahoon, D. (2000). "Pattern and process of land loss in the Mississippi Delta: a spatial and temporal analysis of wetland habitat change." *Estuaries and Coasts*, 23(4): 425-438.

DeLaune, R. D., Jugsujinda, A., Peterson, G. W., and Patrick Jr., W. H. (2003). "Impact of Mississippi River freshwater reintroduction on enhancing marsh accretionary processes in a Louisiana estuary." *Estuarine, Coastal and Shelf Science*, 58(3), 653-662.

Demcheck, D. K., Garrison, C. R., and McGee, B. D. (1996). *Selected water-quality data for the Lower Mississippi River, Bonnet Carré Spillway, and Lake Pontchartrain area, Louisiana, April through June 1994 and 1974-84*. U.S. Geological Survey, Open-file Report 96-652A. Prepared in cooperation with the U.S. Environmental Protection Agency, Baton Rouge, LA.

Dodson, S. I. (2005). *Introduction to limnology*. McGraw Hill, New York, New York.
Dortch, Q., Peterson, T., and Turner, R. E. (1998). "Algal bloom resulting from the opening of the Bonnet Carré Spillway in 1997." *Proceedings of the Basics of the Basin research symposium*, U.S. Geological Survey, New Orleans, LA.
Dortch, Q., Parsons, M. L., Rabalais, N. N., and Turner, R. E. (1999). "What is the threat of harmful algal blooms in Louisiana coastal waters?" *Recent research in coastal Louisiana: Natural system function and response to human influences*. Louisiana Sea Grant College Program, Baton Rouge, LA.
Dortch, M. S., Zakikhani, M., Noel, M. R., and Kim, S. (2007). *Application of a water quality model to Mississippi Sound to evaluate impacts of freshwater diversions*. U.S. Army Corps of Engineers, Environmental Laboratory, Engineer Research and Development Center, ERDC/EL TR-07-20
Gibbs, K. (12 May 2005). *Bonnet Carré Spillway*. U.S. Army Corps of Engineers. 15 Jan. 2008 <http://www.mvn.usace.army.mil/pao/bCarré/bCarré.htm>.
Glysson, G. D., and Gray, J. R. (2002). "Total suspended solids data for use in sediment studies." *Technical paper from the Turbidity and Other Sediment Surrogates Workshop*. April 30 – May 2, Reno, Nevada.
Georgiou, I. Y., McCorquodale, J. A., and Haralampides, K. (1998). "Salinity and dissolved oxygen stratification in Lake Pontchartrain and the vicinity of the Inner Harbor Navigation Canal" *Proceedings of the Basics of the Basin research symposium*, University of New Orleans, New Orleans, LA.
Georgiou, I. Y., and McCorquodale, J. A. (2000). "Salinity stratification from a navigation canal in a shallow Lake" *Stratified flows*, Laurence, G. A., Pieter's, R. and Yemenites, N., Eds., University of British Columbia, Vancouver, Canada, 2: 859 – 864.
Georgiou, I.Y., and McCorquodale, J. A. (2002) "Stratification and circulation patterns in Lake Pontchartrain" *Estuarine and Coastal Modeling*, Malcolm L. Spaulding and Butler Lee H.,Eds., ASCE, New York, 875-887.
Georgiou, I. Y. (2002). *Three-dimensional hydrodynamic modeling of saltwater intrusion and circulation in Lake Pontchartrain*. A dissertation for Doctor of Philosophy in Engineering and Applied Science in the Department of Civil and Environmental Engineering, University of New Orleans, New Orleans, LA.
Haralampides, K. (2000). *A study of the hydrodynamics and salinity regimes of the Lake Pontchartrain system*. A dissertation for Doctor of Philosophy in Engineering and Applied Science in the Department of Civil and Environmental Engineering, University of New Orleans, New Orleans, LA.
Howarth, R. W. (1988). "Nutrient limitation of net primary production in marine ecosystems". *Annual Review of Ecology and Systematics*, 19: 898-910.
Ismail, I. A. (1999). *Lake Pontchartrain water quality and algal bloom assessment*. A Thesis for Master of Science in the Civil and Environmental Engineering Department, University of New Orleans, New Orleans, LA.
Fontenot, R. L. (2004). *An evaluation of reference evapotranspiration models in Louisiana*. A Thesis for Masters of Natural Sciences in the Interdepartamental Program of Natural Sciences, Agriculture and Mechanical College, Louisiana State University, Baton Rouge, LA.

Jenkins, M. C., and Kemp, W. M. (1984). "The coupling of nitrification and denitrification in two estuarine sediments." *Limnology and Oceanography*, 29(3), 609-619.

Kesel, R. H. (1988). "The decline in the suspended load of the Lower Mississippi River and its influence on adjacent wetlands." *Environmental Geology*, 11(3): 271-281.

Kesel, R. H. (1989). "The role of the Mississippi River in wetland loss in south eastern Louisiana, U.S.A." *Environmental Geology*, 13(3): 183-193.

Khairy Ali Gondia, W. M. (2000). *Integrated watershed management for optimum environmental quality of aquatic systems*. A Dissertation for Doctor of Philosophy in Engineering and Applied Science, University of New Orleans, New Orleans, LA.

Lake Pontchartrain Basin Foundation. (2005). *Comprehensive habitat management plan for the Lake Pontchartrain basin*. New Orleans, LA.

Lake Pontchartrain Basin Foundation. (2005). *Tangipahoa River water quality improvement project*. Response to the call for nominations for the 2005 EPA targeted watersheds grant program: Tangipahoa River Watershed: HUC Code 08070205, 303(d) Impaired Subsegment # LA040701_00.

Lane, R. R., Day, J. W., Kemp, G. P., and Demcheck, D. K. (2001). "The 1994 experimental opening of the Bonnet Carré Spillway to divert Mississippi River water into Lake Pontchartrain, Louisiana." *Ecological Engineering*, 17(4), 411-422.

Lane, R. R., Day, J. W., and Thidbodeaux, B. (1999). "Water quality analysis of a freshwater diversion at Caernarvon, Louisiana." *Estuaries*, 22, 327-336.

Leal, J.C., (2004). *Water Quality Study and Plume Behavior Modeling for Lake Pontchartrain at the Mouth of the Tchefuncte River*, M.S. Thesis, Dept. of Civil and Environmental Engineering, University of New Orleans, New Orleans, LA

McCorquodale, J. A., Haralampides, K., and Hannoura, A. (1998). "Lake Pontchartrain monitoring for 1997 opening event." *1998 Basics of the Basin Symposium*, U. S. Geological Survey. New Orleans, LA.

McCorquodale, J. A., Barbé, D., Haralampides, K., Wang, Y., and Carnelos, S. (2001). *Pontchartrain Basin Land Loss – Freshwater inflows into Lake Pontchartrain system in S. Louisiana*. Penland, A. Beall and J. Waters (editors), Environmental Atlas of Lake Pontchartrain Basin. Lake Pontchartrain Basin Foundation, New Orleans, LA.

McCorquodale, J.A., Englande, A.J., Carnelos, S., Georgiou, I., Wang, Y., (2003). *Fate of Pathogen Indicators in Stormwater Runoff.* Final Project Report for the U.S. Environmental Protection Agency, Urban Waste Management and Research Center, University of New Orleans, New Orleans, LA

McCorquodale, J.A., Georgiou, I., Chilmakuri, C. (2004). "*Application of a 3-D Hydrodynamic Model for assessing the risk of an Algal Bloom", Proceedings of the 6th International Conference on Hydro-Science and –Engineering*, M.S. Altinakar, (eds), Brisbane, Australia, 4:11.

McCorquodale, J.A., Georgiou, I., Carnelos, S., and Englande, A.J. (2004). "Modeling Pathogens in Storm Water Plumes", *Special Issue of the Journal of Environmental Engineering and Science*, National Research Council of Canada, Ottawa, ON., p. 419.

McCorquodale, J. A., and Georgiou, I. (2006). *Evaluation of water quality models for Ontario receiving waters*. Prepared for the Ontario Ministry of the Environment, Toronto, Canada.

McCorquodale, J. A., Georgiou, I., Roblin, R. J., and Chilmakuri, C. (2007). *Development of a comprehensive water quality model for the Pontchartrain Basin: application of a 3-D model as a water quality assessment tool*. Prepared for the National Ocean and Atmospheric Administration through Pontchartrain Restoration Program Grant No. NA04NOS4630255.

McCorquodale, J. A., Roblin, R. J., and Georgiou, I. (2007). *Sediment budget for the Chenier Plain*. University of New Orleans, New Orleans, LA.

McCorquodale, J. A. (2007). *Sediment transport fall 2007 course notes*. Department of Civil and Environmental Engineering, University of New Orleans, New Orleans, LA.

McCutcheon, Steve C. (1989). *Water Quality Modeling*. CRC Press, Inc. Boca Raton, FL.

Miller, R.L., Del Castillo, C.E., Chilmakuri, C., McCorquodale, J.A., Georgiou, I., McKee, B.A., and Dapos Sa, E.J. "Using multi-temporal MODIS 250 m data to calibrate and validate a sediment transport model for environmental monitoring of coastal waters" Analysis of Multi-Temporal Remote Sensing Images, *2005 International Workshop on the Volume* , May 16-18, 2005. pp. 200-204.

Penland, S., Beall, A., and Kindinger, J. (2001) *Environmental Atlas of Lake Pontchartrain Basin*. USGS Open File Report 02-206.

Poirrier, M. A., and King, J. M. (1998). "Observations on Lake Pontchartrain blue-green algal blooms and fish kills." *1998 Basics of the Basin Symposium*, U. S. Geological Survey, New Orleans, LA.

Rabalais, N. N. (2002). "Nitrogen in aquatic ecoystsems". *Ambio*, 2: 102-112.

Rabalais, N. N., Turner, R. E., and Wiseman, W. J. (2002). "Gulf of Mexico hypoxia, aka 'The dead zone'". *Annual Review of Ecology and Systematics*, 33: 235-263.

Retana, A. G. (2008). PhD candidate, Civil and Environmental Engineering, University of New Orleans, personal communication.

Schurtz, M. H., and St. Pe', K. (1984) *Report on the Interim Findings of the Environmental Conditions in Lake Pontchartrain, LA*. Department of Environmental, Quality- Water Pollution Control Division.

Smith, V. H. (1990). "Comment on nitrogen, phosphorous, and nitrogen fixation in lacustrine and estuarine ecosystems." *Limnology and Oceanography*, 35(8),1852-1859.

Thomann, V. R., and Mueller, J. A. (1987). *Principles of Surface Water Quality Modeling and Control*, Harper Collins Publishers Inc., New York.

Trotter, P. S., Johnson, G. A., Ricks, R., Smith, D. R., and Wodds, D. (1998). *Floods on the Lower Mississippi: an historical economic overview*. U.S. Department of Commerce, U.S. National Weather Service Technical Attachment SR/SSD 98-9.

Turner, R. E., and Boyer, M. E. (1997). "Mississippi River diversions, coastal wetland restoration/creation and an economy of scale." *Ecological Engineering*, 8(2): 117-128.

Turner, R. E. (1999). "Nitrogen losses in water flowing through Louisiana swamps." *Recent research in coastal Louisiana: Natural system function and response to human influences*. Louisiana Sea Grant College Program, Baton Rouge, LA.

Turner, R. E. Dortch, Q., Justic, D., and Swenson, E.M. (2002). "Nitrogen loading into an urban estuary: Lake Pontchartrain (Louisiana, U.S.A.)". *Hydrobiologia*, 487(1): 137-152.

Uhrich, M. A. (2002). "Determination of total and clay suspended-sediment loads from instream turbidity data in the North Santiam River basin, Oregon: 1998-2000." *Technical paper from the Turbidity and Other Sediment Surrogates Workshop*. April 30 – May 2, Reno, Nevada.

U.S. Army Corps of Engineers. (1982). *Lake Pontchartrain, Louisiana and vicinity Hurricane Protection Project: Environmental Impact Statement*.

U.S. Army Corps of Engineers. (2004). *Louisiana coastal area (LCA) study, Ecosystem restoration study, Hurricane Protection Project: Environmental Impact Statement*. Cooperating agencies: the U.S. Geological Survey (USGS), the Louisiana Department of Natural Resources (LADNR), the National Marine Fisheries Service (NMFS), U.S. Fish and Wildlife (USFW), and the Environmental Protection Agency (EPA)).

U.S. Army Corps of Engineers. (10 April 2008). *Riverside, Special Edition*. 15 April 2008. <http://www.mvn.usace.army.mil/Riverside_April_10_2008.pdf>

Waldon, M. G., and Bryan, C. F. (1999). "Annual salinity and nutrient budget of Lake Pontchatrain and impact of proposed Bonnet Carré Diversion." *Recent research in coastal Louisiana: Natural system function and response to human influences*. Louisiana Sea Grant College Program, Baton Rouge, LA.

Wang, Y. (2003). *Atmospheric deposition of nutrients in an urban area*. A Dissertation for Doctor of Philosophy in Engineering and Applied Science, Department of Civil and Environmental Engineering, University of New Orleans, New Orleans, LA.

Appendix A

Table A.1 USGS Stations used in tributary discharge analysis.

USGS Site Number	Site Name	Drainage Area (km^2)	Length of Discharge Record (years)
7377000	Amite River near Darlington, LA	1,502	48
7378500	Amite River near Denham Springs, LA	3,315	68
7380120	Amite at Port Vincent, LA	4,134	8
7375280	Tangipahoa River at Osyka, MS	409	10
7375500	Tangipahoa River at Robert, LA	1673	68
7375000	Tchefuncte River near Folsom, LA	247	56
7375800	Tickfaw River at Liverpool, LA	232	18
7376000	Tickfaw River at Holden, LA	640	66
7376500	Natalbany River at Baptist, LA	206	63
2490500	Bogue Chitto near Tylertown, MS	1,274	62
2492000	Bogue Chitto River near Bush, LA	3,142	69
2486000	Pearl River at Jackson, MS	8,213	88
2488000	Pearl River at Rockport, MS	11,800	28
2488500	Pearl River near Monticello, MS	12,932	68
2489000	Pearl River near Columbia, MS	14,815	32
2489500	Pearl River near Bogalusa, LA	17,024	68
2492600	Pearl River at Pearl River, LA	21,999	6
301141089320300	East Pearl River at CSX Railrd nr Claimborne, MS	22,466	2
7380224	Black Bayou near Duplessis, LA	9.5	5
7377500	Comite River nr Olive Branch, LA	376	64
7378000	Comite River near Comite, LA	736	62

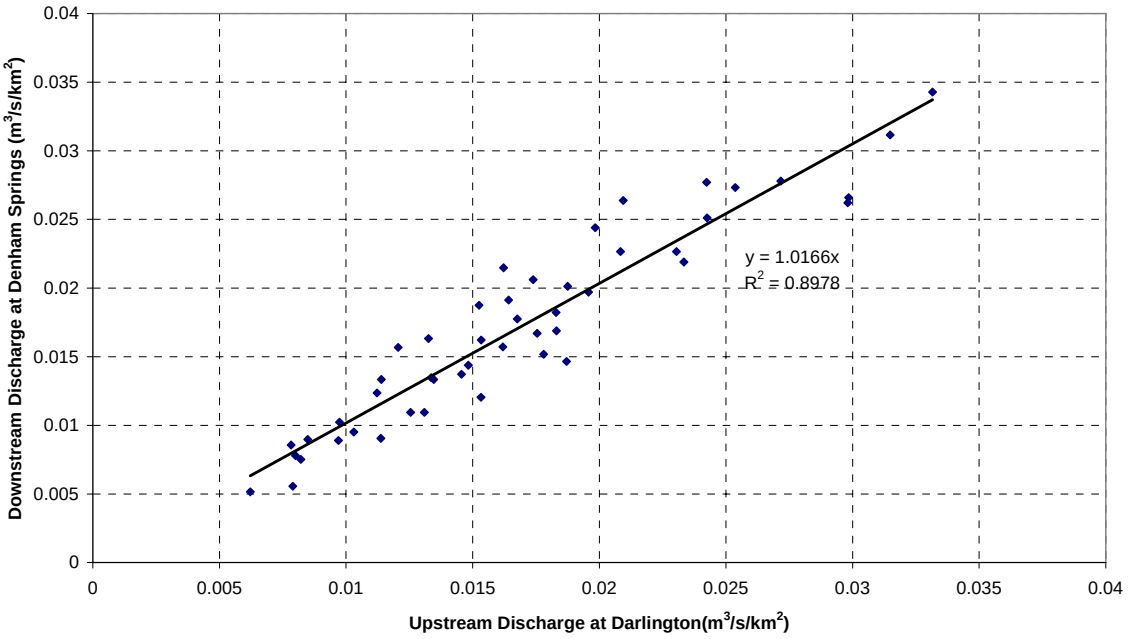

Figure A.1 Relationship between downstream and upstream average annual discharge per unit area for the Amite River

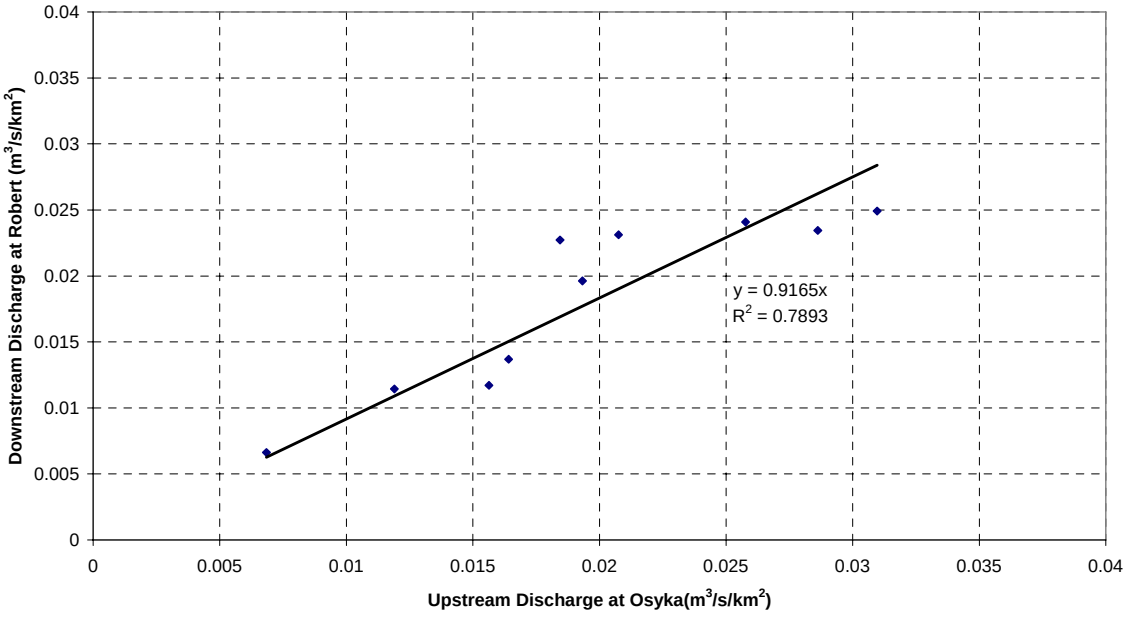

Figure A.2 Relationship between downstream and upstream average annual discharge per unit area for the Tangipahoa River.

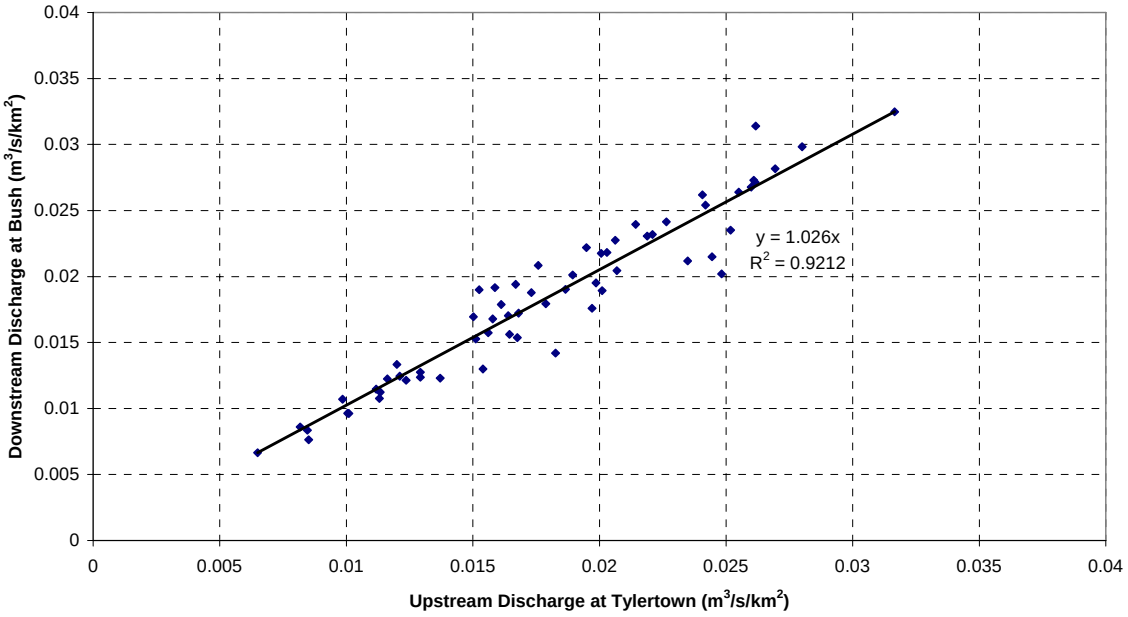

Figure A.3 Relationship between downstream and upstream average annual discharge per unit area for the Bogue Chitto River.

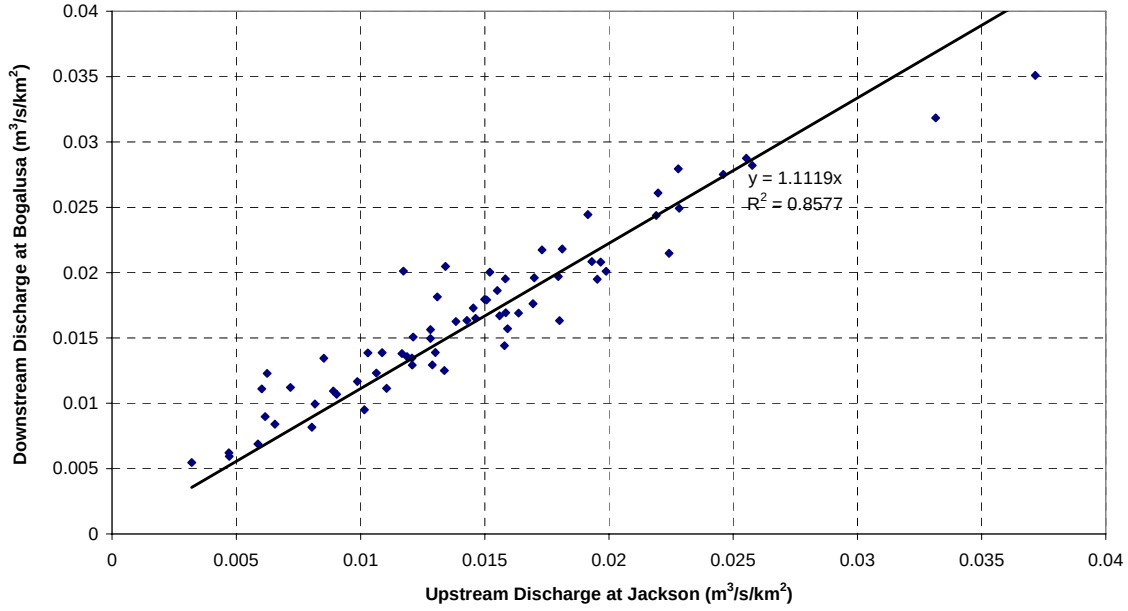

Figure A.4 Relationship between downstream and upstream average annual discharge per unit area for the Pearl River.

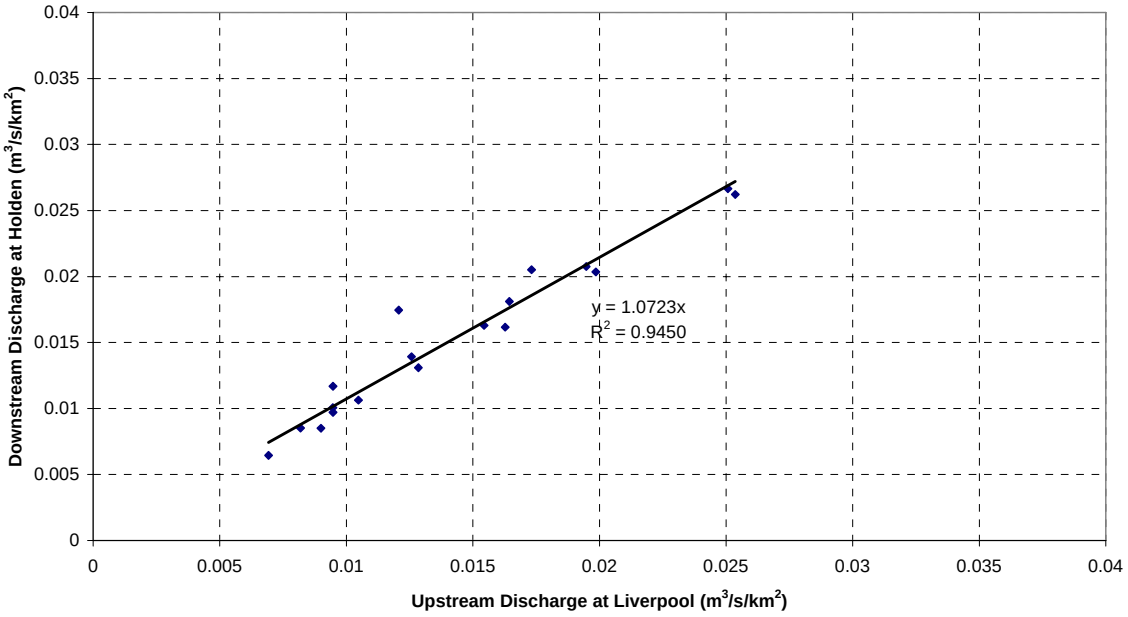

Figure A.5 Relationship between downstream and upstream average annual discharge per unit area for the Tickfaw River.

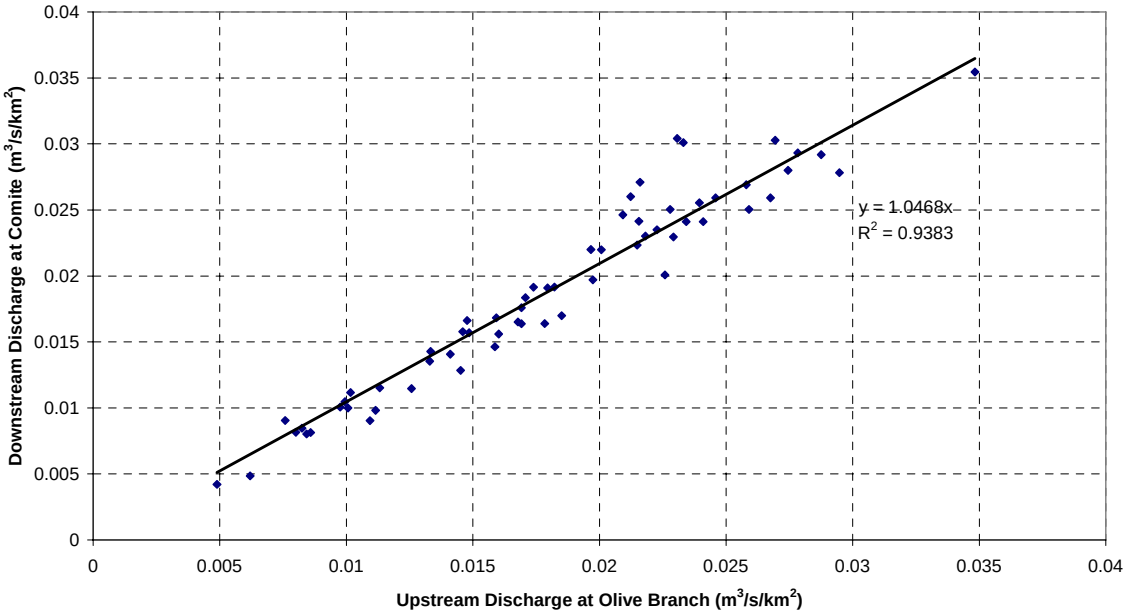

Figure A.6 Relationship between downstream and upstream average annual discharge per unit area for the Comite River.

Table A.2 Relationships between downstream and upstream discharges.

River	Downstream Gage	Upstream Gage	Downstream discharge as a function of upstream discharge ($m^3/s/km^2$)	R^2 Error
Amite	Denham Springs	Darlington	$Q_{downstream} = 1.0166*Q_{upstream}$	0.8978
Bogue Chitto	Bush	Tylertown	$Q_{downstream} = 1.026*Q_{upstream}$	0.9212
Comite	Comite	Olive Branch	$Q_{downstream} = 1.0468*Q_{upstream}$	0.9383
Pearl	Bogalusa	Jackson	$Q_{downstream} = 1.1119*Q_{upstream}$	0.8577
Tangipahoa	Robert	Osyka	$Q_{downstream} = 0.9165*Q_{upstream}$	0.7893
Tickfaw	Holden	Liverpool	$Q_{downstream} = 1.0723*Q_{upstream}$	0.9450

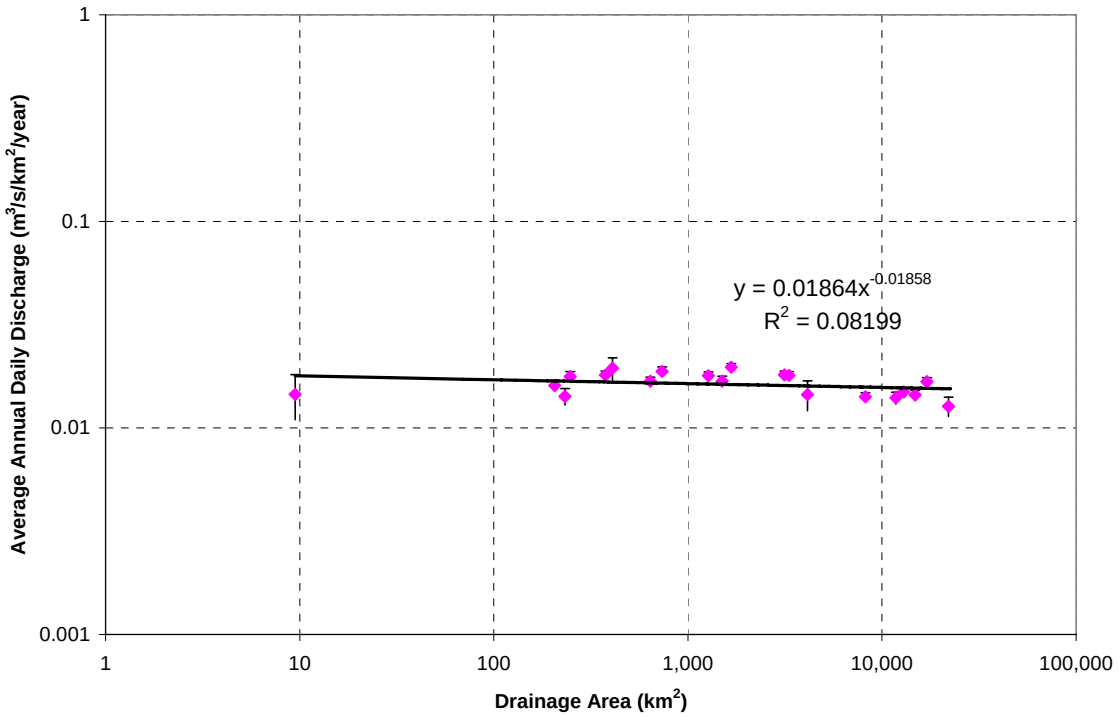

Figure A.7 Relationship between average annual daily discharge per unit area and drainage area.

Table A.3 Stations used in tributary nutrient analyses (table continued).

Entity	Site Number	Site Name	Data	USGS Gage assigned for Discharge
USGS	7377000	Amite River near Darlington, LA	Discharge, Turbidity, NO2+NO3, P	Amite River near Darlington, LA
USGS	7378500	Amite River near Denham Springs, LA	Discharge, Turbidity, SSC, OrgN	Amite River near Denham Springs, LA
USGS	7380120	Amite at Port Vincent, LA	Discharge, Turbidity, SSC, NO2+NO3, P, NH4, OrgN	Amite at Port Vincent, LA
USGS	7378510	Amite River at 4th Camp near Denham Springs	NO2+NO3, Turbidity, SSC, P, NH4, OrgN	Amite River near Denham Springs, LA
LADEQ	43	Amite River at Port Vincent, Louisiana	NO2+NO3, Turbidity, P, TKN	Amite at Port Vincent, LA
LADEQ	228	Amite River at mile 6.5, at Clio, Louisiana	NO2+NO3, Turbidity, P, TKN	Amite at Port Vincent, LA
LADEQ	268	Amite River Diversion Canal north of Gramercy, Louisiana	NO2+NO3, Turbidity, P, TKN	Amite at Port Vincent, LA
LADEQ	44	Amite River west of Darlington, Louisiana	NO2+NO3, Turbidity, P, TKN	Amite River near Darlington, LA
LADEQ	119	Amite River at Grangeville, Louisiana	NO2+NO3, Turbidity, P, TKN	Amite River near Denham Springs, LA
LADEQ	118	Amite River at Magnolia, Louisiana	NO2+NO3, Turbidity, P, TKN	Amite River near Denham Springs, LA
USGS	7375500	Tangipahoa River at Robert, LA	Discharge, Turbidity, SSC, NO2+NO3, P, NH4, OrgN	Tangipahoa River at Robert, LA
USGS	7375690	Tangipahoa River below Bedico Creek near Madisonville, LA	NO2+NO3, P	Tangipahoa River at Robert, LA
LADEQ	108	Tangipahoa River at Arcola	NO2+NO3, Turbidity, P, TKN	Tangipahoa River at Robert, LA
LADEQ	34	Tangipahoa River near Kentwood	NO2+NO3, Turbidity, P, TKN	Tangipahoa River at Robert, LA

Entity	Site Number	Site Name	Data	USGS Gage assigned for Discharge
LADEQ	33	Tangipahoa River west of Robert	NO2+NO3, Turbidity, P, TKN	Tangipahoa River at Robert, LA
LADEQ	1104	Tangipahoa River near Lake Pontchartrain	NO2+NO3, Turbidity, P, TKN	Tangipahoa River at Robert, LA
USGS	2492000	Bogue Chitto River near Bush, LA	Discharge, Turbidity, SSC, NO2+NO3, P, NH4, OrgN	Bogue Chitto River near Bush, LA
LADEQ	1038	Bogue Chitto River upstream from Wilson Slough	NO2+NO3, Turbidity, P, TKN	Bogue Chitto River near Bush, LA
LADEQ	65	Bogue Chitto River at Franklinton	NO2+NO3, Turbidity, P, TKN	Bogue Chitto River near Bush, LA
LADEQ	64	Bogue Chitto River near Bush	NO2+NO3, Turbidity, P, TKN	Bogue Chitto River near Bush, LA
USGS	7375800	Tickfaw River at Liverpool, LA	Discharge, Turbidity, NO2+NO3, P	Tickfaw River at Liverpool, LA
USGS	7376000	Tickfaw River at Holden, LA	NO2+NO3, Turbidity, P, TKN	Tickfaw River at Holden, LA
LADEQ	116	Tickfaw River at Springville	NO2+NO3, Turbidity, P, TKN	Tickfaw River at Holden, LA
LADEQ	1106	Tickfaw River near Lake Maurepas	NO2+NO3, Turbidity, P, TKN	Tickfaw River at Holden, LA
USGS	2488500	Pearl River near Monticello, MS	Discharge, Turbidity, SSC, NO2+NO3, P, NH4, OrgN	Pearl River near Monticello, MS
USGS	2489000	Pearl River near Columbia, MS	Discharge, Turbidity, SSC, NO2+NO3, P, NH4, OrgN	Pearl River near Columbia, MS
USGS	2489500	Pearl River near Bogalusa, LA	Discharge, Turbidity, SSC, NO2+NO3, P, NH4, OrgN	Pearl River near Bogalusa, LA

Entity	Site Number	Site Name	Data	USGS Gage assigned for Discharge
LADEQ	32	Pearl River (East) at Pearlington, Mississippi	NO2+NO3, Turbidity, P, TKN	Pearl River near Bogalusa, LA
USGS	2490193	Pearl River at Pools Bluff near Bogalusa, LA	NO2+NO3, Turbidity, SSC, P	Pearl River near Bogalusa, LA
LADEQ	105	Pearl River (West) southeast of Slidell, Louisiana	NO2+NO3, Turbidity, P, TKN	Pearl River near Bogalusa, LA
LADEQ	1061	Pearl River at Walkian Bluff boat launch	NO2+NO3, Turbidity, P, TKN	Pearl River near Bogalusa, LA
LADEQ	1053	Pearl River Navigation Canal at Lock #1	NO2+NO3, Turbidity, P, TKN	Pearl River near Bogalusa, LA
LADEQ	62	Pearl River at Pools Bluff, Louisiana	NO2+NO3, Turbidity, P, TKN	Pearl River near Bogalusa, LA
LADEQ	12	Pearl River east of Bogalusa, Louisiana	NO2+NO3, Turbidity, P, TKN	Pearl River near Bogalusa, LA
USGS	7375230	Tchefuncte River at Madisonville, LA	NO2+NO3, SSC, NH4, OrgN	Tchefuncte River near Folsom, LA
USGS	7375050	Tchefuncte River near Covington, LA	NO2+NO3, Turbidity, SSC, P, NH4, OrgN	Tchefuncta River near Folsom, LA
LADEQ	106	Tchefuncta River Madisonville	NO2+NO3, Turbidity, P, TKN	Tchefuncta River near Folsom, LA
LADEQ	107	Tchefuncta River west of Covington	NO2+NO3, Turbidity, P, TKN	Tchefuncta River near Folsom, LA
LADEQ	638	Tchefuncta River south of Madisonville	NO2+NO3, Turbidity, P, TKN	Tchefuncta River near Folsom, LA
LADEQ	298	Natalbany River west of Ponchatoula	NO2+NO3, Turbidity, P, TKN	Natalbany River at Baptist, LA
USGS	7378000	Comite River near Comite, LA	Discharge, NO2+NO3, P	Comite River near Comite, LA

Entity	Site Number	Site Name	Data	USGS Gage assigned for Discharge
LADEQ	1109	Comite River at Wilson-Clinton Rd. Bridge	NO2+NO3, Turbidity, P, TKN	Comite River nr Olive Branch, LA
LADEQ	297	Comite River east of Baton Rouge	NO2+NO3, Turbidity, P, TKN	Comite River near Comite, LA
LADEQ	1100	Comite River near Comite Drive Bridge	NO2+NO3, Turbidity, P, TKN	Comite River near Comite, LA
LADEQ	1099	Comite River near Stevensdale Road train bridge	NO2+NO3, Turbidity, P, TKN	Comite River near Comite, LA

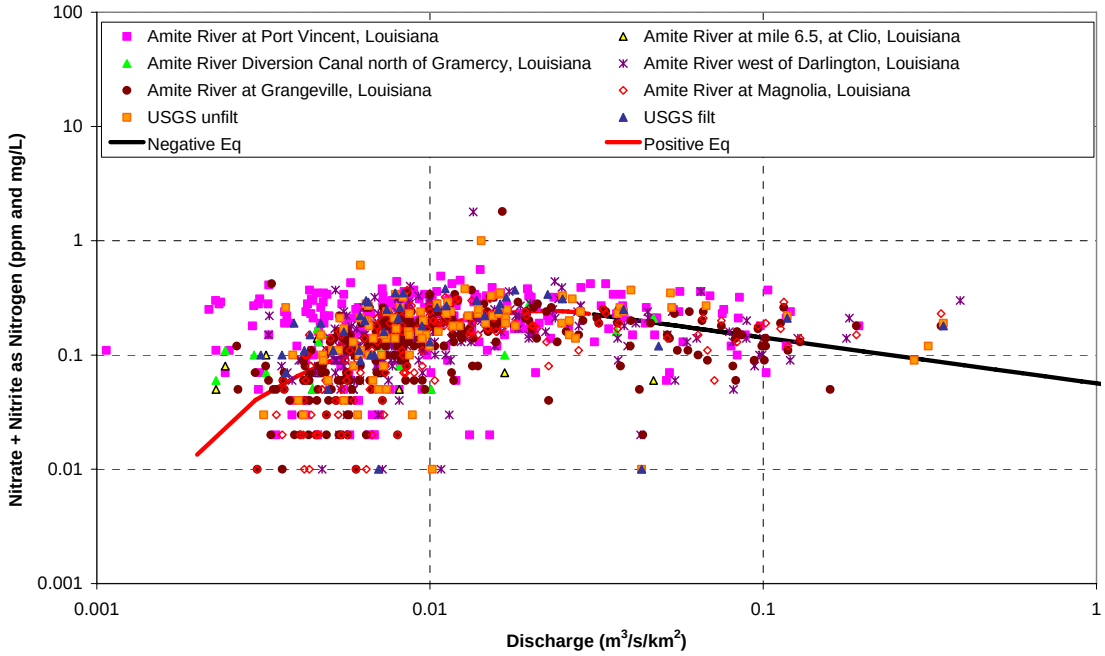

Figure A.8 Relationship between nitrate + nitrite as nitrogen and discharge for the Amite River.

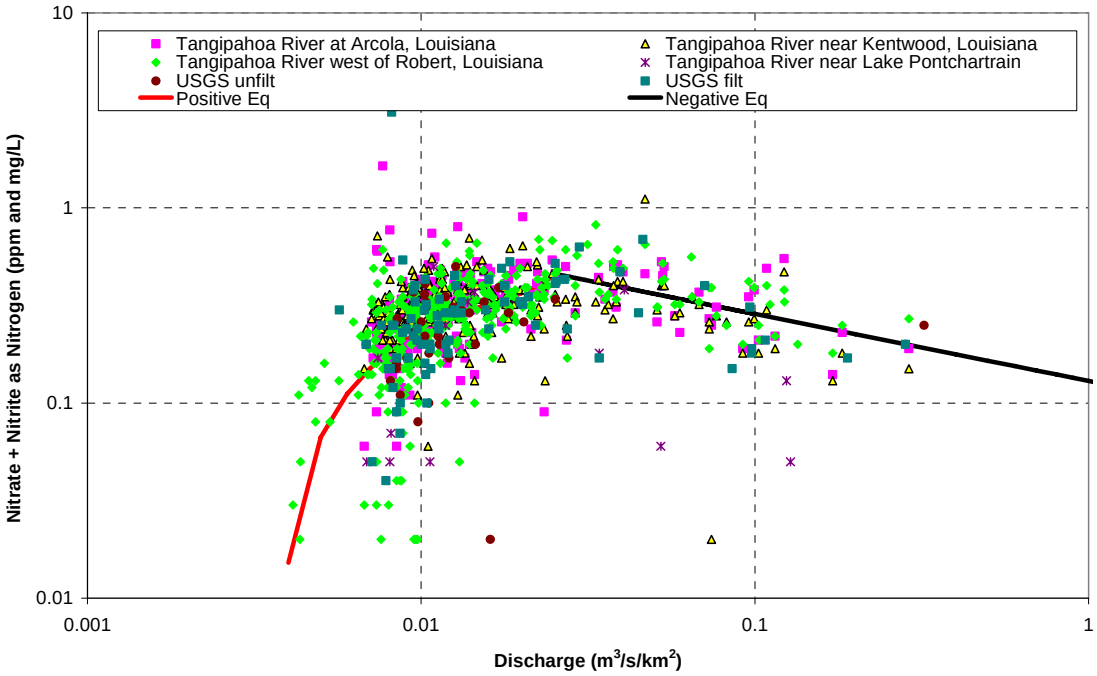

Figure A.9 Relationship between nitrate + nitrite as nitrogen and discharge for the Tangipahoa River.

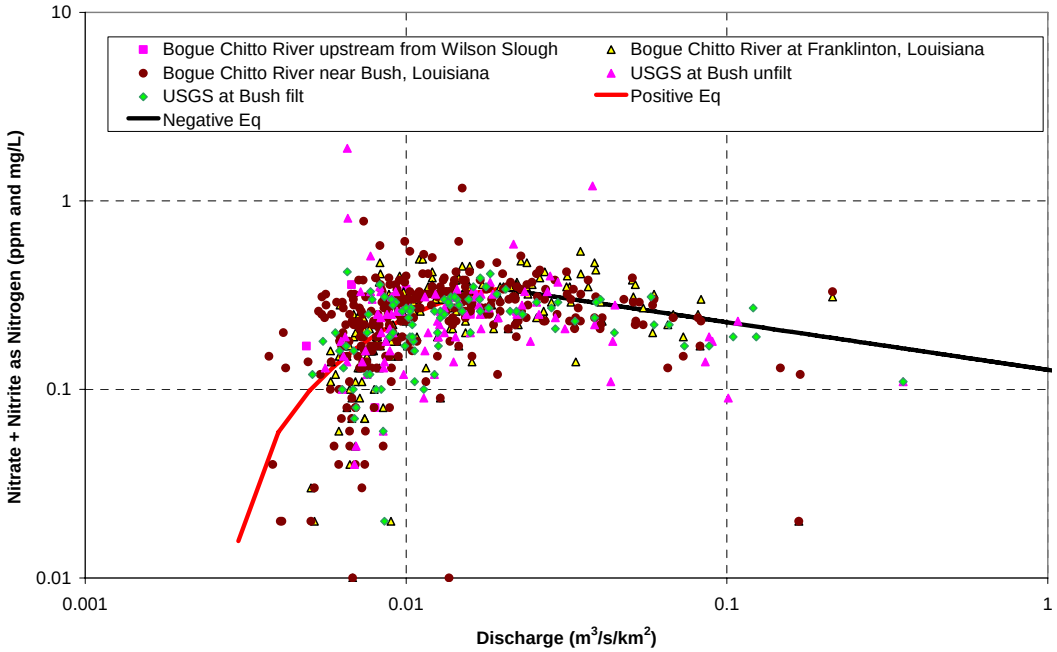

Figure A.10 Relationship between nitrate + nitrite as nitrogen and discharge for the Bogue Chitto River.

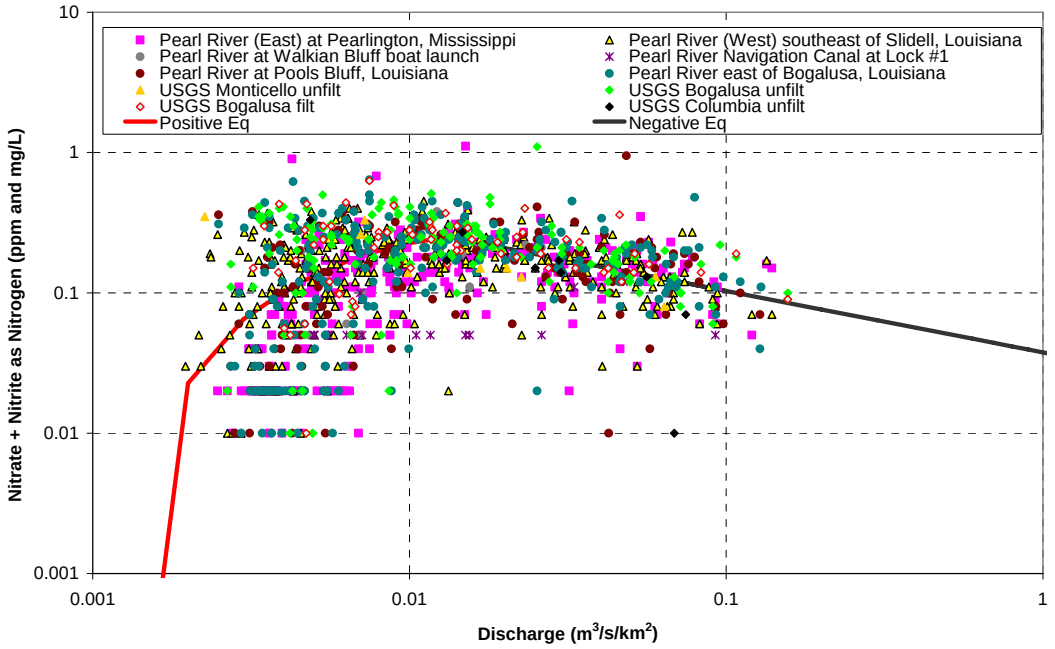

Figure A.11 Relationship between nitrate + nitrite as nitrogen and discharge for the Pearl River.

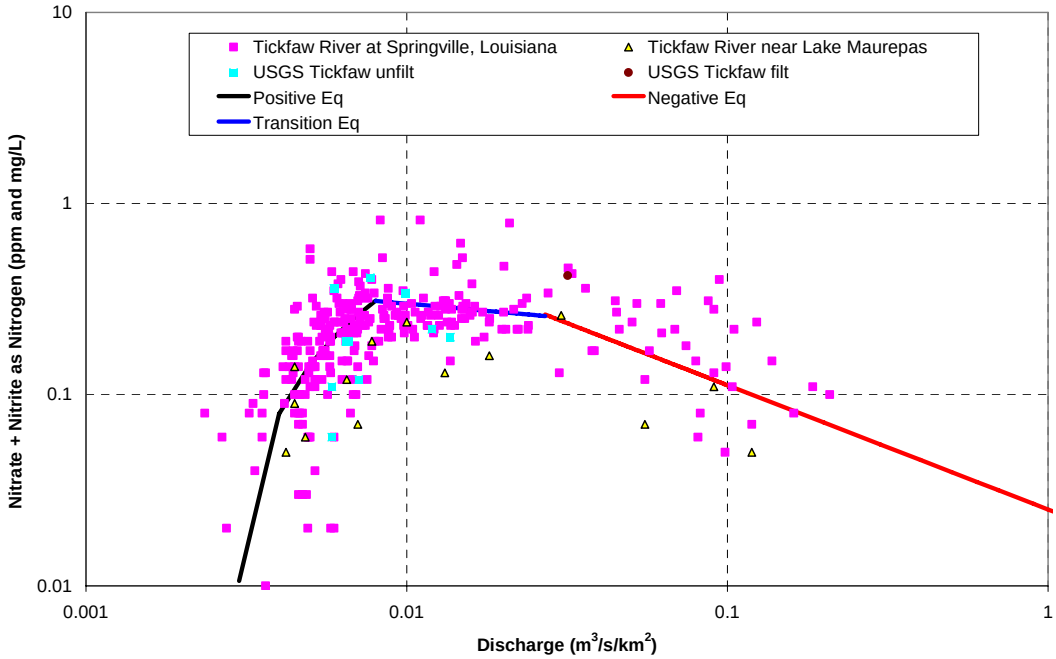

Figure A.12 Relationship between nitrate + nitrite as nitrogen and discharge for the Tickfaw River.

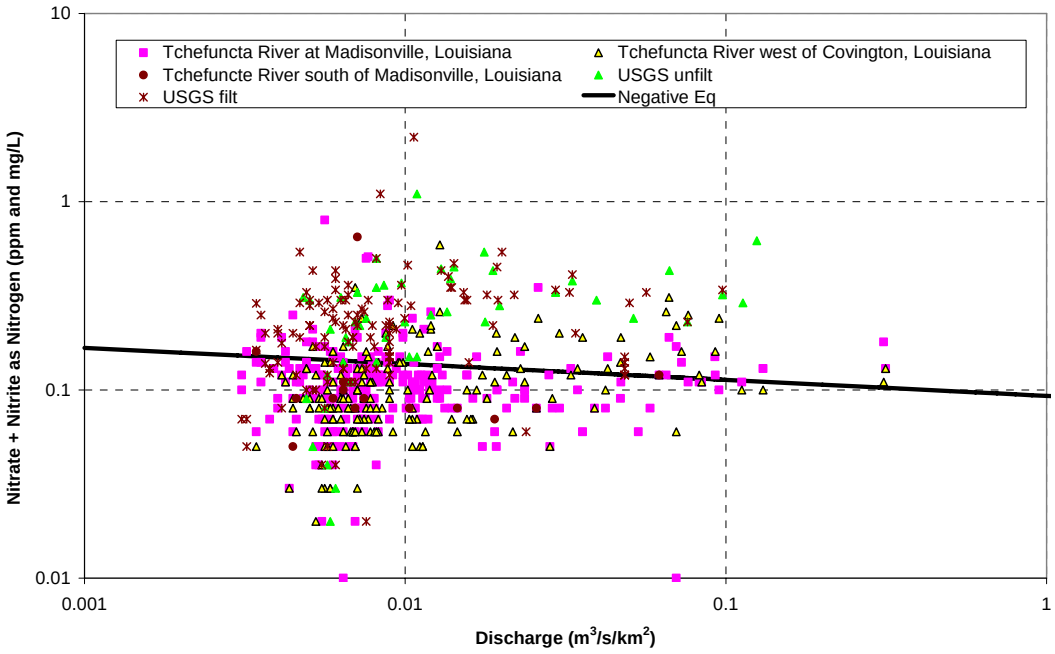

Figure A.13. Relationship between nitrate + nitrite as nitrogen and discharge for the Tchefuncte River.

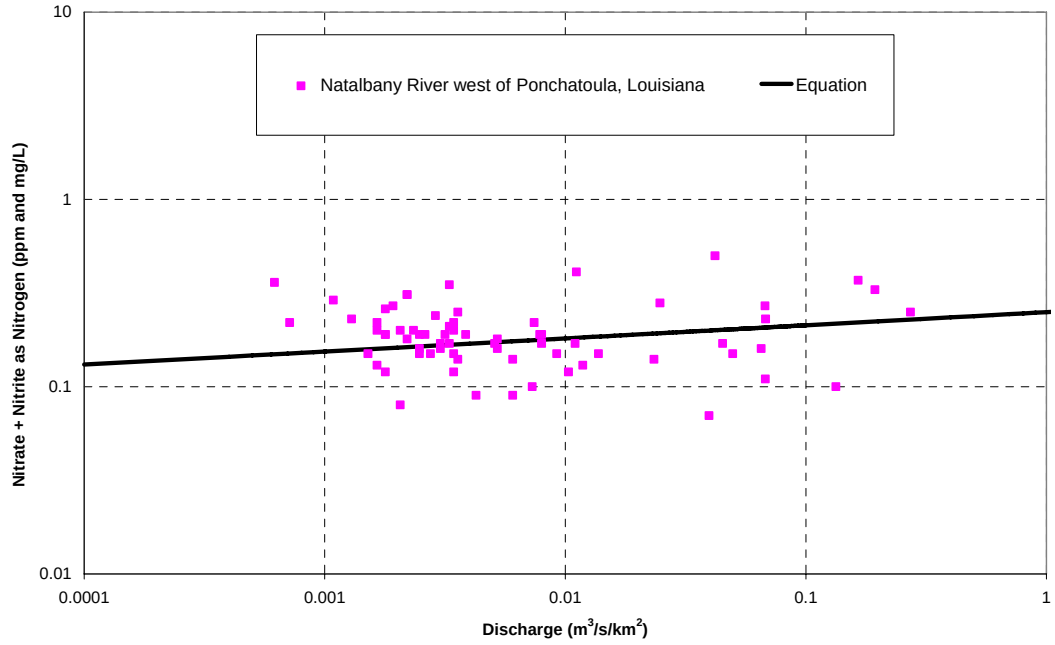

Figure A.14 Relationship between nitrate + nitrite as nitrogen and discharge for the Natalbany River.

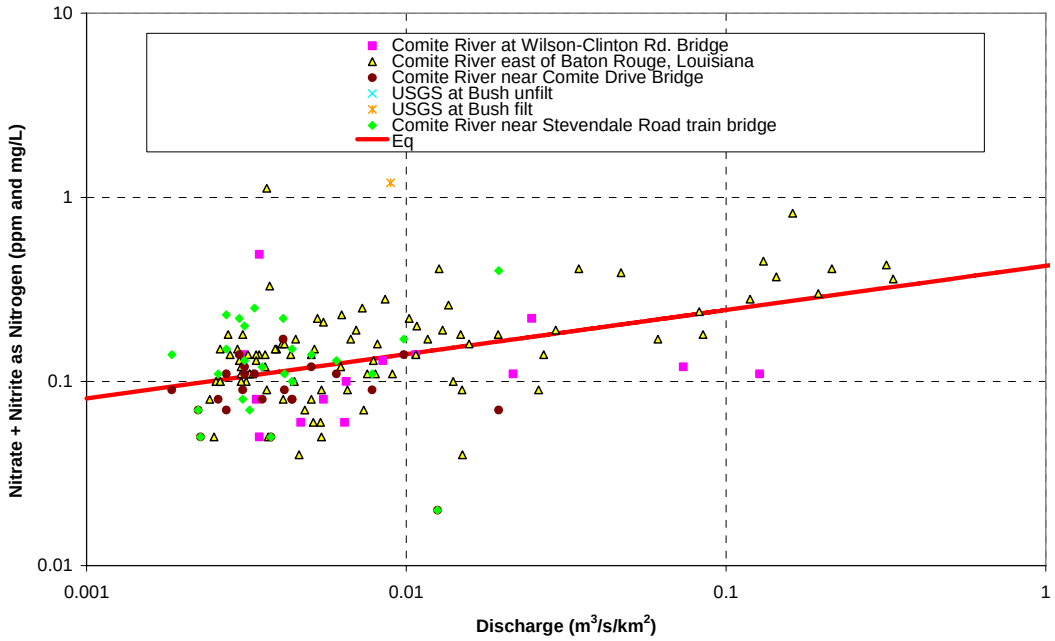

Figure A.15 Relationship between nitrate + nitrite as nitrogen and discharge for the Comite River.

Table A.4 Relationships between discharge and nitrite + nitrate as nitrogen concentrations.

River	Nitrite + Nitrate as Nitrogen Concentration (mg/L) for Discharges less than the Splitting Value ($m^3/s/km^2$)	Splitting Value ($m^3/s/km^2$)	Nitrite + Nitrate as Nitrogen Concentration (mg/L) for Discharges greater than the Splitting Value ($m^3/s/km^2$)
Amite River	$-637673*Q^6 + 514426*Q^5 - 150380*Q^4 + 20231*Q^3 - 1280.5*Q^2 + 33.093*Q - 0.0478$	0.03	$0.0565*Q^{-0.4}$
Tangipahoa River	$-8752700*Q^6 + 1190100*Q^5 - 1225500*Q^4 + 352260*Q^3 - 5621.6*Q^2 + 93.372*Q - 0.27777$	0.0252	$0.1298*Q^{-0.343}$
Bogue Chitto	-5171400*Q6 + 2928600*Q5 - 609660*Q4 + 58800*Q3 - 2794.9*Q2 + 61.067*Q - 0.14389	0.02	$0.127*Q^{-0.2525}$
Pearl	$-24171000*Q^6 + 9579300*Q^5 - 1452100*Q^4 + 105550*Q^3 - 3774.2*Q^2 + 59.312*Q - 0.081608$	0.014	$0.0377*Q^{-0.437}$
Tickfaw	$21{,}000*Q^3 - 2{,}550*Q^2 + 86*Q - 0.225$	0.008	$0.15*Q^{-0.15}$
Tickfaw (cont).		0.027	$0.0251*Q^{-0.65}$
Natalbany	$0.25*Q^{0.07}$		
Comite	$0.4247*Q^{0.2398}$		
Tchefuncte	$0.093*Q^{-0.085}$		

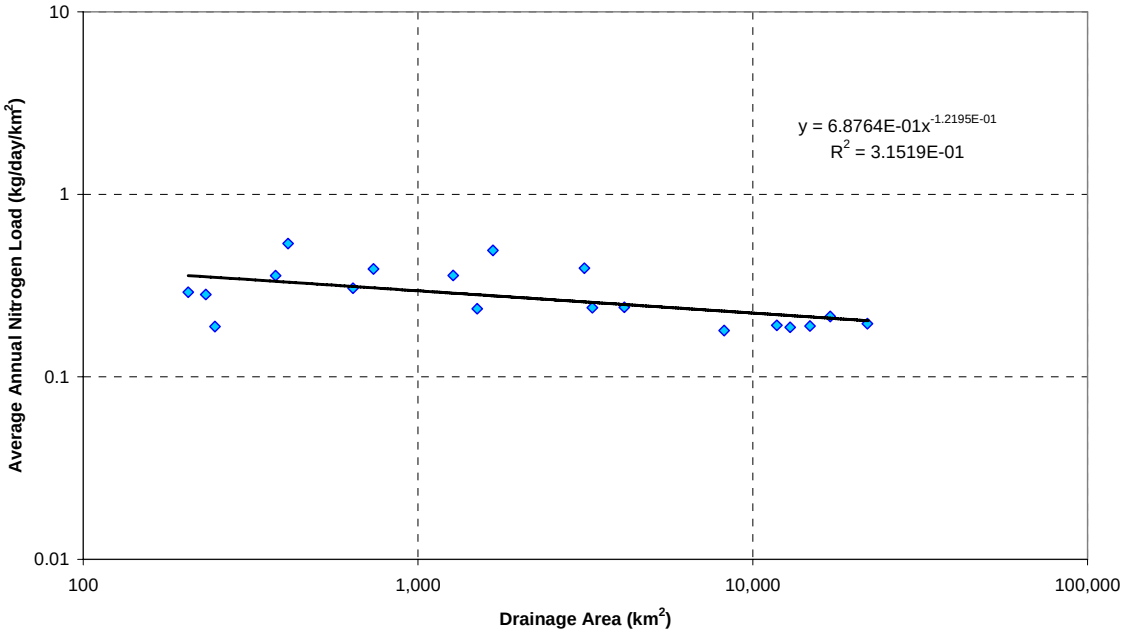

Figure A.16 Relationship between average annual nitrate + nitrite as nitrogen load and drainage area.

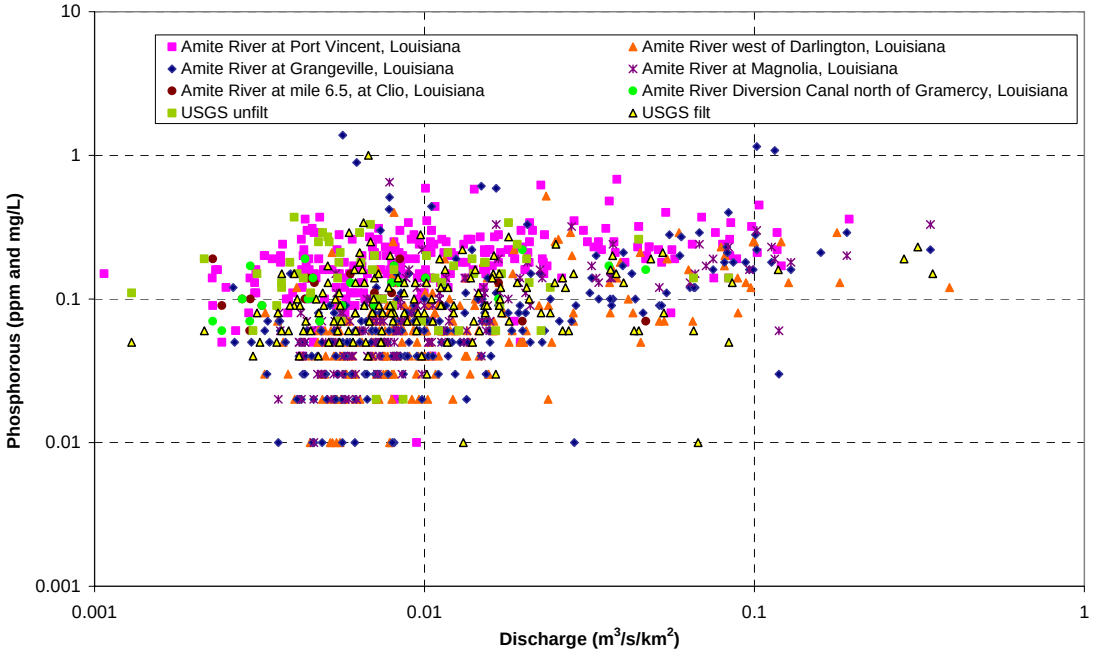

Figure A.17 Relationship between phosphorous concentration and discharge for the Amite River

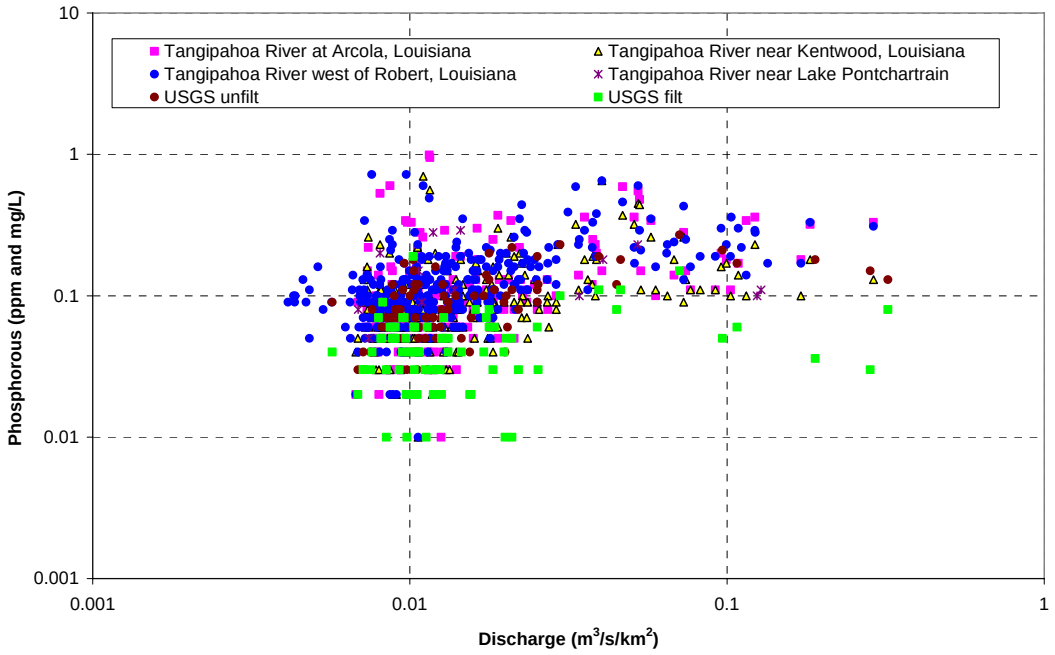

Figure A.18 Relationship between phosphorous concentration and discharge for the Tangipahoa River.

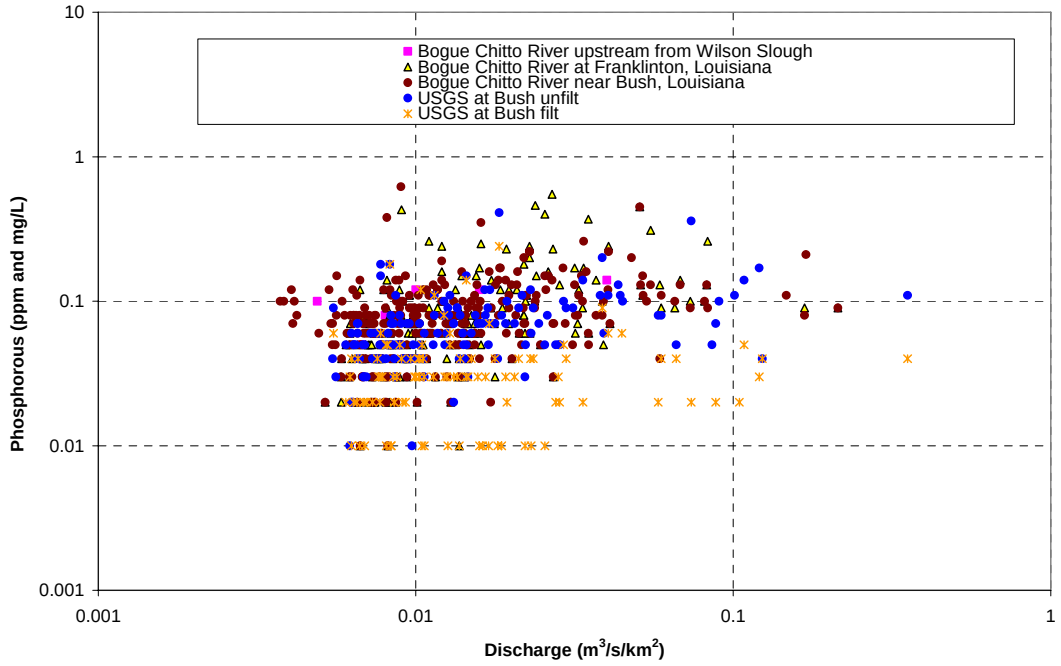

Figure A.19. Relationship between phosphorous concentration and discharge for the Bogue Chitto River

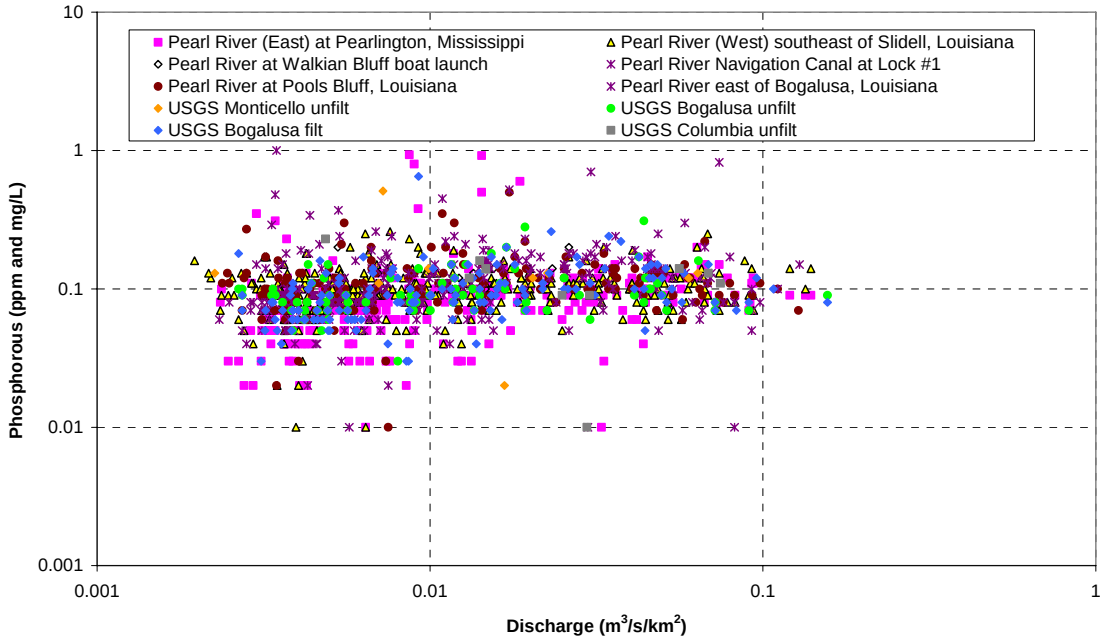

Figure A.20 Relationship between phosphorous concentration and discharge for the Pearl River.

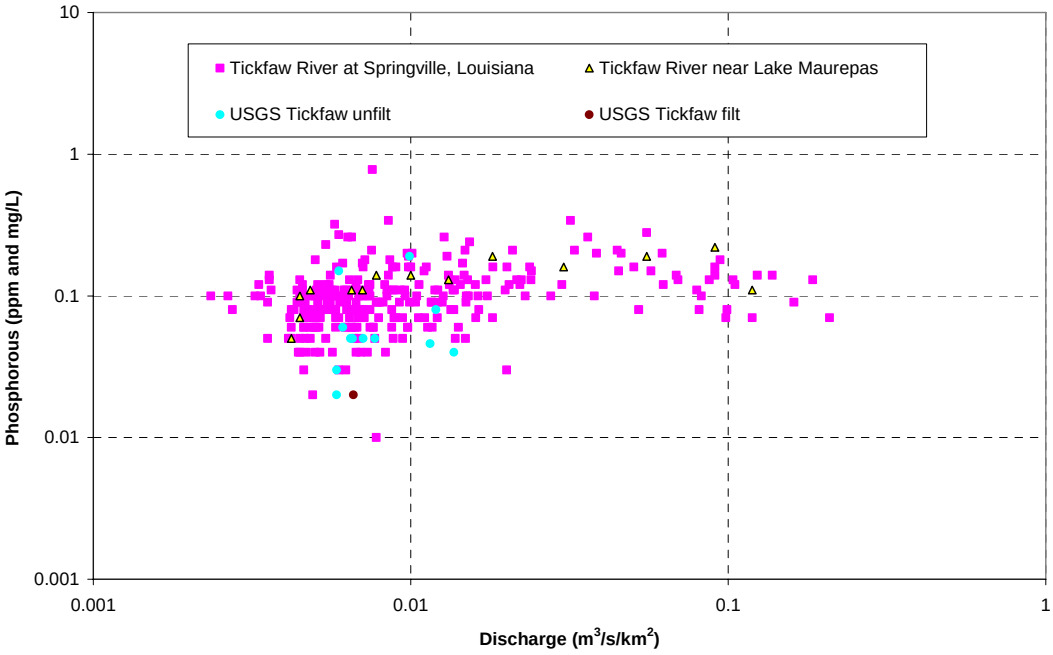

Figure A.21 Relationship between phosphorous concentration and discharge for the Tickfaw River.

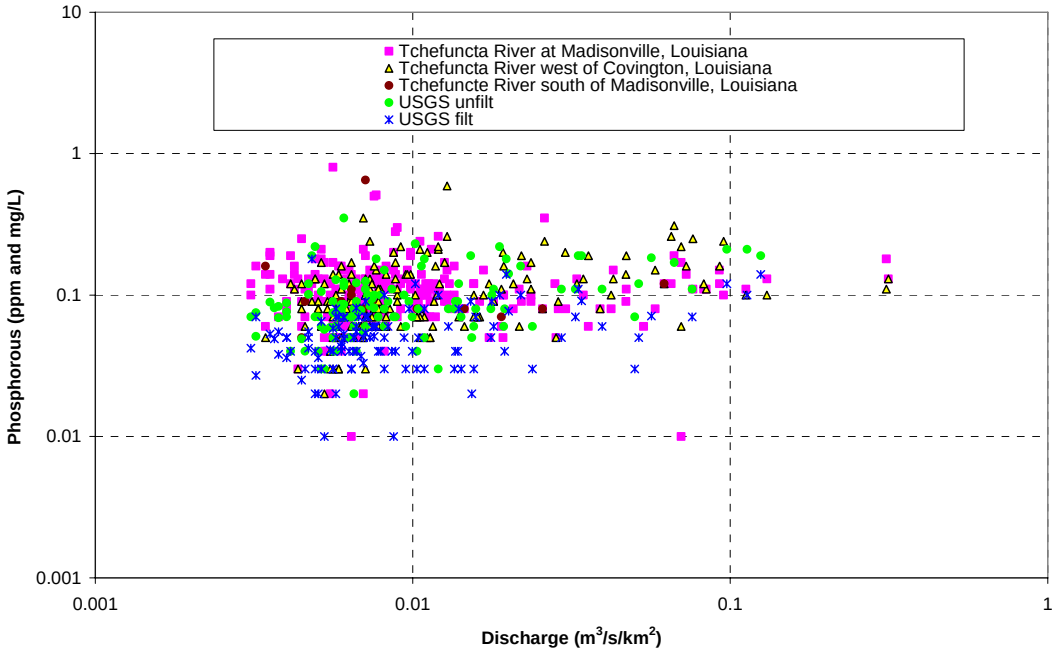

Figure A.22 Relationship between phosphorous concentration and discharge for the Tchefuncte River.

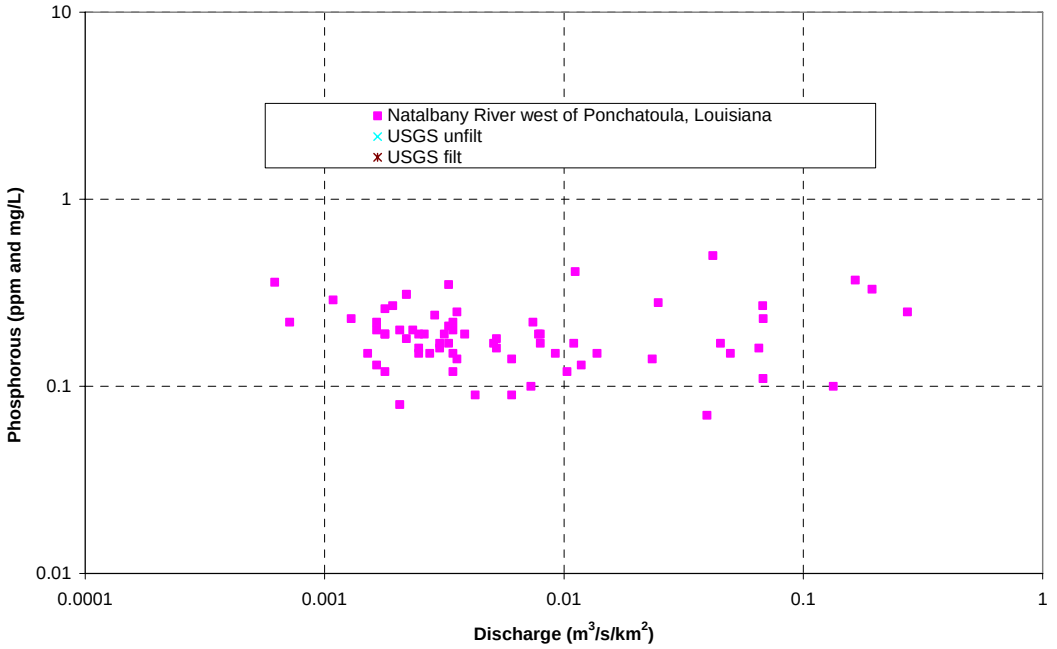

Figure A.23 Relationship between phosphorous concentration and discharge for the Natalbany River.

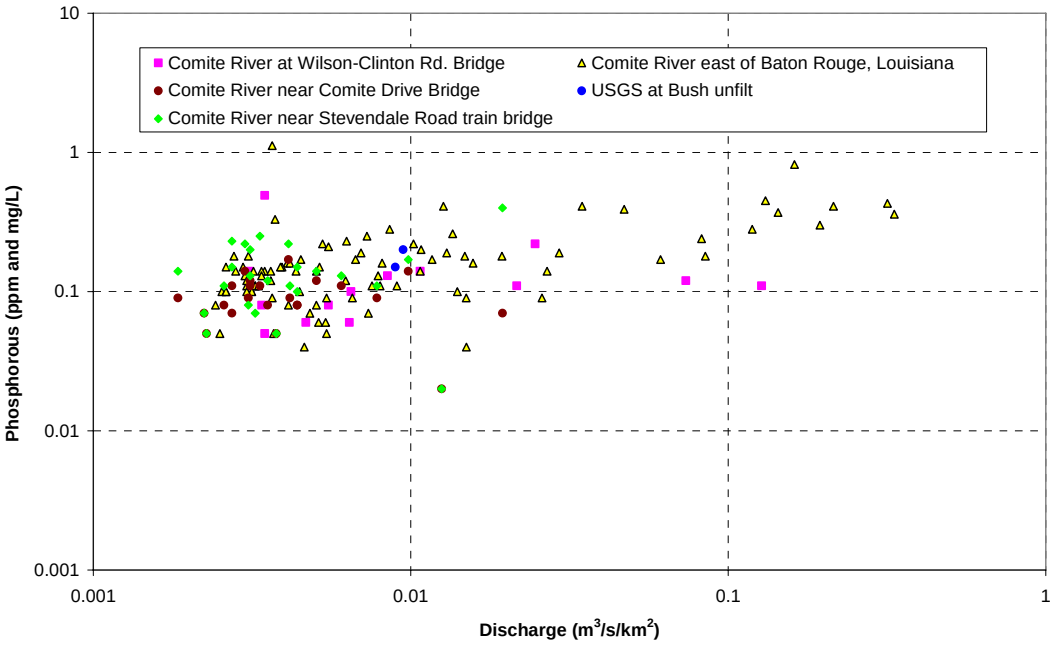

Figure A.24 Relationship between phosphorous concentration and discharge for the Comite River.

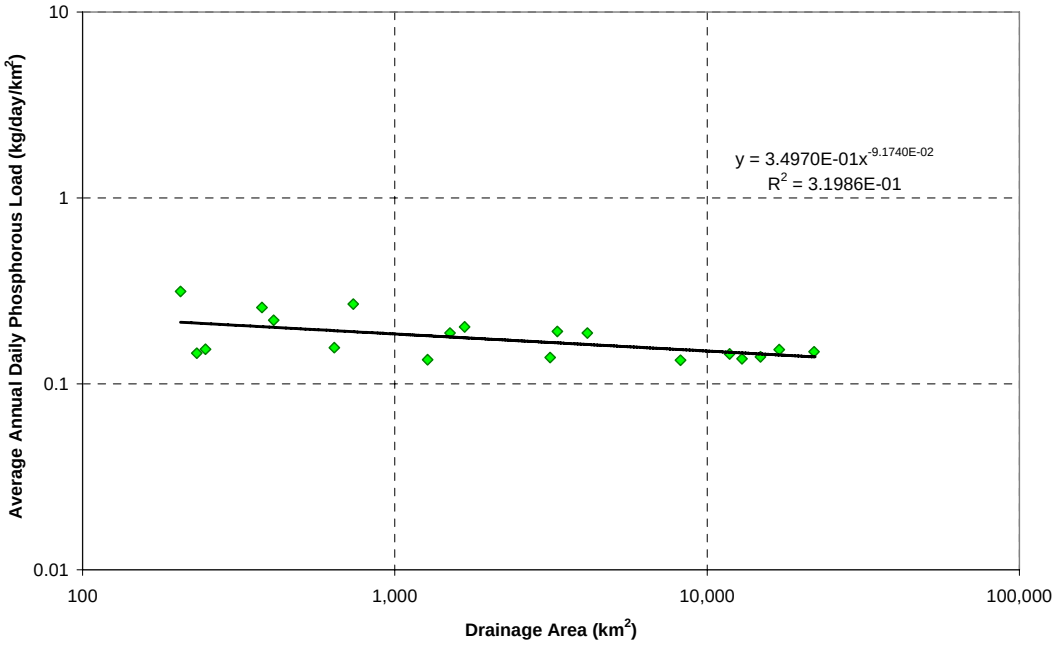

Figure A.25 Relationship between long-term daily phosphorous load and drainage area.

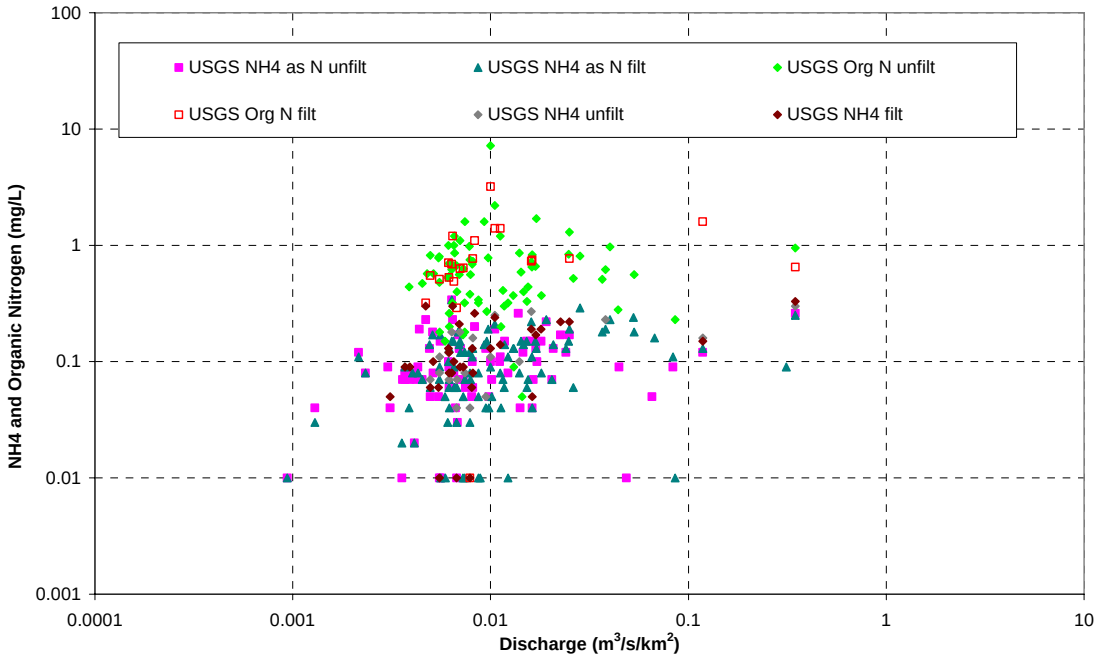

Figure A.26. Relationship between ammonia and organic nitrogen concentration and discharge for the Amite River.

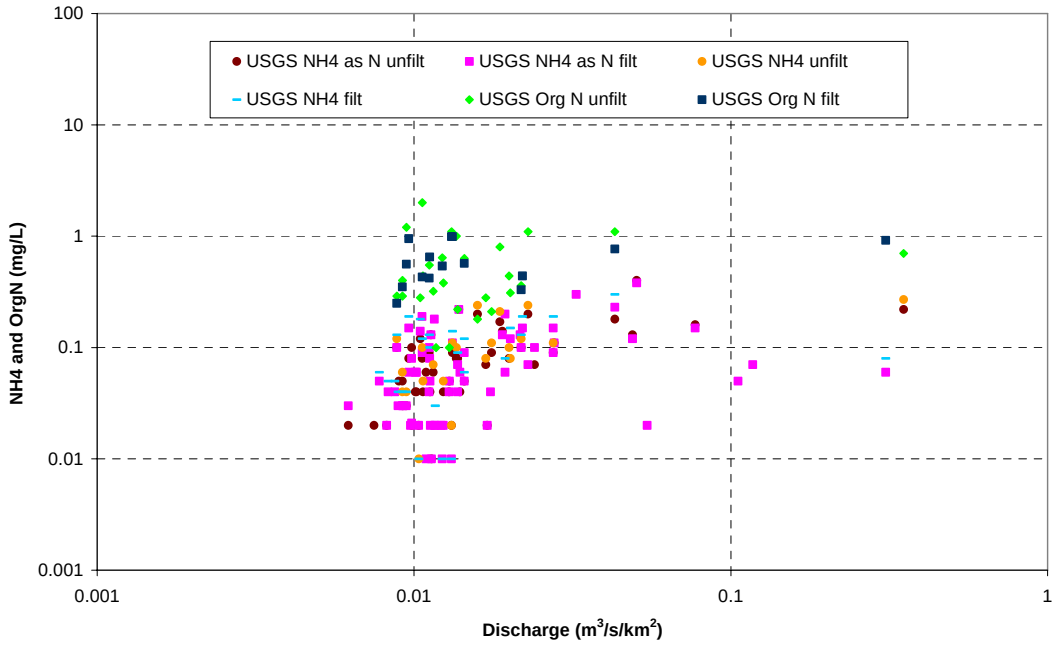

Figure A.27 Relationship between ammonia and organic nitrogen concentration and discharge for the Tangipahoa River.

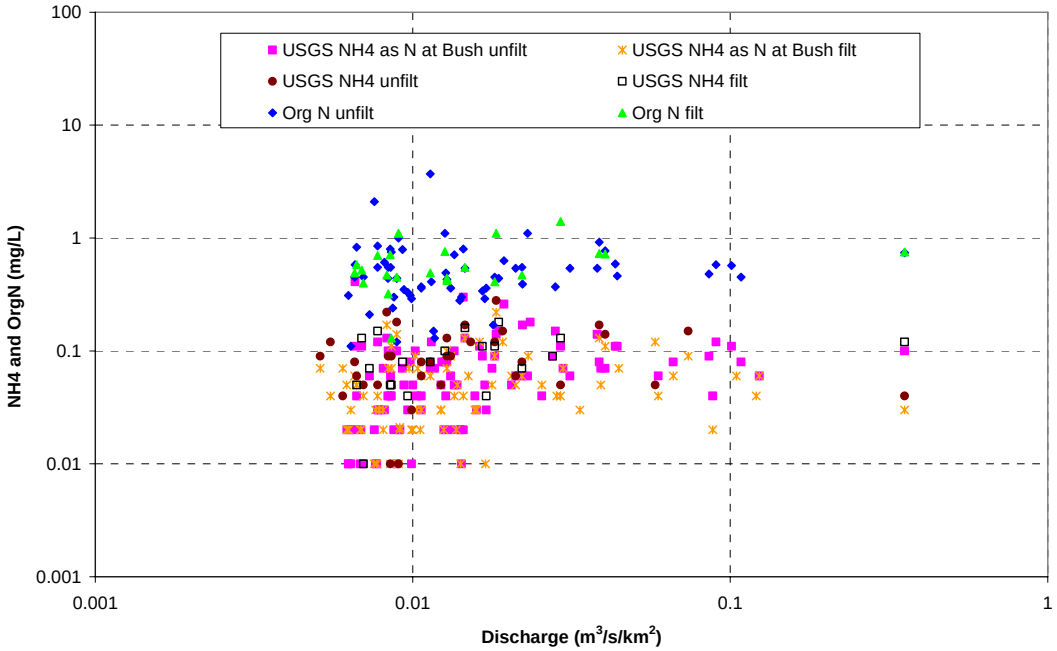

Figure A.28 Relationship between ammonia and organic nitrogen concentration and discharge for the Bogue Chitto River.

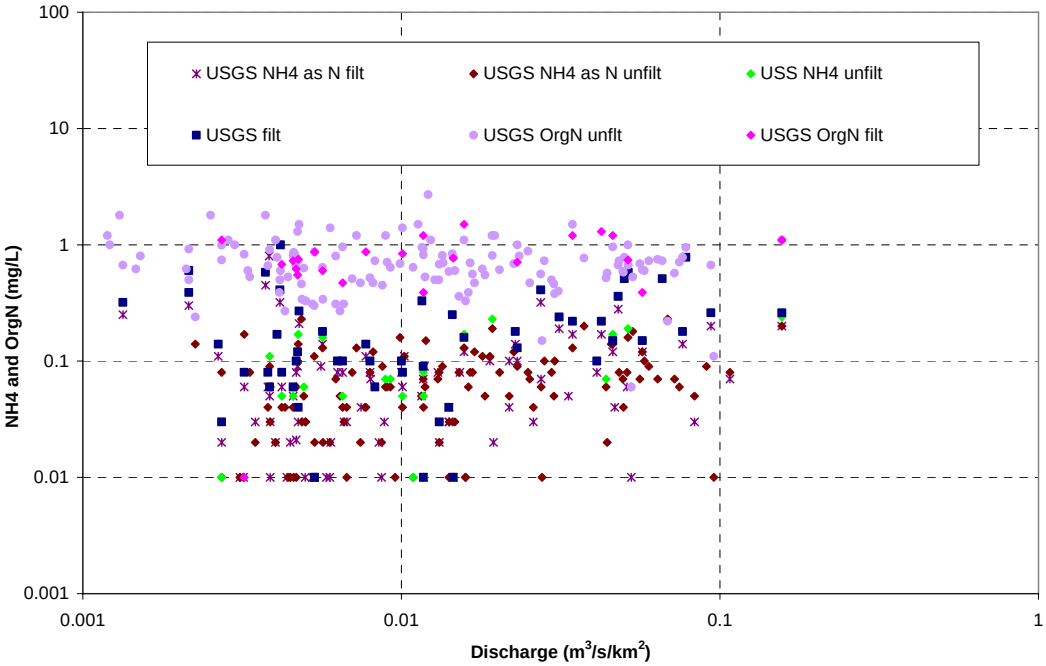

Figure A.29 Relationship between ammonia and organic nitrogen concentration and discharge for the Pearl River.

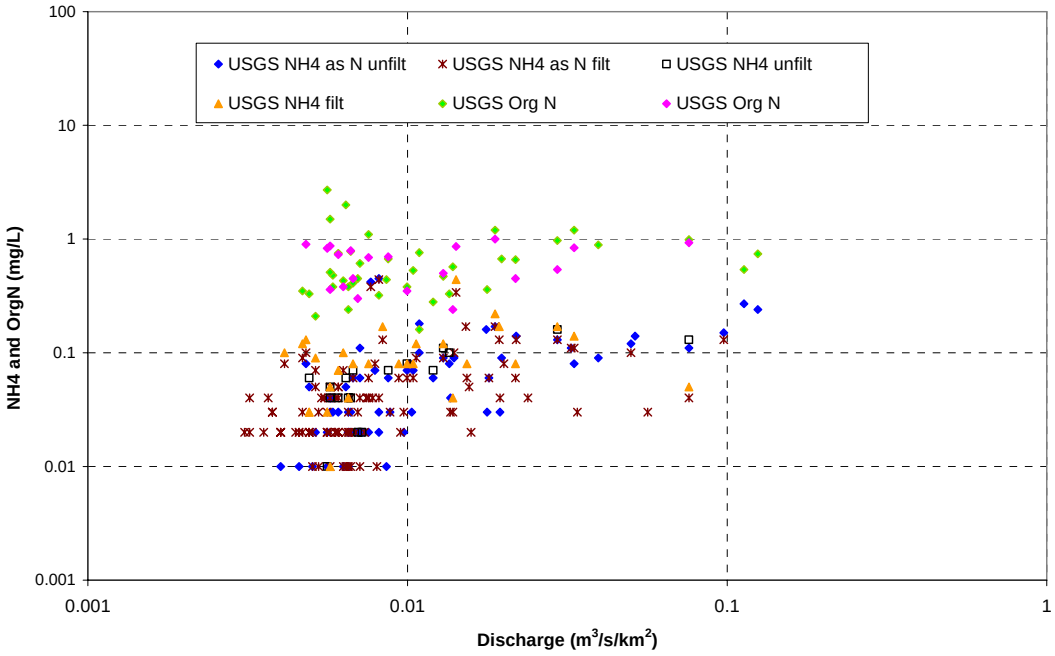

Figure A.30. Relationship between ammonia and organic nitrogen concentration and discharge for the Tchefuncte River.

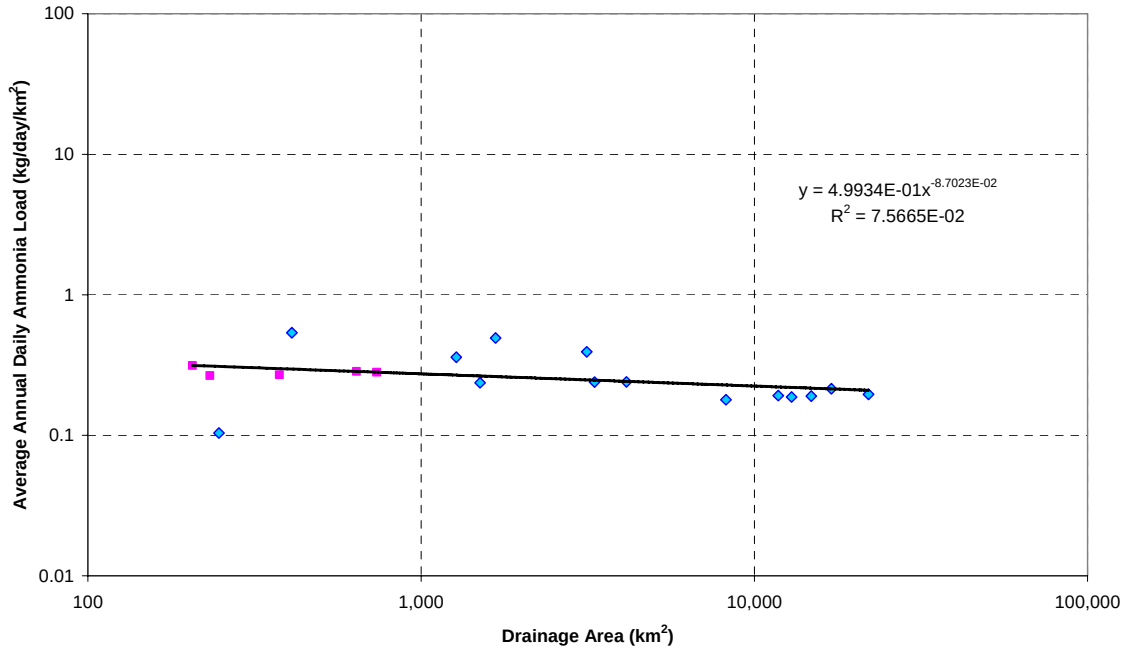

Figure A.31. Relationship between long-term daily ammonia load and drainage area.

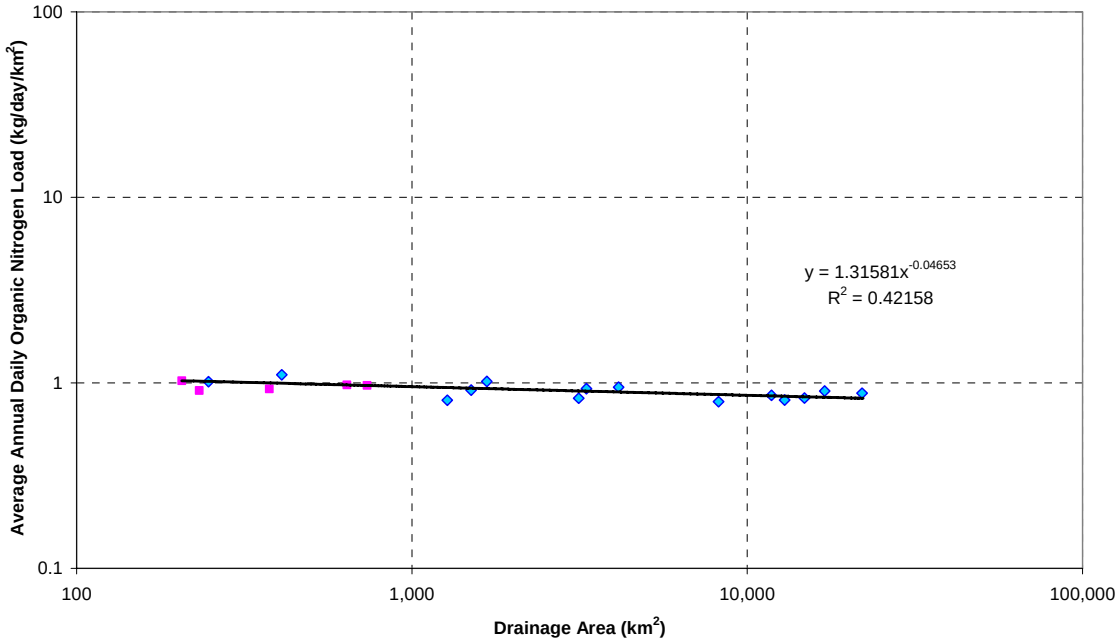

Figure A.32 Relationship between long-term daily organic nitrogen load and drainage area.

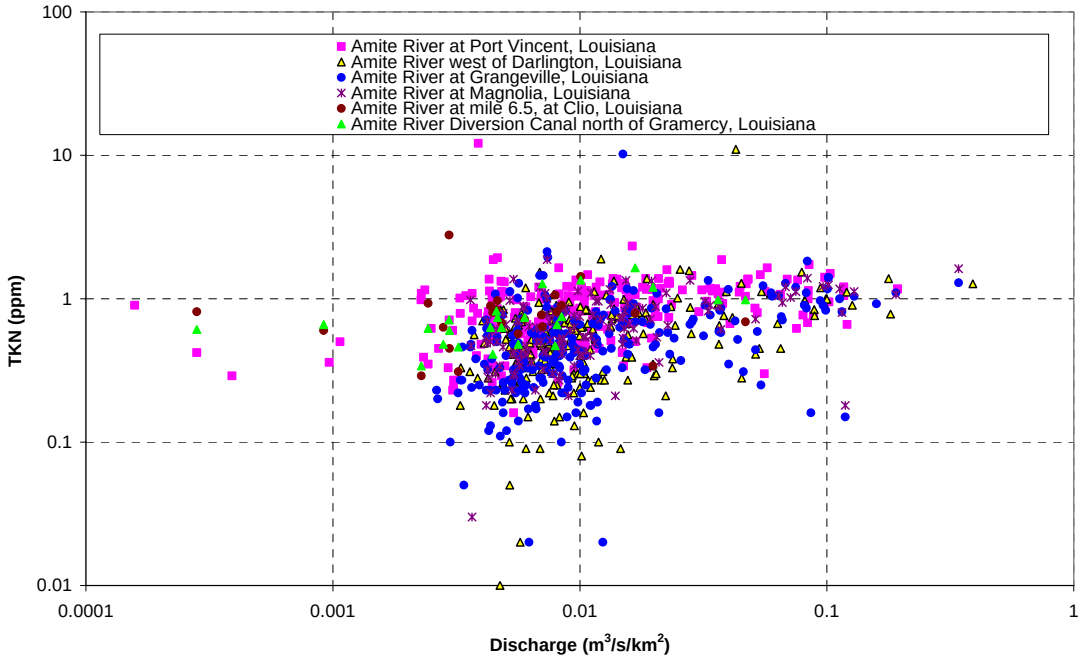

Figure A.33 Relationship between TKN concentration and discharge for the Amite River.

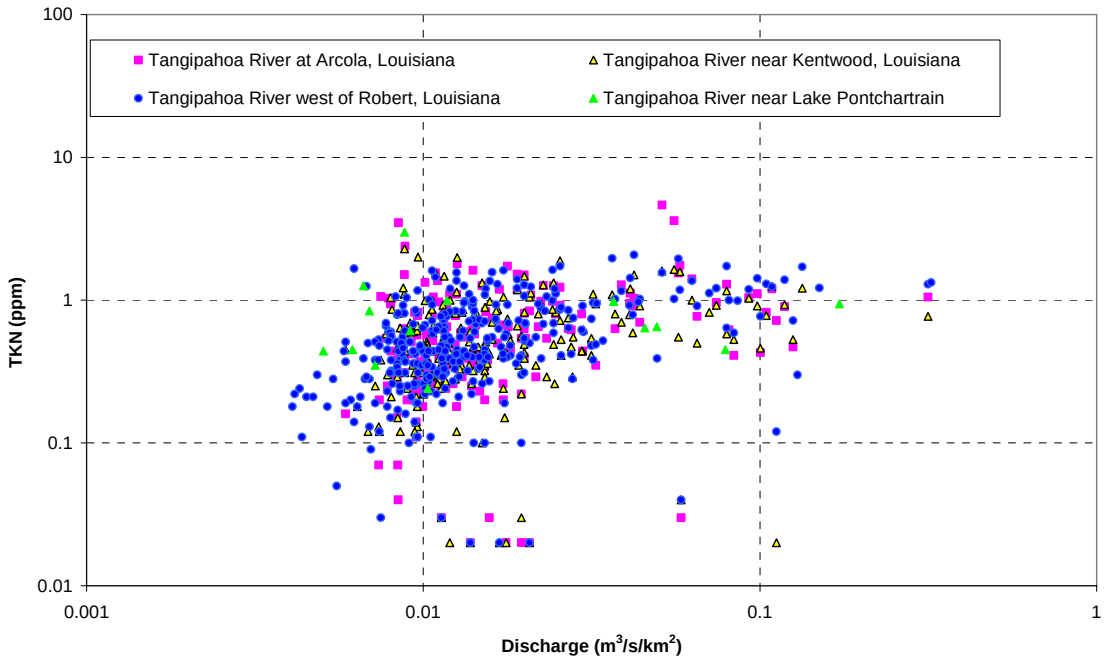

Figure A.34. Relationship between TKN concentration and discharge for the Tangipahoa River.

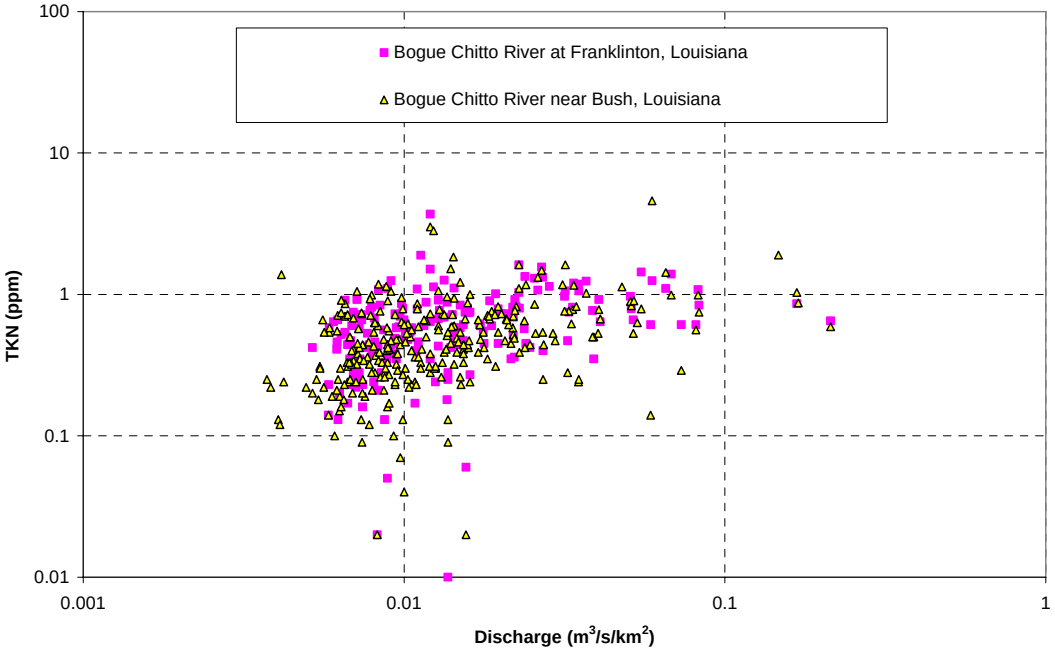

Figure A.35 Relationship between TKN concentration and discharge for the Bogue Chitto River.

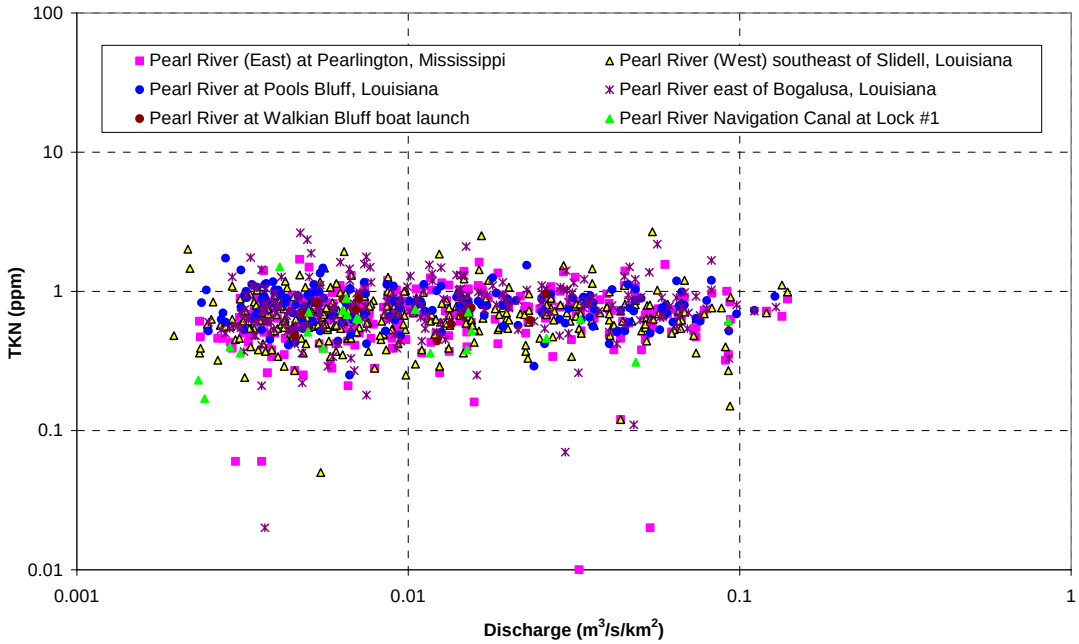

Figure A.36. Relationship TKN concentration and discharge for the Pearl River.

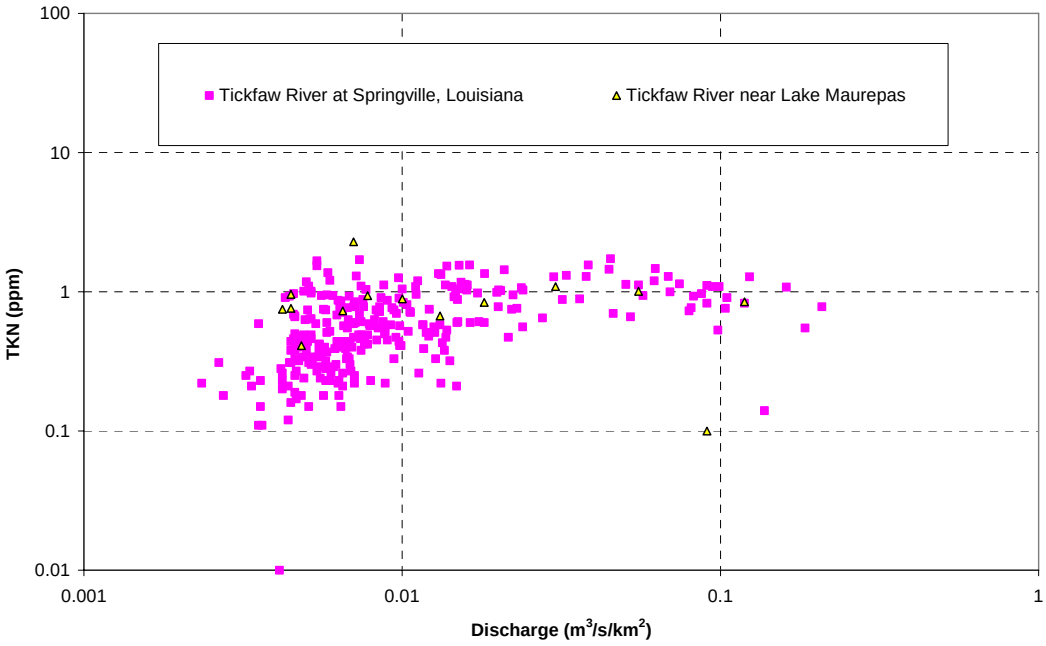

Figure A.37 Relationship between TKN concentration and discharge for the Tickfaw River.

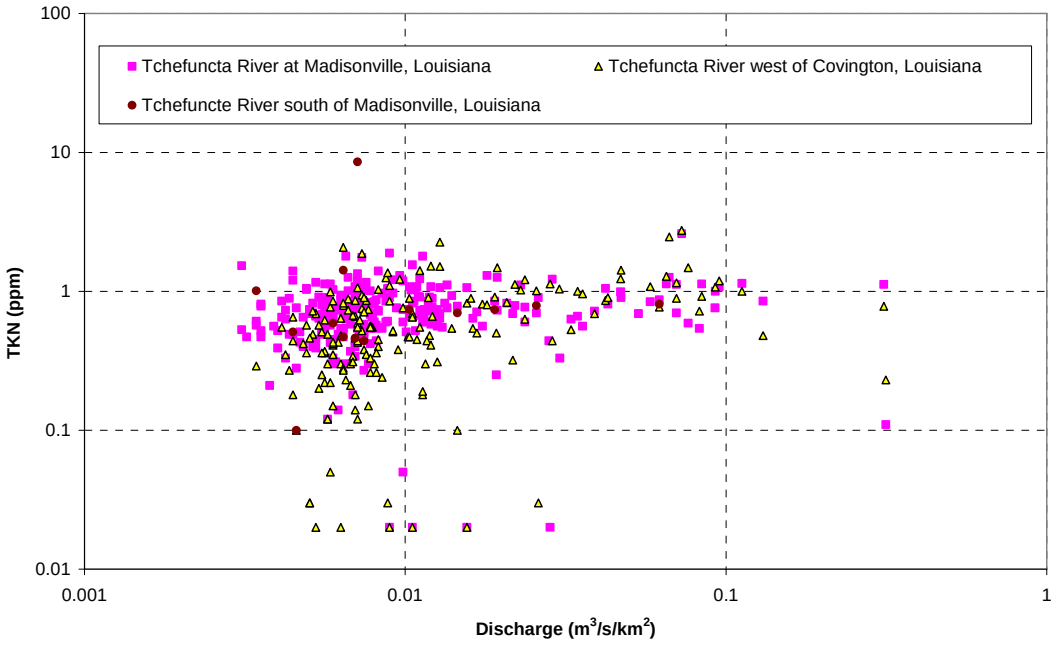

Figure A.38 Relationship between TKN concentration and discharge for the Tchefuncte River.

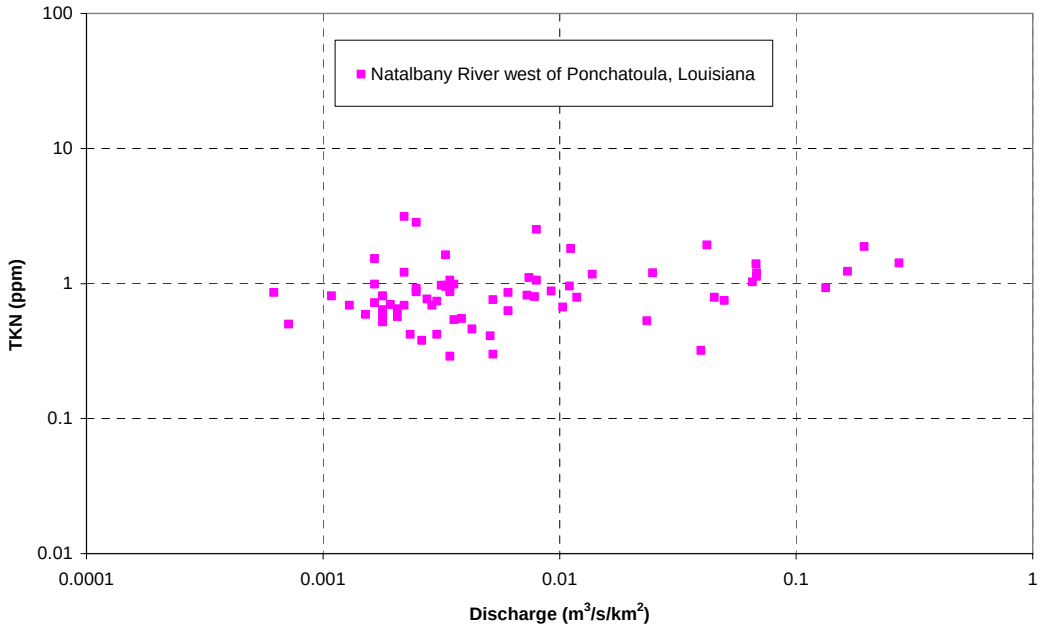

Figure A.39 Relationship between TKN concentration and discharge for the Natalbany River.

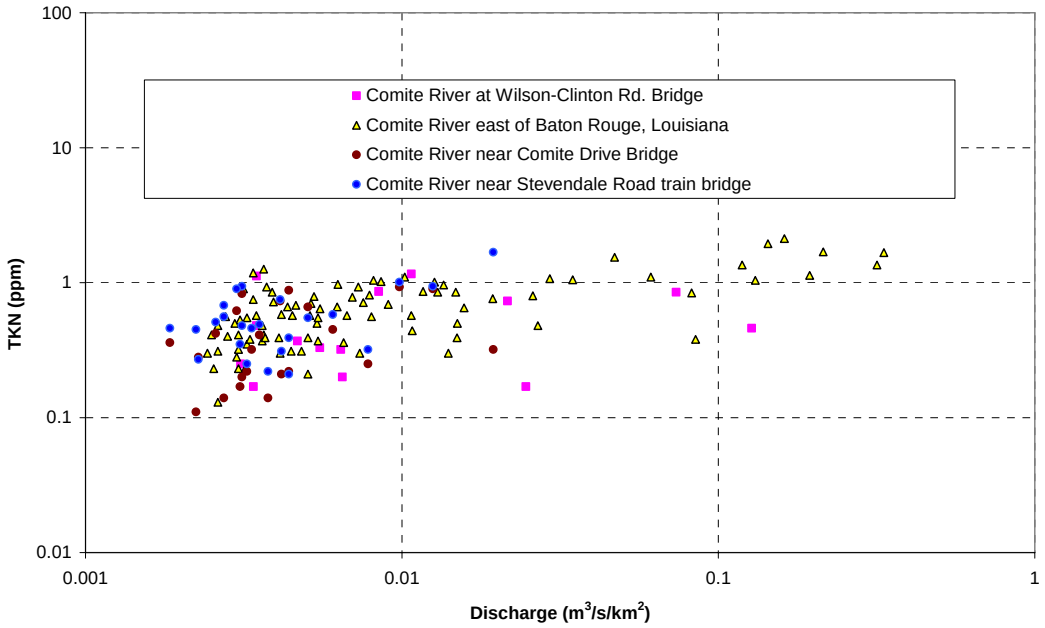

Figure A.40 Relationship between TKN concentration and discharge for the Comite River.

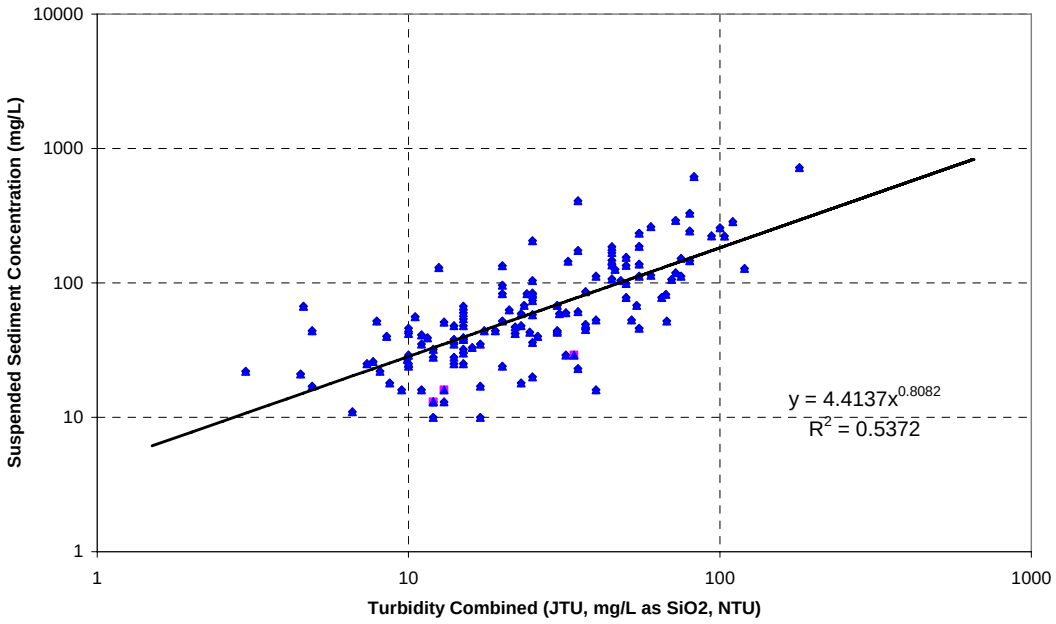

Figure A.41 Relationship between suspended sediment concentration and turbidity for the Amite River.

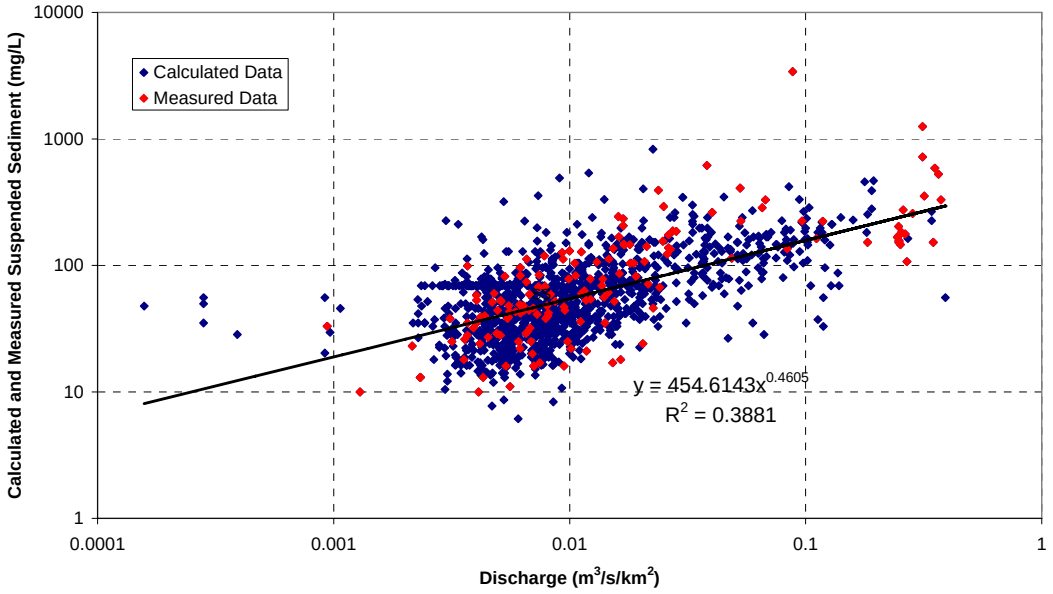

Figure A.42. Relationship between suspended sediment concentration and discharge for the Amite River.

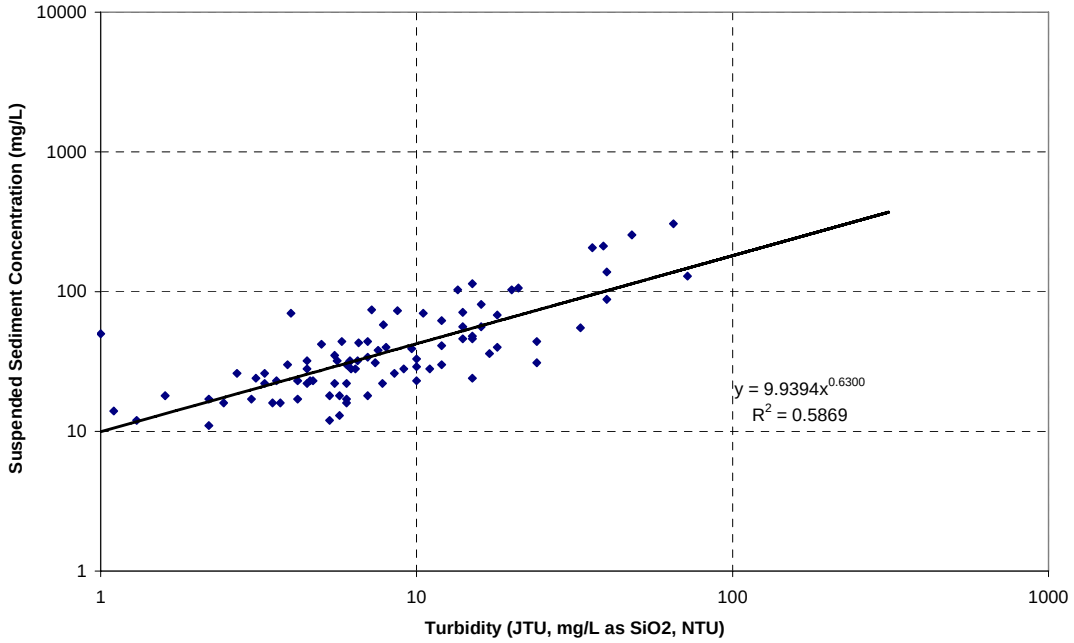

Figure A.43 Relationship between suspended sediment concentration and turbidity for the Tangipahoa River.

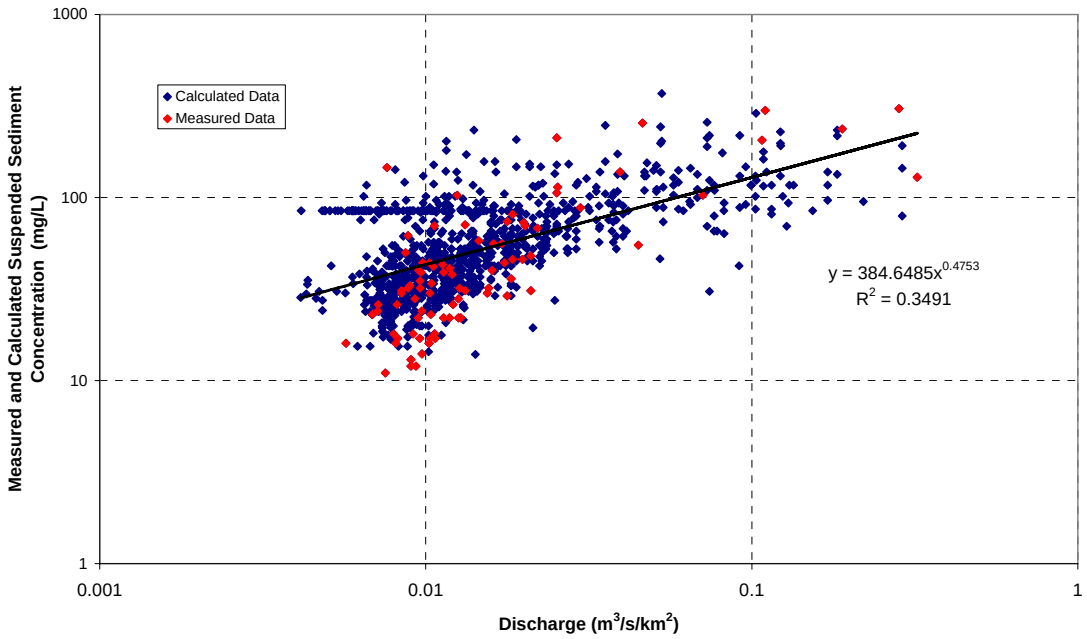

Figure A.44 Relationship between suspended sediment concentration and discharge for the Tangipahoa River.

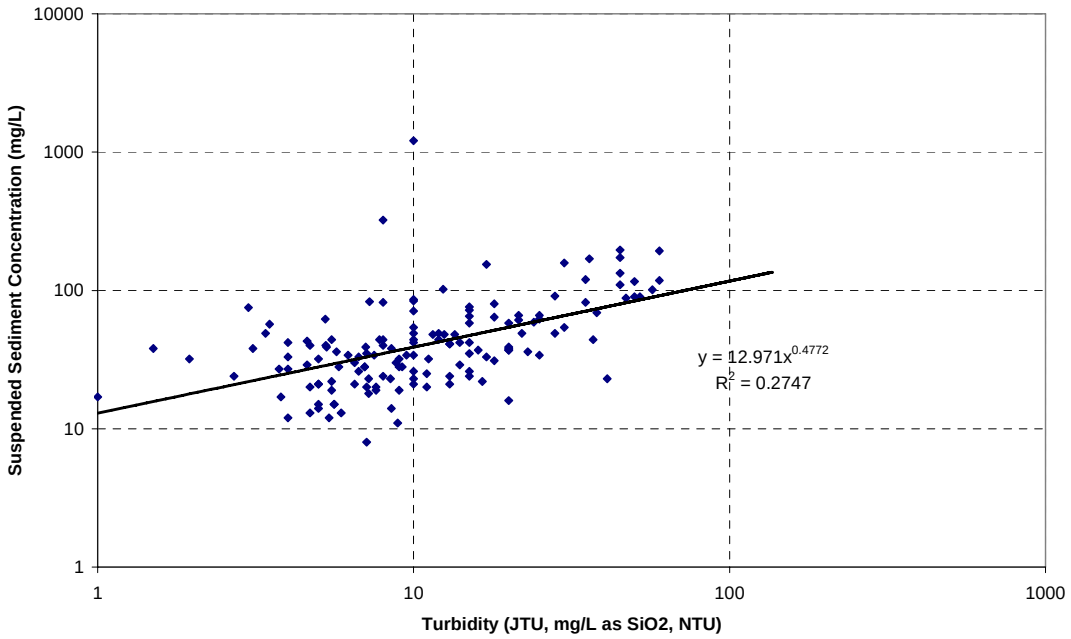

Figure A.45 Relationship between suspended sediment concentration and turbidity for the Bogue Chitto River.

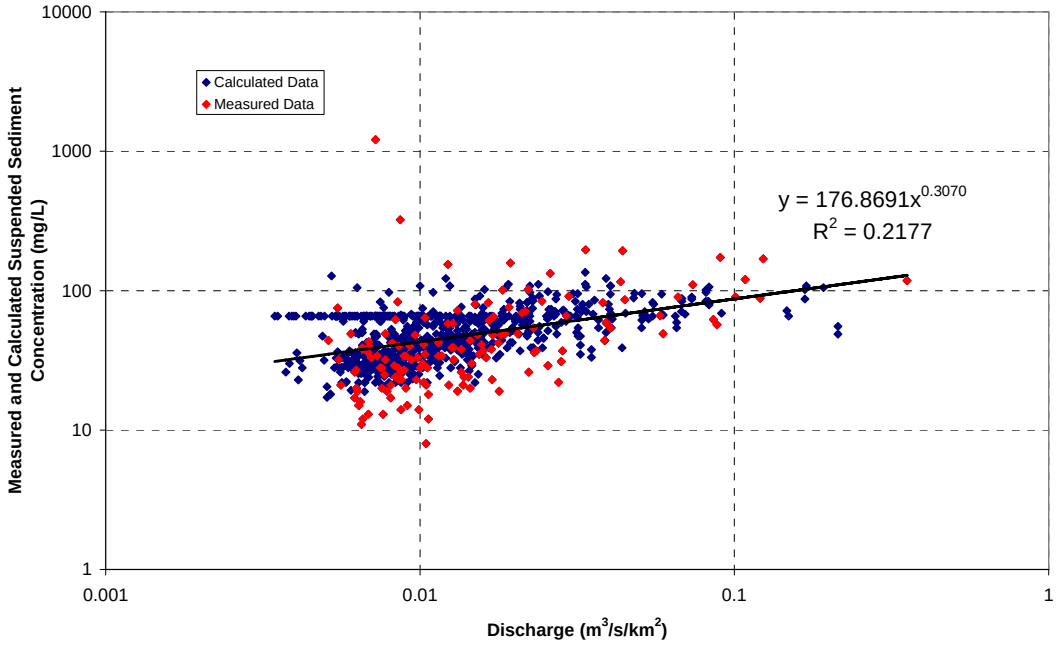

Figure A.46 Relationship between suspended sediment concentration and discharge for the Bogue Chitto River.

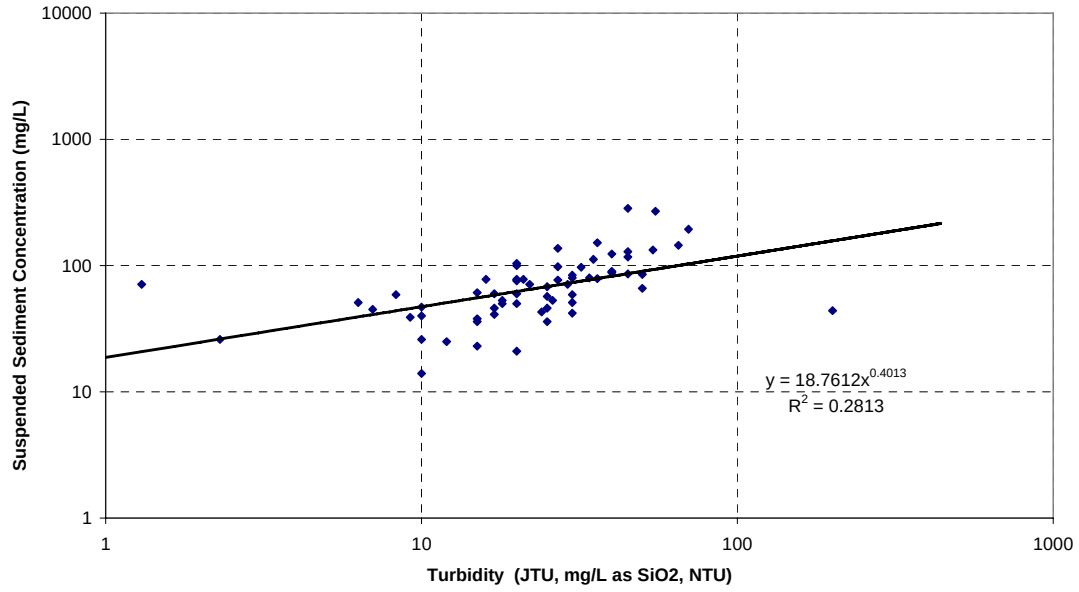

Figure A.47 Relationship between suspended sediment concentration and turbidity for the Pearl River.

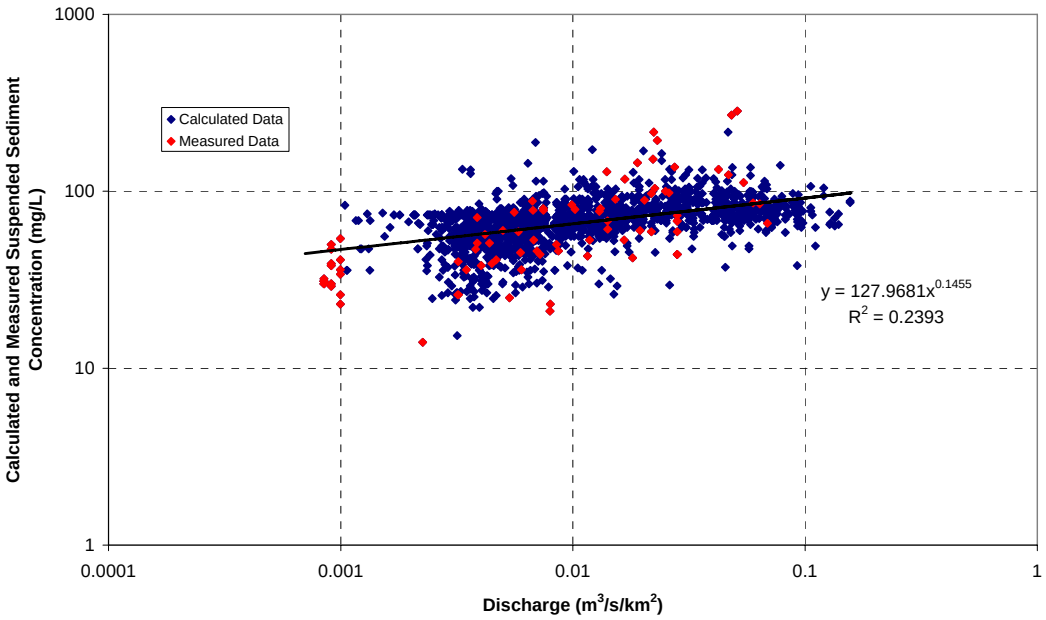

Figure A.48 Relationship between suspended sediment concentration and discharge for the Pearl River.

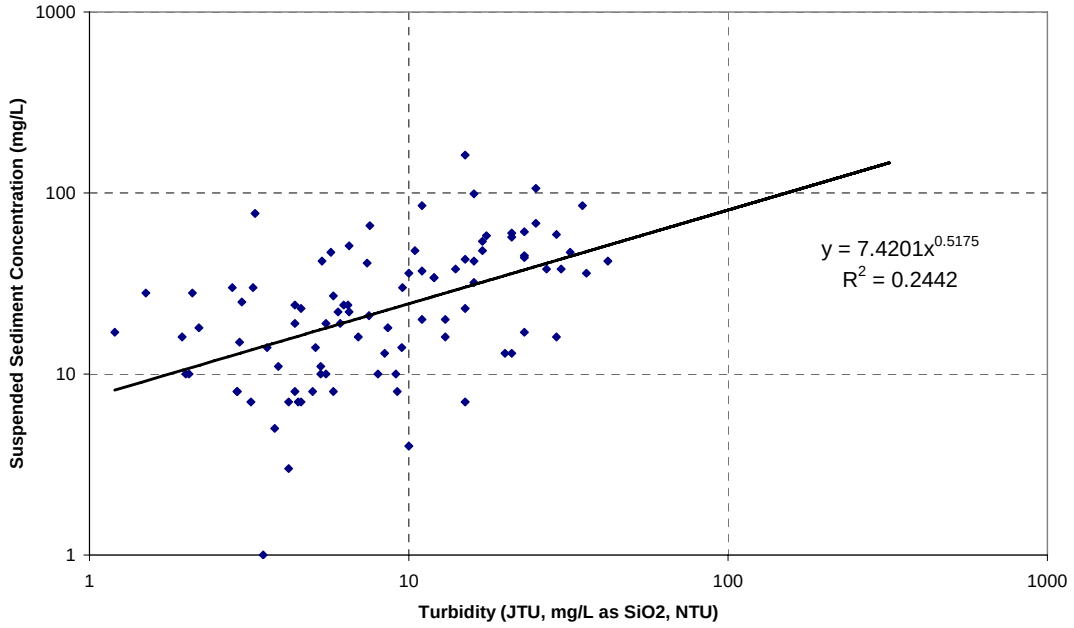

Figure A.49 Relationship between suspended sediment concentration and turbidity for the Tchefuncte River.

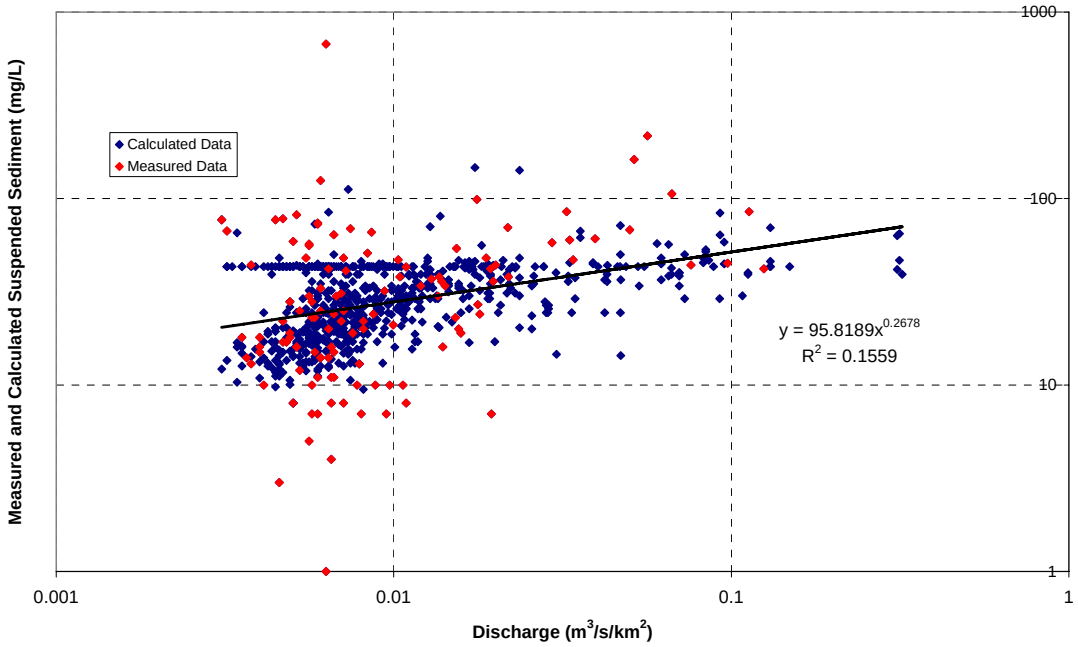

Figure A.50 Relationship between suspended sediment concentration and discharge for the Tchefuncte River.

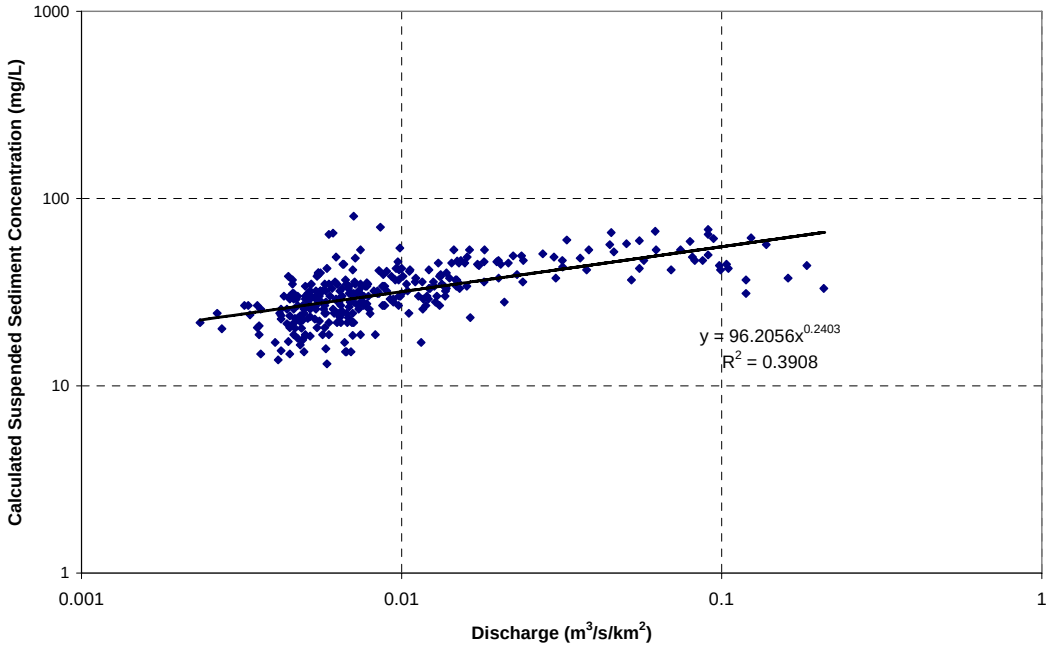

Figure A.51 Relationship between suspended sediment concentration and turbidity for the Tickfaw River.

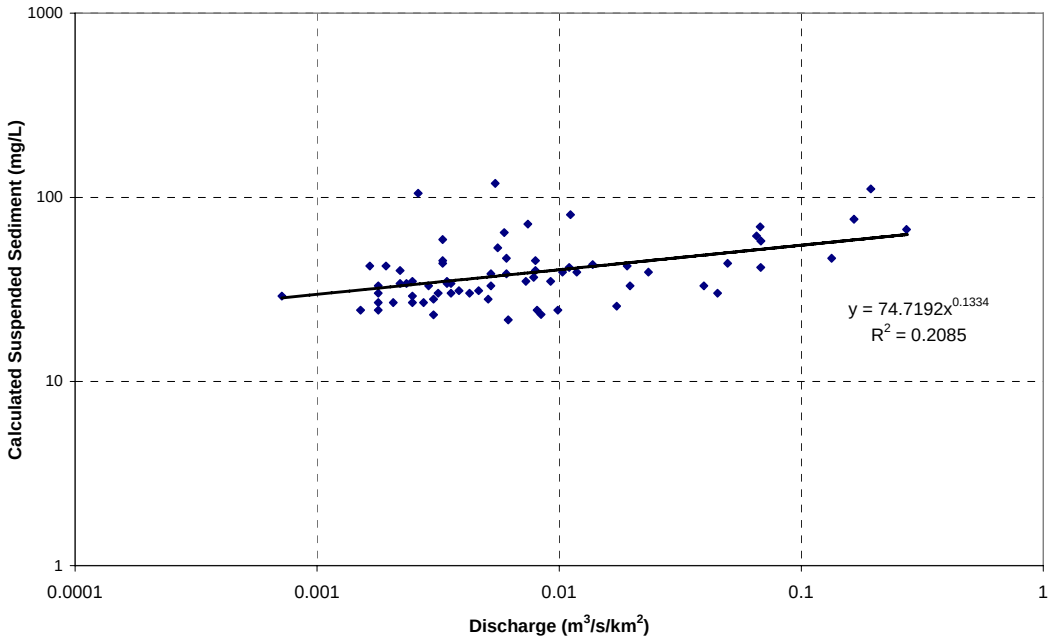

Figure A.52 Relationship between suspended sediment concentration and discharge for the Natalbany River.

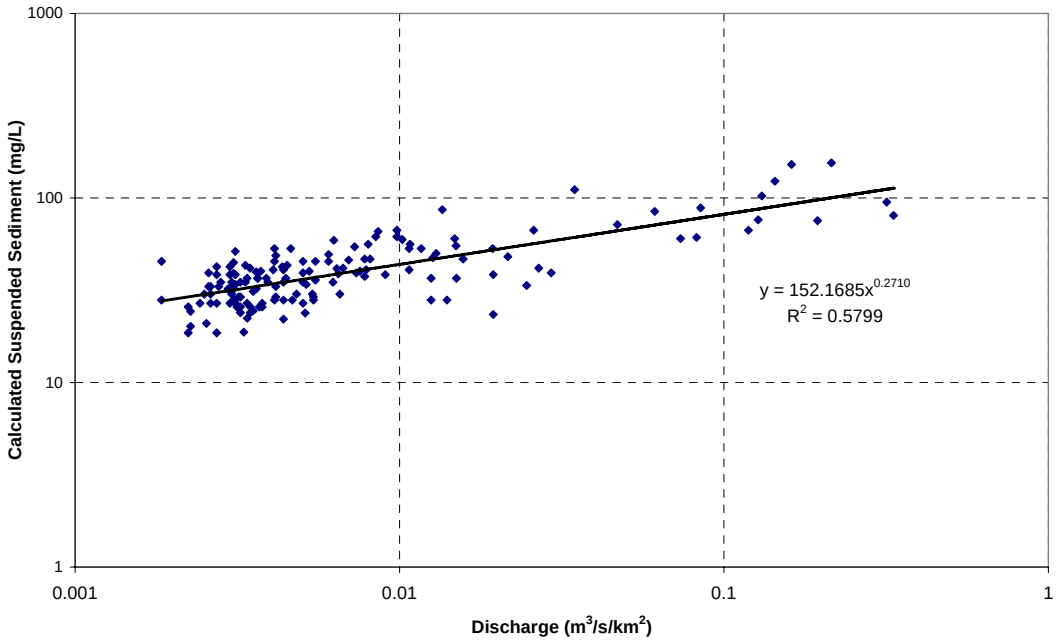

Figure A.53 Relationship between suspended sediment concentration and discharge for the Comite River.

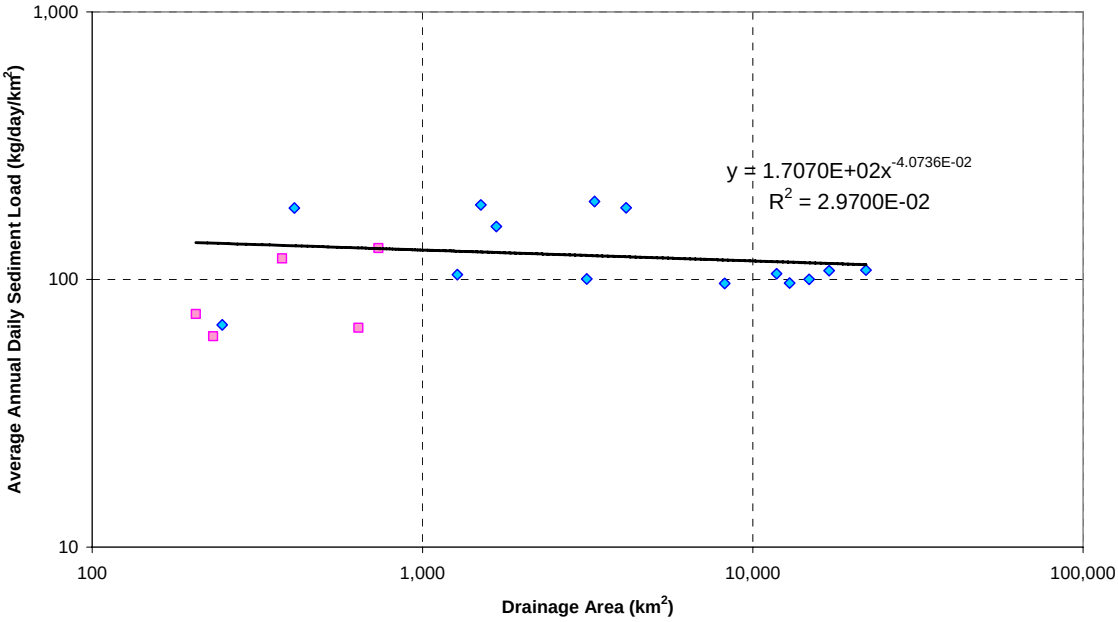

Figure A.54 Relationship between long-term daily sediment load and drainage area.

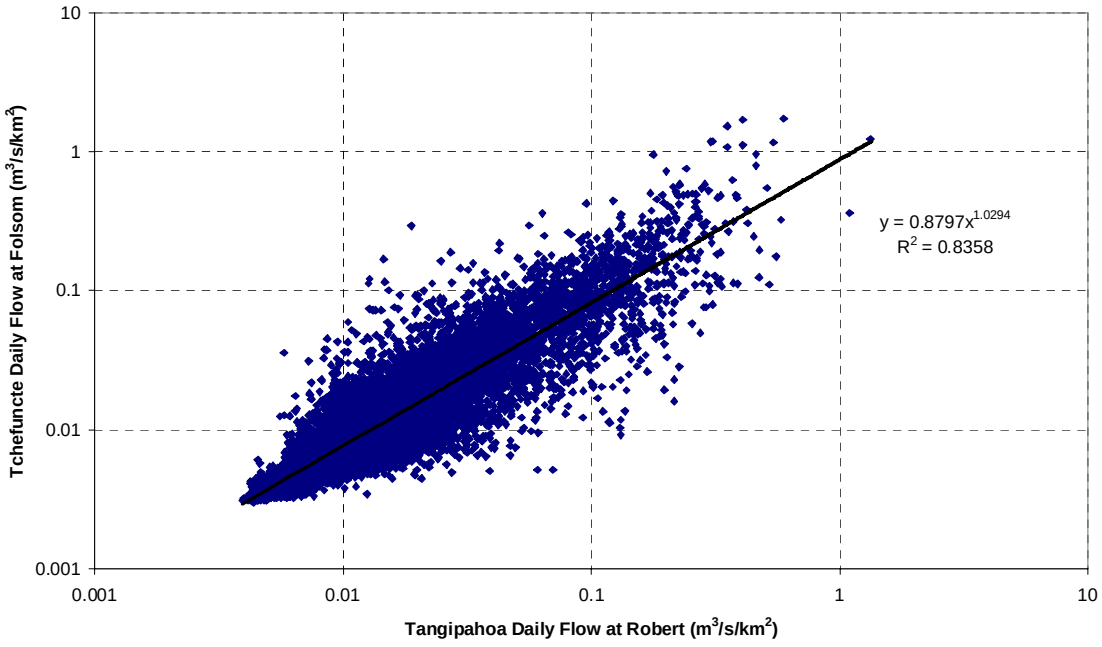

Figure A.55 Relationship between Tchefuncte River and Tangipahoa River flow.

Appendix B

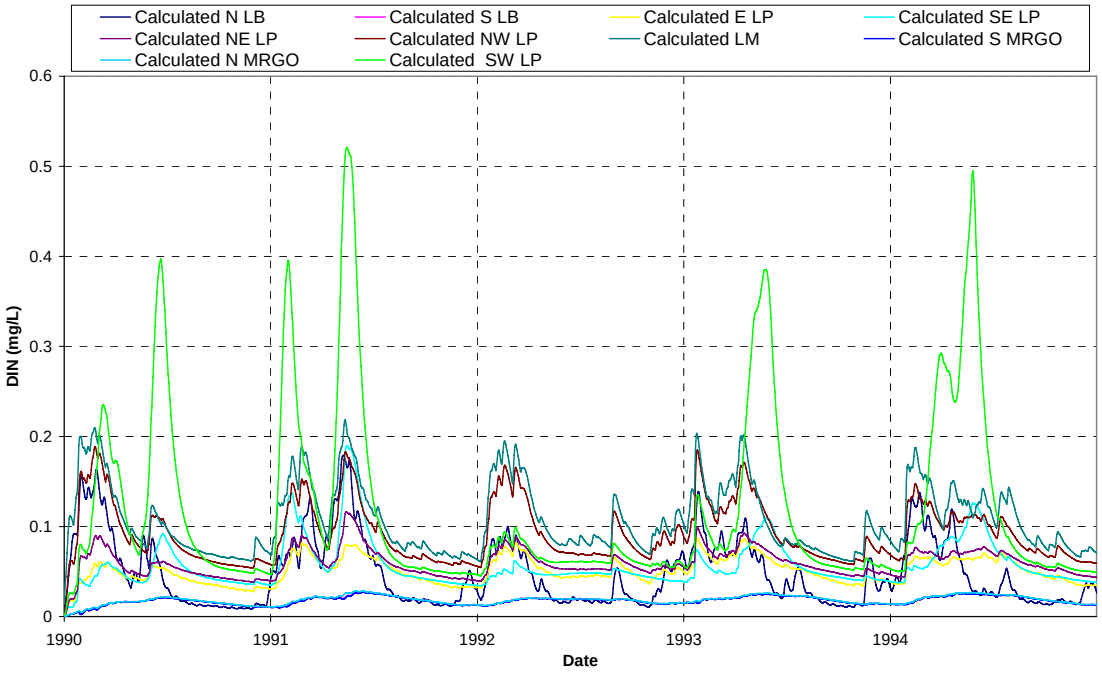

Figure B.1 Calculated DIN concentrations (1990-1995).

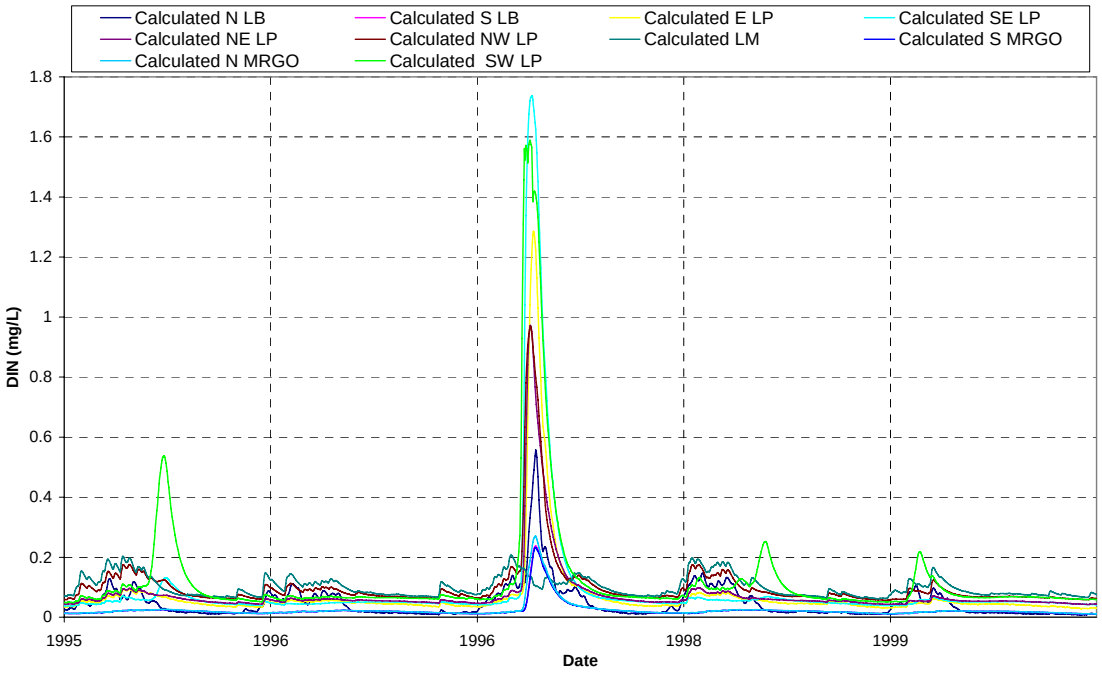

Figure B.2 Calculated DIN concentrations (1995-2000).

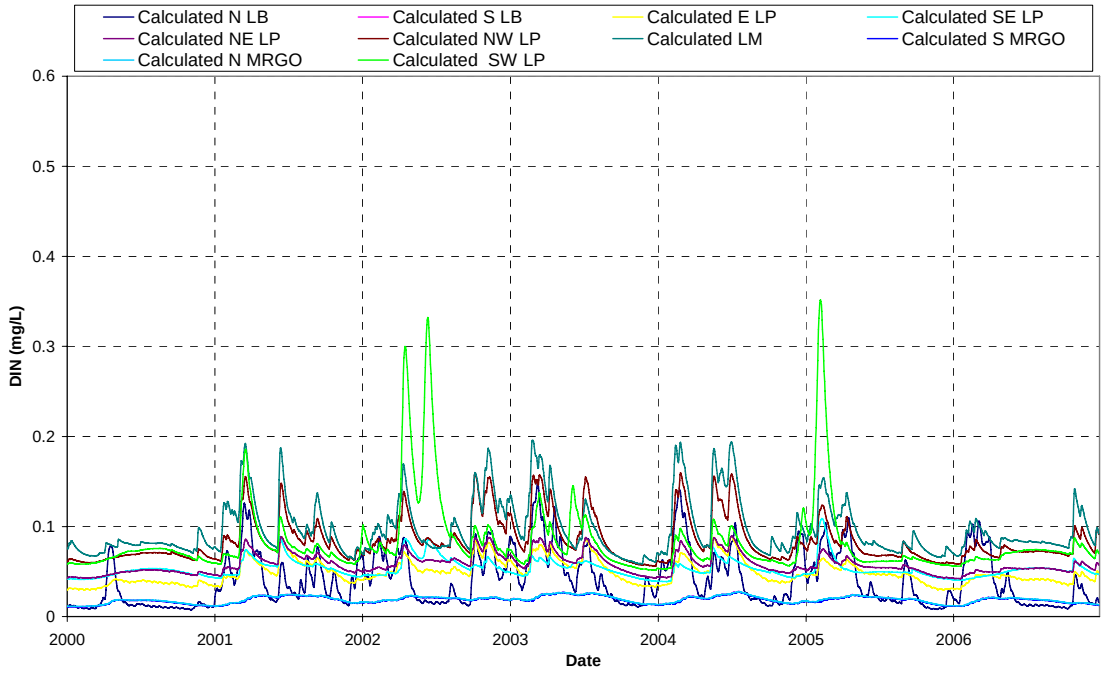

Figure B.3 Calculated DIN concentrations (2000-2006).

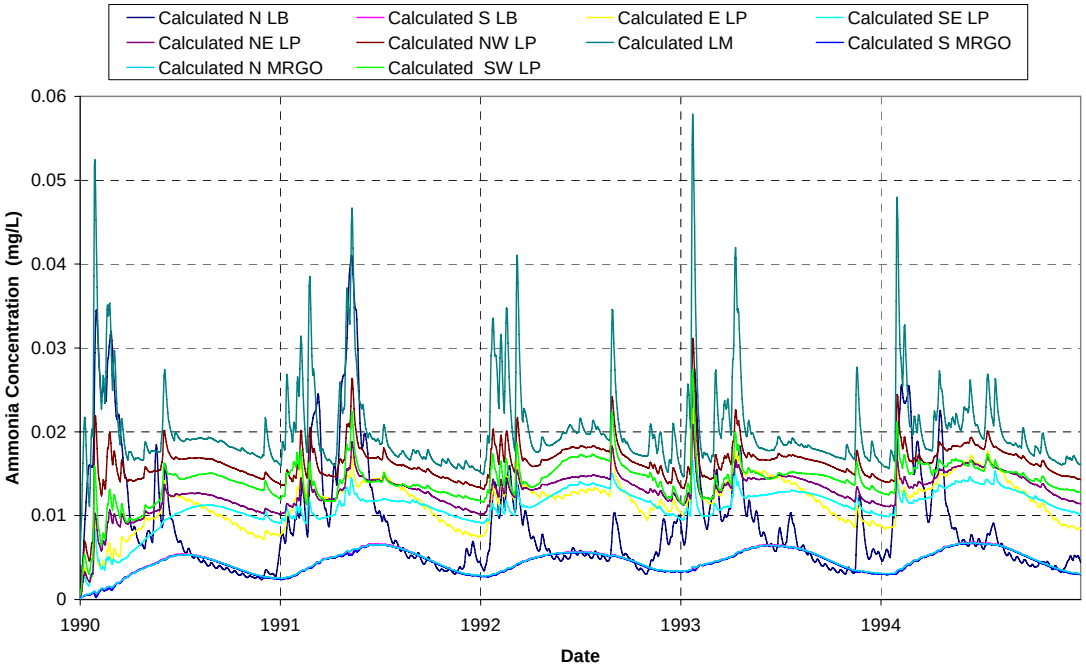

Figure B.4 Calculated ammonia concentrations (1990-1995).

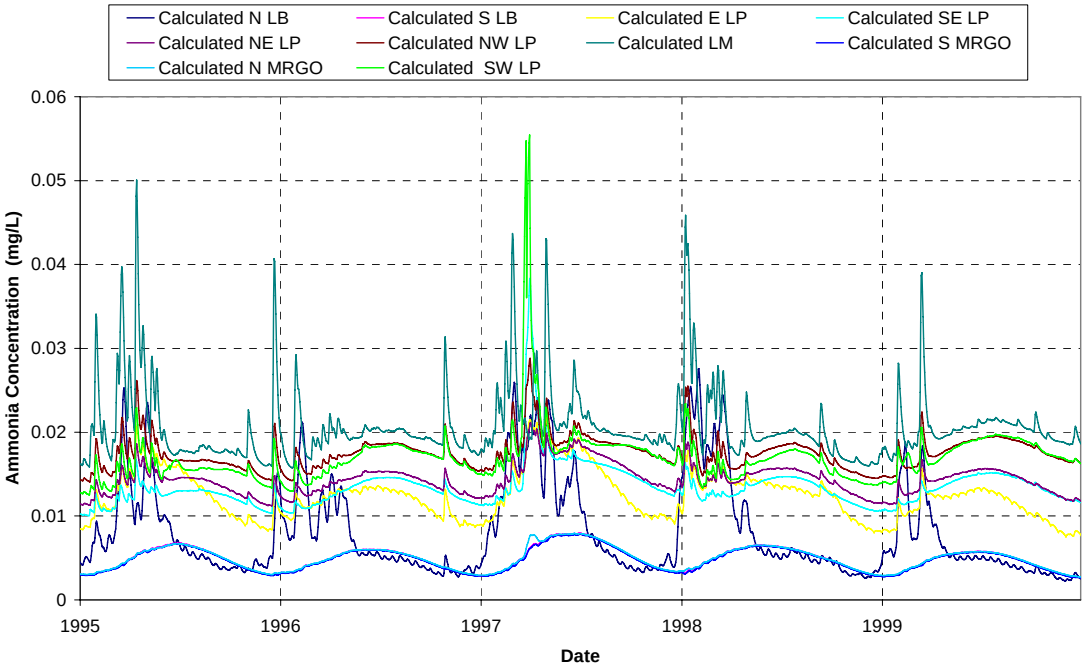

Figure B.5 Calculated ammonia concentrations (1995-2000).

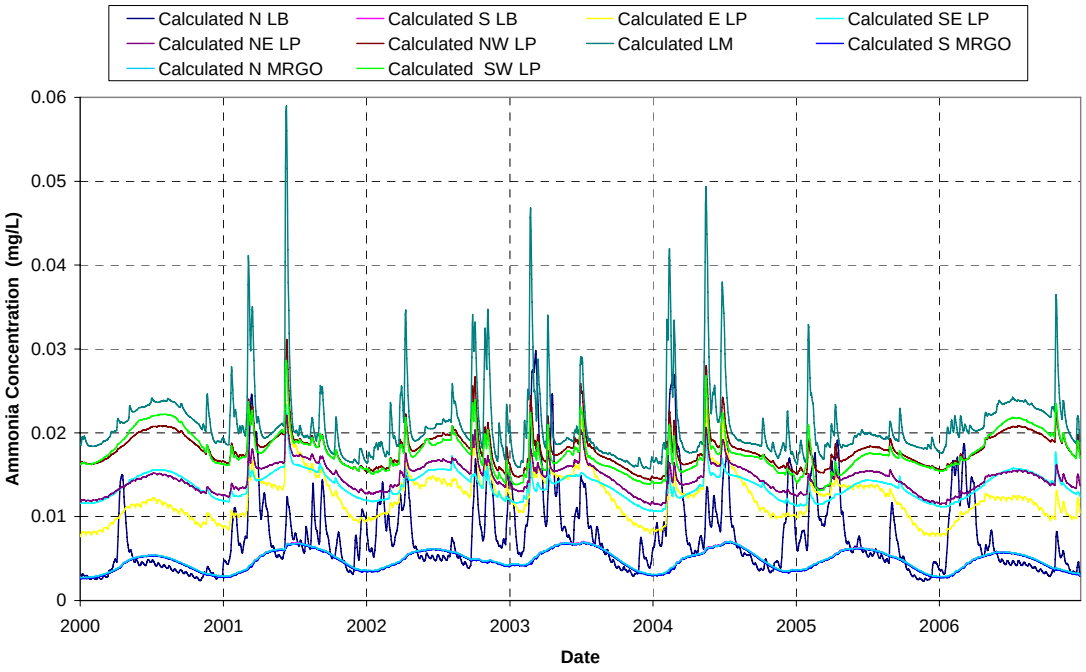

Figure B.6 Calculated ammonia concentrations (2000-2007).

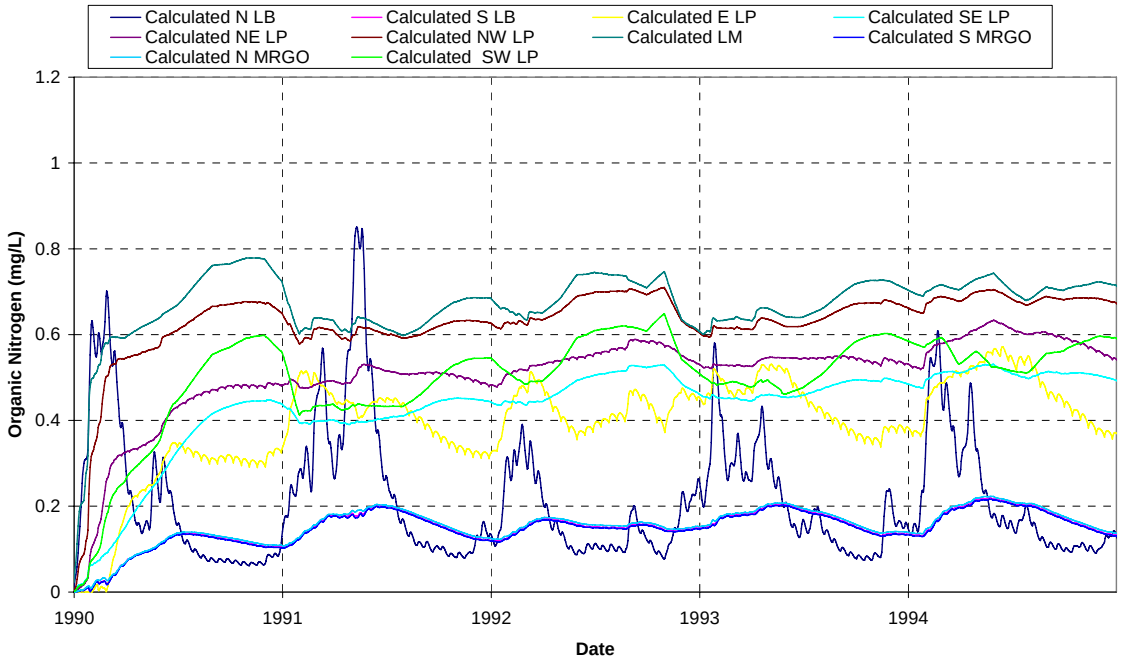

Figure B.7 Calculated organic nitrogen concentrations (1990-1995).

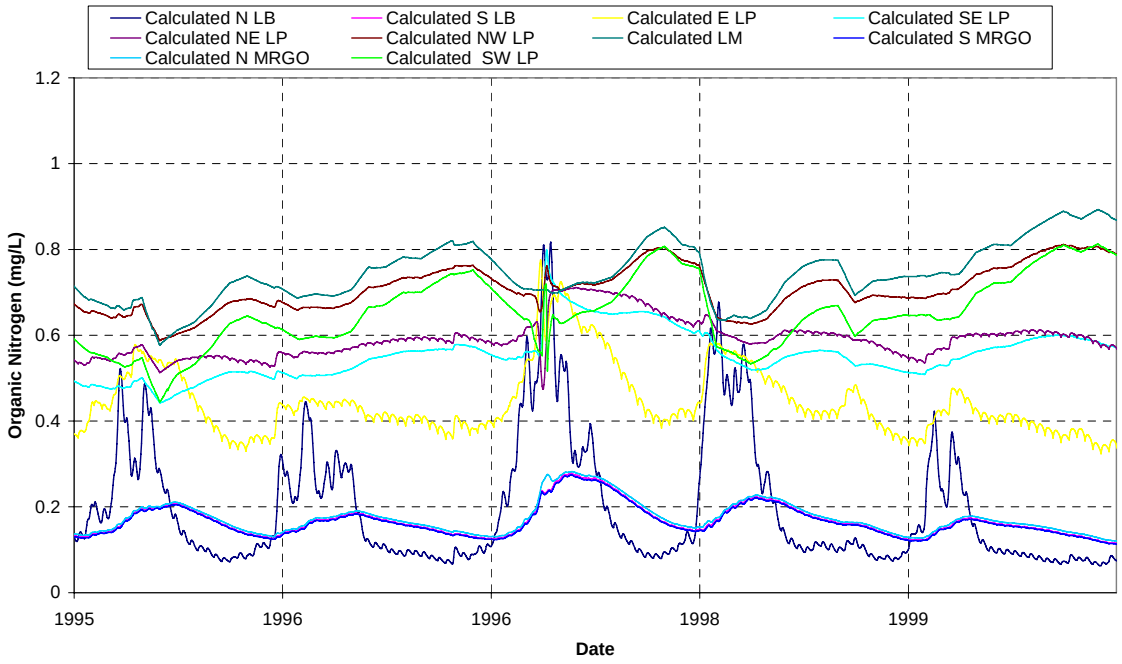

Figure B.8 Calculated organic nitrogen concentrations (1995-2000).

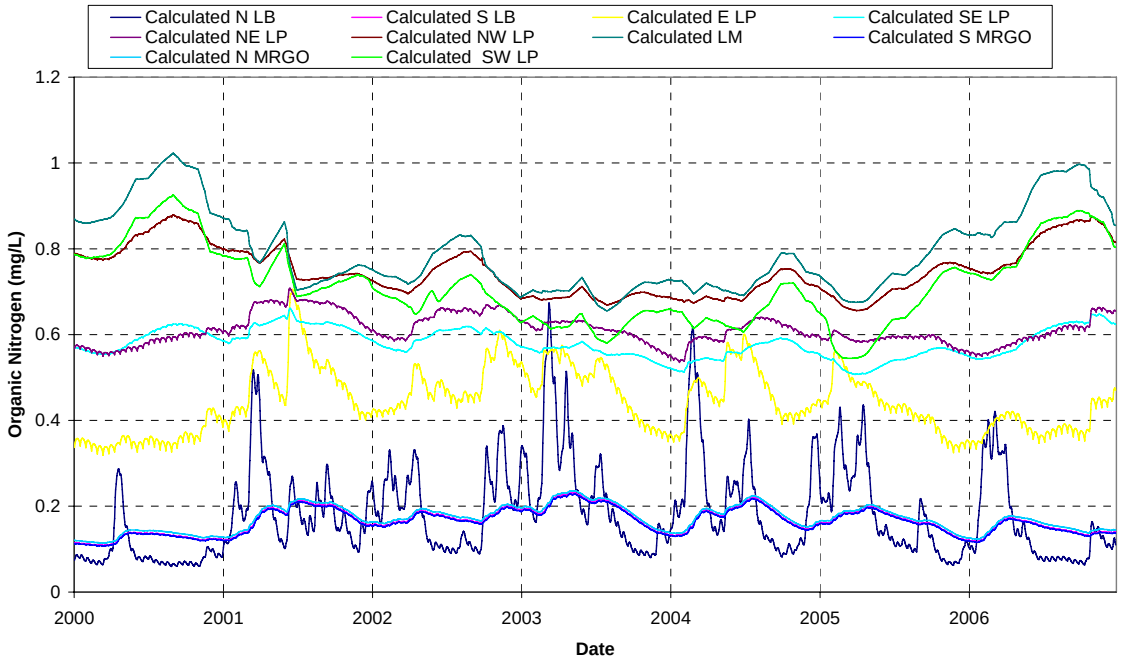

Figure B.9 Calculated organic nitrogen concentrations (2000-2007).

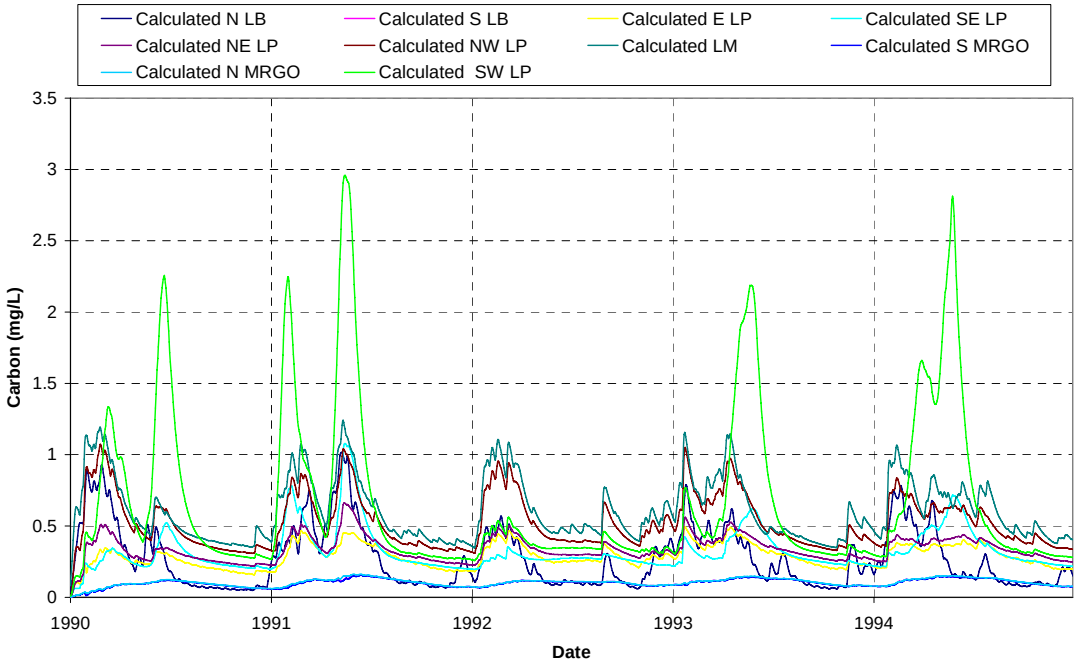

Figure B.10 Calculated carbon concentrations (1990-1995).

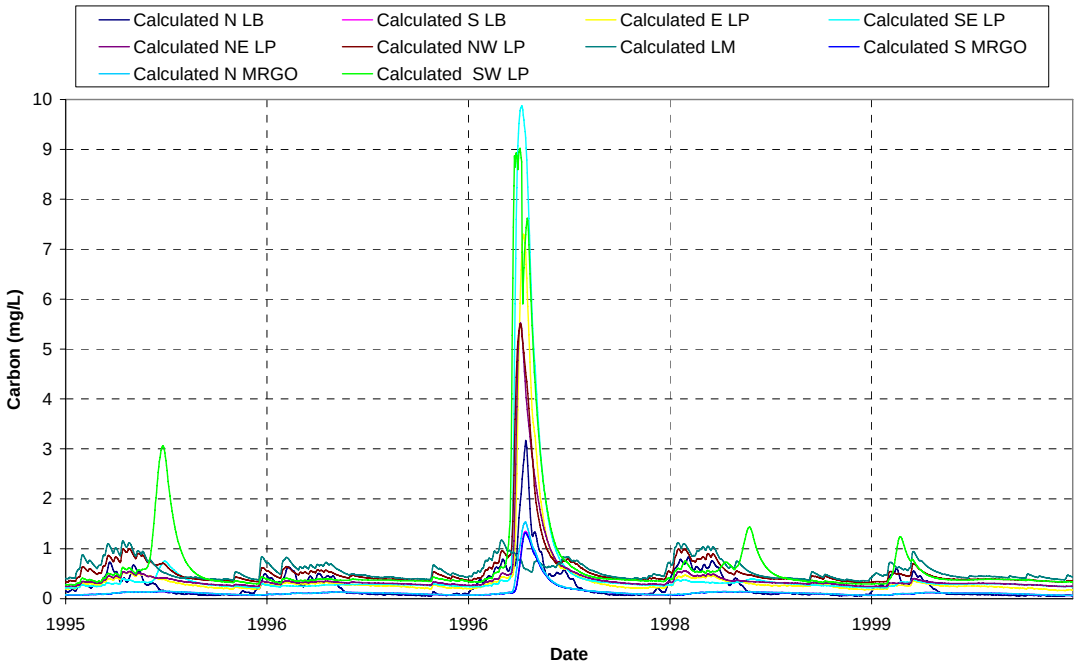

Figure B.11 Calculated carbon concentrations (1995-2000).

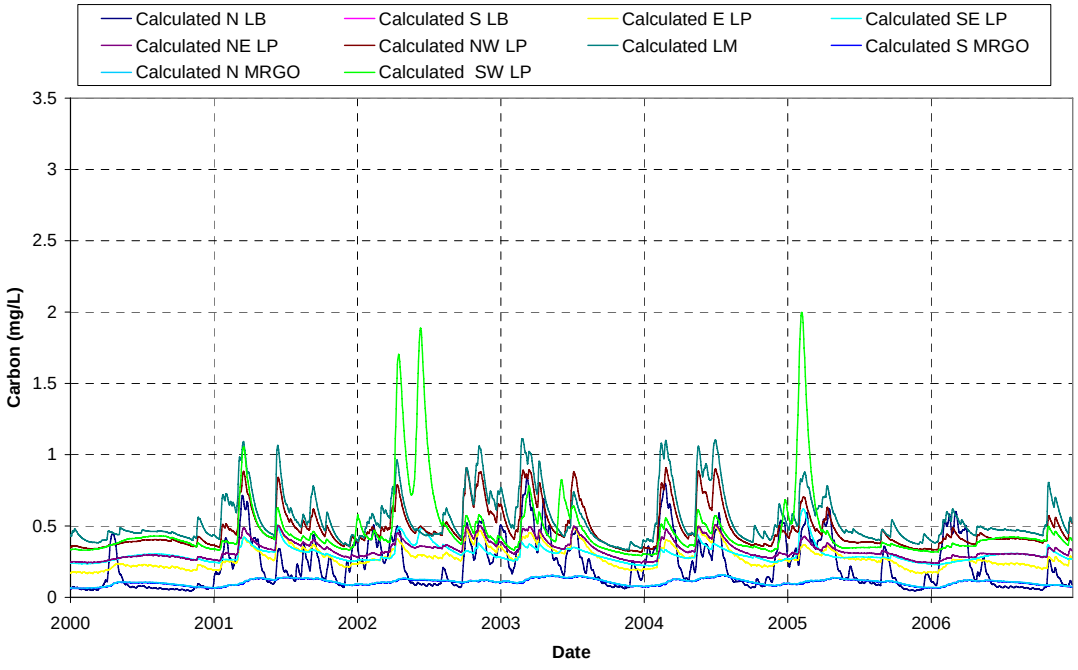

Figure B.12 Calculated carbon concentrations (2000-2006).

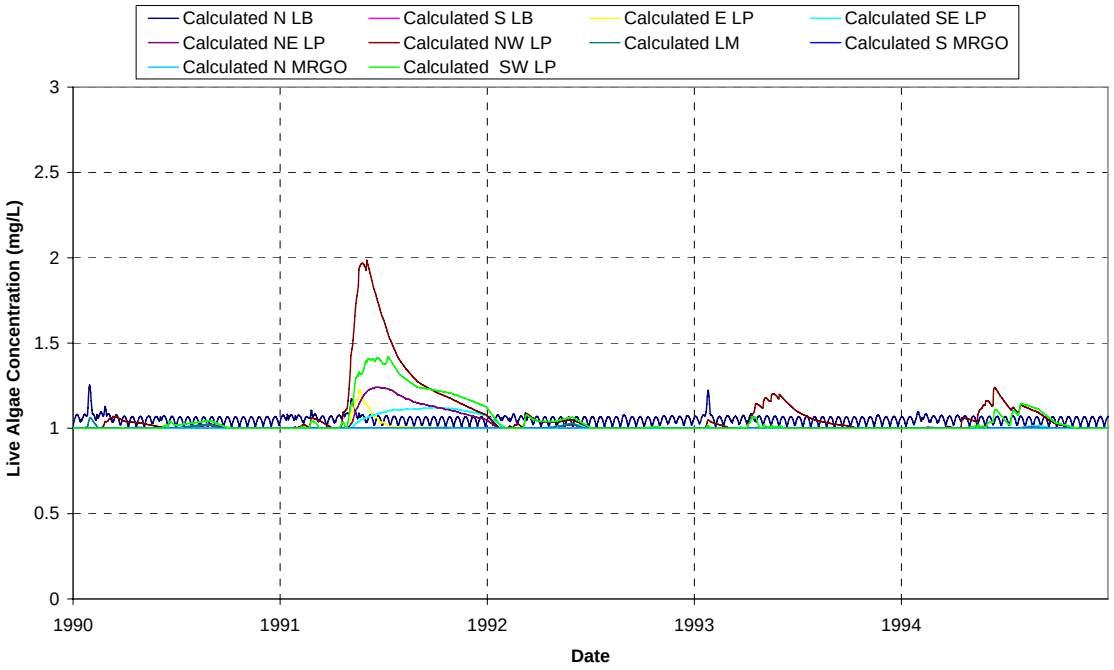

Figure B.13 Calculated live algae concentrations (1990-1995).

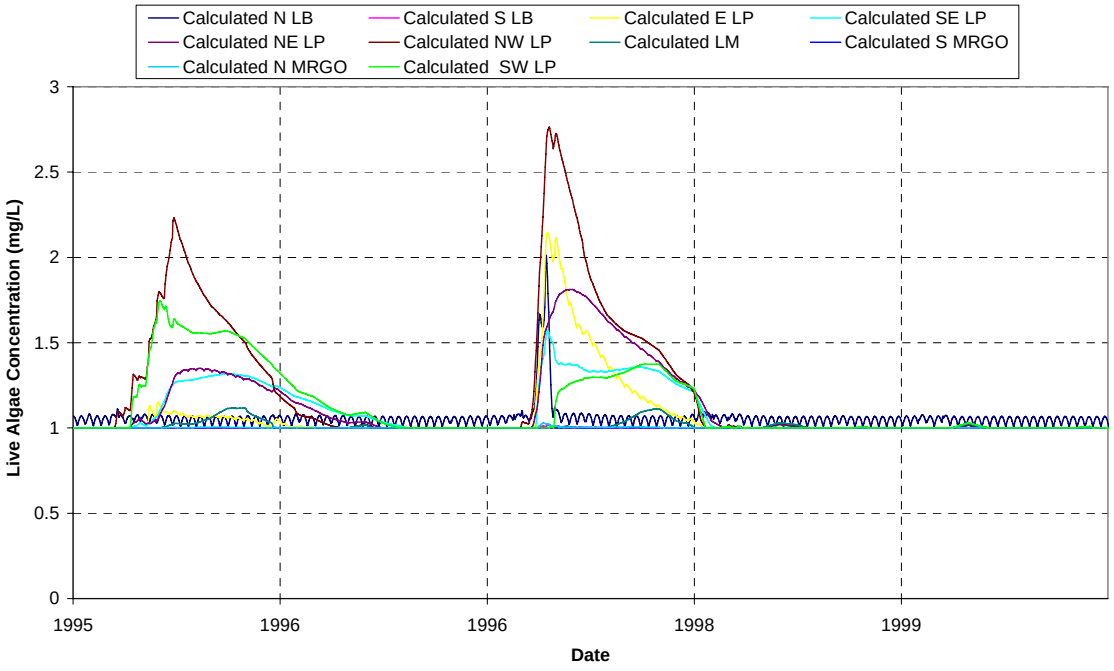

Figure B.14 Calculated live algae concentrations (1995-2000).

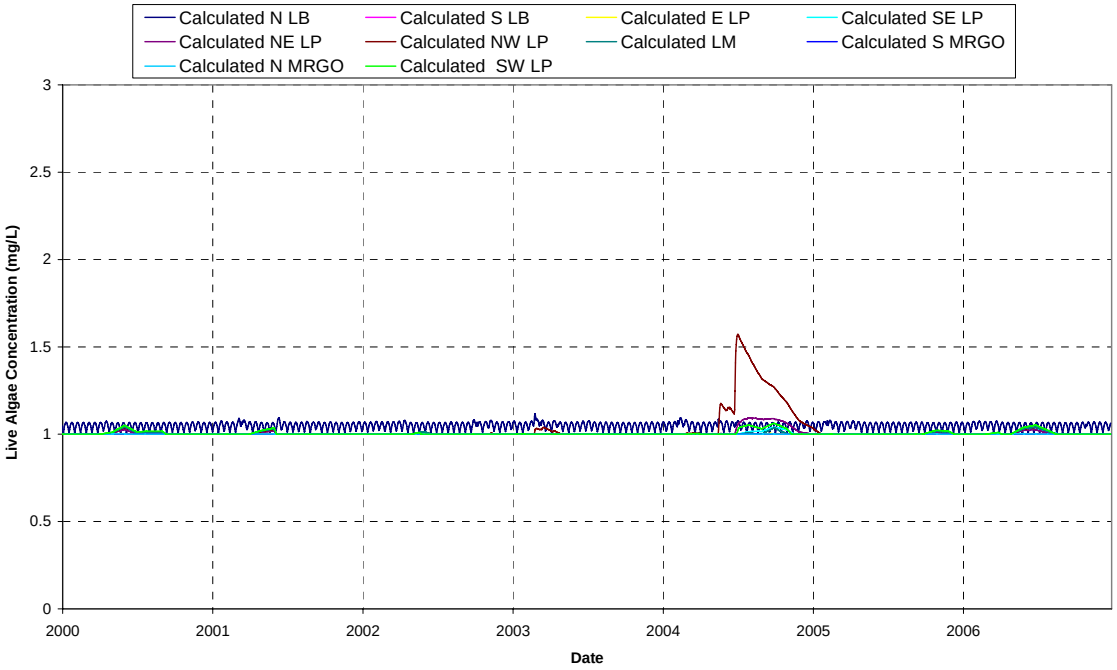

Figure B.15 Calculated live algae concentrations (2000-2007).

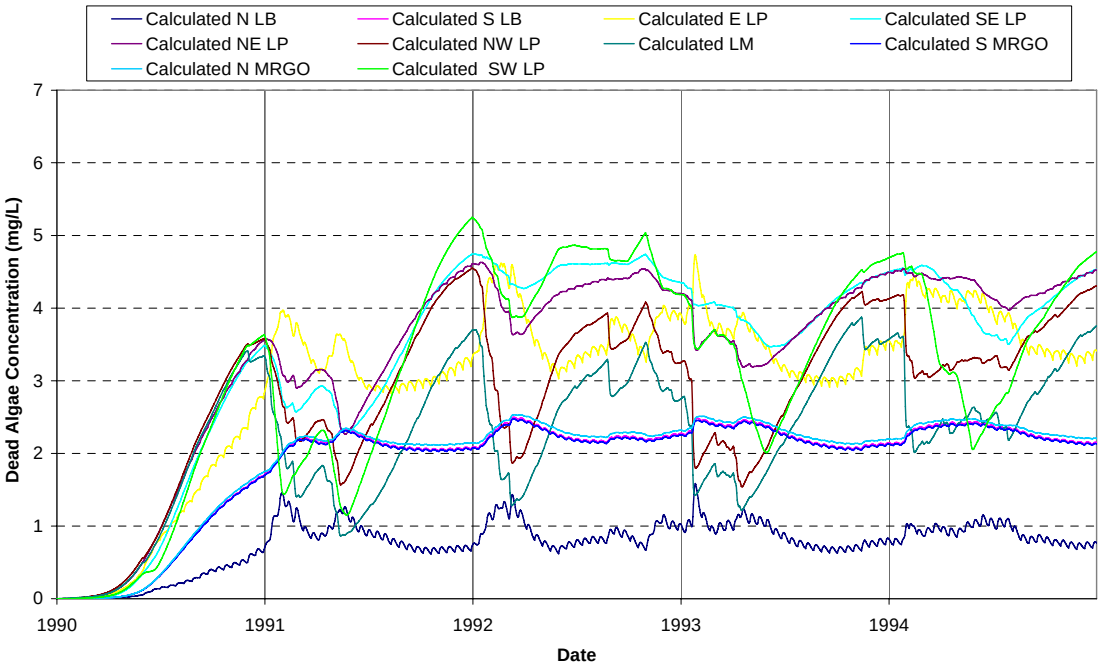

Figure B.16 Calculated dead algae concentrations (1990-1995).

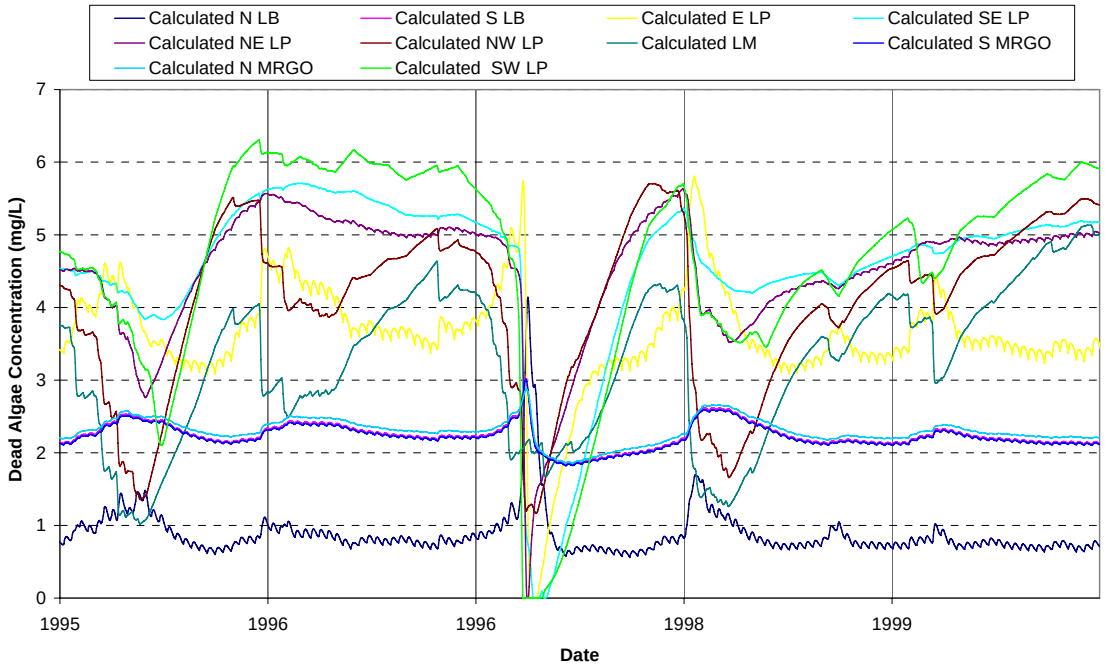

Figure B.17 Calculated dead algae concentrations (1995-2000).

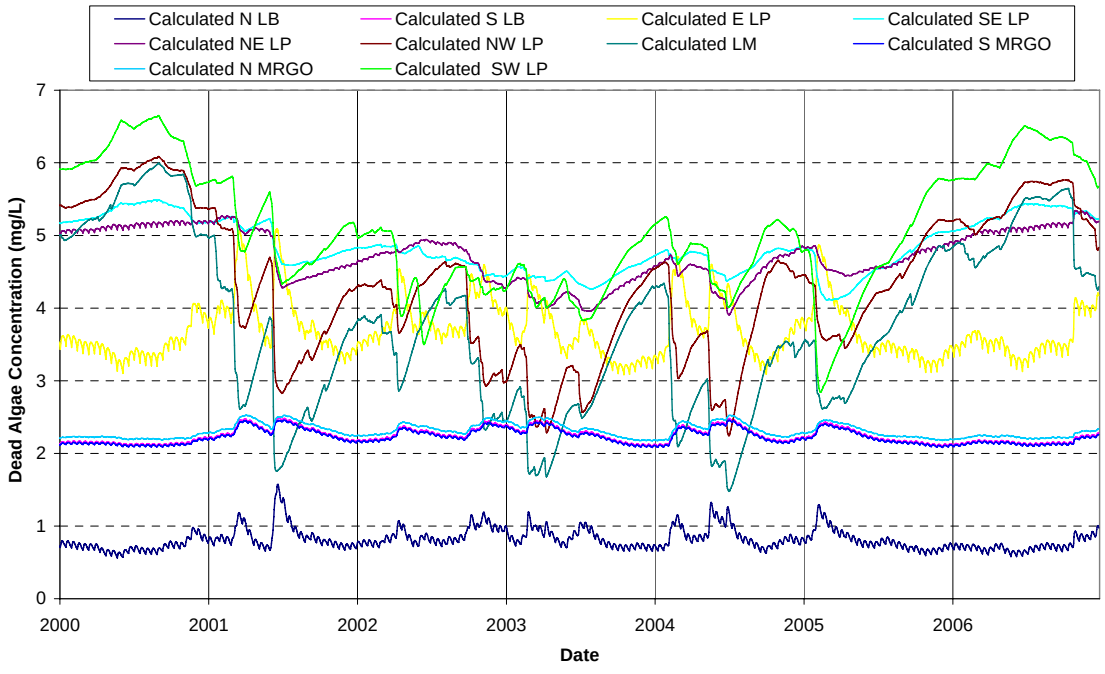

Figure B.18 Calculated dead algae concentrations (2000-2006).

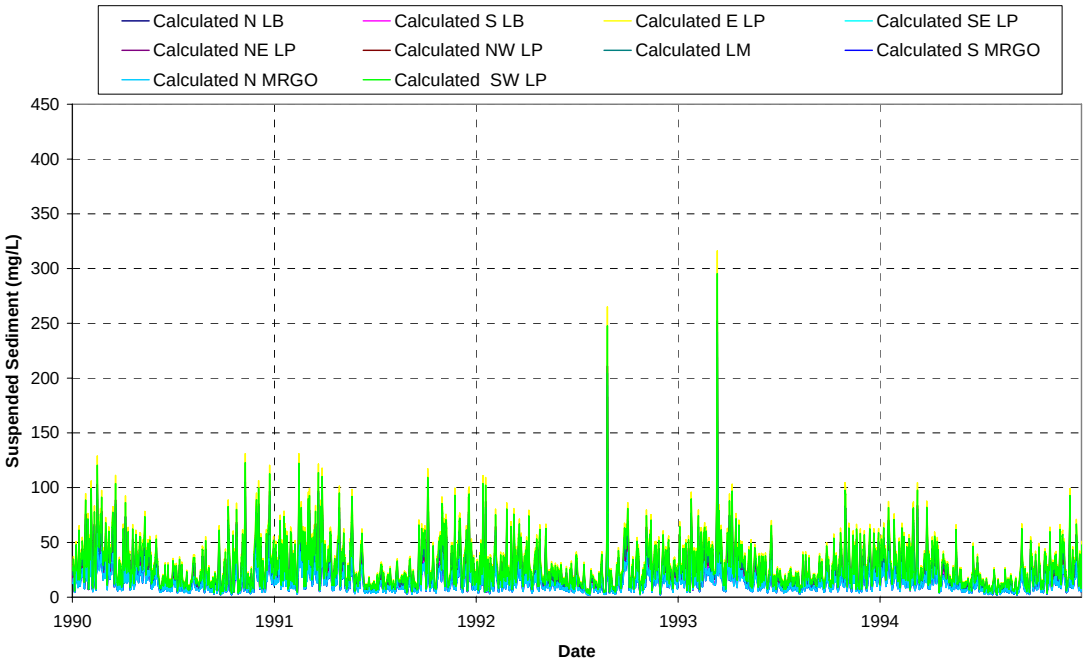

Figure B.19 Calculated suspended sediment concentrations (1990-1995).

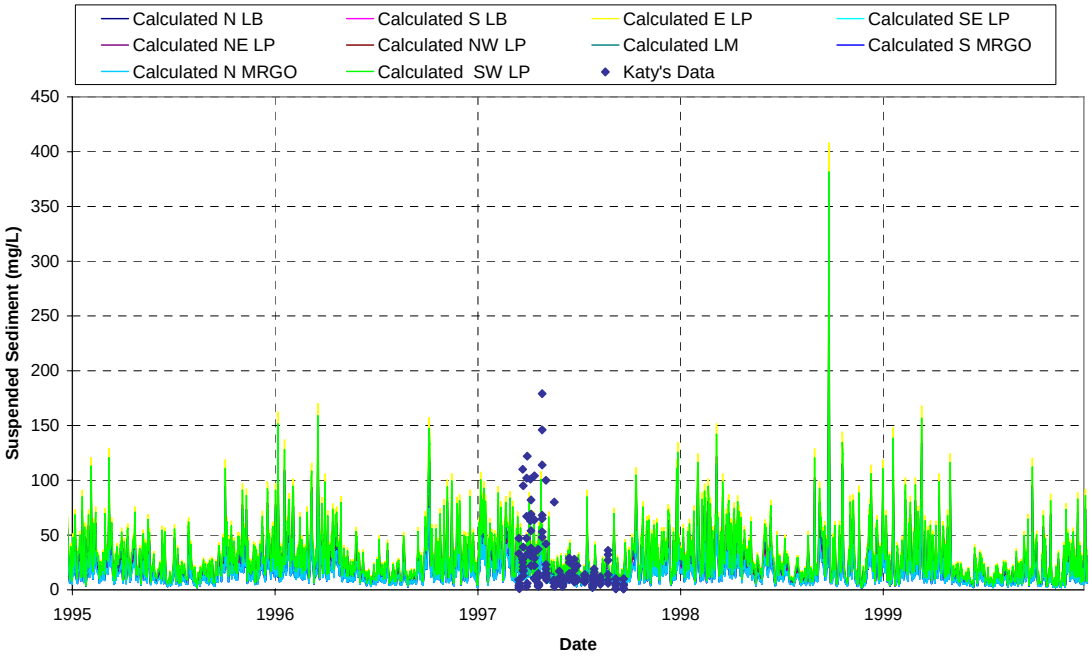

Figure B.20 Calculated suspended sediment concentrations (1995-2000).

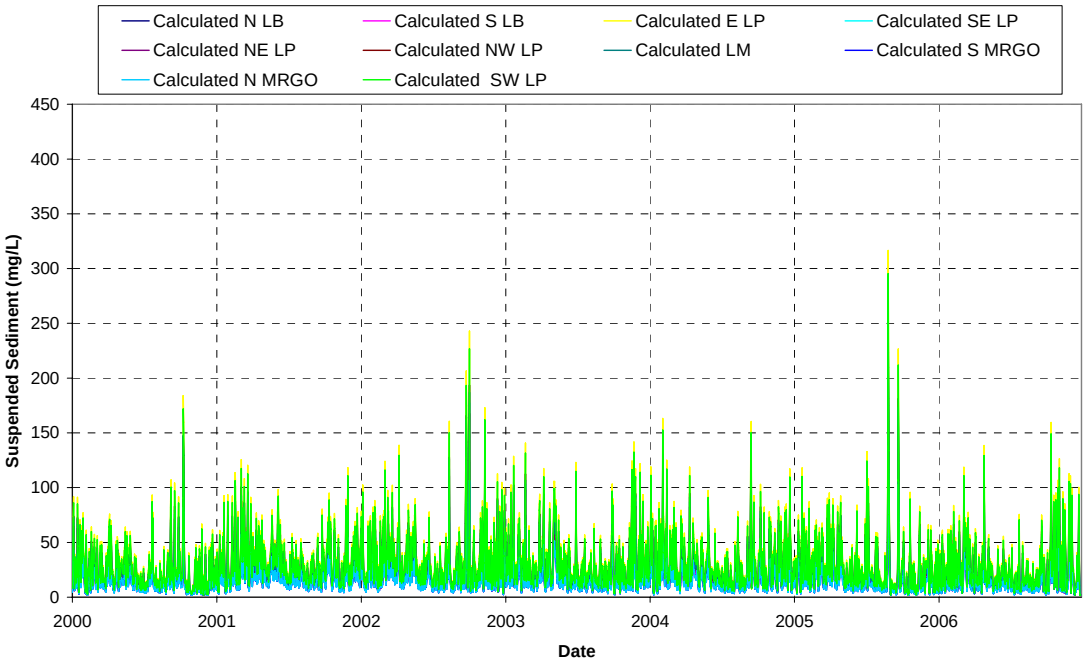

Figure B.21 Calculated suspended sediment concentrations (2000-2006).

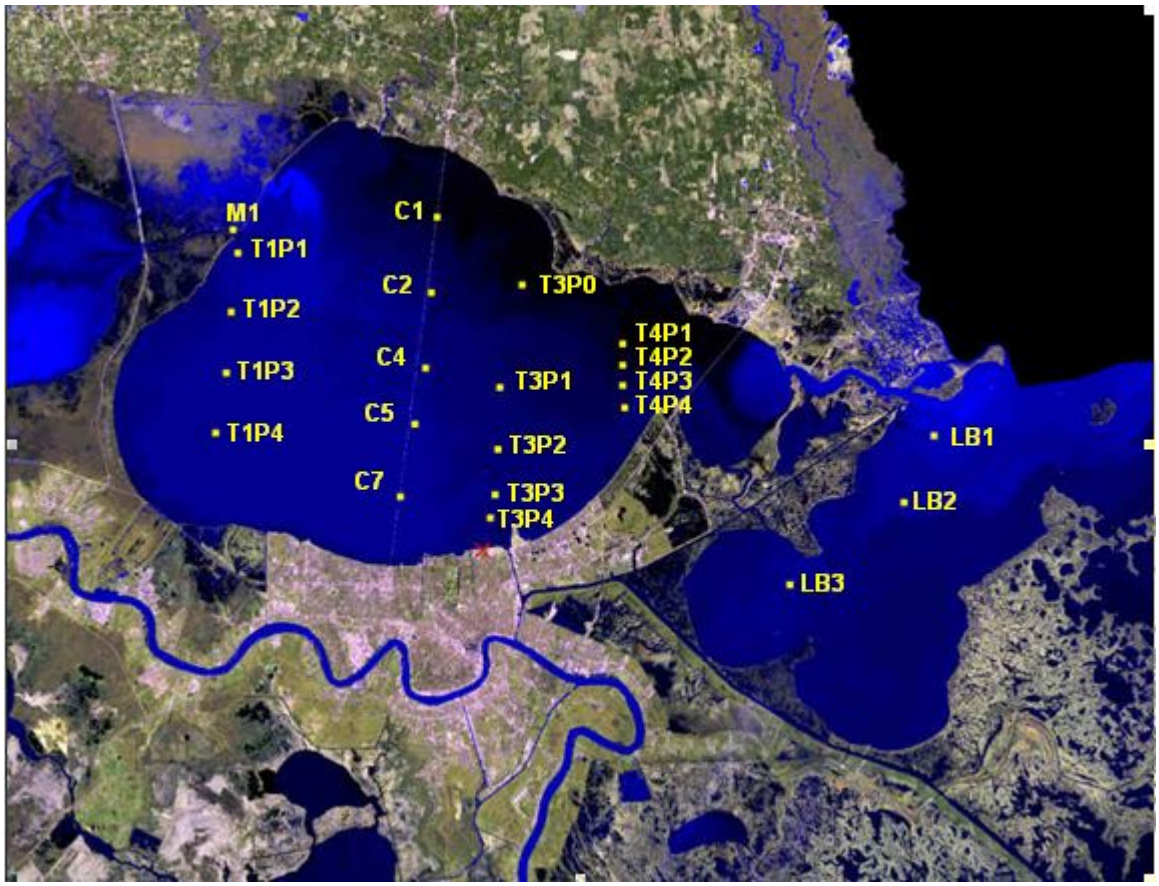

Figure B.22 UNO 1997 research program sampling locations.

Appendix C

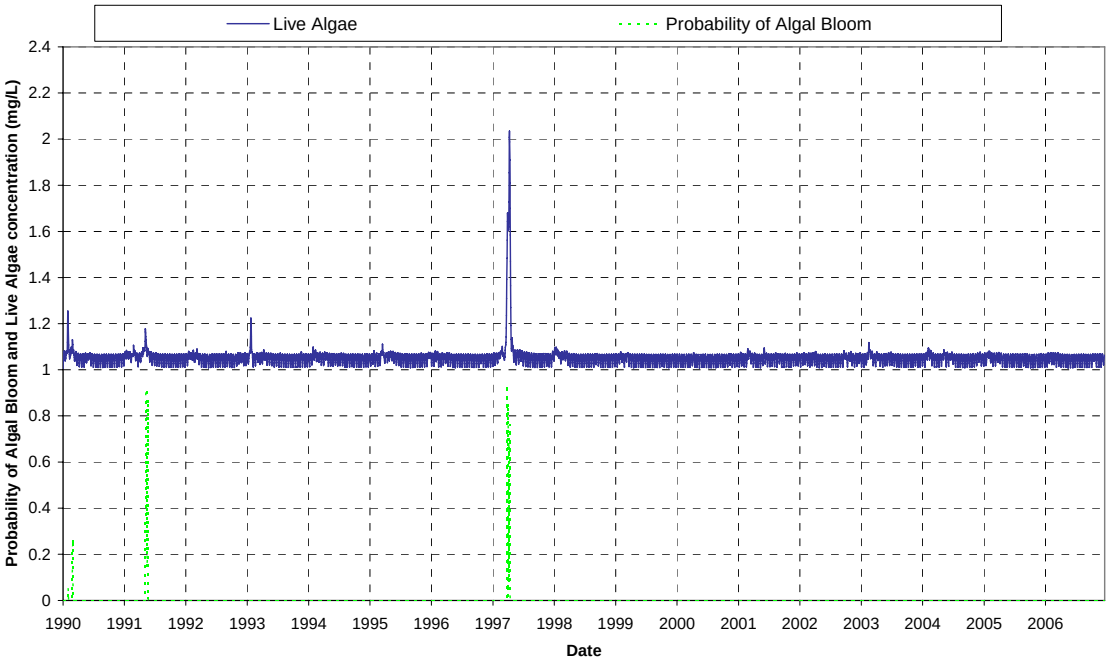

Figure C.1 Probability of an algal bloom on Lake Borgne with predicted live algae concentrations (One diversion, flow of 30 m^3/s).

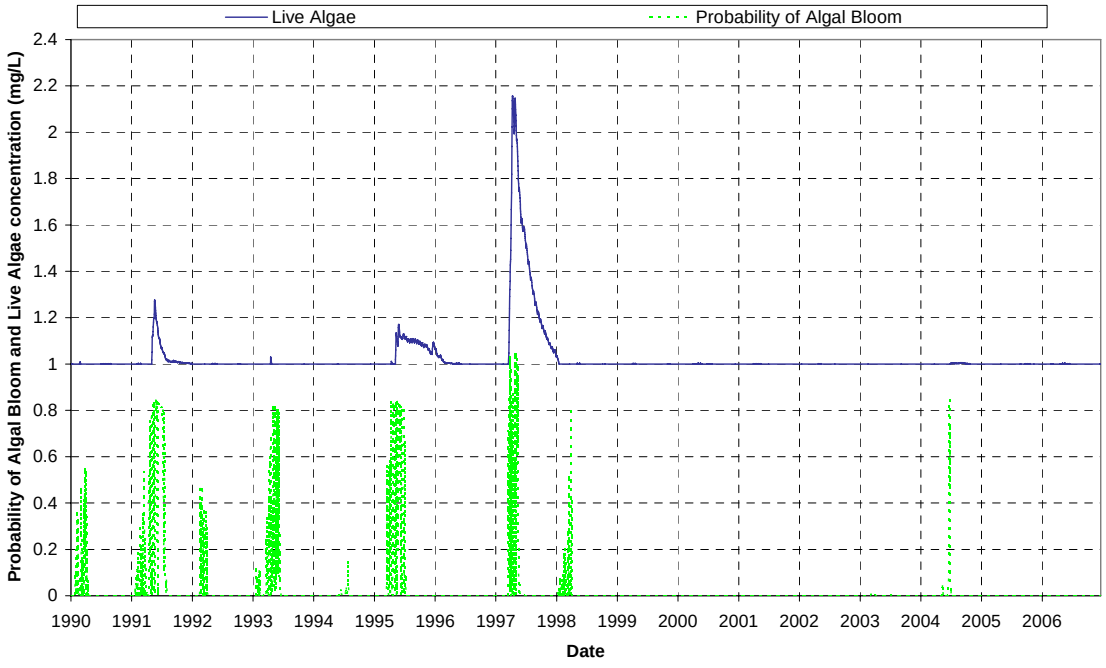

Figure C.2 Probability of an algal bloom on east Lake Pontchartrain with predicted live algae concentrations (One diversion, flow of 30 m^3/s).

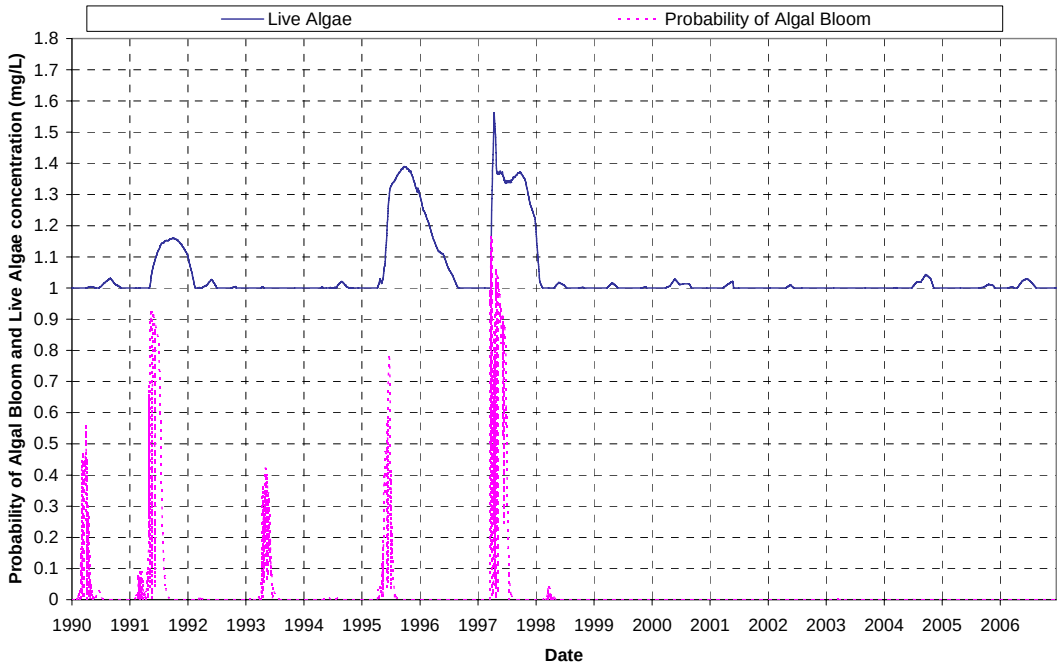

Figure C.3 Probability of an algal bloom on southeast Lake Pontchartrain with predicted live algae concentrations (One diversion, flow of 30 m^3/s).

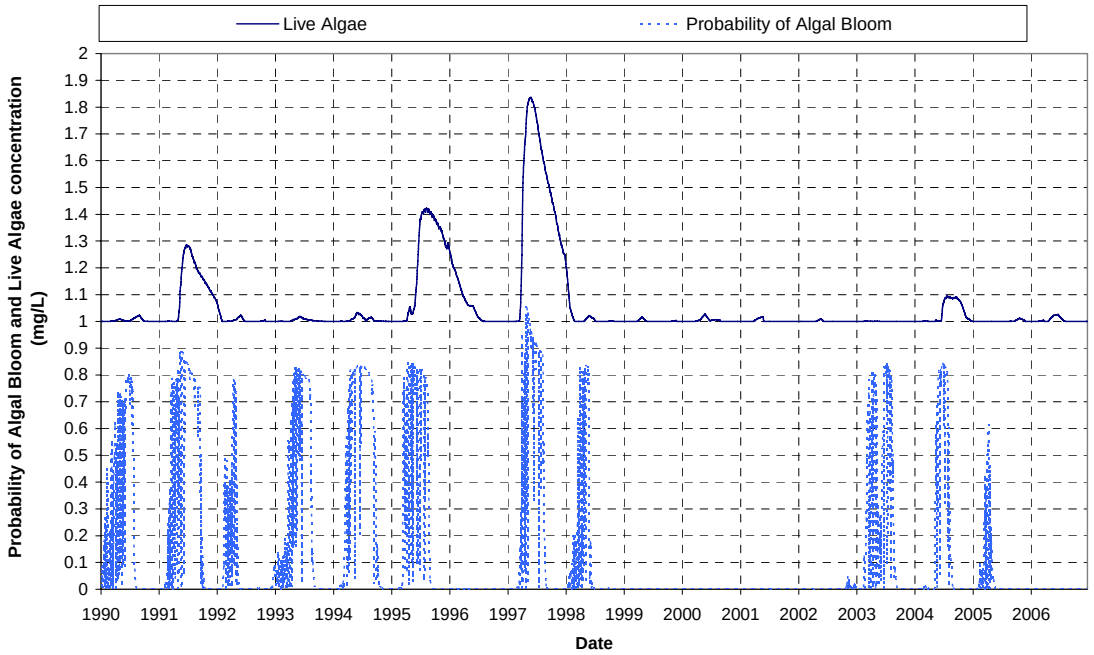

Figure C.4 Probability of an algal bloom on northeast Lake Pontchartrain with predicted live algae concentrations (One diversion, flow of 30 m^3/s).

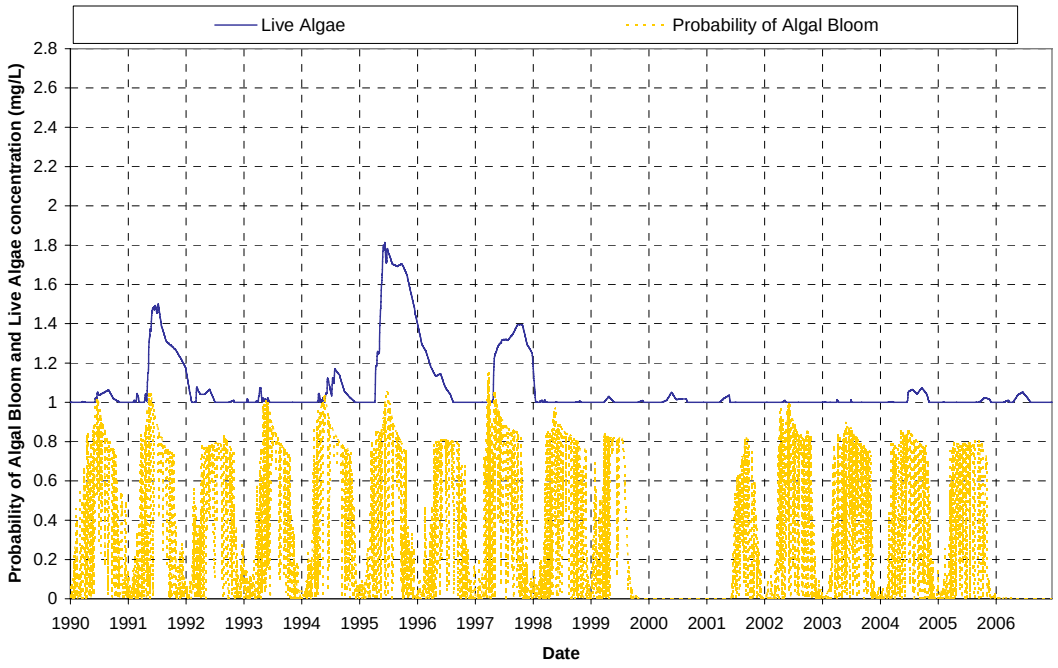

Figure C.5 Probability of an algal bloom on southwest Lake Pontchartrain with predicted live algae concentrations (One diversion, flow of 30 m^3/s).

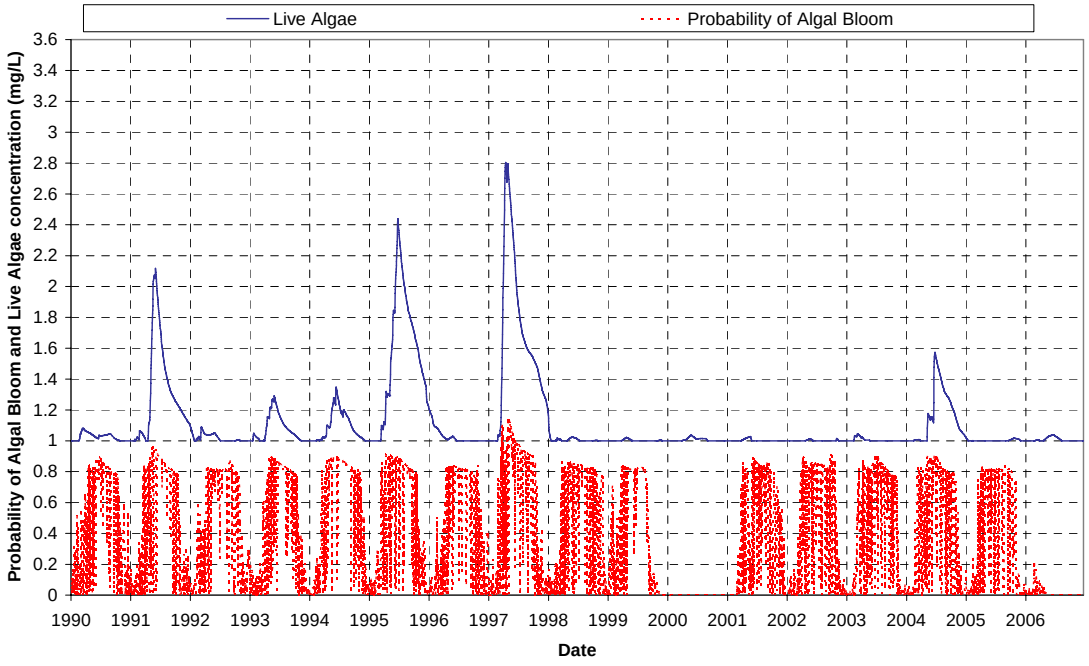

Figure C.6 Probability of an algal bloom on northwest Lake Pontchartrain with predicted live algae concentrations (One diversion, flow of 30 m^3/s).

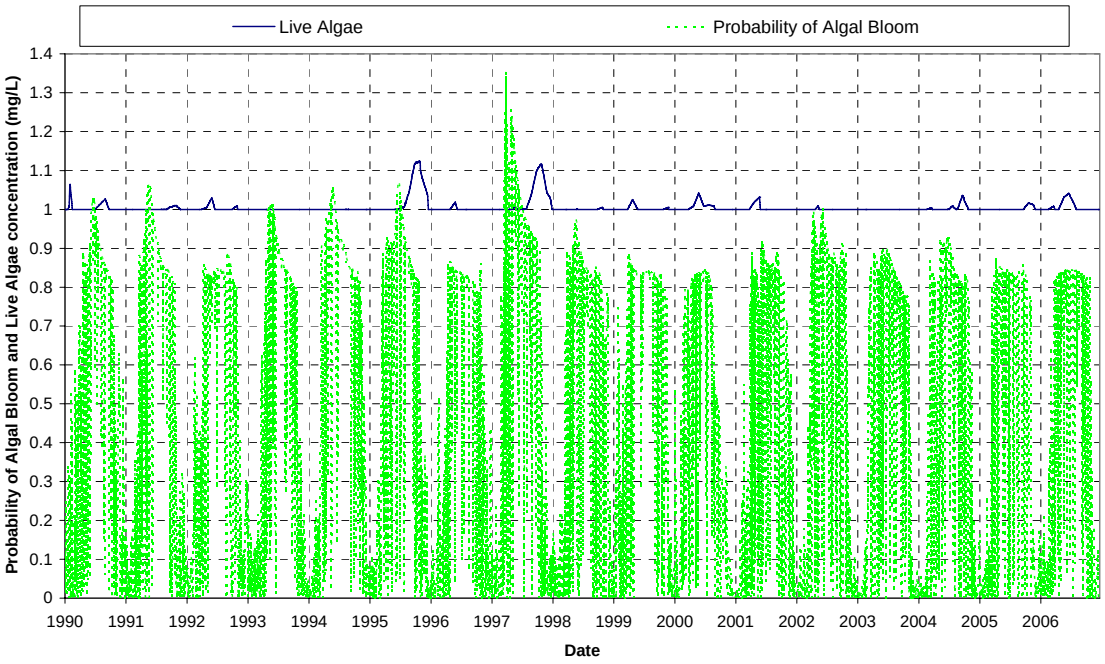

Figure C.7 Probability of an algal bloom on Lake Maurepas with predicted live algae concentrations (One diversion, flow of 30 m^3/s).

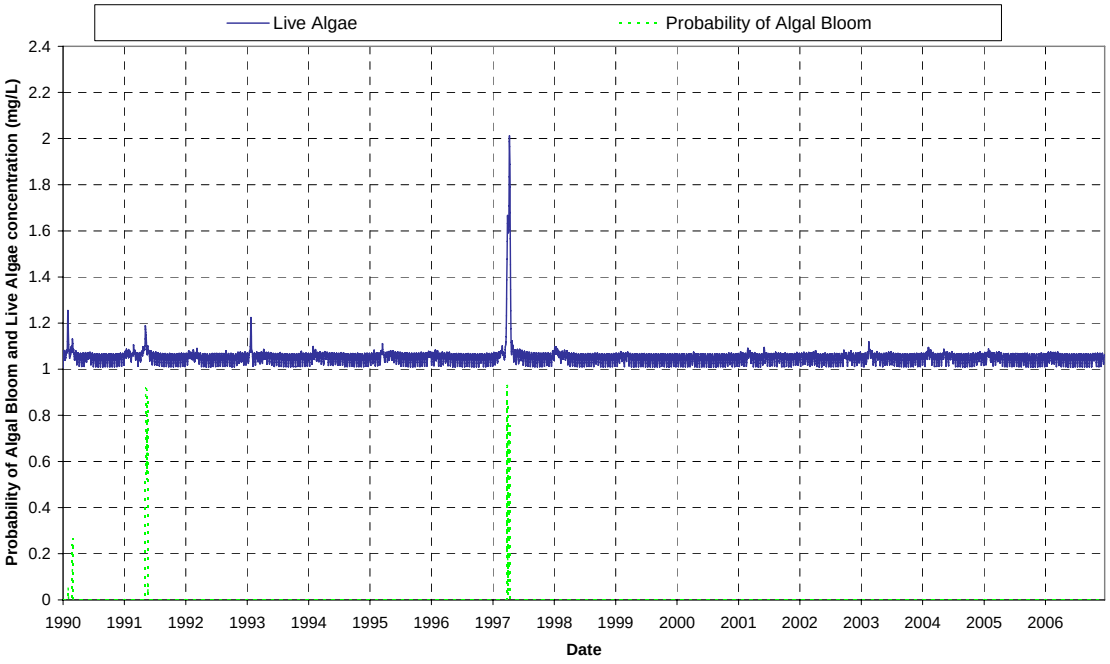

Figure C.8 Probability of an algal bloom on Lake Borgne with predicted live algae concentrations (50% increase to Bonnet Carré Spillway flows).

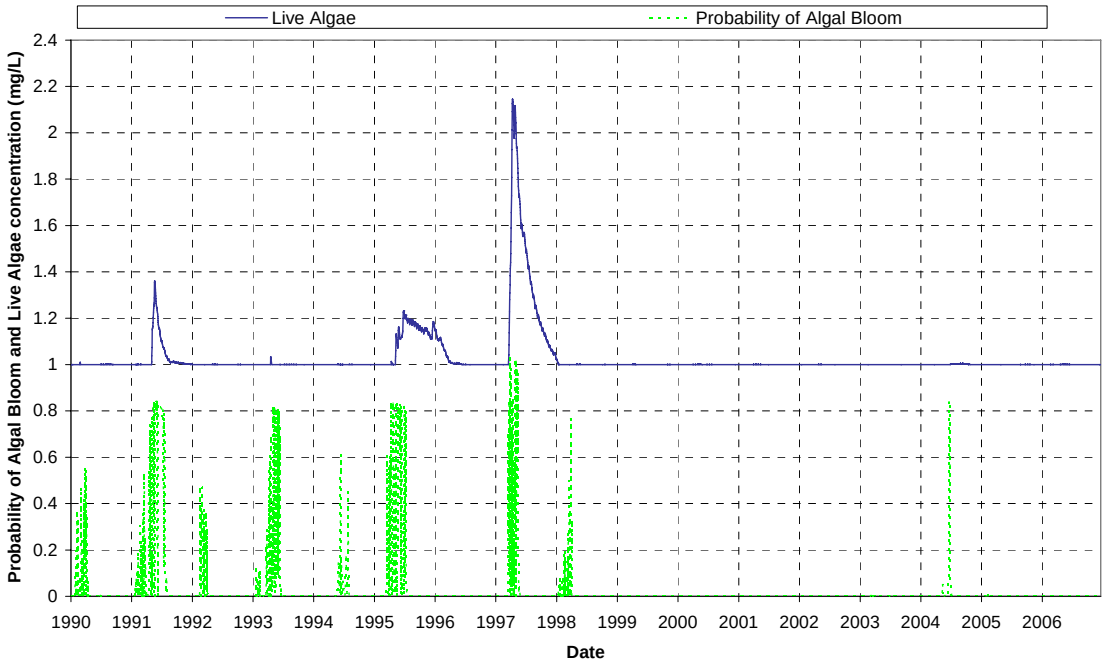

Figure C.9 Probability of an algal bloom on east Lake Pontchartrain with predicted live algae concentrations (50% increase to Bonnet Carré Spillway flows).

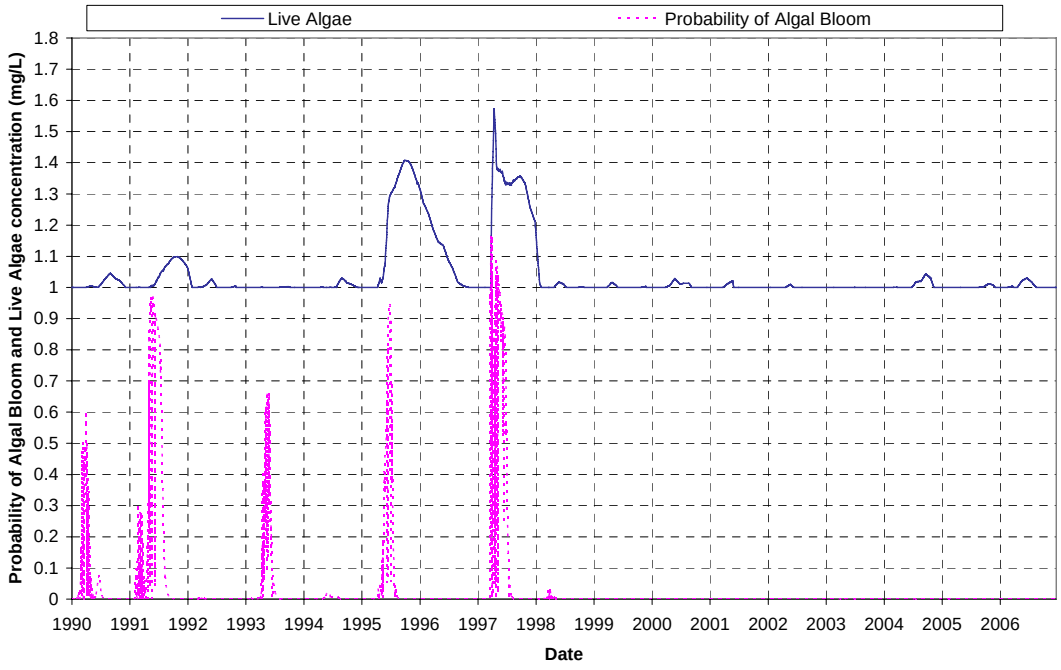

Figure C.10 Probability of an algal bloom on southeast Lake Pontchartrain with predicted live algae concentrations (50% increase to Bonnet Carré Spillway flows).

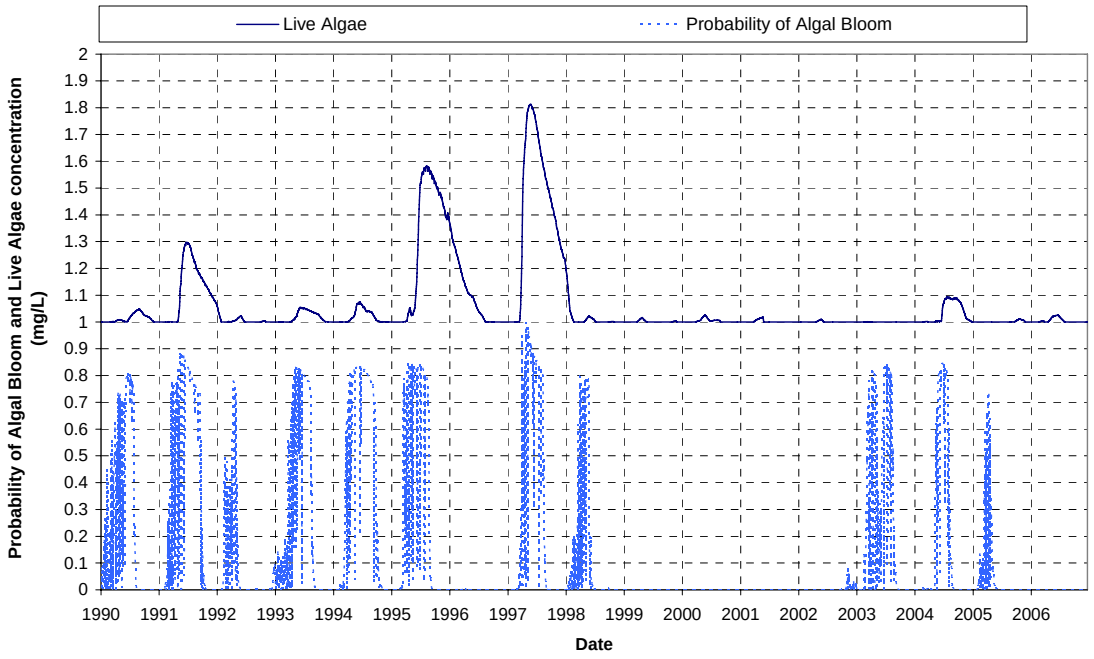

Figure C.11 Probability of an algal bloom on northeast Lake Pontchartrain with predicted live algae concentrations (50% increase to Bonnet Carré Spillway flows).

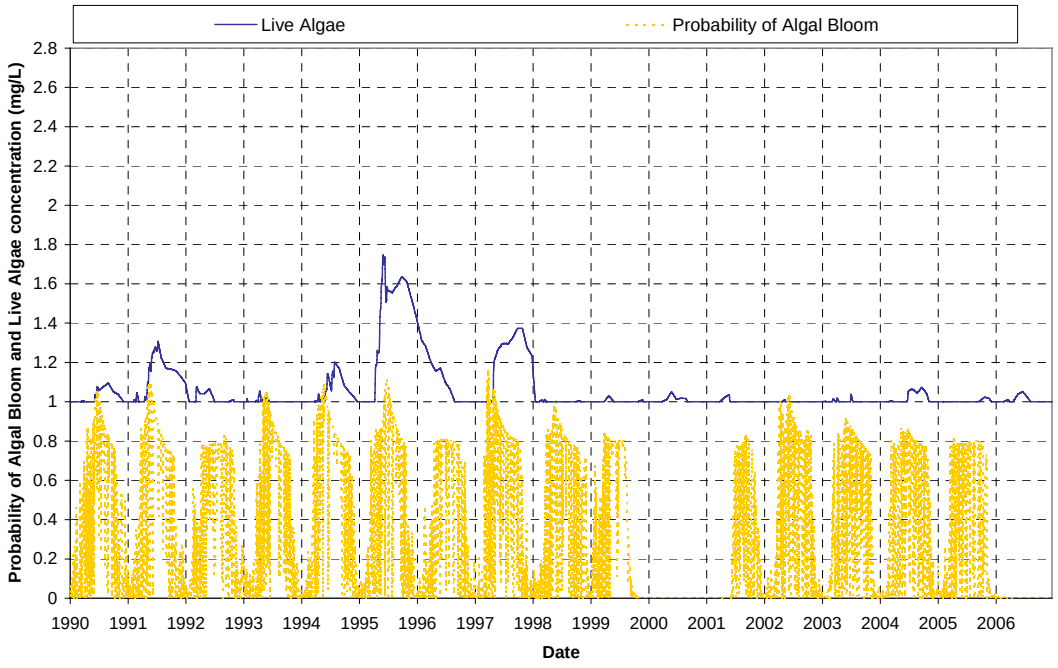

Figure C.12 Probability of an algal bloom on southwest Lake Pontchartrain with predicted live algae concentrations (50% increase to Bonnet Carré Spillway flows).

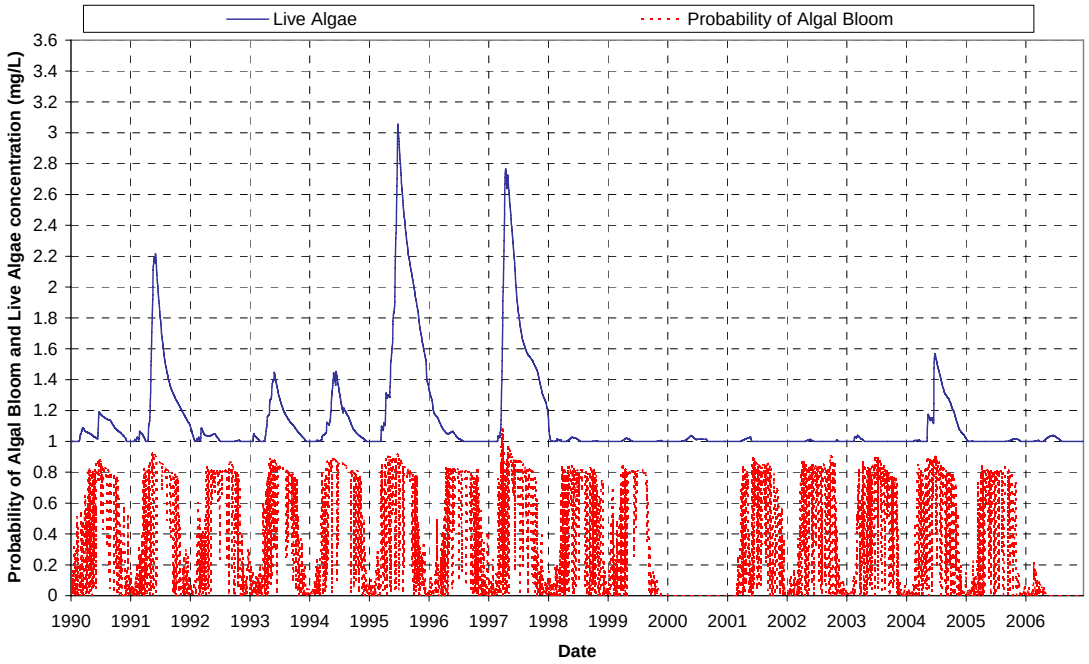

Figure C.13 Probability of an algal bloom on northwest Lake Pontchartrain with predicted live algae concentrations (50% increase to Bonnet Carré Spillway flows).

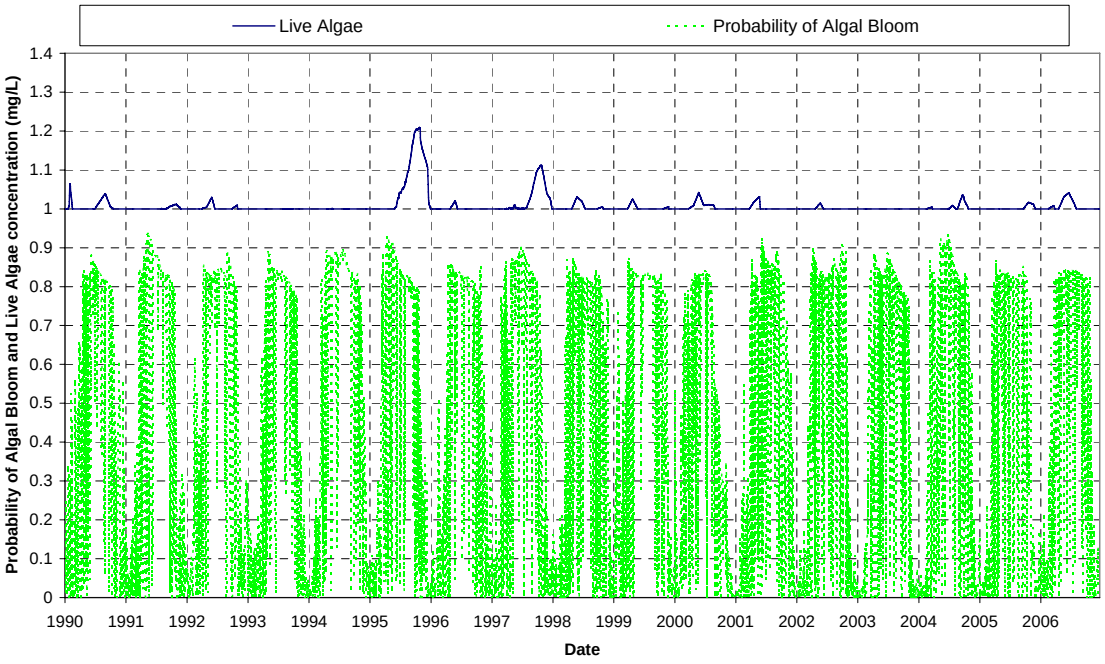

Figure C.14 Probability of an algal bloom on Lake Maurepas with predicted live algae concentrations (50% increase to Bonnet Carré Spillway flows).

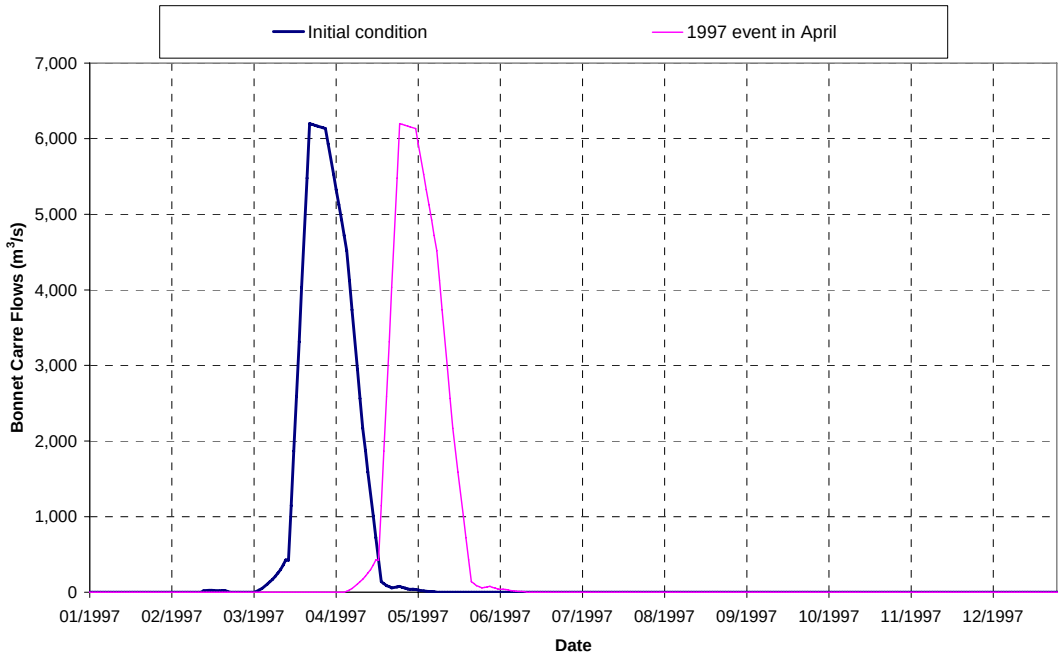

Figure C15. Bonnet Carré Spillway 1997 hydrograph shifted to end of April.

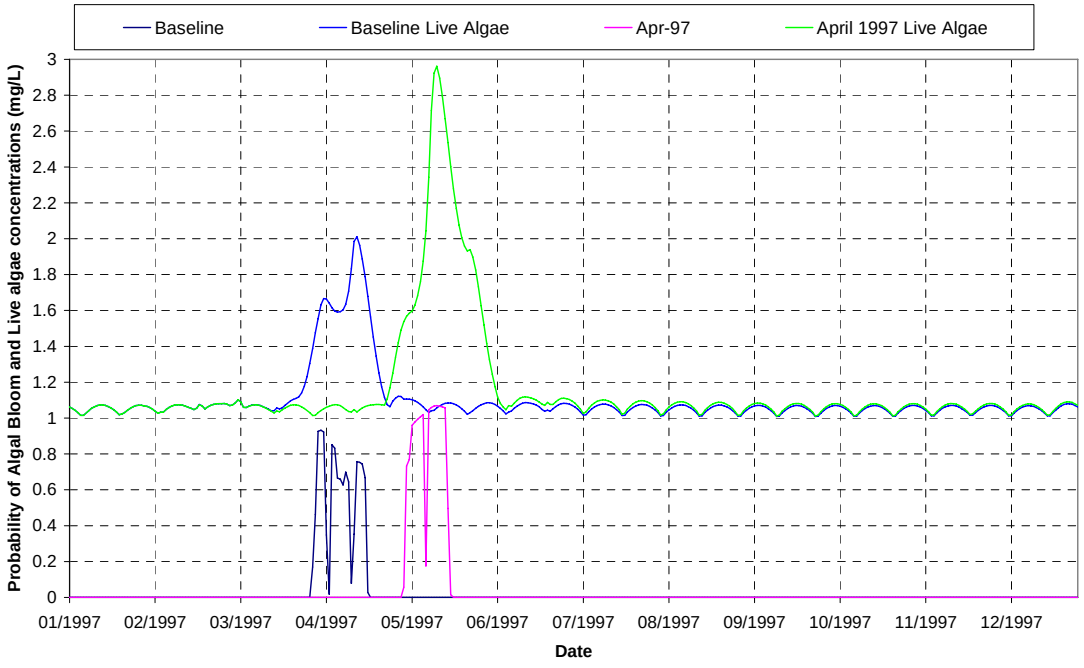

Figure C16. Probability of an algal bloom on Lake Borgne with live algae concentrations (March and April 1997 opening).

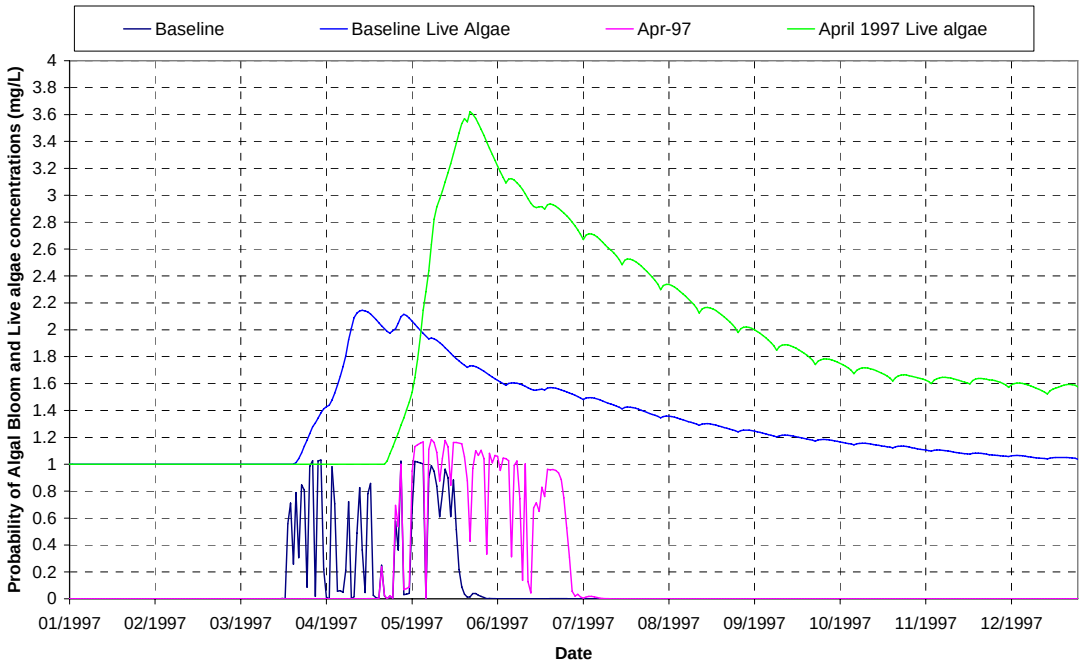

Figure C17. Probability of an algal bloom on east Lake Pontchartrain with live algae concentrations (March and April 1997 opening).

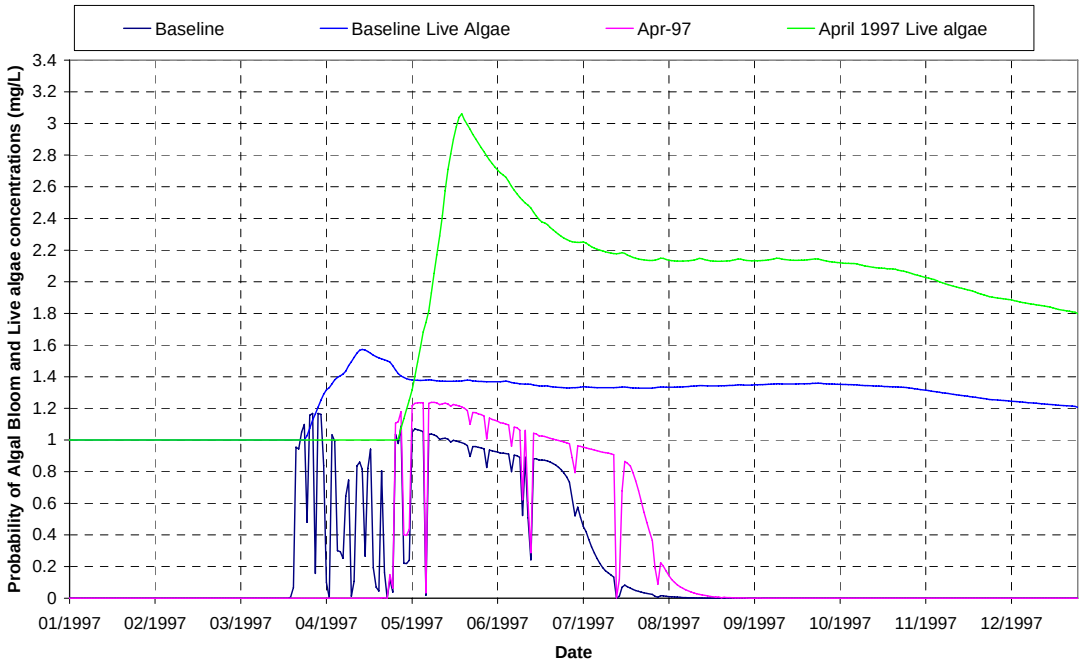

Figure C18. Probability of an algal bloom on southeast Lake Pontchartrain with live algae concentrations (March and April 1997 opening).

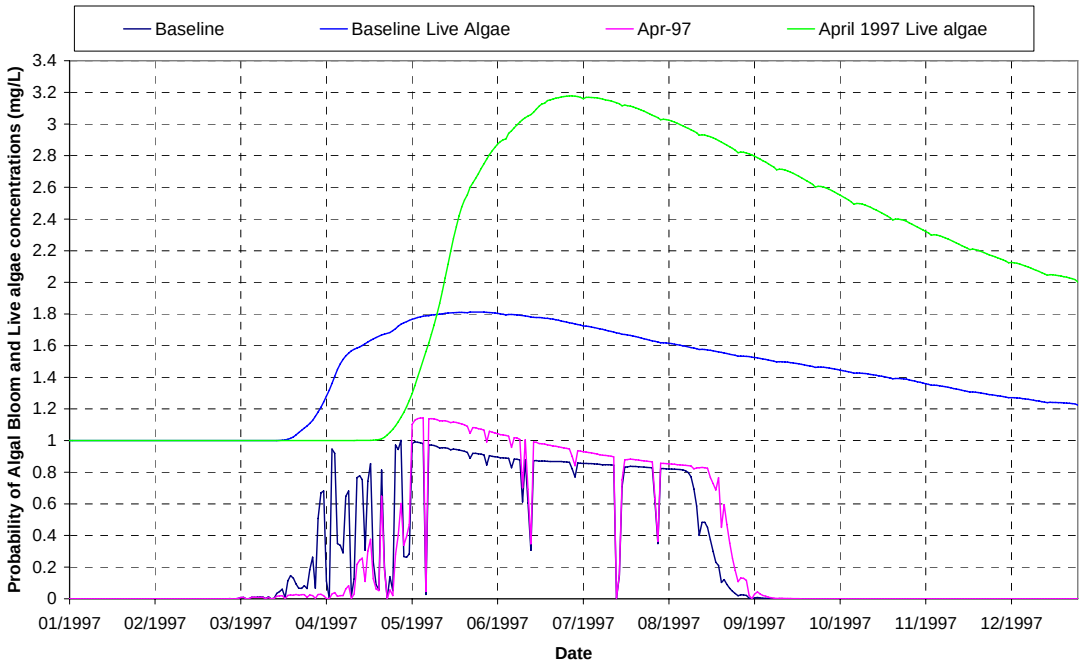

Figure C19. Probability of an algal bloom on northeast Lake Pontchartrain with live algae concentrations (March and April 1997 opening).

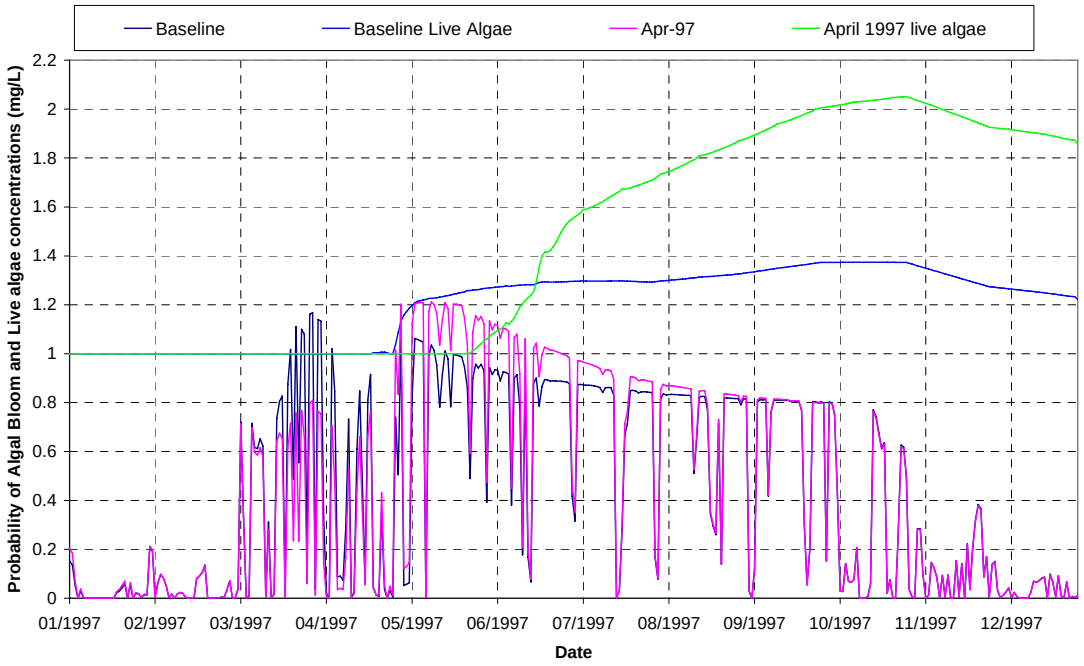

Figure C20. Probability of an algal bloom on southwest Lake Pontchartrain with live algae concentrations (March and April 1997 opening).

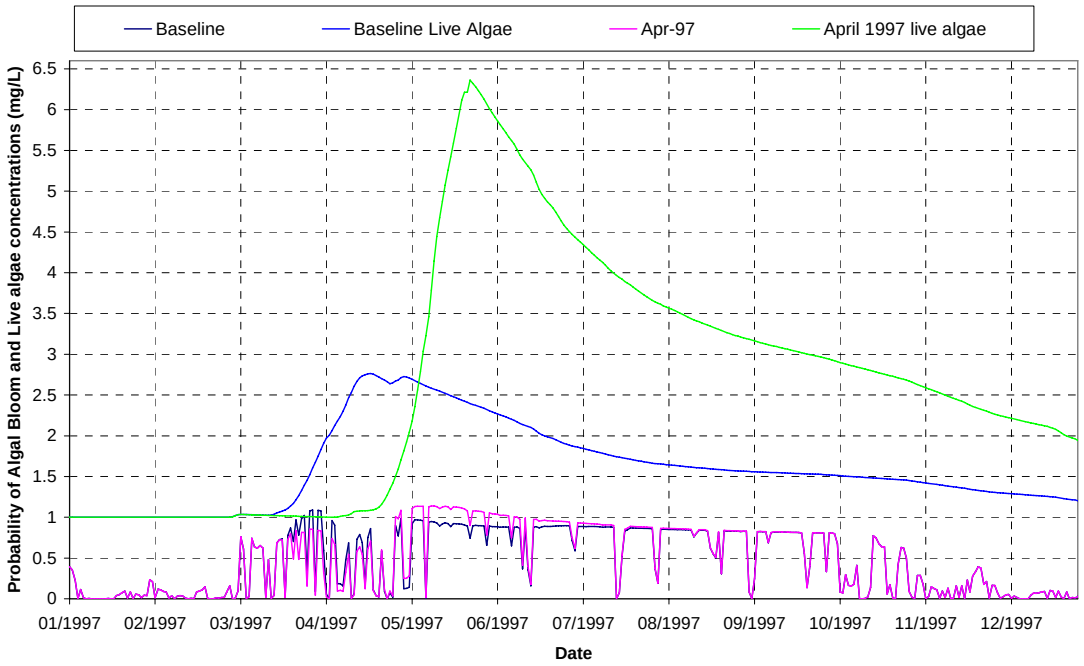

Figure C21. Probability of an algal bloom on northwest Lake Pontchartrain with live algae concentrations (March and April 1997 opening).

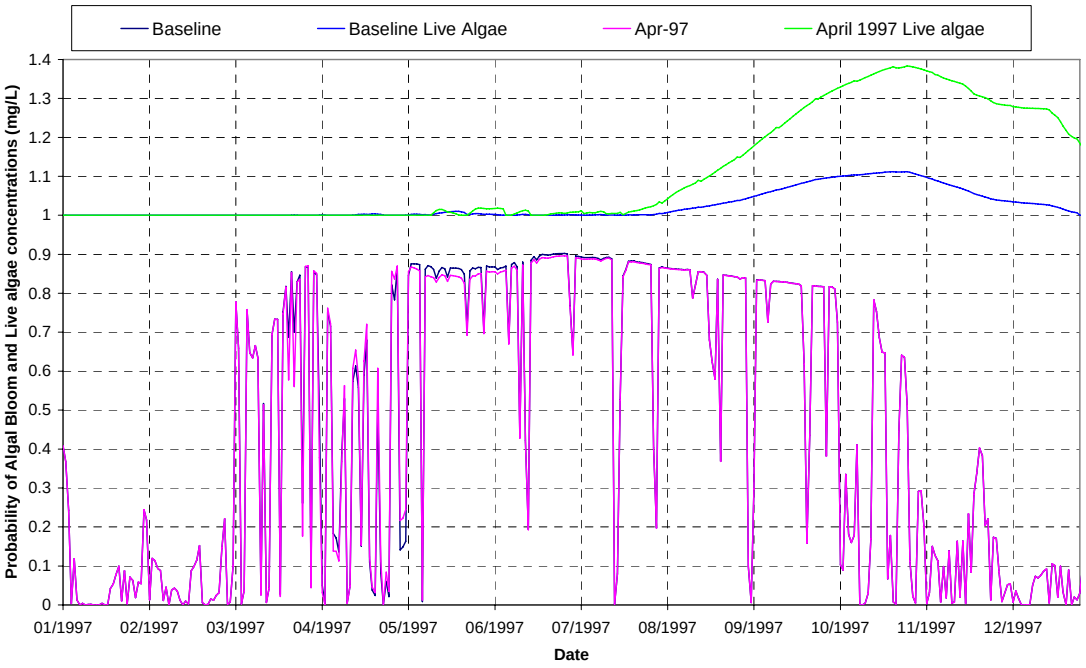

Figure C22. Probability of an algal bloom on Lake Maurepas with live algae concentrations (March and April 1997 opening).

Appendix D

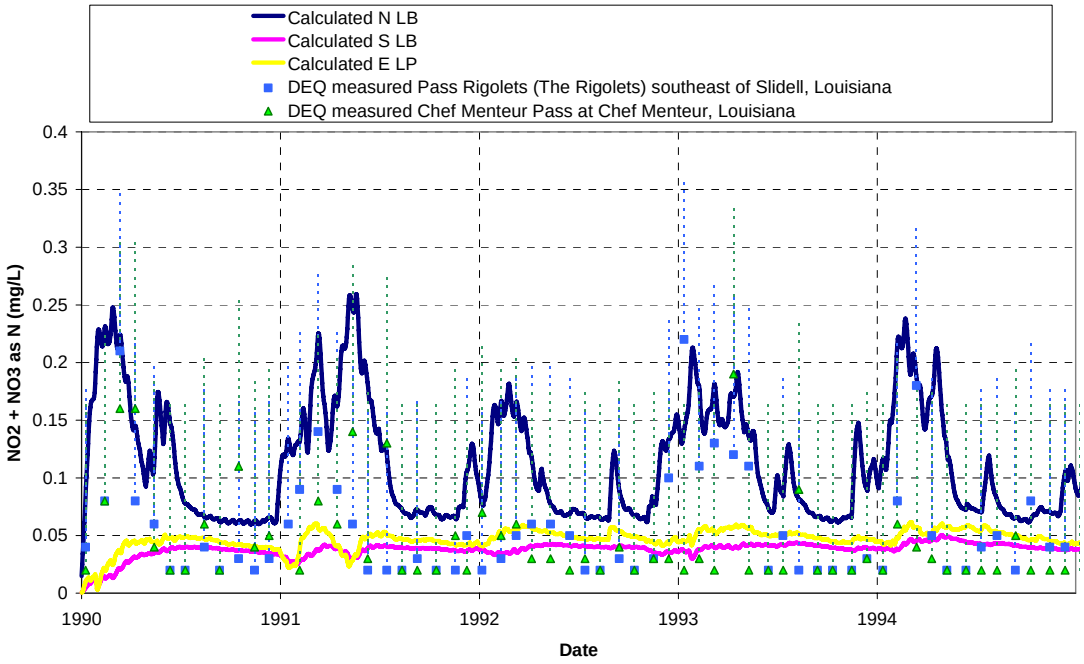

Figure D.1 Nitrite + nitrate as nitrogen concentrations on Lake Borgne with nutrient concentrations applied at the Gulf of Mexico boundary (1990-1995).

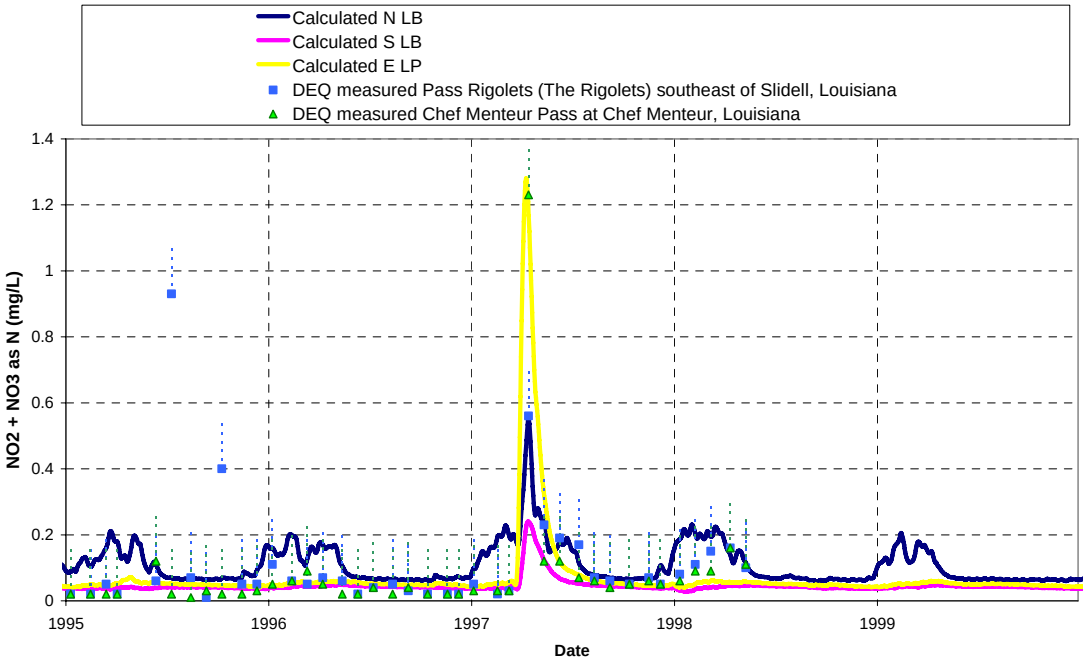

Figure D.2 Nitrite + nitrate as nitrogen concentrations on Lake Borgne with nutrient concentrations applied at the Gulf of Mexico boundary (1995-2000).

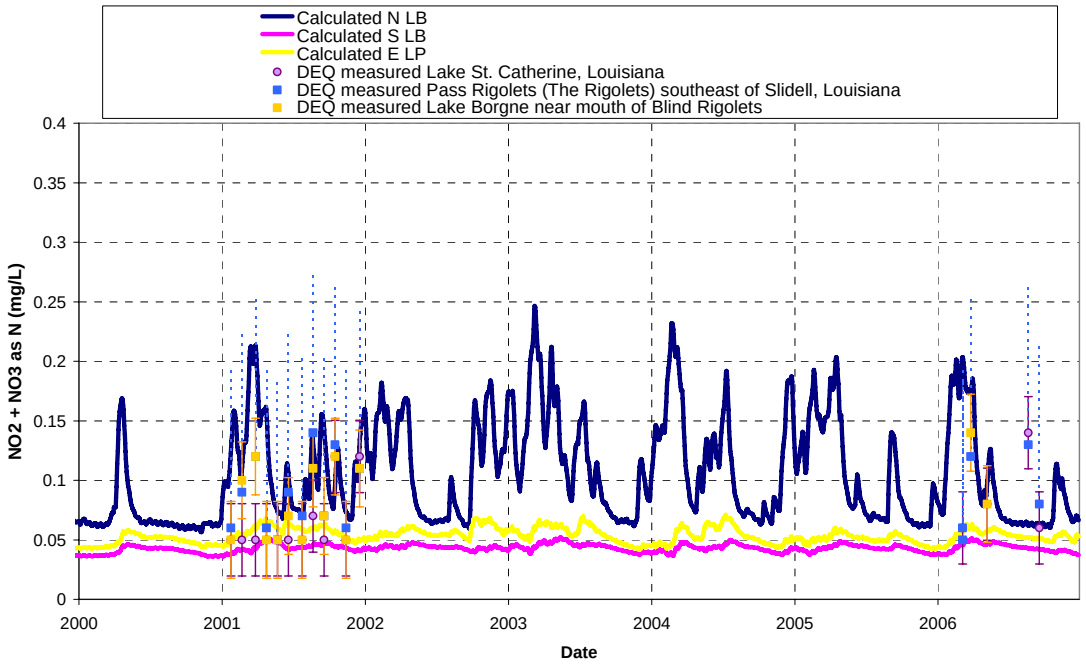

Figure D.3 Nitrite + nitrate as nitrogen concentrations on Lake Borgne with nutrient concentrations applied at the Gulf of Mexico boundary (2000-2007).

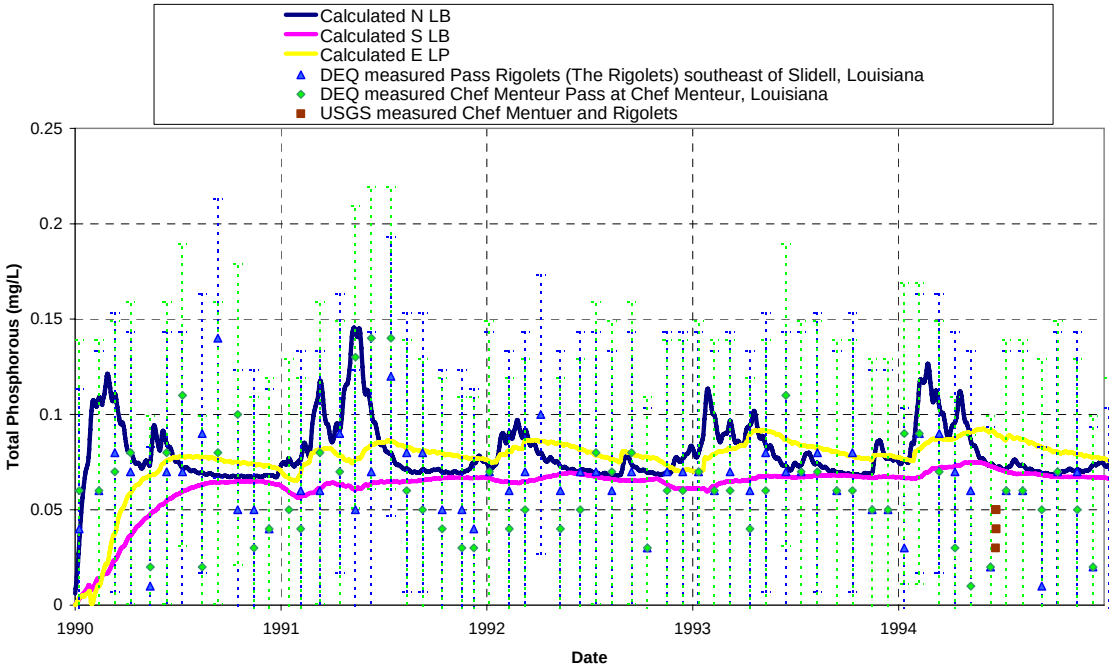

Figure D.4 Total phosphorous concentrations on Lake Borgne with nutrient concentrations applied at the Gulf of Mexico boundary (1990-1995).

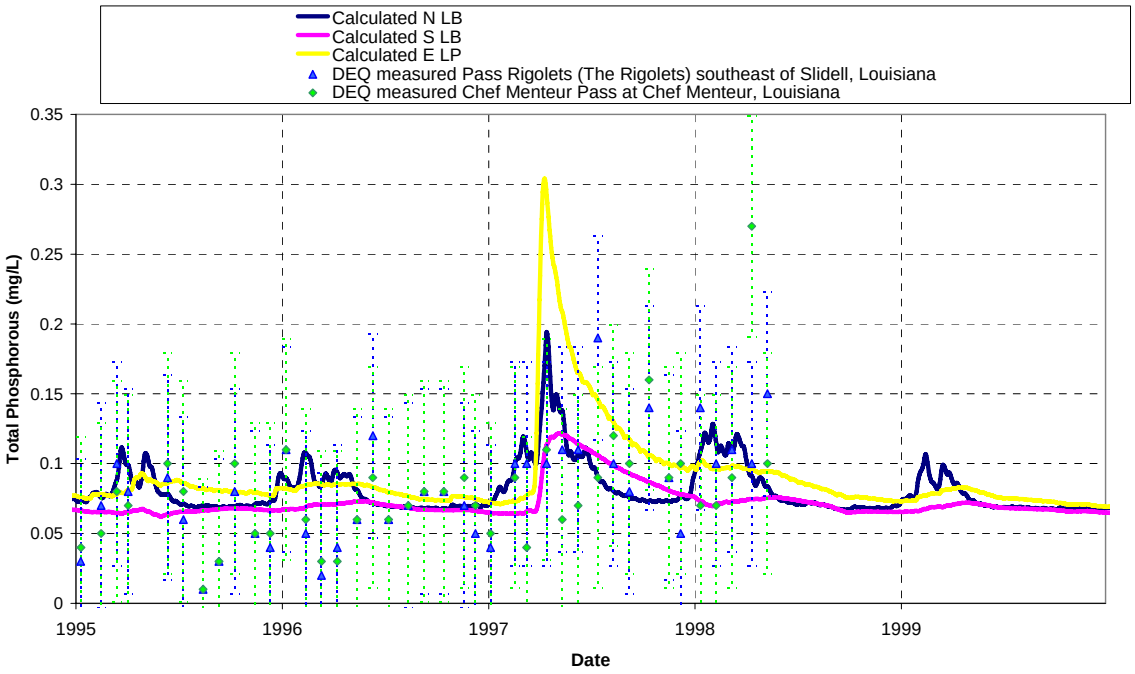

Figure D.5 Total phosphorous concentrations on Lake Borgne with nutrient concentrations applied at the Gulf of Mexico boundary (1995-2000).

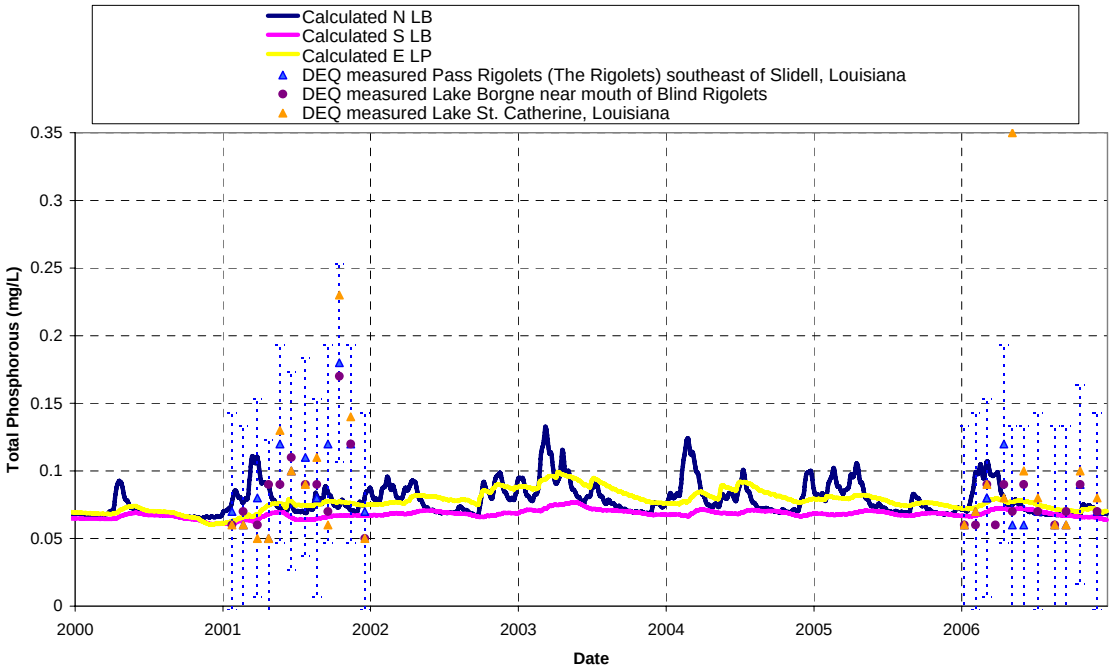

Figure D.6 Total phosphorous concentrations on Lake Borgne with nutrient concentrations applied at the Gulf of Mexico boundary (2000-2007).

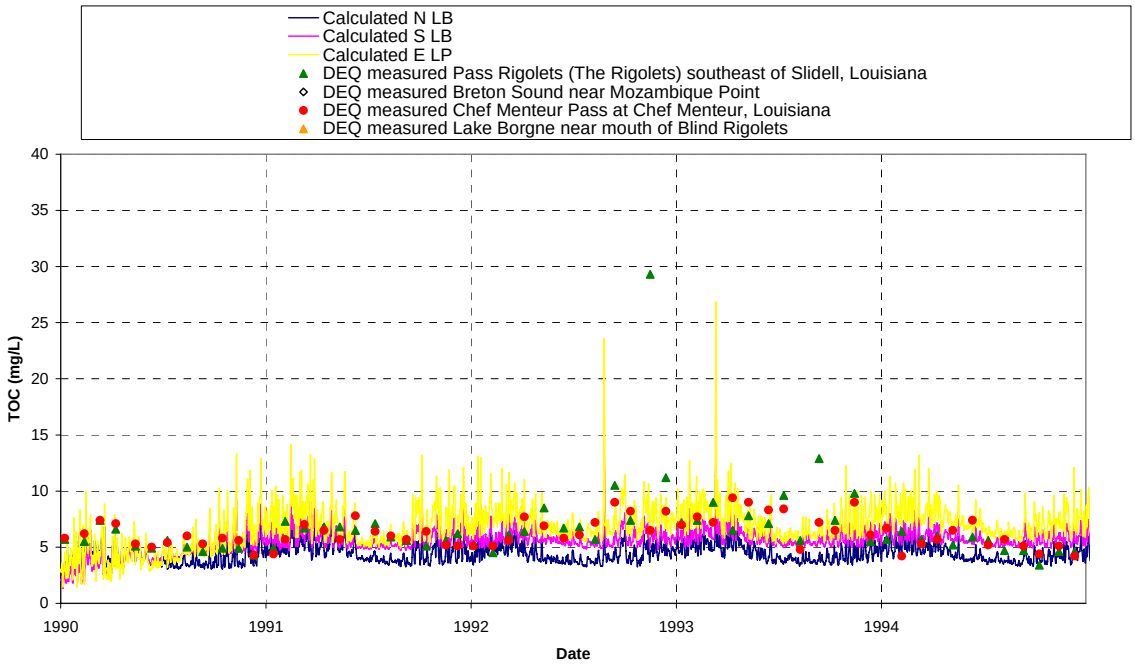

Figure D.7 Total organic carbon concentrations on Lake Borgne with nutrient concentrations applied at the Gulf of Mexico boundary (1990-1995).

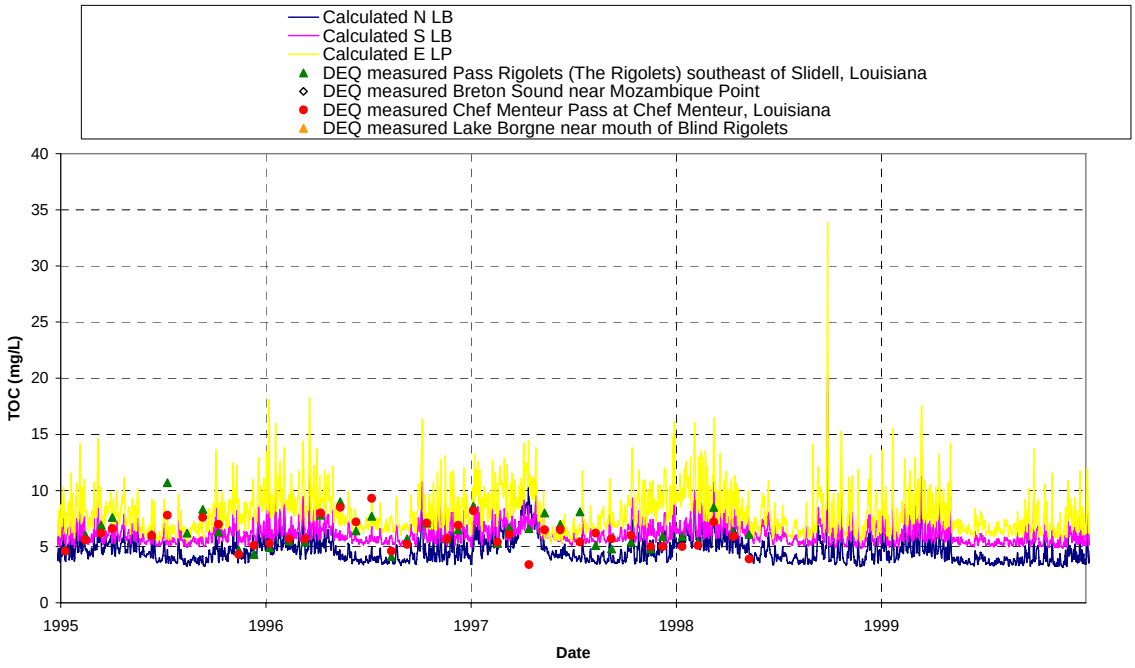

Figure D.8 Total organic carbon concentrations on Lake Borgne with nutrient concentrations applied at the Gulf of Mexico boundary (1995-2000).

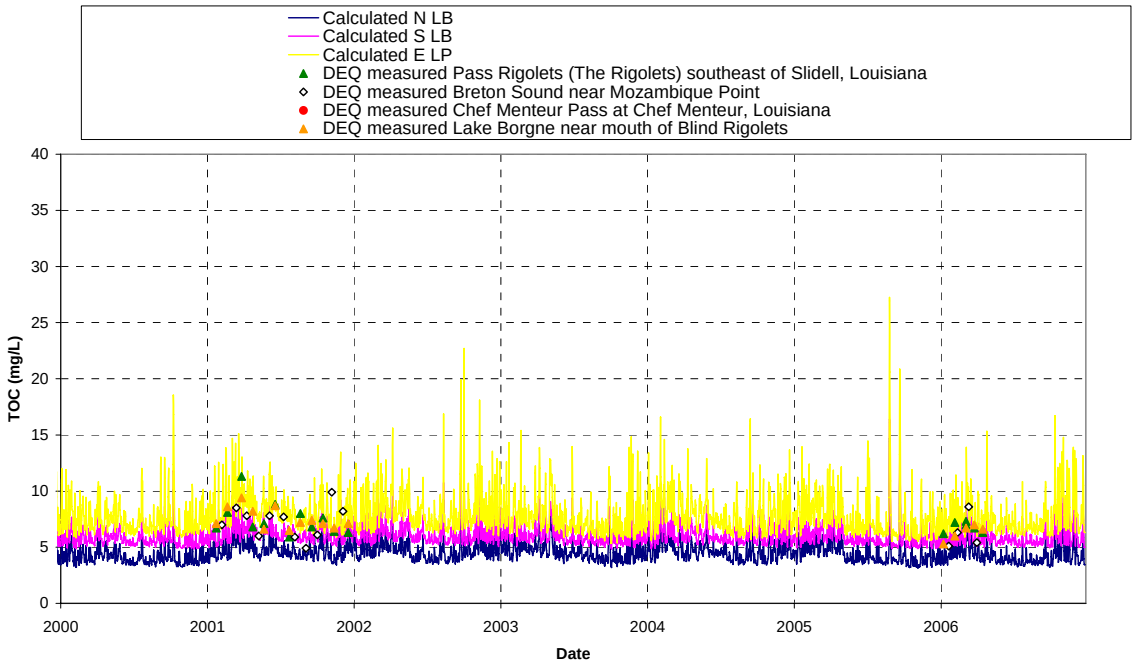

Figure D.9 Total organic carbon concentrations on Lake Borgne with nutrient concentrations applied at the Gulf of Mexico boundary (2000-2007).

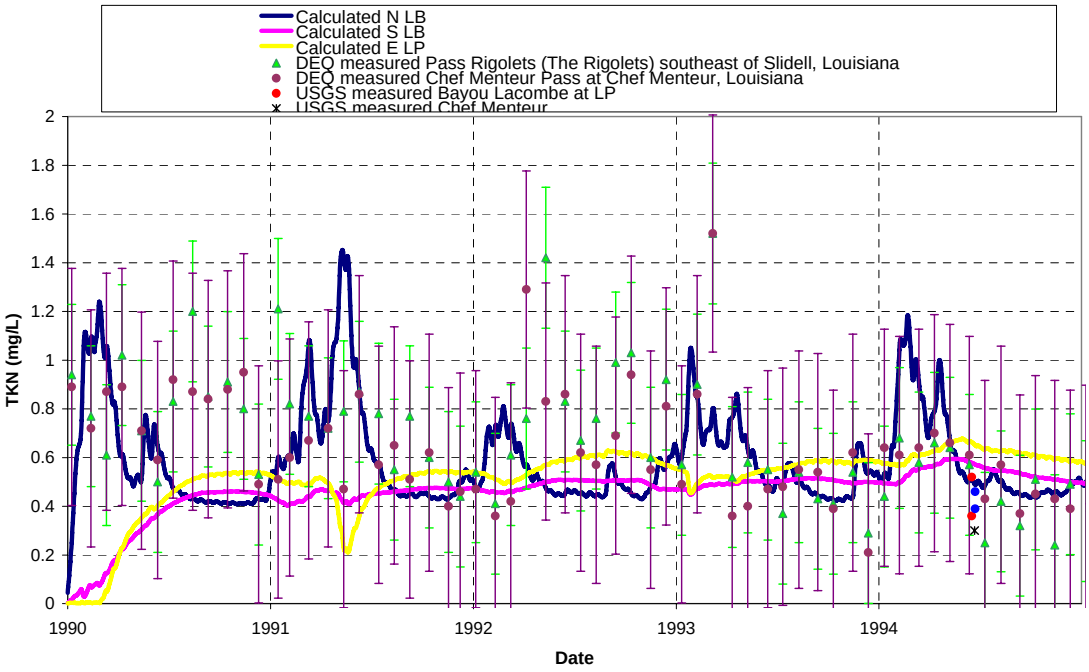

Figure D.10 TKN concentrations on Lake Borgne with nutrient concentrations applied at the Gulf of Mexico boundary (1990-1995).

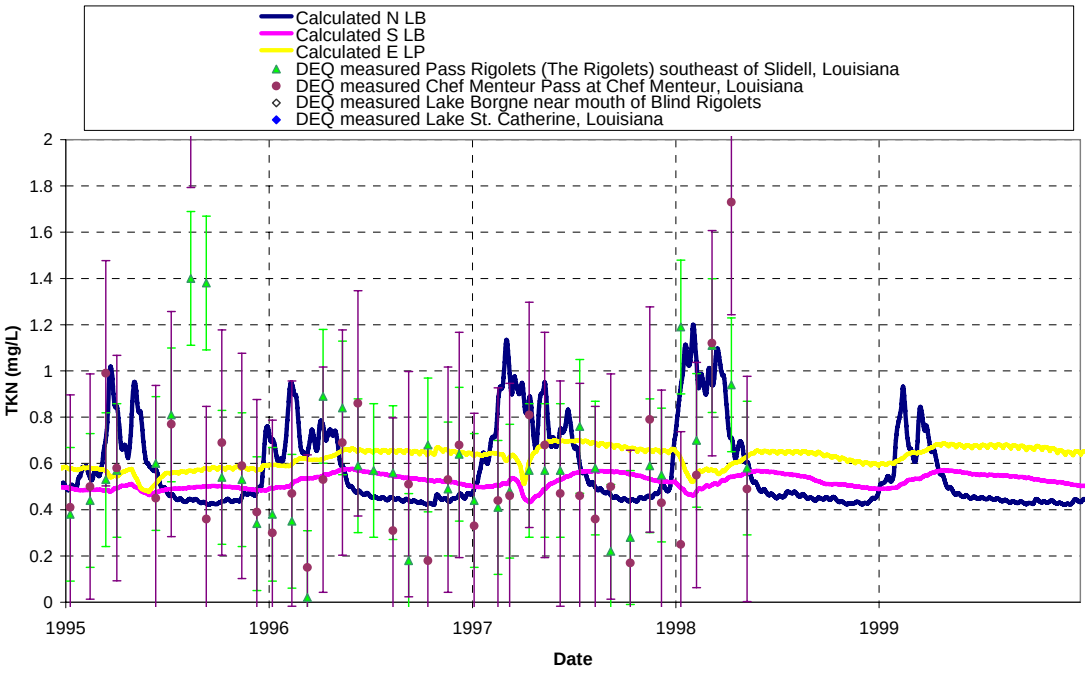

Figure D.11 TKN concentrations on Lake Borgne with nutrient concentrations applied at the Gulf of Mexico boundary (1995-2000).

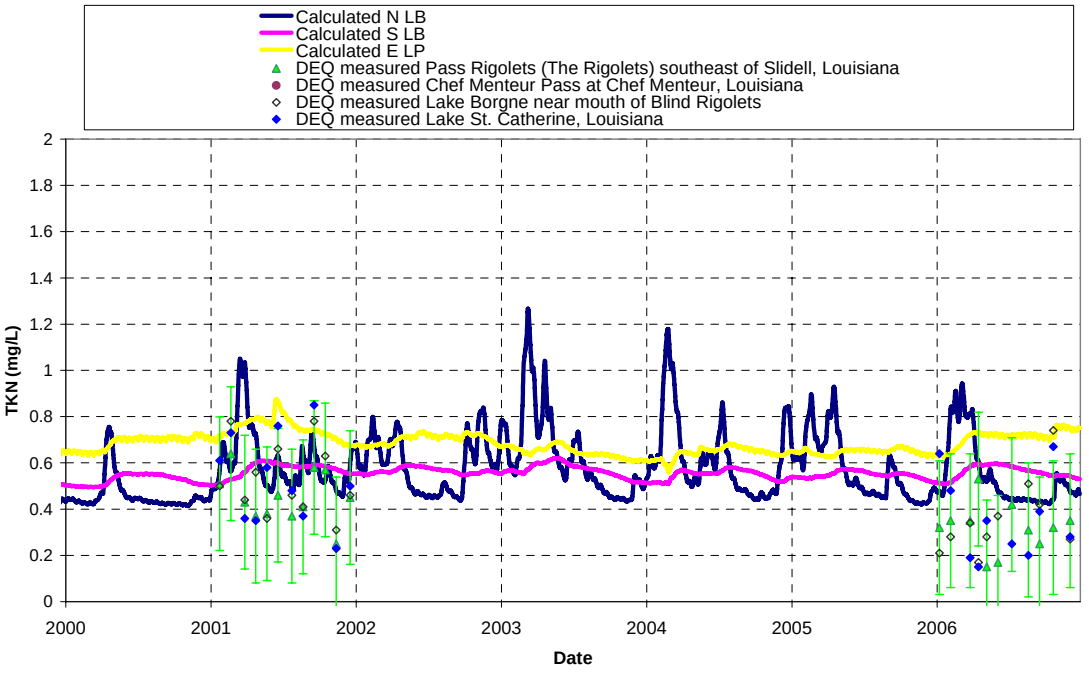

Figure D.12 TKN concentrations on Lake Borgne with nutrient concentrations applied at the Gulf of Mexico boundary (2000-2007).

Vita

Rachel Roblin was born in 1980 in Oshawa, Ontario, Canada. She obtained a Bachelor of Applied Science in Mathematics and Engineering (Civil Engineering Option) in 2003 from Queen's University at Kingston, Ontario, Canada. After graduating in 2003, Rachel worked for a coastal engineering consulting company, W.F. Baird & Associates, in Oakville, Ontario, Canada. In August 2006, Rachel moved to New Orleans to become a graduate assistant and begin her masters degree in the Department of Civil and Environmental Engineering at the University of New Orleans. This thesis was completed in partial fulfillment of the degree Master of Science in Engineering Science for the Department of Civil and Environmental Engineering at the University of New Orleans in May 2008.